SENSORS *in* BIOMEDICAL APPLICATIONS

Fundamentals, Technology and Applications

SENSORS *in* BIOMEDICAL APPLICATIONS

Fundamentals, Technology and Applications

GÁBOR HARSÁNYI, Ph.D.
Department of Electronics Technology
Budapest University of Technology and Economics

CRC PRESS

Boca Raton London New York Washington, D.C.

Library of Congress Cataloging-in-Publication Data

Main entry under title:
Sensors in Biomedical Applications: Fundamentals, Technology and Applications
Full catalog record is available from the Library of Congress

Direct all inquiries to CRC Press LLC, 2000 N.W. Corporate Blvd., Boca Raton, Florida 33431.

Visit the CRC Web site at www.crcpress.com

International Standard Book Number 1-56676-885-3
Library of Congress Card Number 00-100620
Printed in the United States of America 1 2 3 4 5 6 7 8 9 0
Printed on acid-free paper

TABLE OF CONTENTS

FOREWORD

In the twentieth century, technical and technological innovation has progressed at such an accelerated pace that it has permeated almost every aspect of our lives. This is especially true in the field of medicine. With almost continual technological innovations driving medical care, engineering professionals have become intimately involved in many medical ventures. As a result, the discipline of biomedical engineering has emerged as an integrating medium for two dynamic professions: medicine and engineering. In the process, biomedical engineers have become actively involved in the design, development, and utilization of materials, devices, sensors, and techniques for clinical research, as well as the diagnosis and treatment of patients.

The field of biomedical engineering includes many new areas: biomechanics, biomaterials, physiological modeling, simulation and control, and more. One of the most important parts of biomedical engineering is that of biomedical sensors, which enable the detection of biologic events and their conversion to signals. Sensors convert one type of quantity, such as temperature, into an equivalent signal of another type of quantity, for example, an electrical or optical (perhaps mechanical) signal. Biomedical sensors take signals representing biomedical variables and usually convert them into an electrical or optical signal. As such, the biomedical sensor serves as an interface between a biological and an electronic system.

The purpose of this book is to provide a central core of knowledge about sensors in the biomedical field (fundamentals, design, technology, and applications). This field now includes many new areas, each of which is presented in this book:

- sensor technologies
- basic sensor structures

- sensing effects
- physical sensors and their applications in biomedicine
- sensors for measuring chemical quantities in biomedicine
- biosensors

The author, Gábor Harsányi, Ph.D., is presently Associate Professor and Head of the Sensors Laboratory at the Department of Electronics Technology, Technical University of Budapest. He brings his knowledge, as well as his many years of teaching and extensive research expertise, to this book.

For biomedical sensor development, interdisciplinary activities are necessary, and the knowledge of engineers, physicists, chemists, biologists, and physicians has to be combined. This book fulfills this demand, describing in detail processing, devices, recognition principles of sensitive layers, and concrete realizations.

I believe that having all of these useful sensors included in this book will be of great value to scientists, engineers, and biomedical students.

Professor Zoltán Benyó
Chief-Supervisor of Biomedical Engineering Course
Technical University of Budapest

PREFACE

In the second half of the twentieth century, interest in the development of sensors, which conventionally are electric sensing devices, has increased considerably. Scientific research was followed by an emerging demand from various application fields. In the 1960s, the technique of chemical sensors grew rapidly and resulted in the possibility for direct detection of various ion and molecule types with certain selectivity limits. The research and development of conventional macrosensors soon turned in the direction of microsensors as a result of the miniaturization in microelectronics and expanding applications, including biology and medicine.

Currently, digital display thermometers, ear thermometers, personal blood pressure meters, and home glucose monitors are frequently used. Computed tomography and ultrasonography represent well-known modern diagnostic tools. It is less known that all of these instruments would not be available without sophisticated sensor elements. The application of sensors in biomedical diagnostics and bioinstruments has brought revolutionary changes that may already have a positive impact on the quality of life within the next century. Some key current and potential applications are as follows:

- Sensors enabled development computer-based medical imaging tools that could not be available without them, such as computed tomography, ultrasonography and many others.
- Sensors may greatly improve conventional imaging tools, like X-ray photography, by getting more information with smaller radiation doses.
- Portable multiparameter bedside monitoring appliances became available for intensive care.
- Convenient, easy-to-use appliances are available on the market for personal and home monitoring or diagnostics.

- Certain implantable self-regulatory appliances are currently available only for a few applications. However, widespread applications are predicted for the near future.
- Sensor-based systems can replace the functions of human sensing organs, such as artificial retinas, hearing aids, tactile sensing in artificial limbs, etc.
- Rapid diagnostic tools have emerged recently based on immunosensors and DNA chips.

Although the practical application of sensors has been developing rapidly, the theoretical background of their operation is clarified only partly or not at all in many cases. There are debates about the signal excitation mechanisms, signal conditioning methods, and the interpretation of practically measurable and theoretically expected results. Developing new sensors often means conducting considerable basic research at the same time. This is one of the main commercialization barriers of chemical and biosensors in the biomedical area.

A number of edited surveys and monographs have been published during rcent years about bioinstrumentation, bioelectronics and biosensors. Some of them are listed at the end of the preface to orient the reader. Even though the present book unavoidably covers material in certain areas that was discussed in previous works, it also has distinguishing characteristics. Thus, it seems to be important to emphasize what is covered here and what is not:

- The topic is approached from the sensorics side. It does not cover the general topics of bioinstrumentation and bioanalytical measurements. It concentrates only on sensors with existing and potential applications in biomedicine.
- This book gives a broad survey of all kinds of sensor types, including not only chemical and biosensors, but physical ones as well. It is, however, not an encyclopedia; rather, the basic ideas are covered and their combination is illustrated by the examples. Providing all kinds of individual designs and applications would be impossible within this frame.
- The main issue is the biomedical application. Analytical and environmental applications of biosensors are briefly mentioned, without going into details.
- The focus is on sensor elements; related signal conditioning and circuitry are illustrated by block diagrams.
- The main goal is to provide a survey of sensor application. Examples demonstrate how the basic sensing effects, sensor structures, and fabrication technologies could be combined in a particular application, without giving exact design considerations that may need more detailed mathematical discussions and are described in the literature, which is focused on the sensor type in question.

- Physiological aspects are only discussed for better understanding. Doctors cannot use this book as a diagnostic handbook.

The reader will find a strong emphasis not only on "what" and "how" but also on "why." Specialists and newcomers to the field will find this compact book easy to use. Moreover, researchers and development engineers can access the book according to physical, chemical, and technical fundamentals, and since it contains comparisons and assessments of the various types of sensors with respect to their practical applications, users will also benefit. However, a little knowledge in the following areas is helpful (but not necessary) for better understanding: solid state materials, devices and technologies, analytical chemistry, and biochemistry.

Readers of this book will be able to do the following:

- determine which sensor and transducer types are most appropriate for a given application
- understand and comply with the special requirements for sensors used in biomedical applications
- know how transducers can be connected and operated in various medical diagnostic appliances
- select appropriate interfaces between transducers and human bodies when they are in direct contact
- estimate the reliability level that can be expected for various sensor structures and applications

The book is intended for scientists, engineers, and manufacturers involved in the development, design, and application of biomedical sensors. Individuals involved in marketing or technical service will also benefit. Even practicing physicians can extend their knowledge to better understand the results of engineering in this field.

The most important definitions in connection with sensorics are summarized in the first chapter. The second chapter is devoted to the fabrication processing of sensors, including monolithic semiconductor, ceramic, thin-, and thick-film, polymer film, and optical-fiber-based types. It introduces the reader to the most important technologies to see how up-to-date sensor structures can be fabricated and to clarify which processes are compatible.

There are two basic elements in the operation of sensors. The first is a physical or chemical interaction between the environment and sensing material that alters material properties ("sensing effect"), while the second, the so-called "transduction mechanism" inside the sensor structure, converts this material property change into a useful signal that then holds information about the environment-material interaction. In the third chapter, various sensor device structures and their capabilities for some kinds of transduction mechanisms

are described, independent of the actual sensing effects, which are the subject of Chapter 4.

In the subsequent chapter, the discussion then turns to biomedical applications, providing a comprehensive description of the sensor types available presently and potentially in the near future. The survey of the various types is distinguished according to the following grouping:

- Physical sensors and their applications in biomedicine are presented in Chapter 5, including those sensors that measure some kind of physical parameter (i.e., temperature, pressure, etc.) based on a physical interaction.
- Sensors for measuring chemical quantities (practically inorganic analyte concentrations) in biomedicine are described in Chapter 6. Not all of these types are based on chemical interactions; physical sensors can also be used for analytical purposes in some special cases, like photosensors in oximetry (see Section 6.2).
- Biosensors are described in Chapter 7. The operation of biosensors is based on specific biochemical reactions characteristic of living things. Their biomedical application aims mainly at the analysis of organic bioactive molecules. The chapter ends with some chemical sensor examples that are applied for the analysis of the same materials (such as glucose), although they do not belong to the "real biosensor" group.

Chapter 8 gives a short summary of special biocompatibility problems of sensor applications. The description then ends and is followed by a group of tables in Chapter 9 that summarizes detection techniques, sensing effects, sensor structures, and their present status according to the various biomedical application fields distinguished as follows:

- medical imaging appliances
- appliances for personal and clinical use
- sensors for clinical and laboratory applications

Present status and future trends are also described here.

Appendix 1 contains a few examples of realized sensor structures. In Appendix 2, a few reliability aspects are discussed that are out of the scope of the chapters. A Glossary of Acronyms is also provided to make reading easier.

As mentioned, many sources, in addition to the author's personal knowledge and expertise, have been used to compile the information presented here including papers, books, and trade literature containing relevant, up-to-date material. The sources are referred to and listed in the "References" section at the end of each chapter.

RECENT EDITIONS AND MONOGRAPHS OVERLAPPING THE FIELD OF BIOMEDICAL SENSORICS

Bergveld, P. and Sibbald, A., *Analytical and Biomedical Applications of Ion-Selective Field-Effect Transistors*, Elsevier Science, Amsterdam (1999).

Blake-Coleman, B. C., *Approaches to Physical Measurements in Biotechnology*, Academic Press, San Diego, CA (1993).

Buerk, D. G., *Biosensors, Theory and Applications*, Technomic Publishing Co., Inc., Lancaster PA, (1993).

Carr, J. J. and Brown, J. M., *Introduction to Biomedical Equipment Technology*, Prentice Hall, Englewood Cliffs, NJ (1997).

Cunningham, A. J., *Introduction in Bioanalytical Sensors,* John Wiley & Sons, New York (1998).

Diamond, D., *Principles of Chemical and Biological Sensors*, John Wiley & Sons, New York (1998).

Enderle, J., Bronsio, J. and Blandard, S. M., *Introduction to Biomedical Engineering*, Academic Press, San Diego, CA (1997).

Fraser, D. M., *Biosensors in the Body: Continuous in vivo Monitoring*, John Wiley & Sons, New York (1997).

Freitag, R., *Biosensors in Analytical Biotechnology*, Academic Press, San Diego, CA (1996).

Geddes, L. A. and Baker, L. E., *Principles of Applied Biomedical Instrumentation*, 3rd ed., John Wiley & Sons, New York (1989).

Göpel, W., Hesse, J. and Baltes, H., *Sensors Update, Vol. 2-3*, John Wiley & Sons, New York (1998)

Göpel, W., Jones, T. A., Kleitz, M., Lundström, I. and Seiyama, T., *Sensors: A Comprehensive Survey, Vol. 2-3, Pt. H, Chemical and Biochemical Sensors*, John Wiley & Sons, New York (1991).

Ramsay, G., *Commercial Biosensors: Applications to Clinical, Bioprocess, and Environmental Samples*, John Wiley & Sons, New York (1998).

Scheller, F. and Schubert, F., *Biosensors*, Elsevier Science, Amsterdam (1999).

Spichiger-Keller, U. E., *Chemical Sensors and Biosensors for Medical and Biological Applications*, John Wiley & Sons, New York (1998).

Twork, J. V. and Yacynych, A. M., *Sensors in Bioprocess Control*, Marcel Dekker, New York (1997).

Valarcel, M. and de Castro, L., *Flow-Through (Bio)Chemical Sensors*, Elsevier Science, Amsterdam (1999).

Webster, J. G., Neuman, M. R., Olson, W. H., Peura, R. A., Primiano, F. P., Siedband, M. P. and Wheeler, L. A., *Medical Instrumentation: Application and Design, 3rd ed.*, John Wiley & Sons, New York (1997).

Wise, D., L., *Bioinstrumentation and Biosensors,* Marcel Dekker, New York (1991).

ACKNOWLEDGEMENTS

The author is deeply grateful to the many individuals and institutions who made their time and knowledge available to help put this material together. First, I would like to express my deepest thanks and appreciation to the reviewers, to Professor Aicha Eshabini (Professor of Electrical Engineering, University of Arkansas), and to Professor Mark Arnold (Professor of Chemistry, University of Iowa) for reading the material carefully, as well as for providing useful comments and criticisms. Many thanks also go to the publishers and authors who gave their consent to publish borrowed material. Their names and credit are given in the appropriate places.

I am indebted to all the members of the leading committee of the Biomedical Engineering Faculty, Technical University of Budapest, for supporting me in writing and teaching this material to students as a special subject.

Many thanks to my friends and colleagues, especially to my boss Professor Zsolt Illyefalvi-Vitéz, head of the Department of Electronics Technology Technical University of Budapest, for assuring a good environment for working on this material. I must also mention the persons who have been working with me on special biosensor-oriented research topics during the last few years: Professor Csaba Visy (József Attila University, Szeged, Hungary) and Róbert Dobay, Ph.D. student, Technical University of Budapest.

And last but not least, I have to mention the great help and technical assistance provided by Éva Antal in the word processing of the material and by Anikó Gyürki in the preparation of drawings and figures.

I am also grateful to Technomic Publishing Co., Inc. (namely, Joseph Eckenrode, Ph.D. and Ms. Susan G. Farmer) for their willingness to give prompt assistance during the whole period of work. Many thanks also go to Lewis Bass, Ph.D., who encouraged me in bringing this material together for several successful professional seminars long before publishing the book itself.

And I would be remiss if I did not acknowledge those institutions, foundations, and companies that have financially supported my overall systematization, teaching, and research work on biomedical sensor topics through the past few years: the Hungarian National Scientific Research Fund (OTKA, project No. T021102), the Ministry for Culture and Education (MKM, project No. FKFP 0253/97), the Foundation for Hungarian Higher Education and Research (AMFK, project No. 30/96), the National Committee for Technological Development (OMFB), the KOMED Ltd., Hungary, and the ABLESTIC Emca-Remex Co., USA.

This work, of course, would not have been possible without the ongoing support of my family, especially my wife Éva.

Gábor Harsányi, Ph.D.

CHAPTER 1

Introduction

1.1 SENSORS AND THEIR CHARACTERISTICS

The most difficult problem is to define the basic ideas that one is dealing with; it is really difficult to find a correct and up-to-date definition for sensors. Even the technical literature contains contradictory approaches.

The following definition is provided here: *the sensor is a transducer that converts the measurand (a quantity or a parameter) into a signal carrying information.* The nature of the signal can be

- electrical: this has been the most common for many years
- optical: it became a new trend in sensorics
- mechanical: this has been used in several conventional devices

Instrumentation systems using sensors can be categorized into measurement (especially analytical) or control systems (Norton, 1982). In *measurement systems,* a quantity or property is measured, and its value is displayed. In *control systems,* the information about a measurand is used to control it so that its measured value should equal a desired value. (The schematic structure of the latter type is shown in Figure 1.1). The *actuator* converts a signal into an action in order to modify the measurand. *Analyzers* are special measuring systems whose purpose is to display the nature and proportion of the constituents of a substance.

Measuring systems do not always contain sensors, and are not sensors. The simplest measuring system is a measuring device, which also displays the measured value, for example, a mercury-in-glass thermometer. Nobody thinks that it is or that it contains a sensor. A bimetal switching unit cannot be handled as an integrated "sensor-actuator," although it is a controlling device. On

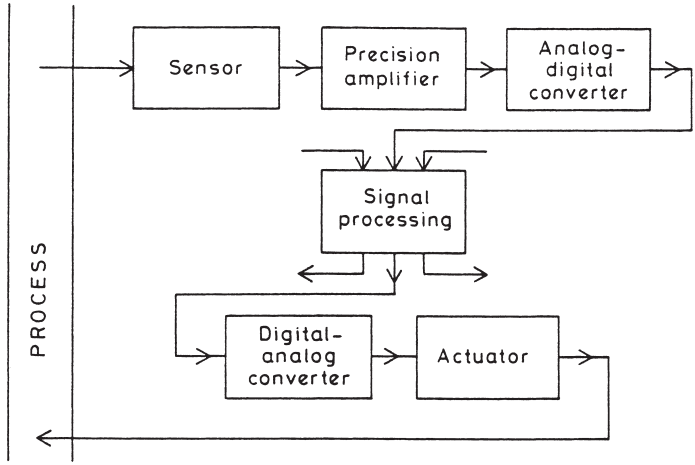

FIGURE 1.1. Schematic structure of a process controlling unit using sensors and actuators. (Reprinted with permission from *Polymer Films in Sensor Applications* by G. Harsányi, ©1995, Technomic Publishing Co., Inc., Lancaster, PA, p. xxi.)

the other hand, a small body thermometer with a liquid crystal display should contain a temperature sensor: there is a stage of processing where a signal can be separated from the system; thus, it really contains a sensor and a display unit. The sensor supplies a signal, an information carrier, and not the information itself, as an output. The signal can also be transmitted directly by one of the information transmission media.

An important property of ideal sensors is that continuous measurement is possible without taking samples and without modifying the measurand or analyte in question. This is the most important difference between chemical sensors and analytical tools or appliances used in analytical chemistry (Janata and Bezegh, 1988). For example, an indicator dye itself is not a sensor because continuous measurement is not possible, even though the function of the dye can be applied in chemical fiber-optic sensors.

Sensors are conventionally classified according to the quantity to be measured:

- mechanical quantities (position, displacement, force, acceleration, pressure, flow rate, rpm, acoustic waves, etc.)
- thermal quantities (temperature, heat flow, etc.)
- electrostatic and magnetic fields and fluxes
- radiation intensity (electromagnetic, nuclear, etc.)
- chemical quantities (concentration of humidity, gas components, ions, etc.)
- biological quantities (concentration of enzyme substrates, antigens, antibodies, etc.)

Another classification is possible *according to the nature of interaction* giving the basis of operation in the groups of physical sensors, chemical sensors, and biosensors. Accordingly, a *biosensor* is such a sensor that uses a living component or products of living things for measurement or indication. Thus, a blood-oxygen sensor is not a biosensor, although it measures a biologically important parameter; it is simply a chemical sensor in a special application. On the other hand, an enzyme-reaction-based alcohol sensor is a biosensor even when used for measuring concentrations in solutions produced by the chemical industry.

Generator-type sensors operate without external excitation, while *modulator-type sensors* need an external source. Thermocouples producing temperature dependent output voltages are generator-type temperature sensors, for example, while thermistors (temperature dependent resistors) need an external voltage or current for producing an output signal and are thus classified as modulator-type sensors.

Static characteristics demonstrate the most important behavior of sensors: the relationship between the output signal and the measurand. *Sensitivity* is defined as the slope of the former function. In linear ranges, it is a constant [see Figure 1.2(a)].

FSO stands for *full-scale output* of the sensor. This is the maximum (or nominal) output signal.

Linearity is the closeness of a sensor's calibration curve to a specified straight line. It is expressed as a percent of FSO, which is the maximum deviation of any calibration point from the corresponding point on the specified straight line [see Figure 1.2(a)].

Hysteresis is the maximum difference in output, at any measurand value within the specified range, when the value is approached first with an increasing and then with a decreasing measurand [see Figure 1.2(b)]. It is also given in percent FSO.

The *limit of detection* is the lowest value of measurand that can be detected by the sensor. *Resolution* is the smallest increment in the output, given in percent FSO.

Repeatability (sometimes called reproducibility) is the ability of a sensor to reproduce output readings when the same measurand value is applied to it consecutively, under the same conditions, and in the same direction.

Interchangeability means the maximum possible error of the measurements when an individual sensor device is changed within the measurement appliance for another of the same type.

The *zero-measurand output* ("the zero" or offset) is the output when the zero measurand is applied. *Zero shift (or drift)* is a change in the zero-measurand output under specified conditions (e.g., temperature change, long-term storage, aging, etc.). Similarly, *sensitivity shift* is a change in the slope of the calibration curve.

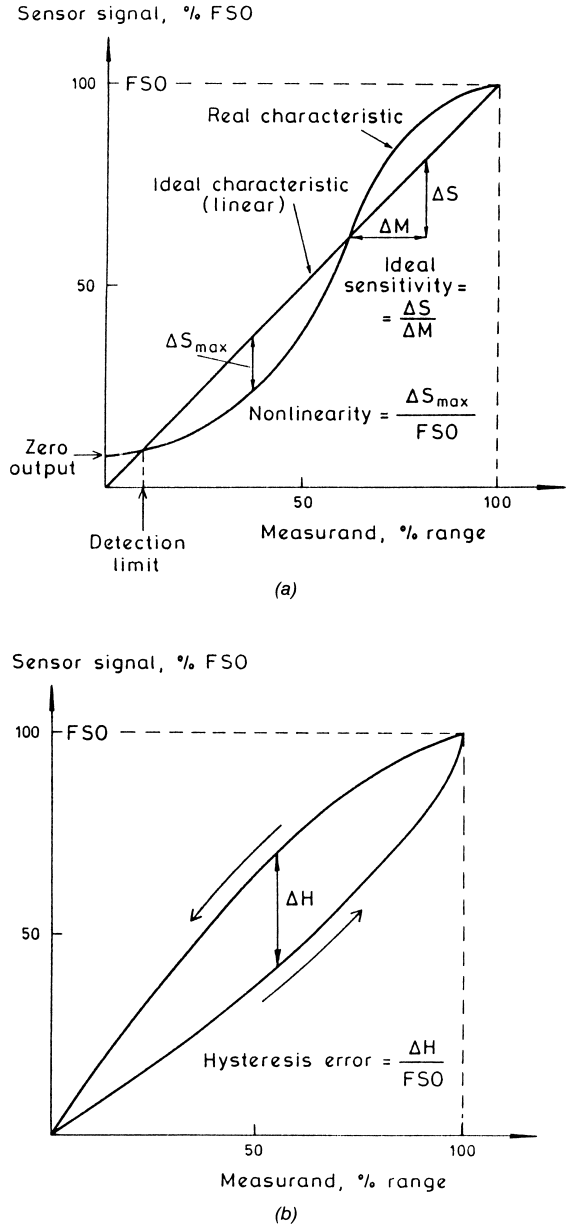

FIGURE 1.2. Calibration curves for sensors indicating the most important properties: (a) sensitivity, nonlinearity, detection limit, and zero output; and (b) hysteresis error. (Reprinted with permission from *Polymer Films in Sensor Applications* by G. Harsányi, ©1995, Technomic Publishing Co., Inc., Lancaster, PA, p. xxiii.)

The *response time* is the length of time required for the output to rise to a specified percentage (generally 90%) of its final value (as a result of a step change in the measurand).

Selectivity is the suppression of the environmental interference. The ideal sensor will only respond to changes in the measurand. However, in practice, sensors can also respond to changes in other quantities, for example, temperature. These cross-effects can be eliminated by compensation or multisensor operation.

Lifetime is also an important property of sensors; it is the length of time that sensors remain sensitive under normal operational conditions.

1.2 INTEGRATED AND SMART SENSORS: UP-TO-DATE REQUIREMENTS

The rapid development of microelectronics, micromechanics, integrated optics, and other related high technologies enabled the miniaturization of sensor elements and the physical integration of various functions and signal-processing elements onto the same substrate.

Sensor arrays are integrated sensors consisting of the same or similar sensor units with the same or similar function.

Multisensors consist of several sensor elements, each having a different function.

A *multifunction sensor* is a single device that can realize several different sensor functions under different conditions.

There are several possible levels of integration when *integrating signal-conditioning units with sensors.* The first level of signal conditioning that can be integrated on a sensor chip is balancing the offset, compensating the temperature drift, and so on. A higher level of integration may include amplification and signal conversion. The third level, which is the visible technology trend of *smart sensors,* is the incorporation of microprocessor and memory for performing different intelligent functions at the sensor level, such as the following:

- digital signal processing and storage
- compensation of static errors
- self-calibration and testing
- automatic switching of the measurement ranges
- recording of the measured data
- calculation of mean values, tolerances, etc.
- possibility of multisensor signal processing (e.g., using self-teaching with neural network processing)
- compensation of time-dependent instabilities (e.g., with fuzzy)

Smart sensors represent the "new wave" of sensors.

Conventional applications of sensors include the measuring and testing of various physical and chemical quantities and industrial process control and/or automation. Advanced technologies enabled not only miniaturization and integration, but also improvements in reliability and low-cost mass production. Newly emerging application areas are mainly in consumer fields (e.g., domestic and automotive electronics, household, safety, and comfort and pleasure) and in highly advanced scientific areas (e.g., medicine, environmental protection, research, etc.). The former area needs low-cost sensors, and the latter area requires very reliable sensors.

The great technical possibilities and the relatively low cost of microprocessor-based systems have also turned the most important requirements into other directions. A few years ago, properties conventionally expected were as follows:

- good linearity
- small hysteresis
- small offset
- low temperature drift
- low interference effects
- good interchangeability
- good long-term stability and reliability

Among these requirements, only the last one should be assured nowadays, but even these properties can be missing in some cases. Linearity and other errors can be compensated or handled using microprocessor-based systems and additional sensors (e.g., temperature sensors for temperature compensation).

The most important new requirements are as follows:

- low cost
- physical compatibility with integrated circuit (IC) and packaging/interconnection technologies to allow the integration of sensors into arrays and together with signal-processing units
- electrical compatibility with microprocessors: it is desirable to provide digital or pseudodigital (e.g., frequency) output
- multifunction sensors and integrated sensor arrays due to the need for compensating interference effects

1.3 SPECIAL REQUIREMENTS OF BIOMEDICAL APPLICATIONS

There are special requirements and challenges for sensors used in biomedical application fields and there are special possibilities for the use of sensors

in these fields that cannot be exploited in other applications. The main areas may be distinguished as follows:

- appliances for diagnosis: measuring or mapping a parameter at a given time
- monitoring devices for measuring parameters within a given period
- built-in controlling units containing not only sensors but also actuators

Although present practical applications are almost entirely in the first two areas, one of the most important research tasks of biomedical sensorics is to develop controlling systems that can be implanted into human bodies and can continuously operate for long periods of time to simulate the function of an internal organ or other controlling mechanism. Many chronic diseases of our age result from the failed operation of one of the controlling systems of the human body (e.g., high blood pressure, diabetes, etc.). These diseases can be managed with the use of medications but the real controlling function cannot be corrected in this way: the danger of overcompensation is always threatening, as, for example, the hypoglycemia with insulin ration in diabetes. The ideal treatment solution calls for continuous blood glucose monitoring and a continuously controlled ration of insulin, always in the necessary amount.

When considering requirements for a sensor, it is very important to determine whether the sensor element is to be applied inside the human body (invasively) to analyze *in vivo* or outside to analyze a sample *in vitro*. Different approaches should be applied for long-term operation of physical sensors and for relatively unstable chemical and biosensors.

Because the various possible application modes result in different requirements, the sensors should be handled separately according to the following groups:

(1) Appliances for medical imaging (CT, PET, ultrasound, etc.)
   - They generally are computer-controlled, high-cost appliances.
   - The cost of the sensing "head," which contains intelligent sensors, sensor arrays or multisensors, is relatively low.
   - The cost of the sensor element is not a determining factor.
   - High reliability, a long lifetime, and the interchangeability of the "head" is required.
   - Integrated smart sensors and sensor arrays are needed.

(2) Small appliances for clinical diagnosis and personal use in measuring or in continuous monitoring of physical parameters
   - These are low-cost, sometimes consumer-like appliances designed to be used for a few years (e.g., digital thermometer, blood-pressure meter, pulse and breath monitoring devices).
   - Low-cost (sometimes disposable) sensor elements are required.
   - They should be interchangeable in many cases.

- They are not exposed to harsh environmental effects (used outside of the body, within narrow operation temperature ranges, etc.).
- Their long-term reliability is not the most important requirement.

(3) Appliances for clinical chemical analysis and for personal domestic analytical diagnosis
- Low-cost disposable sensors can replace competitive conventional methods, like photometry.
- Domestic applications need easy handling, which can be achieved by sensors and connected appliances.
- Interchangeability or easy calibration is a severe requirement.

(4) Chemical and biosensors for clinical *in vivo* monitoring
- Only low-cost and disposable sensor elements can be used for invasive applications in order to avoid sterilization problems or infections (e.g., with AIDS).
- Interchangeability or easy calibration is important.
- In noninvasive cases, the easy refreshment possibility is also a requirement.
- Long-term operation is not needed: operation only for a period of continuous use is required (e.g., one day).
- A harsh chemical environment should be expected in blood and tissues.
- Multisensors for compensating interference effects are needed.
- Integrated sensors for long-distance signal transmission (sometimes telemetry) are desired.
- Miniaturization is essential for catheter-tip applications.
- A number of biocompatibility problems have to be overcome. Tissue-friendly materials and cover layers should be applied (silicone rubber, polysulfones, etc.) to minimize blood clotting and prevent the formation of protein precipitation.

(5) Implanted chemical and biosensors for continuous monitoring and regulation
- Low-cost, disposable, interchangeable sensors are needed.
- Integrated multisensors and actuators are desired.
- Stable long-term operation and reliability are severe requirements.
- Refreshment should be available without recalibration.

The latter list of requirements seems to be the most difficult in practical realization, of course. This is why such systems are mostly still in research stages and represent the future of biomedical sensor applications.

The various biomedical application fields and related detection techniques, sensing effects, sensor structures, and their present status is listed in Chapter 9, Table 9.1.

1.4 REFERENCES AND SUPPLEMENTARY READING

Dakin, J. and Culshaw, B., *Optical Fiber Sensors: Principles and Components,* Artech House, Boston, MA (1988).

Gardner, J. W., *Microsensors: Principles and Applications,* John Wiley & Sons, New York (1994).

Göpel, W., Hesse, J. and Zemel, J. N., eds. *Sensors: A Comprehensive Survey,* Vol.1–6, WILEY-VCH Weinheim, Berlin (1994).

Grandke, T. and Ko, W. H., *Sensors: A Comprehensive Survey, Vol. I, Fundamentals and General Aspects,* John Wiley & Sons, New York (1989).

Harsányi, G., *Polymer Films in Sensor Applications,* Technomic Publishing Co., Inc., Lancaster, PA (1995).

Janata, J. and Bezegh, A., "Chemical Sensors," *Anal. Chem.,* 60 (1988), pp. 62R–74R

Mandelis, A. and Christofides, C., *Solid State Gas Sensor Devices,* John Wiley & Sons, New York (1993).

Norton, H. N., *Sensor and Analyzer Handbook,* Prentice Hall, Inc., Englewood Cliffs, NJ (1982).

Obba, R., *Intelligent Sensor Technology,* John Wiley & Sons, New York (1993).

Prudenziati, M., *Thick Film Sensors,* Elsevier Science, Amsterdam (1994).

Ristic, L., *Sensor Technology and Devices,* Artech House, Boston, MA (1994).

Soloman, S., *Sensors Handbook.* McGraw-Hill, New York (1998).

Sze, S. M., *Semiconductor Sensors,* John Wiley & Sons, New York (1994).

Udd, E., *Fiber Optic Sensors: An Introduction for Engineers and Scientists,* John Wiley & Sons, New York (1991).

CHAPTER 2

Sensor Technologies

Over the years, a number of materials and technologies have been developed in the fabrication of sensors. Some of these are relatively new, while others are well developed and have been mastered to a sufficiently advanced level, such as silicon technology.

Both large categories of materials (i.e., inorganic and organic types) are now used in the fabrication of sensors. Inorganic materials include single crystals like quartz, silicon, and compound semiconductors; polycrystalline and amorphous materials like ceramics, glasses, and their composites; and metals. Organic materials applied in sensors are mainly polymers; however, recently, lipids, enzymes, and biochemical compounds (e.g., antibodies and DNA molecules) have increasingly been used in biosensors.

Because of the great demand for sensors that are compatible with microelectronics, the fabrication processes of microsensors originate from the fabrication of various integrated circuits, packaging, and interconnection systems, as well as from the devices of optoelectronics, mechatronics, and micromechanics. The most important material and related processing techniques are discussed here in the following groups:

- monolithic semiconductor (or other single crystal) processing
- ceramics (and glasses)
- thin- and thick-film technologies
- polymer film deposition techniques
- optical fiber technologies

2.1 MONOLITHIC SEMICONDUCTOR TECHNOLOGIES

Currently, microelectronic circuit fabrication is based on silicon and compound semiconductors, mainly GaAs. However, the former material dominates

semiconductor microsensorics. Therefore, silicon processing will be discussed in detail, and some special processes of the compound semiconductor technology will be mentioned.

Single-crystal silicon has a diamond structure with cubic symmetry. The various directions in the lattice are denoted by three indices. The electrical, chemical, and mechanical properties of silicon depend on the orientation. For example, certain planes of the lattice will etch much more rapidly than others do when the crystal is subjected to chemical etching.

Silicon in single-crystal form is a unique material: its electrical resistivity can be varied many orders of magnitude by adding minute quantities of impurities (dopants). In single-crystal form, every silicon atom is bonded to four other silicon atoms. The dopant atoms are substituted for the silicon in the crystal lattice, and these try to form bonds with four other silicon atoms. However, *p*-type dopants have one electron too few, while *n*-type dopants have one electron too many to make a perfect crystal fit. These "extra" and "missing" electrons impart unique electrical properties to the doped silicon regions. Boron is an example of a *p*-type impurity, while phosphorus and arsenic are examples of *n*-type impurities.

If a boundary exists between a *p*-type region and an *n*-type region, a *p*-*n* junction is formed. Such a junction will allow an electric current to pass only in one direction. Semiconductor devices (diodes, transistors, and integrated circuits) can be fabricated by forming such junctions.

Bulk-form single-crystal silicon is grown from a very pure melt. After crystal growth and purification by zone refining, this bole is sliced into wafers about 0.5 mm thick. These wafers are then chemically mechanically ground and polished to a very high surface quality in preparation for use in producing integrated circuits or silicon sensors. Single-crystal processing methods are used not only in silicon technology, but also in the fabrication of other single-crystal sensor devices, e.g., those made of quartz, $LiNbO_3$, etc.

Although for integrated circuits one side of the silicon wafer is typically polished, for sensors it is more common to begin with wafers that are polished to a mirror surface on both sides. The surface orientation of the silicon wafers is determined by the bole. The most common types of wafers produced have surface (100) or (111) orientation. Silicon sensors almost always employ (100) wafers because of their unique anisotropic etching characteristics.

Single-crystal wafers fabricated by the processes described above still contain surface crystal defects. It is possible to improve the crystal surface structure by growing a thin single-crystal layer on the surface of the wafer by a process known as *epitaxy.* The expression originates from the Greek word meaning "arranging upon." In this, atoms are deposited onto the crystal surface under conditions such that a new crystal is formed layer by layer as long

as the supply of atoms continues. According to the source of silicon, there are several main types of epitaxial layer growing:

- *Liquid phase epitaxy* (LPE) is the simplest crystal growth technique for depositing semiconductor epitaxial films. It is based on the crystallization of semiconductor materials from a solution saturated or supersaturated with the material to be grown.
- In *vapor phase epitaxy* (VPE), the materials to be deposited are brought to the surface of the slice in the vapor phase. The method generally used to carry this out is chemical vapor deposition (CVD). At the appropriate temperature, chemical reactions take place that result in the deposition of atoms onto the surface where they replicate the underlying crystal structure. In the case of silicon, the often-used source of atoms is silicon tetrachloride, which is reduced by hydrogen on a hot silicon surface to deposit silicon atoms and gaseous hydrochloric acid.
- Another possibility is *molecular beam epitaxy* (MBE), which is the most recently developed method for epitaxial layer growth. It is a sophisticated evaporation of materials in an ultrahigh vacuum. The slices are placed in a vacuum chamber, and element species are evaporated from heated sources, impinged on the heated surface, and condensed on the substrate.

CVD is often applied in semiconductor processing for building up epitaxial and polycrystalline or amorphous layers.

Silicon sensors and microstructures are formed on silicon wafers by modifying their mechanical structure and electrical characteristics. To form a mechanical structure, silicon can be etched away from the starting wafer using various etching techniques. Alternatively, silicon can be added to the structure by depositing amorphous or polycrystalline silicon (polysilicon), by growing an "epitaxial" layer of single-crystal silicon onto a single-crystal silicon surface, or by bonding an additional silicon wafer to a partially processed first wafer. When removing silicon by etching, those areas where etching is not required must be protected by a suitable masking layer.

Similarly, the electrical properties of silicon can be modified by selective doping techniques. Solid-state diffusion and ion implantation are two common techniques for increasing the dopant concentration in the silicon. It is desirable to modify the characteristics only in selected areas of the wafer. Suitable masking layers must, therefore, be available for selective doping.

There are a number of techniques for producing *masking layers* on the silicon surface. The most common is the thermal oxidation process. By heating the wafer to a temperature near or about 1000°C in an oxidizing atmosphere, a thin layer of silicon is converted to the insulator silicon dioxide (SiO_2). This dielectric layer is an excellent electrical insulator. In addition, it acts as a mask

to the diffusion of dopants used to vary the conductivity and to the etchants used to shape the mechanical structure of the silicon devices and sensors.

Another common insulator and masking layer is silicon nitride (Si_3N_4). This insulator is deposited by CVD onto the wafers. Phosphosilicate glass deposited by CVD is also an often-used insulating and passivating layer on the top of the chips.

As can be seen, CVD is a commonly used technique for film deposition; single-crystal silicon epitaxial layers, polycrystalline silicon, insulating layers, and even conducting films such as $MoSi_2$ can be deposited. Conventional CVD is performed at atmospheric pressure, but more advanced methods include low-pressure CVD (LPCVD) and plasma-enhanced CVD (PECVD), which employ lower temperature ranges.

Metal layers and interconnections on the silicon surface are deposited using thin-film techniques described in Section 2.3. Polymer films are also often applied as dielectrics and as sensitive films. Their deposition techniques are discussed in Section 2.4.

All films deposited on a wafer are patterned by using a process called lithography and by subsequent etching. *Lithography* is a technique by which patterns are replicated onto the substrate using auxiliary layers, for example, etch-resistant materials that can be shaped easily to the desired pattern (Elliott, 1986). The most widely used conventional photolithography applies photoresists: materials that change their solubility properties when illuminated. For realization of patterns with submicron sizes, techniques other than photolithography must be used. The exposure may also be accomplished using electron beams, X rays, or ion beams. These are new techniques in lithography.

Once the resist pattern is formed and hardened by heat treatment, the wafer is put through various *etching processes* to transfer the pattern from the resist onto the oxide, nitride, or other film (such as metal) to be patterned on the wafer. There are wet chemical etchants and dry etching techniques using plasma reactors. The latter are denoted as plasma etching. In dry etching, the plasma serves as a source of ionized species that produce, or in some manner, catalyze etching. Noble gas ions perform a simple sputtering, while ionized reactive gas molecules can take part in chemical reactions with the particles of the film to be etched. After etching, the photoresist is removed (stripping), and the wafer is ready for further processing steps, which would include doping cycles or further etching steps.

A fundamental process for the production of microstructures in sensors is the *anisotropic etching* of silicon. Certain chemical etchants (such as KOH, hydrazine, etc.) attack the (100) and (110) planes of silicon much faster than the (111) planes. This fact is used to produce a number of accurately defined shapes in a silicon wafer with (100) surface orientation. Typically, the wafer

is oxidized, and then the oxide is patterned using photolithography. When such a wafer is immersed into an anisotropic etchant, silicon will be removed only from the areas where no oxide is present. The etching proceeds downward in the (111) direction very rapidly, but when (111) planes are encountered, the etching effectively stops. In a (100) wafer, the (111) planes are oriented at an angle of 54.7° with respect to the surface. Thus, "V"-shaped grooves and, when an internal etch-stop layer (e.g., a strongly doped p^+ epitaxial layer within an *n*-type wafer) is applied, specially shaped cavities can be precisely formed into the wafers as shown in Figure 2.1.

There are two major techniques of *introducing dopants* into the silicon crystal structure: diffusion and ion implantation. *Diffusion* is a process in which impurity atoms penetrate the crystal lattice because of a concentration gradient at the surface. It is carried out in a high-temperature furnace by depositing a large amount of the dopant on the surface of the silicon. The dopant on the surface is at a very high concentration compared to the silicon, and at high temperatures (usually above 800°C), it will diffuse into the silicon to try to equalize the concentration gradient from the surface to the silicon.

Ion implantation is a process in which the ionized dopant atoms are accelerated through an electromagnetic field and physically blasted into the silicon. The acceleration energy determines how far the dopant ion will penetrate the silicon. Later on, the dopant needs to get a high-temperature annealing (at about 500°C) in order to become incorporated into the crystal structure and become electrically activated. This high-temperature operation may also be used to diffuse the dopant deeper into the wafer from the initially implanted depth.

Although ion implantation is usually more expensive than diffusion, it has an important advantage in that the amount of dopant can be precisely monitored and controlled. As a result, resistors made by ion implantation, for example, have very tight tolerances over resistance values and their temperature coefficients. Equivalent tolerances are usually impossible to obtain with diffusion techniques.

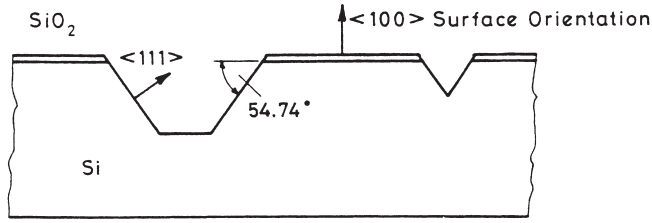

FIGURE 2.1. Cross-section of V-groove and cavity type etch profiles in silicon, made by anisotropic etching. (Reproduced with permission from *Polymer Films in Sensor Applications* by G. Harsányi, ©1995, Technomic Publishing Co., Inc., Lancaster, PA, p. 9.)

In practice, a *technology process flow* should be built up that connects the individual process steps in a series. The optimum technology is the one that minimizes the number of processing steps, while at the same time guaranteeing a specified device performance. In microsensor structures, metal-oxide-silicon-based field-effect transistors, the so-called "MOSFET" devices, are of great importance. The application of individual technology steps in an integrated process is illustrated through the example of conventional complementary MOS, the CMOS technology, which is often used in microsensor fabrication. In this case, both *p*-channel (PMOS) and *n*-channel (NMOS) transistors are realized on the same substrate (see more about MOSFET structures and operation in Section 3.2). It should be stressed that the very large-scale integrated circuits need more sophisticated and much more complicated processes at the present time, however, the given example is a good demonstration for integrated processing, although the aluminum-gate processing has already been replaced by polysilicon gate technology.

The starting material for the CMOS process is a wafer of slightly doped *n*-type silicon. The manufacturing process flow is summarized in Figure 2.2. The individual steps are as follows (Sze, 1985):

(1) Oxidation, photolithography, window etching for the first diffusion
(2) P-well diffusion, oxidation
(3) Photolithography, window etching for the second diffusion
(4) P diffusion and oxidation to define source and drain areas for PMOS transistors and, at the same time, to define a boundary or "channel stop" around the areas where NMOS transistors will be fabricated
(5) Photolithography and window etching for the third diffusion
(6) N diffusion and oxidation to define NMOS transistors and "channel stop" around PMOS transistors
(7) Photolithography and window etching for the gates
(8) Thin-gate oxide growing for MOS-gate dielectric layers
(9) Photolithography and window etching for contacts
(10) Metal deposition, patterning, and passivation

Monolithic semiconductor processing offers the following advantages and disadvantages in sensor fabrication:

(1) Advantages
- batch production of low-cost, uniform elements
- miniaturized elements with low power consumption
- realizable integration in all directions (see Section 1.2)
- possible integration of micromechanical elements

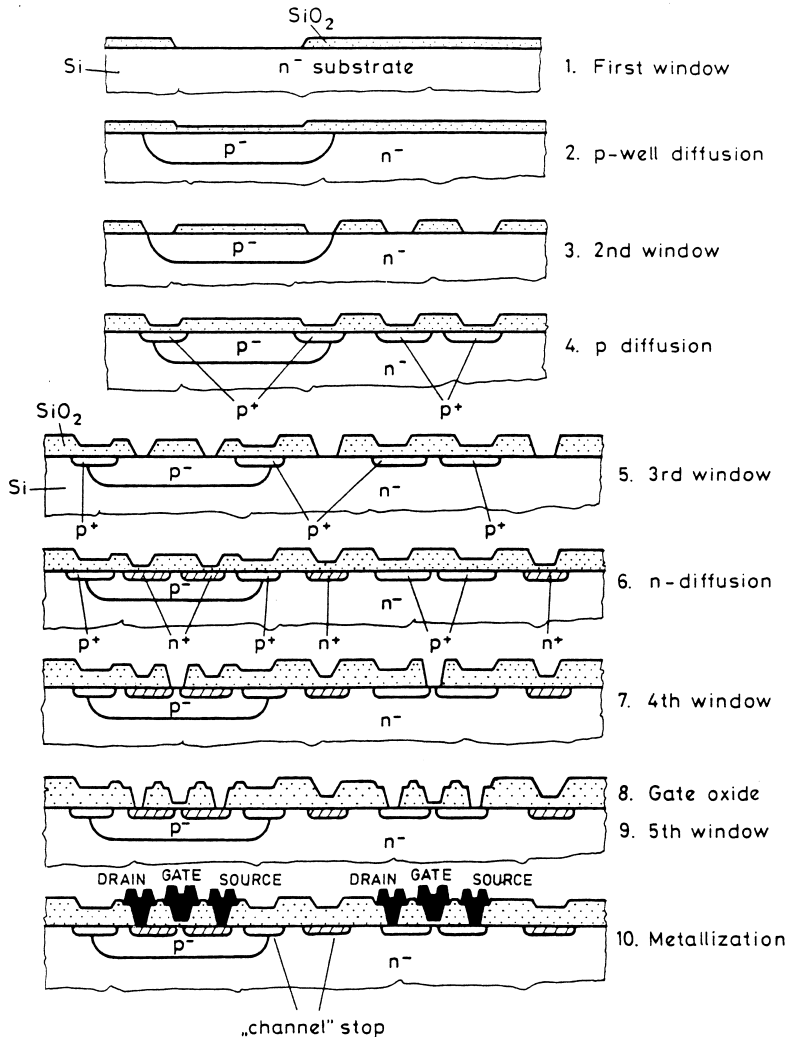

FIGURE 2.2. Processing steps of CMOS structures shown in cross sections. (Reproduced with permission from *Polymer Films in Sensor Applications* by G. Harsányi, ©1995, Technomic Publishing Co., Inc., Lancaster, PA, p. 12.)

(2) Disadvantages

- strong temperature dependence of many electrical parameters
- sophisticated high-cost processing, available only for high batch numbers
- a number of sensor materials cannot be applied on silicon surfaces

- the sophisticated packaging technologies often prevent exploitation of the advantages of low-cost device production

Further details can be found in classical handbooks of semiconductor technology (Sze, 1985; Elliot, 1986; Campbell, 1998).

2.2 CERAMICS

The microstructure of polycrystalline ceramics is usually complex, as shown in Figure 2.3. It can be distinguished by the existence of grain boundaries, which are not seen in single crystals. Furthermore, the existence of pores and imperfections and the multiphase composition enable the production of a great variety of properties (Moulson and Herbert, 1990).

For many years, grain boundaries and additional phases were thought to be undesirable, and the goal was to eliminate them to obtain a structure as close to the single-crystal structure as possible. However, new processes have been found that make positive use of these surfaces and grain boundaries; thus, functional ceramics in which these properties are important are developing rapidly.

In general, ceramics are produced from powdered raw material by a sintering process. Ceramics obtained in this way are polycrystalline, an aggregation of fine crystalline grains, and grain boundaries inevitably exist. They play an important role in the sintering process and have a large influence on chemical and physical properties.

Figure 2.4 shows the typical manufacturing schematic for ceramics. The process begins with the mixing of powdered raw materials and additives by weight. When the starting material is a powder, the synthesis, or refinement, of the powder is one of the most important processes affecting the quality of the final product.

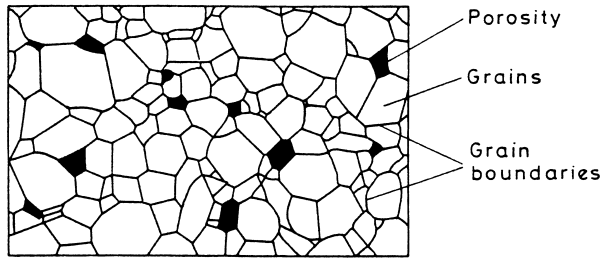

FIGURE 2.3. Typical microstructure of ceramics. (Reproduced with permission from *Polymer Films in Sensor Applications* by G. Harsányi, ©1995, Technomic Publishing Co., Inc., Lancaster, PA, p. 13.)

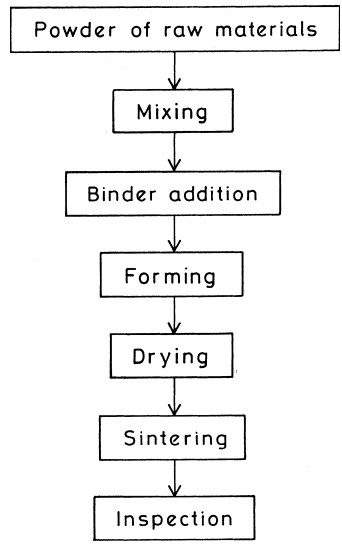

FIGURE 2.4. Flowchart of the processing of ceramics. (Reproduced with permission from *Polymer Films in Sensor Applications* by G. Harsányi, ©1995, Technomic Publishing Co., Inc., Lancaster, PA, p. 14.)

After the mixing, an organic resin—a temporary binder material—is added to the raw material powder. Then, the powder is compacted in a definite form. Prior to sintering, it is necessary to get rid of the organic resin used for forming by heating the compacted material at a low temperature. The formed product is sintered at a high temperature and becomes dense through contraction. Sintering is the consolidation of a powder by means of prolonged use of elevated temperature, which is, however, below the melting point of any major constituents of the ceramic.

Vitrification is densification in the presence of a viscous liquid, and it is the process that takes place in the majority of ceramics produced on a large scale (these are often called "glass-ceramics") (Baker et al., 1970). Upon cooling from the firing temperature, the liquid phase solidifies as a glass, thereby, further increasing the bonding between particles and so forming a solid material, albeit with some porosity. Very similar processes occur in thick-film technology (see Section 2.3).

It should be mentioned here that special technologies have been developed for processing high-quality *alumina and glass-ceramic multilayer substrates* commonly used in IC and sensor laminations (Buchanan, 1986). These technologies originate from IC packaging, where the goal is to make an inexpensive hermetic package with metallization for output-lead connections without

electronic leakage. Currently, this is a technology that is widely used in the processing of sophisticated interconnection systems for multichip modules and for sensors.

The manufacturing of an alumina multilayer system also begins with the mixing of powdered raw materials. A sheet of the powder mixed with organic resin, called a "green sheet," has to be prepared in advance by sheet casting, drying, and cutting processes. Through-holes are then punched into the sheets, and they are filled with a paste composed mostly of tungsten or molybdenum powder. A conductive pattern is subsequently screen-printed on the surface. Several of these sheets are then laminated and sintered over 1500°C in a hydrogen atmosphere to avoid oxidation of the metallization system. The outer surface of the tungsten is nickel-plated, and finally, a fine gold plating is added after the leads have been silver coated.

The technology of multilayer glass-ceramic systems is almost the same, but the sintering temperature is much lower; it is about 850°C which is also the typical firing temperature of thick films (see Section 2.3). Thus, precious metal thick-film conductive layers can be used for the metallization network. The former method is often called HTCC (high-temperature co-fired ceramic) and the latter one LTCC (low-temperature co-fired ceramic) technology. The term "MLC" (multilayer ceramic) is used for both cases.

Ceramics offer the following advantages for sensorics:

- Low-cost, discrete elements can be produced in high batch numbers.
- A great variety of materials can be processed.
- There is no need for very sophisticated processes.

On the other hand, their disadvantages are:

- They need high-temperature sintering processes.
- A direct integration of electronic components is generally not possible.
- Only high batch number production is desirable.
- Compatibility problems occur with other processing technologies.

Further details can be found in classical handbooks of ceramic technology (Buchanan, 1986; Moulson and Herbert, 1990; Licari, 1995; Ginsberg and Schnorr, 1994).

2.3 THIN- AND THICK-FILM TECHNOLOGIES

Originally, thin- and thick-film technologies were developed as metallization techniques of silicon wafers, glasses, and ceramics. Later, resistor and insulating layer materials also appeared. Thus, these technologies began as integrated circuit and microsensor processing methods. The most important

TABLE 2.1. Typical Properties of Thick and Thin Films.

	Thick Films	Thin Films
Raw Materials	Pastes: colloid compounds	High-purity metals, alloys, compounds
Typical Processing	Screen-printing and curing	Vacuum deposition processes, CVD, etc.
Layer Thickness	10–50 μm	10–200 nm
Layer Structure	Active particles in a binder matrix	Polycrystalline, discontinuous, physical thin films

(Reproduced with permission from *Polymer Films in Sensor Applications* by G. Harsányi, ©1995, Technomic Publishing Co., Inc., Lancaster, PA, p. 22.)

differences between the two technologies are in the layer thickness, in the applied materials, and in the processing steps. A short comparison is demonstrated by Table 2.1.

Fabrication technologies of preparing *thin films* may be divided into two main groups, namely, *chemical methods* (including CVD, electrochemical deposition and oxidation, thermal oxidation, and currentless chemical deposition) and *physical deposition methods* (i.e., vacuum evaporation and cathode sputtering). In practice, they are applicable to many substrate types, such as single crystals (e.g., silicon, sapphire, quartz, etc.), borosilicate glasses, ceramics, glass-coated ceramics, polymers (e.g., polyimid, PTFE, epoxy, etc.), and to a great range of thicknesses.

A few chemical methods have already been discussed in Section 2.1, but various other methods are beyond the scope of this book. For a more complete discussion, refer to the literature (Maissel and Glang, 1970).

The process of film formation by *vacuum evaporation* consists of several physical stages (Illyefalvi-Vitéz, 1992): transformation of the material to be deposited by evaporation or sublimation into the gaseous state, transfer of particles to the substrate, deposition onto the substrate, and rearrangement of particles on the surface.

In the *vacuum evaporation technique,* the material to be deposited is heated, usually by putting small lumps of it in an electrically heated "boat" made of tungsten or molybdenum, in an ultra-high vacuum (i.e., 10^{-4} Pa). The schematic diagram of a vacuum deposition unit is shown in Figure 2.5. In the case of metals, the deposition starts when the material has formed a liquid pool in the boat and the shutter is opened. The difference between the various evaporation methods is in the heating method and in the type of evaporation sources.

Electron-beam evaporation is now the most commonly used and most developed evaporation technique. An electron beam of sufficient intensity is

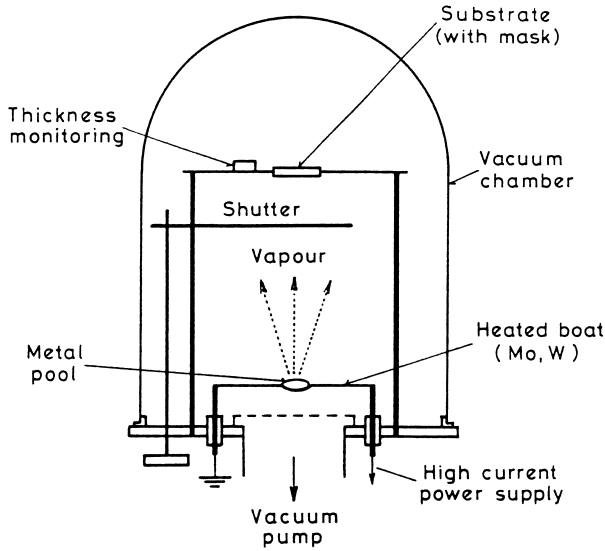

FIGURE 2.5. Schematic diagram of a vacuum evaporation unit. (Reproduced with permission from *Polymer Films in Sensor Applications* by G. Harsányi, ©1995, Technomic Publishing Co., Inc., Lancaster, PA, p. 25.)

ejected from a cathode, accelerated, and focused onto an evaporant material. Impinging electrons heat its surface to the temperature required for evaporation. The method enables the attainment of a very high temperature and the evaporation of materials that would otherwise be difficult to evaporate or not be evaporated at all. An additional advantage of the method is the prevention of contamination by the evaporation source holder material. The beam heats only the evaporant, whereas the support holder is usually cooled.

The simplest arrangement for *cathode sputtering* is shown in Figure 2.6. The material to be sputtered is used as a cathode target in a system in which a glow discharge is established in an inert gas (e.g., argon or xenon) at a pressure of 1 to 10 Pa and a voltage of several kilovolts. The substrate on which the film is to be deposited is placed on the anode of the system. The positive ions of the gas created by the discharge are accelerated toward the cathode (target). Under the bombardment of ions, the material is removed from the cathode (mostly in the form of neutral atoms and, in part, also in the form of ions). The liberated components condense on surrounding areas and, consequently, on the substrate placed on the anode.

In *RF (radio frequency) sputtering,* AC discharges of 5–30 MHz are employed. In the case of the DC process described in the previous paragraph, problems are encountered in initiating the process and with sputtering insu-

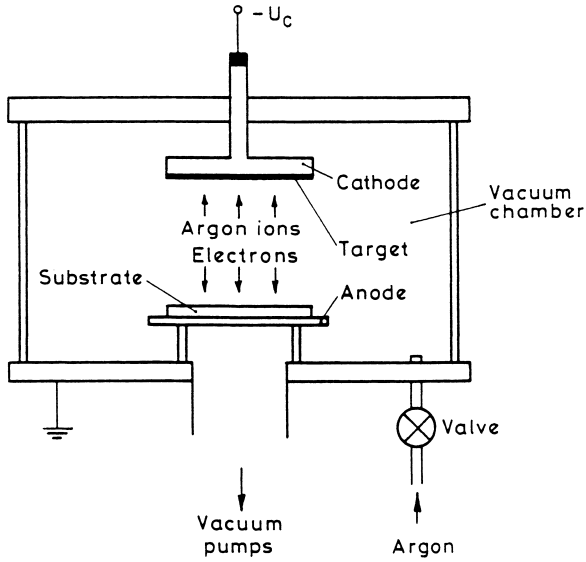

FIGURE 2.6. Apparatus for diode cathode sputtering. (Reproduced with permission from *Polymer Films in Sensor Applications* by G. Harsányi, ©1995, Technomic Publishing Co., Inc., Lancaster, PA, p. 26.)

lating materials. In the RF process, one electrode is coupled capacitively to a RF generator. It then develops a negative DC bias with respect to the other electrode. This is related to the easier response of electrons than ions to an applied RF field.

A special form of deposition by sputtering is called *reactive sputtering.* It is performed in the atmosphere of a pure reactive gas, which is eventually to be a component of the film, or a mixture of inert and reactive gases.

Magnetron sputtering uses magnetic fields to deflect electrons from striking the substrate in order to increase the ionization efficiency. Various magnetically confined discharge configurations have evolved.

For applications in microelectronics and sensorics, it is necessary to form the films in specific, sometimes complicated patterns. For this purpose, a suitable mask is used to prevent condensation on the areas to be kept clean. The mask is usually formed from a metal and is placed in the vapor stream as close as possible to the substrate on which the film is to be deposited. This is the so-called noncontact or masking through-mask-deposition method. There are several technologies for preparation of "in contact" masks, which are deposited directly onto the substrate. The most widely used technology is photolithography combined with selective etching of different layers, similar to the silicon photolithography process. Another often-used tech-

nique is the so-called "lift-off" technique. In this method, the deposition of the film is carried out on a substrate that was previously covered with a photolithographically patterned mask. After the deposition, the mask with the deposited film will be removed by etching or stripping the unnecessary areas.

The most commonly used technology for making *thick films* is *screen printing* and *firing/curing* at an elevated temperature (Harper, 1974; Agnew, 1973). The classical "CERMET" version of the technology uses inorganic-based glasses, glass-ceramics, and ceramic-glass-metal composite raw materials for films, as well as relatively high-temperature firing processes. The emerging polymer thick-film (PTF) technology is based on polymers and conductive polymer-composite materials with low curing temperatures (Martin, 1982; Kirby, 1989).

Raw materials for thick films are available in "paste" form. Thick-film pastes consist of three main ingredients: a finely powdered functional phase (metal and/or metal-oxide powders) of carefully controlled size and composition; finely powdered oxide and glass phases, also of controlled size, shape, and composition (as inorganic binder materials); and an organic vehicle that suspends the inorganic constituents until the paste is fired and must also give the proper rheological characteristics for the screen printing.

The film application method of thick films is basically a screen printing technique. The circuit is fabricated by successively printing each layer until the desired circuitry is achieved. The basic tools used in printing are the squeegee and the screen. The system that incorporates these basic tools and provides adequate means for controlling them precisely in the fabrication is the screen printer. Figure 2.7 shows the steps of the screen-printing process.

The holes of the stainless steel, polyester, or nylon screen are filled with a photolithographically shaped emulsion, which has openings according to the layout pattern. The substrate is placed under the screen, and the squeegee presses the paste through the screen mask openings.

After the film has been printed on a substrate, it should be allowed to "settle," since printing through the screen tends to produce mesh lines in the pattern. The settling time depends on the viscosity of the paste; however, times vary from about 5 minutes to approximately 20 minutes. After settling, the films should be dried before firing. This removes only the volatile and leaves behind the binders. Desirable drying temperatures depend on the solvents and vary from 100 to 150°C for 5 to 15 minutes. The resulting films should be tough enough to permit handling and subsequent printings. Firing is the most critical step of thick-film technology. The temperature profile and atmosphere parameters are the most important. Thick-film pastes require peak temperatures in the range of 700–1000°C (typical value is 850°C) for 10 minutes.

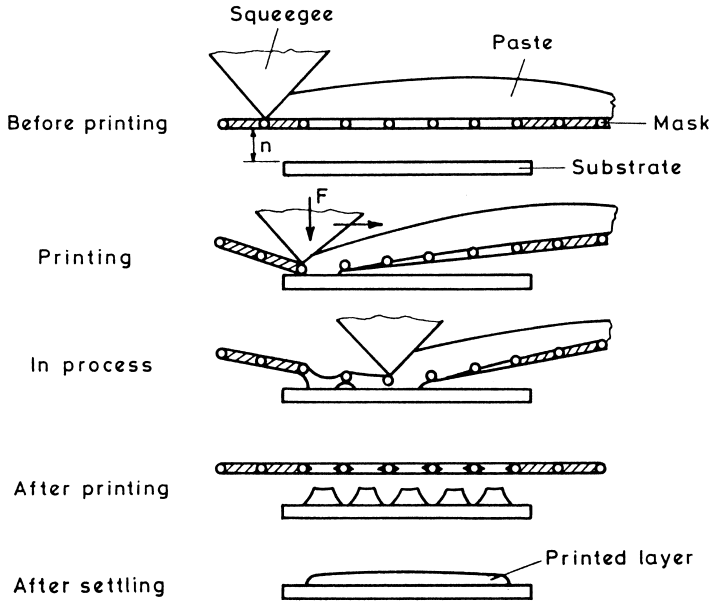

FIGURE 2.7. Process phases of screen printing. (Reproduced with permission from *Polymer Films in Sensor Applications* by G. Harsányi, ©1995, Technomic Publishing Co., Inc., Lancaster, PA, p. 31.)

Temperature should be controlled to better than ± 3 °C at the peak. For firing, belt furnaces are used.

The following advantages and disadvantages may be encountered when applying thin and thick films in microsensor fabrication:

- Cost-effective sensor production is possible with low batch numbers.
- Hybridization of various technologies is possible.
- Integration of passive networks is possible.
- Various substrate types are applicable.
- Various materials can be applied.
- Stable passive elements (resistors) can be realized with low temperature dependency.
- Multilayer structures can be easily realized.
- A high-level of integration, such as at the monolithic ICs, is not available.

Further details can be found in classical handbooks of thin- and thick-film technologies (Agnew, 1973; Harper, 1974; Maissel and Glang, 1970; Haskard and Pitt, 1997; Sergent and Harper, 1995; Elshabini and Barlow, 1998).

2.4 PROCESSING OF POLYMER FILMS

In this section, a general survey will be given about those polymer processes that are compatible or easily applicable with the different inorganic sensor technologies described in the previous sections.

There are two main possibilities when applying polymer films in sensors:

- *Preprocessed polymer films* are synthesized and shaped by extrusion and stretched into sheet forms and covered by metal film separately from the sensor structures. Then, they can be attached to inorganic sensor surfaces, typically by using the gluing method (Münch and Thiemann, 1991).
- *Polymerization directly on sensor surfaces* is the commonly used technique for fabricating thin polymer layers. The synthesis and shaping processes occur on the sensor surface; thus, methods that are compatible with inorganic sensor parts are needed.

Photosensitive polymers for *photolithography* are widely used in integrated circuit technologies as photoresists. Photolithography can be adopted for shaping sensor polymer films (Endo et al., 1987). Photosensitive polymers have a unique advantage in processing, with UV illumination, polymerization and shaping can occur at the same time. A significant advantage of photosensitive polymers is the relative ease of processing using an existing integrated circuit or microsensor fabrication line. Photosensitive polymers can be applied and patterned with the same technology as used for photoresists. Nonphotosensitive polymers can also be patterned by photolithography, but the process is more complex; it is similar to the patterning of thin films using the combination of photolithography and etching. The greatest problem in this case is the prevention of the interaction between the soft-baked polymer layer and the photoresist. The reaction can take place if the soft-bake temperature is not high enough or if the photoresist is applied to a hot polymer film. It is important to select a suitable temperature to make the polymer hard enough to prevent the reaction with photoresist, but not too hard for etching (Hijikigawa et al., 1983).

Screen printing and curing are widely used technologies in processing polymer composite materials that are available in paste form; the process is called polymer thick-film (PTF) technology (see Section 2.3). Thermoset- and thermoplastic-type binder materials are applied; the curing temperature is kept within the range of 150–400°C, depending on the type of the applied binder. Special printing processes have also been developed, such as employing etched metal masks instead of screen masks and special squeegees with a rectangular pipe structure cross section filled with the solution of a monomer or with a paste (Takasago et al., 1987).

Conducting and semiconducting polymers can be synthesized and deposited onto a conductive surface of a given substrate from monomer solutions by *electrochemical polymerization.* The advantage of this method is that precise flow control and rate of film deposition can be maintained by varying the potential/current conditions of the working electrode in the system. Use of this method yields a high-quality thin film and has great prospects in biosensors, where enzymes may be entrapped into conducting polymer films (Yon Hin and Lowe, 1992; Bidan, 1992).

Electropolymerization, like the well-known radical polymerization, is a chain process. While the growing end groups in radical polymerization are electrically neutral, they are charged in electropolymerization. During synthesis, charge transfer also takes place. Polymerizing systems are electrically neutral; hence, some negatively charged ions are present in cationically polymerized systems, while positively charged ions are present in anionically growing species. The participation of these counter-ions makes this polymerization intrinsically more complex than radical polymerization. Since the oppositely charged ions attract each other and strongly interact with the molecules surrounding them, many species coexist in the polymerized medium. This is the basis of the conductivity modifying mechanism of electropolymerized layers.

Various aromatic compounds can be polymerized by electrochemical oxidation in a solution containing a supporting electrolyte. The reaction involves the subtraction of hydrogen from the monomer, forming fully conjugated polymers. The simultaneous electrochemical doping of electrolyte anions may render these polymers highly electrically conductive.

For example, the electropolymerization mechanism for conducting polypyrrole (PPy) is shown in Figure 2.8 (Bidan, 1992). The electropolymerization process [see Figure 2.8(a)] is a simultaneous growth and doping that enables negatively charged A^- species (acting as dopants) to be irreversibly captured.

The reaction is, in fact, a condensing oxidation, which follows an electronic stoichiometry, allowing a coulombmetric control of the film thickness to be deposited. For reasons of electroneutrality, the dopant counterions are inserted into the polymer matrix, which can be considered a polymeric organic salt. In the reaction scheme, k represents the doping level, which can also be changed by subsequent electrochemical processes [see Figure 2.8(b)]. In fact, this doping-dedoping reaction is a completely reversible redox process that results in conductivity changes over several orders of magnitude. In practice, electrosynthesis is carried out by simultaneous deposition and doping-dedoping using cyclic anodic-cathodic reactions.

Vacuum deposition processes are also possible methods of obtaining thin polymer films that have high density, thermal stability, and insolubility in organic solvents, acids, and alkalis. The layers can be deposited on any sub-

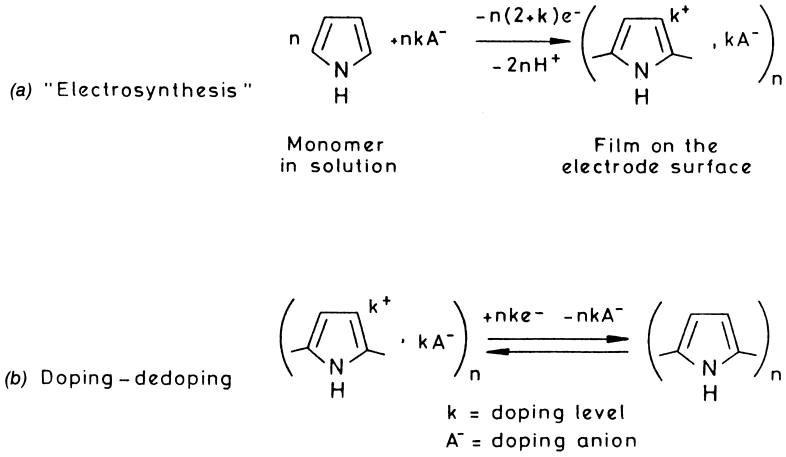

FIGURE 2.8. Schematic electrochemical polymerization mechanism for polypyrrole: (a) synthesis and (b) doping-dedoping. (Reproduced with permission from *Polymer Films in Sensor Applications* by G. Harsányi, ©1995, Technomic Publishing Co., Inc., Lancaster, PA, p. 43.)

strates that cannot be attacked by vacuum processes. Polymer films can be grown by the following methods:

- vacuum pyrolysis, which consists of a sublimation, a pyrolysis, and a deposition-polymerization process (Taylor and Welber, 1975)
- vacuum polymerization stimulated by electron bombardment (Hill, 1965)
- vacuum polymerization initiated by ultraviolet irradiation
- vacuum evaporation using a resistance-heated solid polymer source and, more effectively, using an electron beam (Luff and White, 1970)
- RF sputtering of a polymer target in a plasma composed of polymer fragments and with argon added to the plasma (Morrison and Robertson, 1973)
- plasma or glow discharge polymerization of monomer gases or vapors (Holland et al., 1976)

Figure 2.9 shows a schematic comparison of the different vacuum deposition processes.

There are a lot of conventional coating methods, such as *spin-coating, dipping, casting, bath immersion,* and various curing technologies using ovens, hot plates, vacuum ovens, conveyor belt furnaces, and infrared (IR) irradiation, that are widely used in polymer film applications. *Microwave assisted curing,* a newly developed process, provides ease of use and precise control of the temperature profile and distribution.

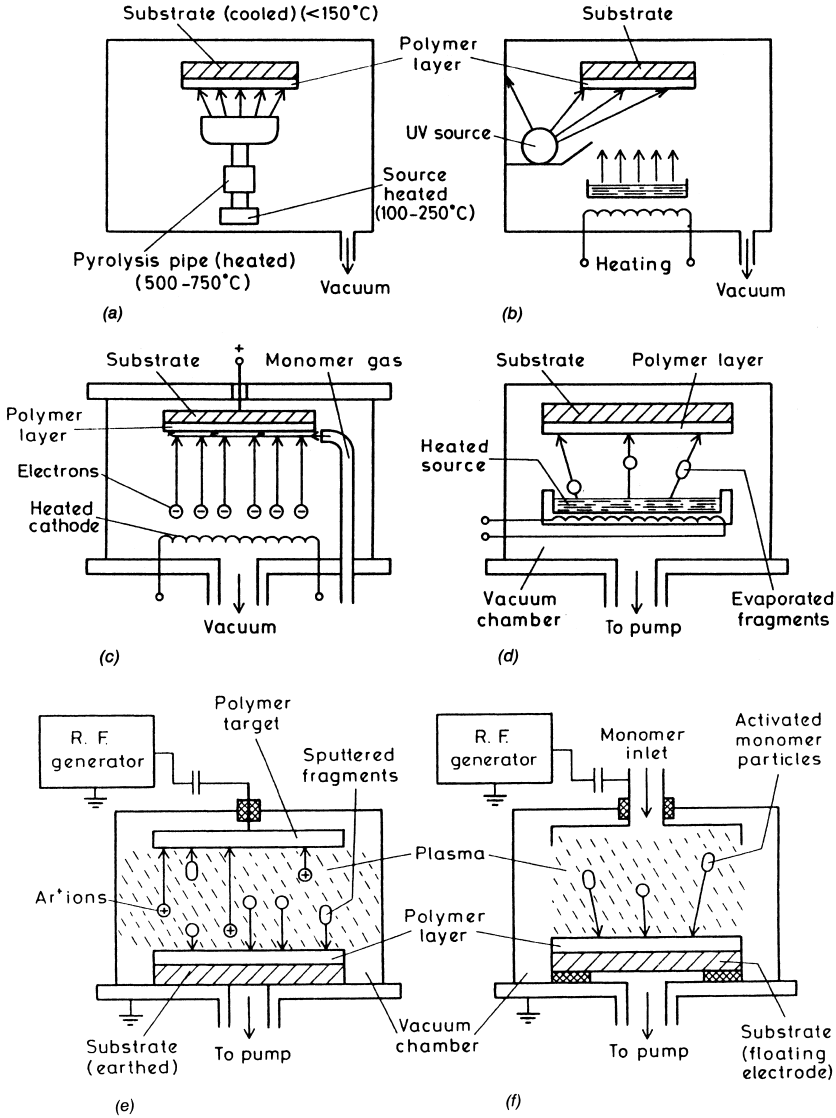

FIGURE 2.9. Schematic illustration of the vacuum deposition processes used for polymer films: (a) vacuum pyrolysis, (b) vacuum UV-polymerization, (c) electron-beam polymerization, (d) vacuum evaporation, (e) RF sputtering, and (f) glow discharge (plasma) polymerization. (Reproduced with permission from *Polymer Films in Sensor Applications* by G. Harsányi, ©1995, Technomic Publishing Co., Inc., Lancaster, PA, p. 45–46.)

Cross-linking of highly oriented monomer films made by the *Langmuir-Blodgett method* can be achieved by UV irradiation or by chemically initialized reactions. The whole process is illustrated in Figure 2.10 (Imai et al., 1989). A small amount of a high-molecular-weight substance, which has polar molecules possessing hydrophobic tails and hydrophilic heads (e.g., fatty acids or higher alcohols), is dissolved in a volatile solvent, and one drop of the solution is sprinkled on the surface of the water. The solvent evaporates, and the molecules of the substance diffuse over the surface of the water, all orientated in the same manner due to their polarity. According to their concentration, either a "two-dimensional gas" or a monomolecular film of liquid or solid is formed. Such a film can be lifted and placed on a plate or directly deposited onto the surface of a plate-shaped substrate by dipping. Several such films can be applied on top of each other, and in this way, even films of several hundreds of nanometer thickness can be built up gradually, and finally cross-linked to form a polymer film.

Applying polymer films in sensors may offer the following advantages and disadvantages:

- Relatively low-cost materials are applicable.
- Their fabrication techniques are quite simple (there is no need for a special clean room and/or high-temperature processes).
- The films can be deposited on a great variety of substrates.
- The wide choice of molecular structure and the possibility of building side chains, charged or neutral particles, and even grains of specific behavior into the bulk material or on its surface region enables the production of films with various physical and chemical properties, including sensing behavior.
- Biocompatibility can be easily realized.
- Devices based on polymer films show much bigger instabilities compared to sensors that are built entirely from inorganic materials.

Further details about sensor polymer film technologies can be found in the literature (Harsányi, 1995).

2.5 OPTICAL-FIBER TECHNOLOGIES

Recently, a great competition between electric and fiber-optic sensing devices has begun. The importance of fiber-optic sensing devices is increasing since optical telecommunication channels are becoming widespread.

In optical communication links, it is the optical fiber that provides the transmission channel. The fiber consists of a solid cylinder of transparent material, the *core,* surrounded by a *cladding* of similar material (see Figure 2.11). Light

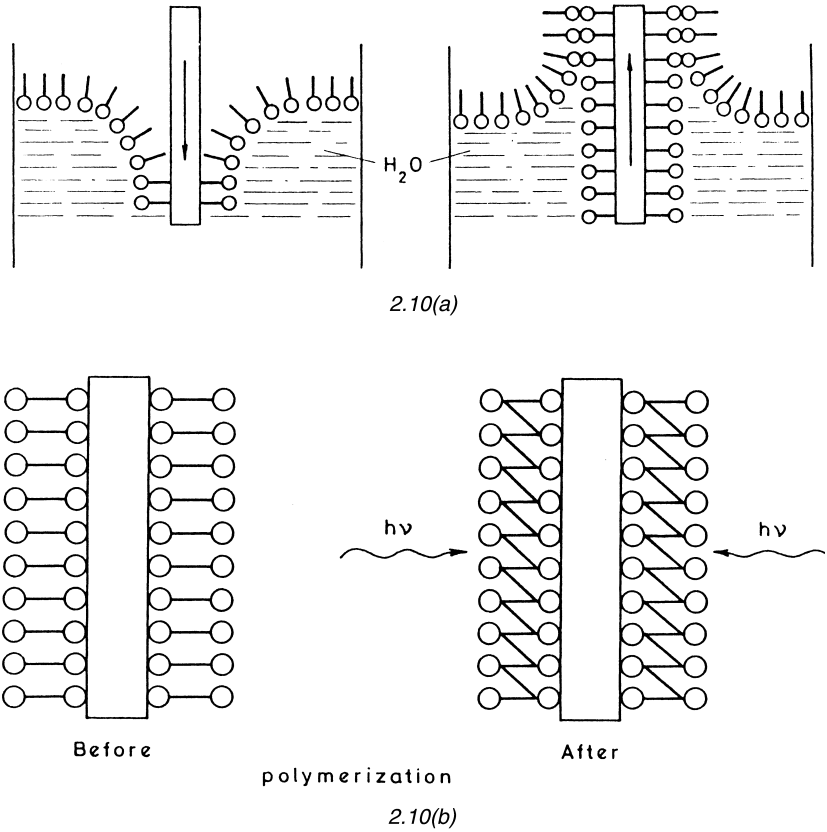

FIGURE 2.10. Langmuir-Blodgett deposition (a) and polymerization (b) of organic thin films. (Reproduced with permission from *Polymer Films in Sensor Applications* by G. Harsányi, ©1995, Technomic Publishing Co., Inc., Lancaster, PA, p. 24, 49.)

waves propagate through the core in a series of plane wave fronts, or *modes*—the simple light ray path used in elementary optics is an example of a mode. For this propagation to occur, the refractive index of the core must be larger than that of the cladding. There are two basic structures that have this property: step-index fibers with two different refractive index values for core and cladding and graded-index fibers providing a continuous transition of refractive index from core to cladding. There are multimode fibers that allow a great number of modes to propagate and single-mode fibers that allow only one mode to propagate. The propagation in the fibers can be described with the effective refractive index, which depends on core and cladding refractive indices, as well as on the type and thickness of the fiber.

Optical fibers can basically be made from two different materials: silica

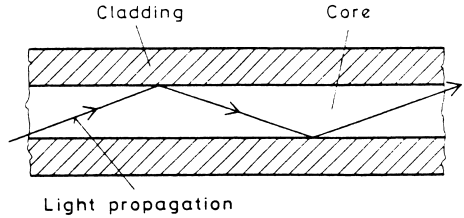

FIGURE 2.11. Light propagation in optical fibers. (Reproduced with permission from *Polymer Films in Sensor Applications* by G. Harsányi, ©1995, Technomic Publishing Co., Inc., Lancaster, PA, p. 83.)

glass (SiO_2) and plastic polymer, generally polymethyl-methacrylate (PMMA). The addition of certain dopants to the glass will vary the refractive index. All-plastic fibers use different plastics for the core and the cladding. All-glass fibers with 10–50 μm diameter exhibit very low losses and high bandwidths, which make them ideal for use in long-haul telecommunication routes. Large-core (1 mm diameter) fibers for use in medical and industrial applications are generally made of plastic, making them more robust than all-glass fibers, and are cheaper to produce. However, the very high attenuation and low bandwidth of these fibers tend to limit their uses, for instance, to the field of sensors. In integrated optics, silicon, compound semiconductors, and $LiNbO_3$ are used for optical wave guide purposes.

A specially developed technique is applied for forming glass optical fibers. The *fiber* can be *drawn* directly from the core and cladding glasses, which results in a continuous process, making the fiber cheap to produce. Such a process is the double crucible method of fiber manufacturing (also known as the direct melt technique). A double crucible pulling tower consists of two concentric funnels. The outer funnel contains the cladding material, while the inner funnel contains the core glass. The crucibles are usually made of platinum to reduce contamination. The crucibles are heated to melt the glasses, and the fiber can then be drawn from the tip and attached to a take-up drum at the base of the tower. As the drum rotates, it pulls the fiber. The rate of drum rotation determines the thickness of the fiber. A noncontact thickness gauge regulates the drum speed by means of a feedback loop. Below the gauge, the fiber passes through a funnel containing a plastic coating to protect the fiber from impurities and structural damage. A curing lamp ensures that the coating is a solid before the fiber reaches the take-up drum.

Optical fibers offer the same advantages to transducer systems that they have in telecommunication systems:

- low signal attenuation and high information transfer capacity
- compatibility with optical telecommunication systems

- elimination of electromagnetic interference problems
- flexibility, both physically and technologically

Further advantages, especially for sensors, include the following:

- explosion safety
- biocompatibility and corrosion resistance of most materials applied

Their disadvantage is, however, their incompatibility with most other microelectronics and microsensor technologies, as well as signal processing methods.

Further details about optical systems can be found in the literature (Kongston, 1995).

2.6 REFERENCES

Agnew, J., *Thick Film Technology,* Hayden Book Co., Inc., Rochelle Park, NJ (1973).

Baker, D., Koehler, D. C., Fleckenstein, W. O, Roden, C. E. and Sabia, R., *Physical Design of Electronic Systems,* Vol. II, Prentice Hall, Englewood Cliffs, NJ (1970).

Bidan, G., "Electroconducting Conjugated Polymers: New Sensitive Matrices to Build Up Chemical or Electrochemical Sensors. A Review," *Sensors and Actuators B,* 6 (1992), pp. 45–56.

Buchanan, R. C., *Ceramic Materials for Electronics,* Marcel Dekker, New York (1986).

Campbell, S. A., *Semiconductor Micromachining, Vol. 1–2, Techniques and Industrial Applications,* John Wiley & Sons, New York (1998).

Elliott, D. J., *Microlithography, Process Technology for IC Fabrication,* McGraw-Hill, New York (1986).

Elshabini, A. R. and Barlow, F. D., *Thin Film Technology Handbook,* McGraw-Hill, New York and International Microelectronics and Packaging Society (IMAPS), Reston, VA (1998).

Endo, A., Takada, M., Adachi, K., Takasago, H., Yada, T. and Onishi, Y., "Material and Processing Technologies of Polyimide for Advanced Electronic Devices," *J. Electrochem. Soc.,* Vol. 134, No. 10 (1987), pp. 2522–2527.

Ginsberg, G. L. and Schnorr, D. P., *Multichip Modules & Related Technologies, MCM, TAB, and COB Design,* McGraw-Hill, New York (1994).

Harper, C. A., *Handbook of Thick Film Hybrid Microelectronics,* McGraw-Hill, New York (1974).

Harsányi, G., *Polymer Films in Sensor Applications,* Technomic Publishing Co., Inc., Lancaster, PA (1995).

Haskard, M. R. and Pitt, K., *Thick-Film Technology and Applications,* Electrochemical Publications, British Isles (1997).

Hijikigawa, M., Miyoshi, S., Sugihara, T. and Jinda, A., "A Thin-Film Resistance Humidity Sensor," *Sensors and Actuators,* Vol. 4 (1983), pp. 307–315.

Hill, G. W., "Electron Beam Polymerization of Insulating Films," *Microelectronics,* Vol. 4, No. 3 (1965), pp. 109–116.

Holland, L., Biederman, H. and Ojha, S. M., "Sputtered and Plasma Polymerized Fluorocarbon Films," *Thin Solid Films,* 35 (1976), pp. L19–L21.

Illyefalvi-Vitéz, Zs., *Electronics Technology,* Textbook for Undergraduate Students, TU Budapest, Hungary (1992).

Imai, Y., Nishikata, Y. and Kakimoto, M., "Preparation and Microelectronic Applications of Langmuir-Blodgett Films of Polyimides and Related Polymers," *Proc. of the 32nd Midwest Symp. on Circ. and Syst.,* Champaign, IL (1989), pp. 735–748.

Kirby, P. L., "Origins and Advances in Polymer Thick Film Technology," *Proc. of the 7th European Hybrid Microel. Conf.,* Hamburg, Germany (1989), p. 4.1.

Kongston, R. H., *Optical Sources, Detectors, and Systems,* Academic Press, San Diego, CA (1995).

Licari, J. J., *Multichip Module Design, Fabrication & Testing,* McGraw-Hill, New York (1995).

Luff, P. P. and White, M., "The Structure and Properties of Evaporated Polyethylene Thin Films," *Thin Solid Films,* 6 (1970), pp. 175–195.

Maissel, L. I. and Glang, R., *Handbook of Thin Film Technology,* McGraw-Hill, New York (1970).

Martin, F. W., "The Use of Polymer Thick Film for Making Printed Circuit Boards," *Hybrid Circuits,* (1982), p. 22.

Morrison, D. T. and Robertson, T., "RF Sputtering of Plastics," *Thin Solid Films,* 15 (1973), pp. 87–101.

Moulson, A. I. and Herbert, I. M., *Electroceramics. Materials, Properties, Applications,* Chapman and Hall, London (1990).

Münch, W. V. and Thiemann, U., "Pyroelectric Detector Array with PVDF on Silicon Integrated Circuit," *Sensors and Actuators A,* 25–27 (1991), pp. 167–172.

Sergent, J. and Harper, C., *The Handbook of Hybrid Microelectronics,* McGraw-Hill, New York (1995).

Sze, S. M., *VLSI Technology,* McGraw-Hill, New York (1985).

Takasago, H., Takada, M., Adachi, K., Endo, A., Yamada, K., Makita, T., Gofuku, E. and Onishi, Y., "Advanced Copper/Polyimide Hybrid Technology," *IEEE Transactions on Components, Hybrids and Manufacturing Technology,* Vol. 10, No. 3 (1987), pp. 425–432.

Taylor, R. C. and Welber, B., "Laser-Monitored Deposition of Parylene Thin Films," *Thin Solid Films,* 26 (1975), pp. 221–226.

Yon Hin, B. F. Y. and Lowe, C. R., "Amperometric Response of Polypyrrole Entrapped Bienzyme Films," *Sensors and Actuators B,* 7 (1992), pp. 339–342.

CHAPTER 3

Basic Sensor Structures

There are two basic elements of sensor operation. The first is the physical or chemical interaction between the environment and the sensing material that alters the material properties ("sensing effect"), while the second is the "transduction mechanism" inside the sensor structure that converts this material property change into a useful signal, which then holds information about the environment-material interaction. In this chapter, various sensor device structures and their transduction mechanisms are described independent of the possible real sensing effect, which is the subject of Chapter 4. The most important sensor device structures can be categorized into the following groups:

- *Impedance-type sensors* follow the sensing phenomena with capacitance, resistance, and/or inductance changes.
- *Sensing semiconductor devices* are more complicated; the sensing effect can change the most important characteristic and/or parameter of the devices, for example, shift the diode characteristics, alter the threshold voltage of the MOSFET, etc.
- In *sensor structures operated with acoustic waves,* the shift of the resonance frequency or wave phase can be measured as a function of the quantity in question.
- *Electrochemical cells* are widely used in chemical sensors; the electrode potential, the cell current, and/or the cell resistance can be measured as a function of the analyte composition.
- *Calorimetric sensors* are based on the measurement of excess heat or heat loss caused by physical or chemical processes that took place due to environmental effects.
- *Fiber optic sensors* represent a new generation of sensors; they are based on the changes of light propagation, absorption, and/or emission properties within the devices and provide an optical output signal.

3.1 IMPEDANCE-TYPE STRUCTURES

The structure and operation principles of impedance-type sensors are the most simple. Figures 3.1(a) and (b) show some possible device structures: the sheet capacitor and the film resistor, respectively. The basic equations expressing the capacitance and resistance values are also given in the figures. These expressions are also used in the design of discrete and integrated passive components. Measurand changes alter the permittivity and/or resistivity of the sensitive layer, which, in turn, produces the variation of capacitance and/or resistance values of the sensor. There are also generator-type effects that can be applied to produce voltage output at sheet capacitors; the basis is the polarization or surface charge density variations within the dielectrics (e.g., as a result of the piezoelectric or pyroelectric effect, see in Sections 4.6 and 4.7).

Figure 3.1(c) shows the interdigital device structure that is rarely used in integrated devices because only small capacitance and resistance values can be realized. It is, however, a very popular structure in sensorics because of its large free surface that can interact with the environment. The mathematical expressions for this design are much more complicated (Mansour and Brown, 1963). The capacitance value is determined not only by the geometry and the permittivity of the dielectric layer, but also by the permittivity of the substrate and the gas or liquid environment. This interdigital structure can also be used as a resistor. At AC investigations of the interdigital structure, both capacitive and resistive behaviors must be taken into account (Tsuchitani et al., 1988). Figure 3.2 shows the equivalent circuit model, including interface impedance. In the figure, R_b is the bulk resistance of the film; R_e and C_e are the dielectrics/electrode interface resistance and capacitance values, respectively; and C_g is the geometric capacitance, which consists of the bulk dielectrics capacitance and the stray capacitance. The parameters can be measured experimentally by the complex impedance spectra method using Cole-Cole plots. Figure 3.2 also shows a typical complex impedance diagram for interdigital structures using layers with relatively low permittivity and large resistivity. If C_g-R_b and C_e-R_e pairs are dominating different frequency ranges, R_b and C_g can be determined simply from the complex impedance spectra, as shown in the figure.

Further details are available in the literature (Göpel et al., 1994; Grandke and Ko, 1996).

3.2 SEMICONDUCTOR DEVICES AS SENSORS

Silicon or compound semiconductors are used for fabricating semiconductor devices for transducer device parts. Their sensitive layers may be insulating, semiconductor, or conductive materials.

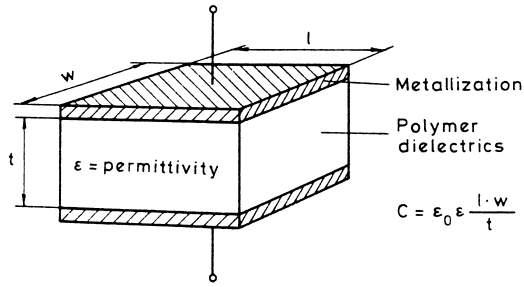

3.1(a)

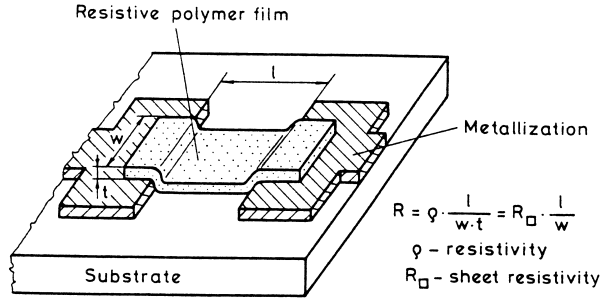

3.1(b)

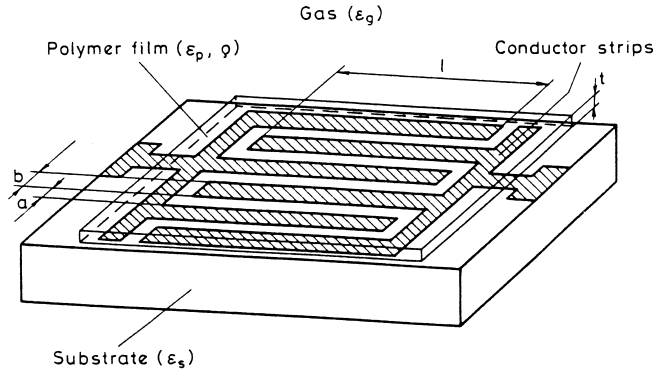

3.1(c)

FIGURE 3.1. Structure impedance-type sensors: (a) sheet capacitor, (b) film resistors, and (c) interdigital structure. (Reproduced with permission from *Polymer Films in Sensor Applications* by G. Harsányi, ©1995, Technomic Publishing Co., Inc., Lancaster, PA, p. 55.)

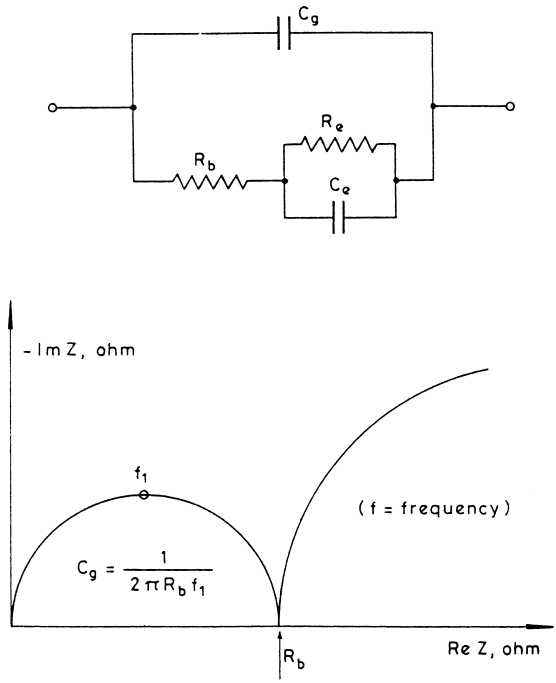

FIGURE 3.2. Complex impedance spectra and equivalent circuit to interpret them: C_g, geometrical capacity; R_b, bulk resistance; R_e, polymer/electrode interface resistance; and C_e, polymer/electrode interface capacity. (Reproduced with permission from *Polymer Films in Sensor Applications* by G. Harsányi, ©1995, Technomic Publishing Co., Inc., Lancaster, PA, pp. 56, 57.)

In sensor devices based on the *field-effect principle,* the semiconductor surface potential is modulated by potential or electric charge variations elsewhere in the structure, usually called a gate, which is actually an insulator/(metal)/(sensitive layer)/environment interface. Figure 3.3 shows the cross section of the conventional *p*-channel metal-oxide-semiconductor field effect transistor, the PMOSFET device, as well as the typical structure used in FET-based sensors. In both structures, the two *p*-type regions are known as the source and drain and can be interchanged principally without affecting the electrical behavior of the device.

The thin insulating layer (SiO_2 and/or Si_3N_4) and the covering (metallization and/or sensing) layer comprise the gate, and it is this electrode that mainly controls the action of the transistor. In the conventional MOS transistor, a bias voltage is applied to the gate, which is called the controlling gate voltage. If an increasing negative bias is applied to the gate, a positive charge is first in-

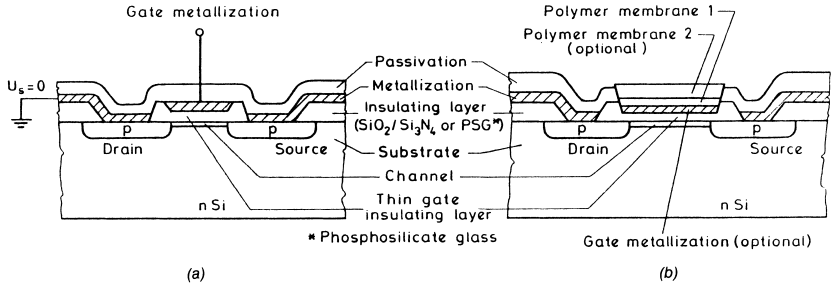

FIGURE 3.3. Field effect device structures used in (a) transistors (MOSFETs) and (b) in sensors. (Reproduced with permission from *Polymer Films in Sensor Applications* by G. Harsányi, ©1995, Technomic Publishing Co., Inc., Lancaster, PA, p. 58.)

duced at the silicon surface, and electrons are repelled away from this region. A depletion region results that will deepen as the bias increases. A point called the turn-on (or threshold) voltage, U_t is reached when inversion occurs, and movable free holes are induced at the surface; thus, the transistor channel starts to conduct between the source and drain (Wolfendale, 1973).

In the sensor FET devices, the gate metallization and/or coating environment interaction produce the controlling potential (through charge and work function condition changes) that is a function of the quantity to be measured and can be detected only as a threshold voltage variation. Practically, these devices are operated at the threshold point by an external regulation, and the gate voltage variations, which are sufficient for the compensation, can be followed.

There are a number of special sensitive FET structures, but their names are not always used in their entirety. Following is a brief survey of the typical abbreviations:

- POSFET: polymer-oxide-semiconductor FET (Mo et al., 1990)
- ISFET: ion-selective FET (Bergveld, 1972)
- REFET: reference FET that compensates interference effects for other sensor FETs (Müller et al., 1991)
- CHEMFET: chemically sensitive FET (Reinhoudt, 1992)
- MEMFET: membrane modified FET (Reinhoudt, 1992)
- ENFET: enzyme modified FET (Schul'ga et al., 1995)
- ImmunoFET: immune-reaction based FET (Schasfoort et al., 1990)
- SOSFET: silicon-on-sapphire-technology-based FET (Saito et al., 1991)

The basic idea (to follow environmental effects by the characteristic shifts of a device) can also be realized by using other types of semiconductor devices, e.g., diodes. A *pn*-junction can be applied to a temperature- or photo-

sensitive device because of its characteristic shifts. A similar effect can be used in chemical sensors; metal semiconductor diodes, the so-called Schottky-barrier devices, built from *n*-GaAs and discontinuous platinum films, can be used as detectors of different gases over a wide range of temperatures (Lechuga et al., 1992).

Further details of semiconductor sensors can be found in the literature (Sze, 1994; Ristic, 1994; Göpel et al., 1994; Gardner, 1994; Soloman, 1998).

3.3 SENSORS BASED ON ACOUSTIC-WAVE PROPAGATION

Sensors based on acoustic-wave propagation apply acoustic waves within the bulk or on their surfaces for sensing. Resonant sensors generally have an electromechanical resonance frequency (when standing waves are present in the structure) that is a function of the measurand. The output is a quasi-digital frequency signal that is much less prone to noise and interference and can be directly measured in digital systems. This provides a great advantage over conventional analog sensors. The operation of another group of sensors is based on the phase shift of acoustic wave propagation caused by environmental effects.

A common approach for obtaining a frequency output is to use electronic oscillators in which the sensor element itself is the frequency-determining element. Piezoelectric resonant sensors use the elastic properties of various piezoelectric materials (see Chapter 3) to sense and measure a physical or chemical phenomenon. These sensors are based on the propagation of elastic bulk or surface waves.

Bulk acoustic wave (BAW, also called thickness-shear mode, or TSM) sensors have been applied to a wide variety of mass, chemical, and biochemical measurement applications. For BAW sensors, small quartz crystal disks of 10–15 mm diameter and 0.1–0.2 mm thickness are used [see Figure 3.4.(a)]. The resonance frequencies are between 6 and 20 MHz (Lucklum et al., 1991). The historic development of BAW quartz sensors originated from the use of quartz resonators as time bases for frequency control. The high reliability and stability of quartz oscillators are based on the stability of a mechanical resonance in a structure composed of single-crystal quartz.

It has been well known that the deposition of a small mass of material on the surface of a quartz microbalance (QMB) lowers its resonance frequency. QMB sensors are commonly used for thin-film thickness monitoring in vacuum evaporation equipment. Similarly, the gravimetric sensor principle is based on changes in the fundamental oscillation frequency, f_0, upon adsorption or absorption of particles from the surrounding gas phase. For the first

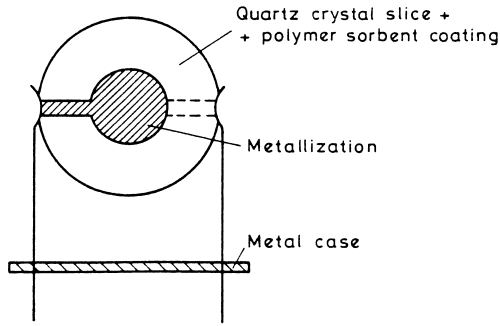

3.4(a)

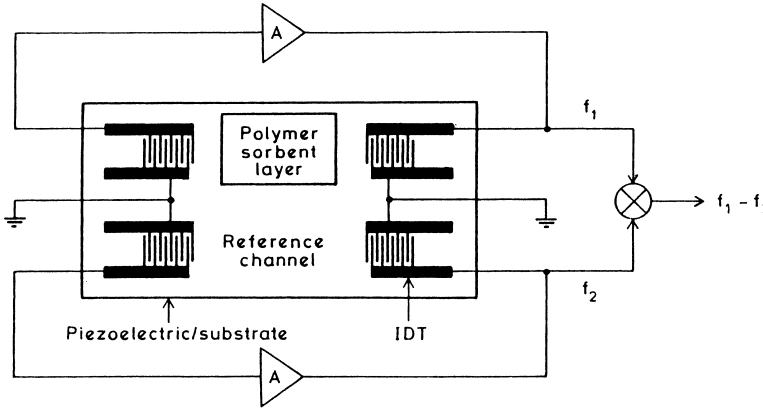

3.4(b)

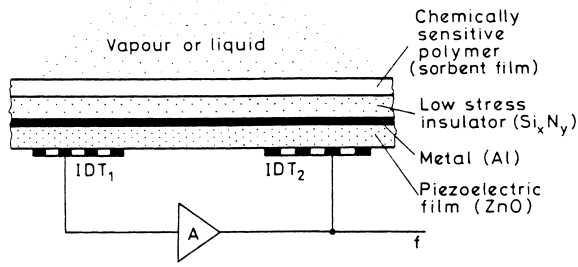

3.4(c)

FIGURE 3.4. Sensors based on acoustic wave propagation: (a) bulk acoustic wave (BAW) quartz microbalance (QMB), (b) dual delay line surface acoustic wave (SAW) resonator, (c) Lamb-wave (LW)-type composite plate sensor.

(continued)

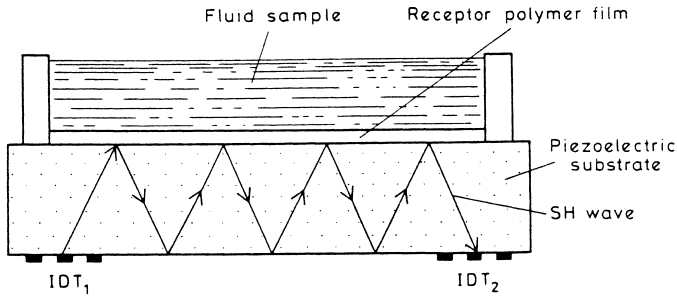

3.4(d)

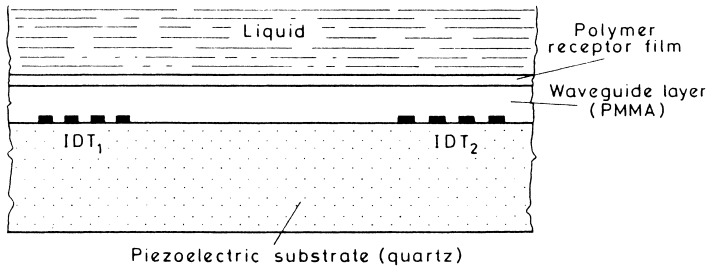

3.4(e)

FIGURE 3.4 (continued). (d) shear horizontal (SH), and (e) guided (Love) wave sensor types. (Reproduced with permission from *Polymer Films in Sensor Applications* by G. Harsányi, ©1995, Technomic Publishing Co., Inc., Lancaster, PA, pp. 68–73.)

harmonic, the frequency shift (Δf) can be described as follows (Sauerbrey, 1959):

$$\Delta f/f_0 = -\Delta m/m \tag{3.1}$$

where Δm is the mass change; m is the mass; and f_0 is the operating frequency.

For a 10-MHz crystal, the detection limit is at the 0.1 ng/mm^2 level. The sensitivity is limited by the mass of the whole crystal.

In *surface acoustic wave* (SAW) devices, the acoustic wave energy is constrained to the surface; the wave propagates along the surface of a solid medium. SAWs normally include different waves, the most important of which are the Rayleigh waves (Rayleigh, 1885). The displacement of the particles near the surface of the solid that is propagating the Rayleigh wave has two components: a longitudinal component and a shear vertical component (Wohltjen, 1984). The superposition of these two components results in surface tra-

jectories that follow a retrograde elliptical path around their quiescent positions.

Waves can be generated quite easily in piezoelectric substrates using an interdigital transducer (IDT) electrode, which can be fabricated by microlithography from thin-film metallization (White and Voltmer, 1965). The time-varying voltage at the transmitter will result in a synchronously varying deformation of the piezoelectric substrate and the subsequent generation of a propagating surface wave. The counterpart of the phenomenon can also occur; SAWs can generate alternating voltage in another IDT called a receiver. Delay line is a configuration consisting of two (or more) IDTs and a propagation path between them [see Figure 3.4(b)]. The first interdigital transducer excites a SAW. The frequency of the SAW is mainly determined by the elastic constants of the piezoelectric material and the geometrical sizes of the generator IDT. The receiver IDT will receive this wave after traveling along the surface of the substrate. The propagation path is the sensitive area. All changes in the boundary conditions for SAW propagation lead to a variation of the SAW received by the second IDT. This well-known fact can be used for sensor applications.

The SAW resonator is, in fact, a delay line with an amplified feedback [see Figure 3.4(b)]. It can be used as a sensor in a similar way to the delay line; standing waves are formed by reflection from gratings. Any change in the environment leads to a change in the resonance frequency and can be registered (Grate et al., 1993).

The response behavior for a SAW device coated with a sorbing film is as follows:

$$\Delta f/f_0 = -K\Delta m\, f_0 /A \tag{3.2}$$

where A is the active surface area; K is a constant; and the other symbols are the same as in the previous equation. The SAW sensors typically operate at high frequencies up to the GHz ranges. Because the sensitivity of the device increases as the square of the fundamental frequency, SAW sensors have greater potential sensitivity than BAW types. Many SAW sensor applications use a dual delay line configuration; one delay line can be coated with the sorptive or reactive film, while the other remains inert or protected from environmental effects. Typically, the frequency difference will be measured, which is in the order of kHz and can be easily sampled. The uncoated or protected resonator acts as a reference to compensate undesired effects, for instance, frequency fluctuations caused by temperature or pressure changes.

When a good coating is available, it is usually possible to detect species at the 10–100 ppb concentration level, with a selectivity of 1000:1 or more over commonly encountered interfaces (Rapp et al., 1991). The mass detection limit is in the range of 0.05 pg/mm^2.

A new resonator sensor concept similar to SAW sensors, but employing *Lamb waves* (LW), was recently applied in sensors (Wenzel and White, 1988). Lamb waves propagate in the bulk of plates with thicknesses that are small compared to the ultrasonic wavelength: the thickness/wavelength ratio is less than one. Particle motions of Lamb waves are similar to those of Rayleigh waves; however, in a thin plate, the waves give rise to a series of symmetric and antisymmetric plate modes. The lowest order antisymmetric modes have a unique flexural character, hence, the name "flexural plate wave," or FPW.

Figure 3.4(c) shows a schematic cross section of an FPW sensor device (Wenzel and White, 1990). The core of the device is an ultrasonic delay line consisting of a composite plate of a low stress insulation, metallization, and piezoelectric film. IDTs on the piezoelectric layer launch and receive the waves and, together with the amplifier, form a feedback oscillator whose output frequency depends on the mass per unit area of the membrane, including the chemically sensitive film. The advantages of FPW sensor devices are that they operate in the low-MHz frequency range and that they may operate while immersed in a liquid. Theoretical and experimental results also show that, compared to BAW and SAW gravimetric sensors, LW sensors and especially FPW devices are more sensitive to added mass. They are very attractive for chemical and biological sensing.

Recent advances in the design and construction of *acoustic plate mode* (APM) devices have allowed their use as sensors (Grate et al., 1993). Figure 3.4(d) shows the cross section of a typical APM sensor. The sensor consists of a piezoelectric plate, a receptor film, a fluid containment cell, and appropriate signal processing electronics. The piezoelectric plate supports APMs that are primarily horizontally polarized shear waves. Therefore, the device is called a shear horizontal acoustic plate mode (SH-APM) sensor. Typical plates are a few acoustic wavelengths thick. The waves are generated and detected by IDTs on the lower surface and reflect between the upper and lower surfaces of the substrate. This beam interacts with the receptor polymer film and viscously coupled fluid sample when it reflects from the upper surface. Changes in the film due to mass loading or viscoelastic stiffening will alter the phase of the reflected wave and result in a phase shift in the electrical signal. Similar to SAW sensors, a dual delay line configuration can be used to compensate nonspecific responses and undesired environmental effects. The advantage of the APM sensor is that electrical connections can be made on the surface of the device, which is not immersed in solution. Typical APM device frequencies are 25–200 MHz.

Because a wave reflection mechanism occurs, acoustic energy cannot be concentrated at the surface unless very thin plates are used. An alternative approach (Gizeli et al., 1992) is to apply another geometry to excite another type of guided SH wave, the *Love wave.* Mass loading of this surface skimming

bulk wave (SSBW) device results in a composite acoustic device, known as Love plate, with an SH wave guided at the interface of the deposited polymer overlayer and the SSBW substrate. SSBWs are acoustic waves with only a shear displacement component propagating just below the surface of a piezoelectric substrate. SSBW suffers from a considerable acoustic loss. A thin overlayer of a dielectric material on the surface may convert the SSBW into a guided SH or Love wave, increasing the coupling coefficient of the wave and reducing the losses.

Generally, devices using thin films to help guide the waves are called Love wave devices. Figure 3.4(e) demonstrates the geometry used in Love plates. The substrate is generally piezoelectric quartz crystal and the overlayer is silica or polymethyl-methacrylate (PMMA), which exhibits much lower shear acoustic velocities than quartz, and so fulfills the necessary requirement for the guidance of a Love wave. PMMA shows much lower viscoelasticity than a lot of other polymers; thus, it shows low acoustic losses. Application of PMMA in the field of sensors is based on the sensing mechanisms of SH-AMP sensors. Changes in the receptor film, due to mass loading or viscoelastic stiffening, alter the phase of the reflected wave. Phase shifts ($\Delta\Phi$) can be measured as a function of the mass-load ($\Delta m/A$):

$$\Delta\Phi = C(\Delta m/A) \tag{3.3}$$

where C is a constant. Typical sensitivities that can be reached by this type of sensor are in the range of 5–30 deg/(10^{-6} gcm^2), depending on the applied material system and layer thicknesses.

Further details about acoustic wave devices can be found in the literature (Ballantine et al., 1996).

3.4 CALORIMETRIC SENSORS

The basis of transduction in calorimetric sensors is a temperature variation resulting from the environmental effect to be detected. The latter may involve heat generation, heat consumption, or variations in heat transfer abilities. Typical examples are as follows:

- endo- or exotherm chemical reactions on the sensor surface
- heat generation of incoming IR (infrared) or another type of radiation
- varying heat transfer from a heat-flow or a flowing medium

The sensors may operate at room temperatures, however, an elevated temperature is often desired, which is stabilized by a heating control. Dual structures are typically used in which the reference element is isolated from the

environmental effects and operates, therefore, at a fixed temperature, while the sensing element follows the environmental effects by temperature variations; thus, a temperature difference is practically measured.

Calorimetric sensors are widely used for the detection of reactive gas components; they are often called pellistors. Their operation principle utilizes the heat generated or consumed during kinetically controlled catalytic chemical reactions of reactive gas molecules for reactive gas component detection (Walsh and Jones, 1991). The sensor element consists of a substrate that is heated continuously by the heating resistor (see Figure 3.5). Its temperature is determined by the heat flow from the substrate to the environment. In a stationary state, the temperature difference is constant, and the power dissipation is equal to the heat flow. The temperature of the substrate can be monitored using a temperature sensor (thermistor, thermoelement, or Pt-resistor, see Section 4.1). A Pt-resistor can be used for heating and for temperature monitoring purposes. The polymer catalyst coating can adsorb and absorb gas components from the environment that can take part in catalytic chemical reactions. The reaction heat generated or consumed by the chemical reaction will disturb the stationary state heat flow from the sensor to the environment, and a temperature change can be detected, which is a function of the partial pressure of the gas component in question.

Calorimetric sensor applications generally use dual sensor configurations; one substrate is coated with the catalyst polymer film, while the other remains inert or protected from environmental effects (see Figure 3.5). The uncoated or protected substrate acts as a reference to compensate undesired effects, for instance, temperature fluctuations caused by the ambient temperature, heat conductivity, or ambient gas velocity changes.

In the case of adiabatic sensor types, power dissipation is the same in both substrates, and the temperature difference is measured. In the isothermic-type sensors, the temperatures are held at the same value, and the heating power difference necessary to keep the same temperatures will be monitored.

Conventional calorimetric sensors utilize themodynamically controlled catalytic reactions. In this case, steady-state signals are obtained under continuous flow conditions at constant partial pressure of chemically active components. These signals are proportional to the generated catalytic reaction heat obtained for constant partial pressure of the given component (Walsh and Jones, 1991). With this type of sensor, the greatest problem may be the continuous consumption of the analyte that can alter the concentration level in small volumes.

Some new types of sensors, in contrast, monitor kinetically controlled reactions between the sensor material and the detected molecules under chopped flow conditions. Only changes in the equilibrium concentration of ad- or absorbed molecules lead to time-dependent nonequilibrium heat generation,

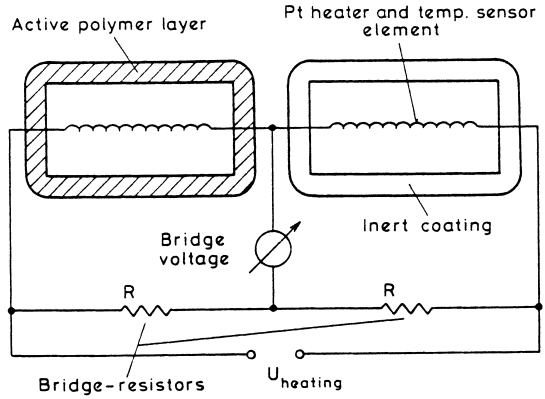

FIGURE 3.5. Application of calorimetric sensors in dual structure. (Reproduced with permission from *Polymer Films in Sensor Applications* by G. Harsányi, ©1995, Technomic Publishing Co., Inc., Lancaster, PA, p. 82.)

which only occurs during pressure variations. Fast and rectangular-shaped partial pressure variations should be produced, and the maximum temperature change that occurs during heat generation upon adsorption or desorption of molecules has to be determined (Schierbaum et al., 1992).

Further details about thermal sensors can be found in the literature (Ricolfi and Scholtz, 1990).

3.5 ELECTROCHEMICAL CELLS AS SENSORS

Electrochemical cells are widely used as sensors for the measurement of chemical quantities, typically ion or gas-molecule concentrations in different media. It is expected that electrochemical cells will find wide applications in biosensors. In the simplest cases, an electrochemical cell consists of a minimum of two electrodes and an ionic conductive material, called an electrolyte, between them (see Figure 3.6). For the practical operation, the whole cell must be built up, although, the sensor element itself is often only a part of that. Accordingly, the following cases can be distinguished:

- The sensor element is the whole electrochemical cell that is isolated from the environment, for example, by a semipermeable membrane.
- The sensor consists of the two electrodes; and the electrolyte between them is the actual analyte.
- The sensor element is a single electrode (the counterelectrode serves only the practical measurement purposes).

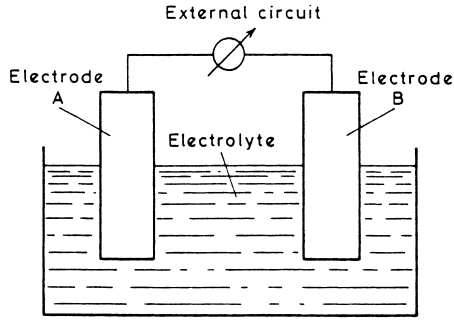

FIGURE 3.6. General structure of an electrochemical cell. (Reproduced with permission from *Polymer Films in Sensor Applications* by G. Harsányi, ©1995, Technomic Publishing Co., Inc., Lancaster, PA, p. 74.)

Electrochemical-cell-type sensors can be classified into three main categories according to the characteristics of the electrode reaction (Wiemhöfer and Göpel, 1991):

- Type A is characterized by direct participation of the mobile ions, which are originally present in the electrolyte.
- Type B cells use the electrolytes as "solvents" for the charged products formed by redox reactions from neutral molecules that are present in the electrolyte or in its surrounding medium.
- Type C cells are characterized by competing or several step electrode reactions.

Electrochemical sensors are based upon potentiometric, amperometric (more generally, voltammetric), or conductivity measurements. The different principles always require a specific design of the electrochemical cell. The operation of the sensors is based on the reactions and their equilibrium at the interfaces between electronic and ionic conductors on the electrode surfaces. Sometimes, their transient behavior may also be applied for analytical purposes. Their operating and measurement principles will be summarized in the next sections according to the types listed above.

3.5.1 Potentiometric Sensors

In potentiometric sensors, the potential difference between the reference electrode and the working electrode is measured without polarizing the electrochemical cell, that is, very small current is allowed. In that case, the equilibrium electrode potential difference can be monitored. This difference is given by the Nernst-Nicolsky-Eisenman equation (Sudhölter et al., 1989):

$$E = E_0 + \frac{R \cdot T}{z_i \cdot F} \cdot \ln \left[a_i + \sum_j S_{ij} \cdot (a_j)^{z_i/z_j} \right] \tag{3.4}$$

where E_0 is the standard electrode potential of the sensor electrode; a_i is the activity of the primary ion; a_j represent the activities of the interfering ions; S_{ij} represent the selectivity coefficients of the primary ion over the interfering ions; R is the universal gas constant; T is the absolute temperature; F is the Faraday constant; z_i is the valency of the primary ion; and z_j is the valency of the interfering ion. The ion activity is generally approximated as a simple linear function of the concentration:

$$a_i = k_i c_i \ (k_i < 1) \tag{3.5}$$

where k_i is the activity coefficient of the particular ion.

In the case of ideal ion selective electrodes (ISEs), the selectivity or cross-sensitivity constants (S_{ij}'s) could be neglected. In practice, they must be taken into consideration.

The conventional electrodes generally use metal, metal-salt, or metal-electrolyte-glass structures. Recently, for ISE purposes, another generation of electrodes—the membrane electrodes—is also used. These contain an internal reference electrode and an internal reference electrolyte in an isolation tube that is closed by an ion-selective membrane that is generally a special polymer material. One side of the membrane is in contact with the analyte solution to be probed. The structure is shown in Figure 3.7(a). The polymer-sample solution interactions can be divided into the following groups:

- The membrane contains active grains or ionic sites (called ionophores) that are the basis of ion exchange and/or complexion within the membrane. By reversible exchange of the ions between the analyte solution and the membrane phase or by a reversible penetration of the ions accompanied by the complexion process, a membrane potential will be developed, which can be described by the Nernst-equation. Recently, sensor electrodes with nonionic grains, so-called neutral charge carriers, are preferably used for complexion processes with ions of the analyte.
- A surface charge and potential shift may also be developed by the sorption of ions onto the membrane surface. The process is typical for the adsorption of H^+ ions onto the surface of a glass electrode with special composition that causes its pH-dependent electrode potential variations. Glass electrodes are used as pH sensors.

Figure 3.7(a) shows the cell configuration of a conventional liquid junction ion-selective electrode. A reversible ion or electron transport mechanism is

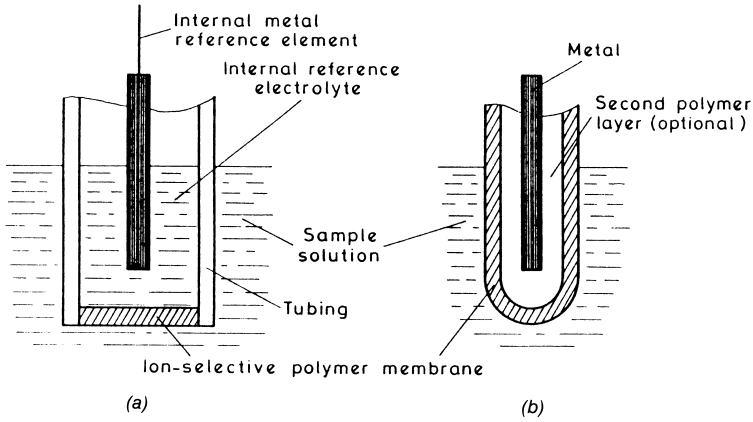

FIGURE 3.7. Schematic structure of the membrane electrodes: (a) conventional-liquid-electrolyte-based type and (b) solid-contact electrode. (Reproduced with permission from *Polymer Films in Sensor Applications* by G. Harsányi, ©1995, Technomic Publishing Co., Inc., Lancaster, PA, p. 76.)

present not only at the membrane-analyte solution interface, but also at every phase boundary, resulting in well-defined interfacial potentials. Electrodes of this type usually exhibit little potentiometric drift, however, the evaporation of water alters the electrolyte composition causing problems with long-term stability (Goldberg et al., 1991).

Another type of ion sensor was developed in which ion-selective polymeric membranes are deposited directly onto solid electrode surfaces with no internal electrolyte solution. Figure 3.7(b) illustrates the cell configuration for this sensor, called solid-contact ISE, which is similar to a coated-wire electrode. Often, in this type of ISE, the membrane/solid interface is ill defined, leading to significant potentiometric drifts. A stable and reversible transition from electronic conductivity in the metal electrode to ionic conductivity in the polymeric membrane can be maintained by using double-membrane structures. Polymer electrolytes or hydrogel buffers are generally combined with perm- and/or ion-selective membranes. The mechanisms responsible for the improvement are still the subject of debate. Adhesion and reaction mechanisms may influence the behavior of the electrodes.

The application of electroconducting conjugated polymers (ECPs) results in many new possibilities for building up electrochemical sensors (see in Section 2.4). In these materials, a semiconductor polymer contains ionic dopants and/or specific molecules covalently grafted to the ECP (Bidan, 1992). The great advantage of ECPs is in the phenomenon that the ion exchange or ion sorption occurs directly within the electroconducting material or on its sur-

face. The ion exchange process directly changes the doping level and also the conductivity and work function of the semiconductor polymer. Thus, ECPs can be used directly as sensitive electrodes. ECPs even enable the molecular "ion-sieving" effect. This means that it is possible to vary the permeability of electropolymerized films via their controlled anodic growth. The cut-off size of ions can be determined by the size of the anion that was used as dopant during the electropolymerization, removing them during an electrochemical dedoping process. By choosing suitable electropolymerization conditions, enzymes acting as negative dopants can be entrapped through coulombic interactions. This is a technique for immobilizing enzymes at the surface of electrodes, which is the most promising fabrication method of enzyme-reaction-based bioelectrodes (see Section 7.1.5).

In connection with potentiometric sensors, the role and nature of reference electrodes should also be clarified. These are so-called electrodes of second class that is, the metal electrode is covered by its solid salt and by the saturated solution of the latter one. Their electrode potential is rather independent from the current density; thus, it can be handled as a constant. The silver/silver-chloride electrode (SSC), a silver wire coated by its chloride within a saturated KCl solution, is typical. Actually, it is a chloride sensitive electrode surrounded by a constant concentration solution. Their application in the non-polarized potentiometric measurement methods is unnecessary, but they are much more important in the amperometric cells (see Section 3.5.2).

3.5.2 Amperometric Sensors

Amperometry is a method of electrochemical analysis in which the signal of interest is a current that is linearly dependent upon the concentration of the analyte. As the chemical species approach the working (or sensing) electrode, electrons are transferred from the analyte to the working electrode or to the analyte from the electrode. The direction of flow of electrons depends upon the properties of the analyte and can be controlled by the electric potential applied to the working electrode. To maintain charge neutrality within the sample, a counter-reaction occurs at a second electrode, the counterelectrode. If a constant potential difference is maintained by the external circuit, a continuous current flow can be measured. Linear current via ion-concentration characteristics can be obtained by amperometry at diffusion controlled processes in the "limiting current operating mode." Diffusion control can occur at several interfaces in the electrochemical cell:

- Diffusion of ions from the electrolyte to the surface of the electrode is used in the analytical method called polarography (Buttner et al., 1990). Applying the Fick law of diffusion and Faraday's law for the charge

transfer, it can be easily shown that the current density, i, is proportional to the concentration, c, of the active component in the electrolyte:

$$i = \text{constant} \times c \tag{3.6}$$

- Diffusion of molecules from the surrounding gas or liquid through a capillary into the electrolyte and/or to the surface of the electrolyte counterelectrode interface, where they will be ionized, may occur. In that case, of course, the electrical current density is a function of the partial pressure, p, of the analyte (Yan and Lu, 1989).
- Diffusion will also control the charge transfer process when particle flow limiting membranes are used on the surface of the electrolyte. This phenomenon is the basis of concentration measurements in the Clark-type O_2 sensors (Clark, 1956, see Chapter 6, Section 6.1.1). The current density is proportional to the partial pressure of the dissolved gas analyte:

$$i = \text{constant} \times p \tag{3.7}$$

- Particle flow limiting membranes can also be used on the surface of electrodes or within the electrolyte (Van den Berg et al., 1991).

Figure 3.8(a) shows the typical voltage-current characteristics of diffusion-controlled processes. Figure 3.8(b) gives the typical limiting current value and analyte concentration relationship. By setting the operation mode of the sensor in the limiting current region and keeping the voltage on a constant value, a current proportional to the concentration can be measured.

To guarantee the constant potential difference between the working and counterelectrodes independent from the current that polarizes the electrodes, the application of a potentiostat and a reference electrode is often necessary. Figure 3.8(c) shows a simple circuit diagram (Schelter et al., 1992). The function of the circuit is to set the electrode potential of the working electrode to a given value, always with respect to the reference electrode. The electrode potential of the reference electrode is independent of the current flowing through the cell, and it is also inert to the analyte to be examined. At the same time, the cell current is converted into an output voltage signal using a simple current-voltage converter circuit.

3.5.3 Other Types of Electrochemical Measurements

The amperometric method is a special case of the *voltammetric measurements* where potential-current diagrams are used for the analysis. Generally, the potential of the working electrode controlled by a potentiostat is changed

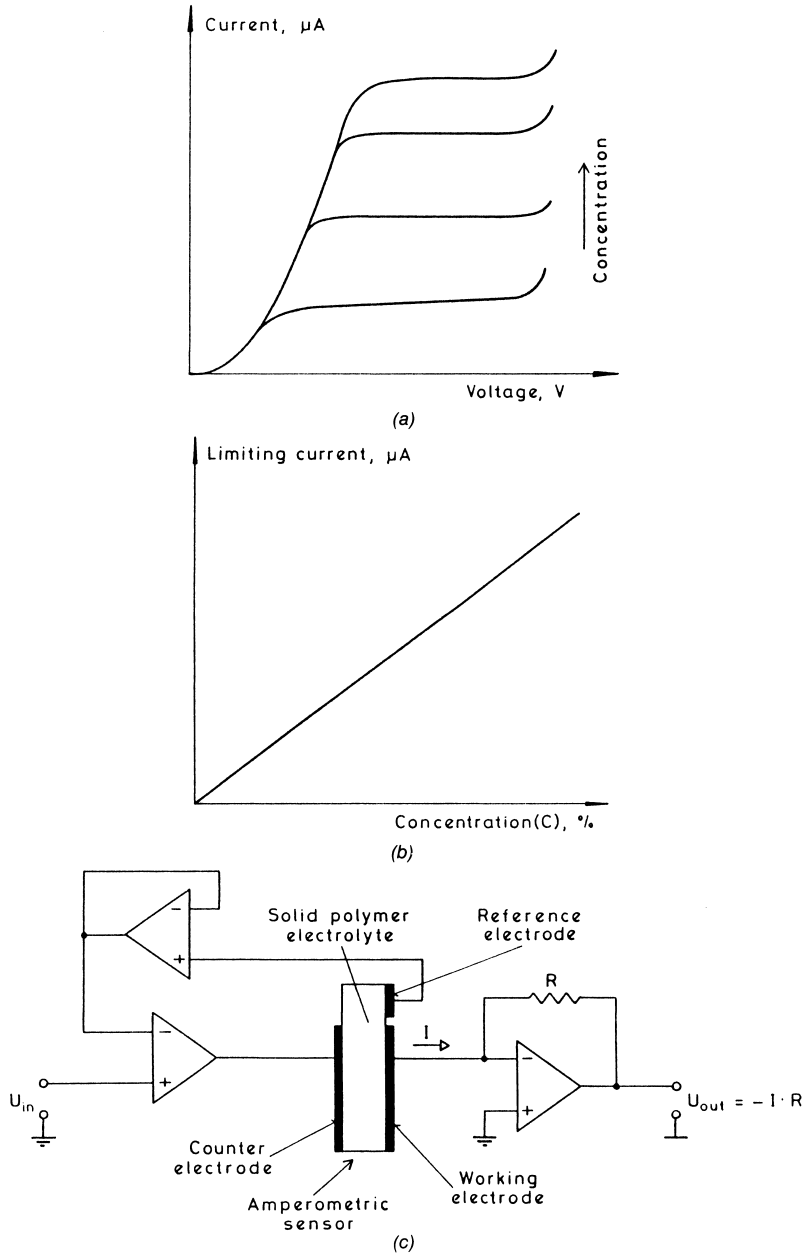

FIGURE 3.8. Structure and characteristics of amperometric sensors: (a) voltage-current characteristics, (b) limiting current-concentration characteristic, and (c) schematic structure and circuit connection. (Reproduced with permission from *Polymer Films in Sensor Applications* by G. Harsányi, ©1995, Technomic Publishing Co., Inc., Lancaster, PA, p. 79.)

continuously with a constant scan rate. Any reaction at the electrode surface can usually be detected as a current superimposed to the base current due to double-layer charging. Thus, in these voltammograms, current peaks can be observed. The peak potential values can be used for qualitative analysis, and the height of the peaks is a function of analyte concentration (Tieman et al., 1992). Figure 3.9 shows typical cyclic voltammograms at different concentrations.

The structure of voltammetric sensors is generally the same as that of the amperometric sensors. They are generally fabricated with reference, auxiliary, and working electrodes.

Conductimetric sensors are based on the measurement of electrolyte conductivity, which varies when the cell is exposed to different environments. The sensing effect is based on the change of the number of mobile charge carriers in the electrolyte. If the electrodes are prevented from polarizing, the electrolyte shows ohmic behavior. Conductivity measurements are generally performed with AC supply (Watson et al., 1987). As a first approximation, the conductivity (σ) can be expressed as follows:

$$\sigma = \sum_i c_i \cdot z_i \cdot e \cdot \mu_i, \tag{3.8}$$

where e is the elementary electric charge; μ_i is the mobility; z_i is the valency; and c_i is the volume number of ionic carriers in the electrolyte. Accordingly,

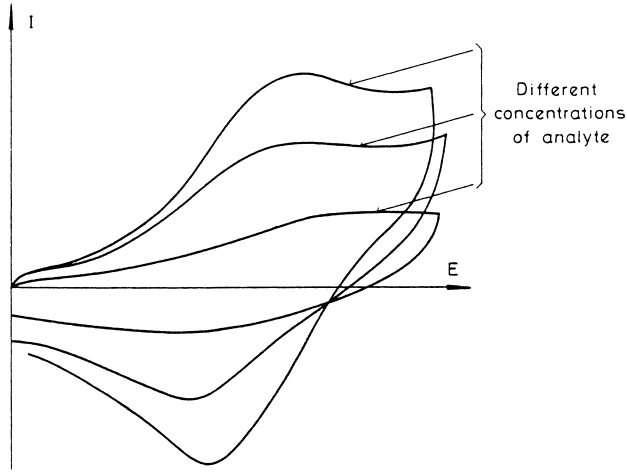

FIGURE 3.9. Typical cyclic voltammograms depending on the analyte composition. (Reproduced with permission from *Polymer Films in Sensor Applications* by G. Harsányi, ©1995, Technomic Publishing Co., Inc., Lancaster, PA, p. 80.)

the conductivity is a linear function of the ion concentration; therefore, it can be used for sensor applications. However, it is nonspecific for a given ion type. On the other hand, both the polarization and the limiting current operation mode must be avoided. Thus, small amplitude alternating bias is used for the measurements with frequencies where the capacitive coupling is still not determining the impedance measurement.

All electrochemical sensor and measurement types discussed above are based on equilibrium or stationary process stages. This is their main disadvantage: the response time is rather long and may be comparable to the time constants of the variations within the observed medium. Another disturbing circumstance might be that the long-lasting electrochemical processes at the electrode surfaces might alter the composition of analytes that are present in small volume. In such cases, techniques that are based on equilibrium stages cannot be applied because the equilibrium stage can never be reached.

Thus, the application of *transient electrochemical measurement methods* is necessary. In these techniques, the time-dependent responses of a given parameter are followed when a special excitation is applied. By measuring the response and decay times, asymptotic solutions can be determined without reaching equilibrium stages. According to the type of external excitation, the following methods can be distinguished (Buerk, 1993):

- potentiostatic measurements: the excitation is a voltage, the output is the current response
- galvanostatic measurements: the cell current is the excitation and the electromotive force of the cell is measured
- coulostatic measurements: the cell is excited by a given electric charge, while the cell current or electromotive force responses are measured

The transient methods apply various excitation curve shapes, like the step function, linear time dependent curve, periodic sinusoidal, rectangular or triangular signals, impulses superimposed on linear functions, or impulses with heights that increase proportionally to time.

Further details on electrochemical sensors can be found in the literature (Rubinstein, 1995; Lacourse, 1997; Christensen and Hamnett, 1994).

3.6 SENSORS WITH OPTICAL WAVEGUIDES

The advantages of applying optical fibers as transducers were summarized in Chapter 2, Section 2.5. Optical fibers can be made sensitive to a wide variety of phenomena where the basis of operation is that the environmental effect alters the parameters of the propagating light. Generator-type operation is also possible, if light is emitted (e.g., chemiluminescence effect). Accord-

ing to the variable to be measured, the following cases and measurement techniques can be distinguished:

- intensity measurement: the intensity changes of the transmitted, reflected, or emitted light are followed
- spectrum analysis: the spectral changes of the transmitted, reflected, or emitted light are followed; since its measurement technique is rather complicated, it is generally replaced by a simple intensity measurement within narrow wavelength ranges
- phase shifts of the transmitted or reflected beams may also be followed by applying monochromatic and coherent beams; in interferometer arrangements, simple intensity changes are measured
- polarization changes can also be followed by applying linearly polarized excitation light; using rotating polar filters, intensity measurement can be made; this type is rarely applied in sensors

Fiber optic sensors can be categorized in many ways. A basic division is into intrinsic and extrinsic. In the first, the measured parameter causes a change in the transmission properties of the fiber itself; in the second, the fiber acts just as a light conductor to and from the sensor.

Figure 3.10 shows a number of optical sensor structures and measurement arrangements that have widespread application in optical sensorics.

Figure 3.10(a) shows a typical structure of a chemical or biochemical fiber optic sensor called an *optrode* (or *optode*). It consists of two (maybe one or more than two) fibers for the input light and output light. The operation is based on the spectral change of the output light caused by different physical and chemical effects at the tip of the sensor:

- *Colorimetric detection* is based on the color changes of indicators entrapped in the material at the sensor tip (Sadaoka et al., 1991). Practically, the reflected light spectra are to be measured. A special case of that method is the simple reflectance/absorbance measurement using a monochromatic light source or a special wavelength region (Czolk et al., 1992). Sometimes the spectral change is caused directly by the color change of the analyte of interest.
- *Fluorimetric detection* is based on the phenomenon of fluorescence quenching. The absorbed incident light excites a secondary light wave, the spectrum of which differs from that of the incident light spectrum. The intensity of the emitted light may vary according to environmental changes (Wolfbeis, 1991).
- *Phosphorescence* behavior is a secondary light emission as an answer for the excitation, however, the emission decays slowly and is present for a given period of time even when the excitation has already been switched

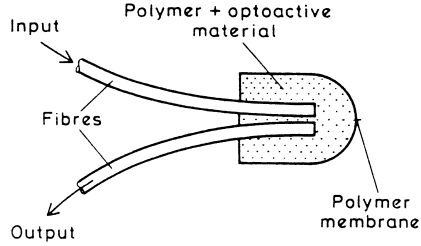

3.10(a)

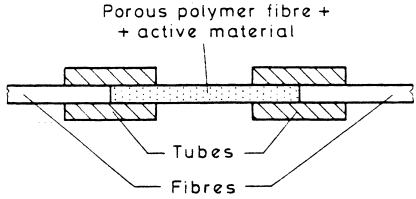

3.10(b)

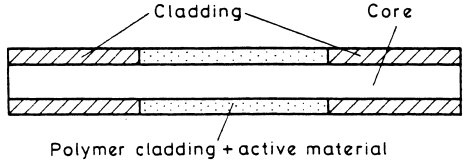

3.10(c)

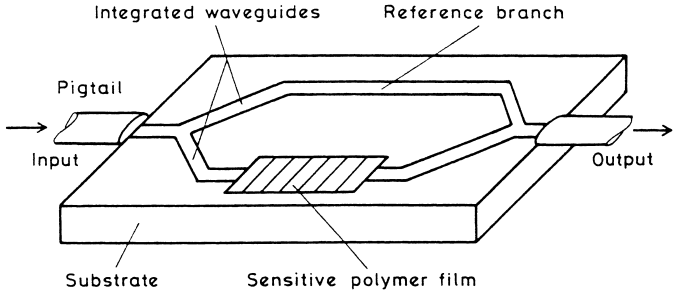

3.10(d)

FIGURE 3.10. Typical optical sensor structures using optical waveguides: (a) optrode, (b) core-based sensor using porous polymer core, and (c) fiber optic sensor with sensitive cladding; interferometer sensors: (d) transmission type.

(continued)

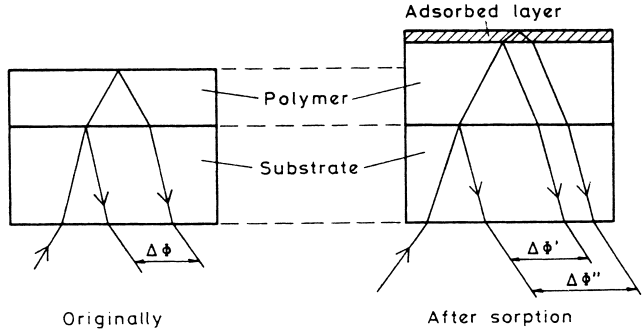

3.10(e)

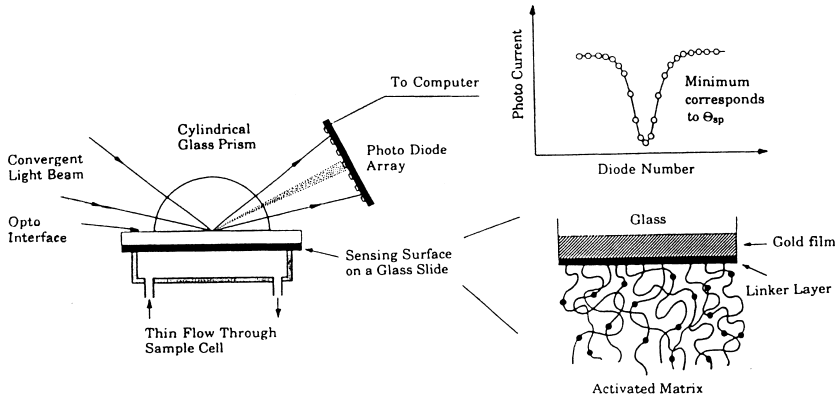

3.10(f)

FIGURE 3.10 (Continued). (e) reflection type; and (f) principle of the surface plasmon resonance sensor. [Figures (a)–(e): reproduced with permission from *Polymer Films in Sensor Applications* by G. Harsányi, ©1995, Technomic Publishing Co., Inc., Lancaster, PA, pp. 85–88; Figure (f) reprinted from *Sensors and Actuators B* by B. Liedberg, I. Lundström and E. Stenberg, "Principles of Biosensing with an Extended Coupled Matrix and Surface Plasmon Resonance," 11, pp. 63–72, ©1993, with permission from Elsevier Science S.A., Lausanne, Switzerland.]

out. Not only spectral changes, but also decay time measurements can be used for analytical purposes (Buerk, 1993).

- Catalyzed light emission caused by *chemiluminescence* or *bioluminescence* reactions can also be used for sensor purposes. There is no need for incident input light in this case (Gautier et al., 1990).

Optrodes can be used for the detection of gases, ions, enzyme substrates,

and macromolecules. The active material and the membrane at the tip may contain immobilized ionophores, indicators, fluorescent dyes, chemi- or bioluminescence enzymes, organic adsorbents, etc., according to the application purposes and operation principles. Immobilizing selective reagents and/or applying permselective membranes can increase chemical sensitivity and selectivity.

In *core-based sensors,* the core-analyte interaction is directly utilized as the basis of operation [see Figure 3.10(b)]. Some core-based sensors use *porous fibers* with chemically sensitive reagents immobilized physically or chemically on the surfaces of the pores to sensitize them to the analyte of interest (Zhou et al., 1989). Porous fibers may exhibit very high gas permeability and liquid impermeability so they can be used for the detection of gases in liquids. Vapors permeating into the porous zone can produce a spectral change in transmission. For better sensitivity and selectivity, colorimetric reagents can be trapped in the pores. The observed light intensity is a function of the concentration of the analyte to be measured, c, and can be expressed as follows:

$$I = I_0 \exp[-hlf(c)], \tag{3.9}$$

where I_0 is the intensity of the incident light; h is the extinction coefficient, both of light absorption and of light scattering; l is the light passing length of the sensing segment; and $f(c)$ is the concentration of the absorption and scattering centers.

Cladding-based chemical fiber-optic sensors can be made using microporous or other types of sensitive claddings, as shown in Figure 3.10(c) (Lieberman, 1993). *Evanescent-wave refractometric cladding-based sensors* detect the absorption of the species in the polymeric cladding, which leads to a variation of its refractive index, thus, also to a variation of the overall transmission efficiency of the fiber. Porous polymer cladding-type sensors can be used, for instance, for humidity measurements (Ogawa et al., 1988). The quantity of moisture absorbed by the microporous cladding varies with humidity. The optical power level of the transmitted light in the core varies according to the moisture absorption quantity because of the refractive index change of the cladding. Another example is the application of organopolysiloxanes as cladding materials since they can change their refractive index when they adsorb and/or absorb molecules from the surrounding medium (see Section 4.16). Also, evanescent wave excited fluorescence quenching can be used for detection. In special cases, the surrounding medium itself plays the role of the cladding; the decoupling light from a fiber core having no special cladding on its surface follows the refractive index changes of the environment.

Both conventional fiber-optic and integrated optical *interferometers* can also be used as sensors. Their operation is based on the optical interference be-

tween reference and sensitive light waves. According to the well-known rules of light interference, the resultant intensity is a function of the difference in optical path length of the branches, which can be modulated by a change of either the refractive index or the geometrical length difference between the paths. Figures 3.10(d) and 3.10(e) show a transmission type and a reflection type interferometer structure, respectively.

The former is the *Mach-Zehnder interferometer* consisting of two Y-branches (Brandenburg et al., 1993). Incoming light is split into two parts that are guided in the two branches of the interferometer. For sensor applications, one branch is usually affected by the quantity to be measured, while the other provides the reference phase. If one of the branches of the integrated structure is covered with a sensitive polymer film, the refractive index of which is a function of its surrounding medium, the effective refractive index of this waveguide branch is a function of the quantity to be measured. Thus, the interferometer acts as a sensor based on the refractive index modulation caused by the evanescent field effect in the branch covered with the sensitive polymer.

Figure 3.10(e) illustrates the operation of *reflection-type interferometer sensors* (Gauglitz et al., 1993). The superposition of the two partial beams reflected from the waveguide/polymer and polymer/air interfaces, respectively, can be influenced either by swelling of the film caused by permeation of gases and liquids or by adsorption of particles on the top of the film, which will introduce an additional reflection. Moreover, the introduced analyte can interact with the polymer film, thus influencing the value of the refractive index. Spectral interferometry allows these effects to be discriminated to a certain extent.

Surface plasmon resonance (SPR) is one of the surface-oriented biosensing techniques that can be used to monitor biomolecular interactions. Surface plasmons are the quanta of plasma waves propagating along a metal interface. Surface plasmons can be excited by light waves when an intensity decrease occurs in the propagating beam; this phenomenon is called SPR. For sensor purposes, the most used excitation arrangement is the attenuated total reflection (ATR) or Kretschmann configuration (Kretschmann, 1971). A recently developed version is shown in Figure 3.10(f) (Lindberg et al., 1993). It consists of a glass chip coated by a thin gold film closed into a flow-through cell. The surface of the gold is activated by receptor molecules. Plasmons are excited optically on the metal-glass interface at a characteristic angle of the incident light (Θ_{sp}). In practical arrangements, a convergent light beam falls through a cylindrical prism onto the sensitive area. The reflected light is detected by a photodiode array, where the critical angle can be determined directly. The resonance-angle shifts are measured when molecules or clusters are bound to the receptors. Further chemical reactions of the immobilized molecules may also be followed.

Further details about optical sensing devices can be found in the literature (Wagner et al., 1992; Udd, 1991; Dakin and Culshaw, 1988).

3.7 REFERENCES

Ballantine, D. S., White, R. M., Martin, S. J., Ricco, A. J., Frye, G. C., Zellers, E. T. and Wohltijen, Y. H., *Acoustic Wave Sensors,* Academic Press, San Diego (1996).

Bergveld, P., "Development, Operation and Application of the Ion Sensitive Field Effect Transistor as a Tool for Electrophysiology," *IEEE Trans. Biomed. Eng.,* Vol. BME-19 (1972), pp. 342–351.

Bidan, G., "Electroconducting Conjugated Polymers: New-Sensitive Matrices to Build Up Chemical or Electrochemical Sensors. A Review," *Sensors and Actuators B,* Vol. 6 (1992), pp. 45–56.

Brandenburg, A., Edelhauser, R. and Hutter, F., "Integrated Optical Gas Sensors Using Organically Modified Silicates as Sensitive Films," *Sensors and Actuators B,* Vol. 11 (1993), pp. 361–374.

Buerk, D. G., *Biosensors, Theory and Applications,* Technomic Publishing Co., Inc., Lancaster, PA (1993).

Buttner, W. J., Maclay, G. J. and Stetter, J. R., "An Integrated Amperometric Microsensor," *Sensors and Actuators B,* Vol. 1 (1990), pp. 303–307.

Christensen, P. A. and Hamnett, A., *Techniques and Mechanism in Electrochemistry,* Blackie Academic, London (1994).

Clark, L. C., Jr., "Monitor and Control of Blood and Tissue Oxygen Tensions," *Trans. Am. Soc. Art. Int. Organs,* Vol. 2 (1956), pp. 41–45.

Czolk, R., Reichert, J. and Ache, H. J., "An Optical Sensor for the Detection of Heavy Metal Ions," *Sensors and Actuators B,* Vol. 7 (1992), pp. 540–543.

Dakin, J. and Culshaw, B. (ed), *Optical Fiber Sensors: Principles and Components,* Artech House, Boston, MA (1988).

Gardner, J. W., *Microsensors: Principles and Applications,* John Wiley & Sons, New York (1994).

Gauglitz, G., Brecht, G., Kraus, G. and Nahm, W., "Chemical and Biochemical Sensors Based on Interferometry at Thin (multi)layers," *Sensors and Actuators B,* Vol. 11 (1993), pp. 21–27

Gautier, S. M., Blum, L. J. and Coulet, P. R., "Alternate Determination of ATP and NADH with a Single Bioluminescence-Based Fiber-Optic Sensor," *Sensors and Actuators B,* Vol. 1 (1990), pp. 580–584.

Gizeli, E., Goddard, N. J., Lowe, C. R. and Stevenson, A. C., "A Love Plate Biosensor Utilising a Polymer Layer," *Sensors and Actuators B,* Vol. 6 (1992), pp. 131–137.

Goldberg, H. D., Cha, G. S., Meyerhoff, M. E. and Brown, R. B., "Improved Stability at the Polymeric Membrane/Solid Contact Interface of Solid-State Potentiometric Ion Sensors," *Proc. of the 1991 Int. Conf. on Solid State Sensors and Actuators (Transducers '91),* San Francisco, CA (1991), pp. 781–784.

Göpel, W., Hesse, J. and Zemel, J. N. (ed.): *Sensors, A Comprehensive Survey,* Vol. 1–6, WILEY-VCH, Weinheim (1994).

Grandke, T. and Ko, W. H., *Sensors: A Comprehensive Survey, Vol. 1, Fundamentals and General Aspects, Update,* John Wiley & Sons, New York (1996).

Grate, J. W., Martin, S .J. and White, R. M., "Acoustic Wave Microsensors, Part I," *Analytical Chemistry,* Vol. 65, No. 21 (1993), pp. 940A–948A.

Kretschmann, E., "Die Bestimmung optischer Konstanten von Metall en durch Anregung von Oberflächenplasmaschwingungen," (Determining Optical Parameters of Metals by Exciting Surface Plasmons) *Z. Phys.,* Vol. 241 (1971), pp. 313–324.

Lacourse, W. R., *Pulsed Electrochemical Detection in High-Performance Liquid Chromatography (Techniques in Analytical Chemistry Series),* John Wiley & Sons, New York (1997).

Lechuga, L. M., Calle, A., Golmayo, D., Briones, F., De Abajo, J. and De La Campa, J. G., "Ammonia Sensitivity of Pt/GaAs Schottky Barrier Diodes. Improvement of the Sensor with an Organic Layer," *Sensors and Actuators B,* Vol. 8 (1992), pp. 249–252.

Lieberman, R. A., "Recent Progress in Intrinsic Fiber-Optic Chemical Sensing II," *Sensors and Actuators B,* Vol. 11 (1993), pp. 43–55.

Lindberg, B., Lundström, I., and Stenberg, E., "Principles of Biosensing with an Extended Coupled Matrix and Surface Plasmon Resonance," *Sensors and Actuators B,* Vol. 11 (1993), pp. 63–72.

Lucklum, R., Henning, B., Hauptmann, P., Schierbaum, K. D., Vaihinger, S. and Göpel, W., "Quartz Microbalance Sensors for Gas Detection," *Sensors and Actuators A,* Vol. 25–27 (1991), pp. 705–710.

Mansour, J. and Brown, P. M., *Field Analysis and Electromagnetics,* McGraw-Hill, New York (1963).

Mo, J-H., Andrew, L., Robinson, L., Terry, F. L., Jr., Fitting, D. W. and Carson, P. L., "Improvement of Integrated Ultrasonic Transducer Sensitivity," *Sensors and Actuators A,* Vol. 21–23 (1990), pp. 679–682.

Müller, E., Woias, P., Hein, P. and Koch, S., "Differential ISFET/REFET Pairs as a Reference System for Integrated ISFET-Sensor-Arrays," *1991 Int. Conf. on Solid State Sensors and Actuators (Transducers '91),* San Francisco (1991), pp. 267–470.

Ogawa, K., Tsuchiya, S., Kawakami, H. and Tsutsui, T., "Humidity-Sensing Effects of Optical Fibers with Microporous SiO_2 Cladding," *Electronic Letters,* Vol. 24, No. 1 (1988), pp. 42–43.

Rapp, M., Binz, P., Kabbe, I., Van Schickfus, M., Hunklinger, S., Fuchs, A., Schrepp, W. and Fleischmann, B., "A New High-Frequency High-Sensitivity SAW Device for NO_2 Gas Detection in the Sub-ppm Range," *Sensors and Actuators B,* Vol. 4 (1991), pp. 103–108.

Rayleigh, Lord, "On Waves Propagated Along the Plane Surface of an Elastic Solid," *Proc. London Math. Soc.,* London, Vol. 17 (1885), pp. 4–11.

Reinhoudt, N., "Application of Supramolecular Chemistry in the Development of Ion-Selective CHEMFETs," *Sensors and Actuators B,* Vol. 6 (1992), pp. 179–185.

Ricolfi, T. and Scholz, J., *Sensors: A Comprehensive Survey, Vol. 4, Thermal Sensors,* John Wiley & Sons, New York (1990).

Ristic, L., *Sensor Technology and Devices,* Artech House, Boston, MA (1994).

Rubinstein, I., *Physical Electrochemistry,* Marcel Dekker, New York (1995).

Sadaoka, Y., Matsuguchi, M. and Sakai, Y., "Optical-Fiber and Quartz Oscillator Type Gas Sensors: Humidity Detection by Nafion Film with Crystal Violet and Related Compounds," *Sensors and Actuators A,* Vol. 25–27 (1991), pp. 489–492.

Saito, A., Miyamoto, Sh., Kimura, J. and Kuriyama, T., "ISFET Glucose Sensor for Undiluted Serum Sample Measurement," *Sensors and Actuators B,* Vol. 5 (1991), pp. 237–239.

Sauerbrey, G., "Verwendung von Schwingquarzen zur Microwagung," (Applying Quartz Resonators for Microbalancing) *Z. Phys.,* Vol. 155 (1959), pp. 206–222.

Schasfoort, R. B. M., Keldermans, C. E. J., Kooyman, R. P. H., Bergveld, P. and Greve, J., "Com-

petitive Immunological Detection of Progesterone by Means of the Ion-step Induced Response of an ImmunoFET," *Sensors and Actuators B,* Vol. 1 (1990), pp. 368–372.

Schelter, W., Gumbrecht, W., Montag, B., Sykora, V. and Erhardt, W., "Combination of Amperometric and Potentiometric Sensor Principles for On-Line Blood Monitoring," *Sensors and Actuators B,* Vol. 6 (1992), pp. 91–95.

Schierbaum, K. D., Gerlach, A., Haug, M. and Göpel, W., "Selective Detection of Organic Molecules with Polymers and Supramolecular Compounds: Application of Capacitance Quartz Microbalance and Calorimetric Transducers," *Sensors and Actuators A,* Vol. 31 (1992), pp. 130–137.

Schul'ga, A. A., Koudelka-Hep, M., de Rooij, N. F. and Netchiporouk, L. I., "Glucose-Sensitive ENFET Using Potassium Ferricyanide as an Oxidizing Substrate: The Effect of an Additional Lysozyme Membrane," *Sensors and Actuators B,* Vol. 24–26 (1995), pp. 117–120.

Soloman, S., *Sensors Handbook.* McGraw-Hill, New York (1998).

Sudhölter, E. J. R., Van der Wal, P. D., Skawronska-Ptasinska, M., Van den Berg, A. and Reinhoudt, D. N., "Ion-Sensing Using Chemically Modified ISFETs," *Sensors and Actuators,* Vol. 17 (1989), pp. 189–194.

Sze, S. M., *Semiconductor Sensors,* John Wiley & Sons, New York (1994).

Tieman, R. S., Heineman, W. R., Johnson, J. and Seguin, R., "Oxygen Sensors Based on the Ionically Conductive Polymer Poly(dimethyldiallylammonium chloride)," *Sensors and Actuators B,* Vol. 8 (1992), pp. 199–204.

Tsuchitani, S., Sugawara, T., Kinjo, N. and Ohara, S., "A Humidity Sensor Using Ionic Copolymer and its Application to a Humidity-Temperature Module," *Sensors and Actuators,* Vol. 15 (1988), pp. 375–386.

Udd, E., *Fiber Optic Sensors: An Introduction for Engineers and Scientists,* John Wiley & Sons, New York (1991).

Van den Berg, A., Grisel, A., Koudelka, M. and Van der Schoot, B. H., "A Universal on Wafer Fabrication Technique for Diffusion-limiting Membranes for Use in Microelectrochemical Amperometric Sensors," *Sensors and Actuators B,* Vol. 5 (1991), pp. 71–74.

Wagner, E., Danliker, R. and Spenner, K., *Sensors: A Comprehensive Survey, Vol. 6, Optical Sensors,* John Wiley & Sons, New York (1992).

Walsh, P. T. and Jones, T. A., "Calorimetric Chemical Sensors" in Göpel, W. et. al. (ed.) *Sensors: A Comprehensive Survey* Vol II. WILEY-VCH Verlag, Weinheim (1991).

Watson, L. D., Maynard, P., Cullen, D. C., Sethi, R. S., Brettle, J. and Lowe, C. R., "A Microelectronic Conductimetric Biosensor," *Biosensors,* Vol. 3 (1987), pp. 101–115.

Wenzel, S. W. and White, R. M., "A Multisensor Employing an Ultrasonic Lamb-Wave Oscillator," *IEEE Trans. Electron Devices,* Vol. ED-35, (1988), pp. 735–743.

Wenzel, S. W. and White, R. M., "Flexural Plate-Wave Gravimetric Chemical Sensor," *Sensors and Actuators A,* Vol. 21–23 (1990), pp. 700–703.

White, R. M. and Voltmer, F. W., "Direct Piezoelectric Coupling to Surface Elastic Waves," *Appl. Phys. Lett,* Vol. 7 (1965), pp. 314–316.

Wiemhöfer, H. D. and Göpel, W., "Fundamentals and Principles of Potentiometric Gas Sensors Based upon Solid Electrolytes," *Sensors and Actuators B,* Vol. 4 (1991), pp. 365–372.

Wohltjen, H., "Mechanism of Operation and Design Considerations for Surface Acoustic Wave Device Vapour Sensors," *Sensors and Actuators,* Vol. 5 (1984), pp. 307–325.

Wolfbeis, O. S., "Biomedical Applications of Fiber Optic Chemical Sensors," *Int. J. Optoelectronics,* Vol. 6, No. 5 (1991), pp. 425–441.

Wolfendale, E., (ed.), *MOS Integrated Circuit Design,* Butterworth & Co. Publishers Ltd., London (1973).

Yan, H. and Lu, J., "Solid Polymer Electrolyte Based Electrochemical Oxygen Sensor," *Sensors and Actuators,* Vol. 19 (1989), pp. 33–40.

Zhou, Q., Kritz, D., Bonell, L. and Siegel, Jr., G. H., "Porous Plastic Optical Fiber Sensor for Ammonia Measurement," *Applied Optics,* Vol. 28, No. 11 (1989), pp. 2022–2025.

CHAPTER 4

Sensing Effects

There are two basic elements in the operation of sensors. The first is the physical or chemical interaction between the environment and the sensing material altering the material properties ("sensing effect"). The second, the so-called "transduction mechanism" inside the sensor structure, converts this material property change into a useful signal that then holds information about the environment-material interaction. In this chapter, a selected group of those sensing effects will be described that may have important roles in biomedical sensors. The reason for devoting a special chapter for this description is that many sensors may be built based on similar sensing effects, although they use different transducer structures and may be used for the measurement of different parameters. Thus, we cannot distinguish all sensing phenomena according to the measurand.

4.1 THERMORESISTIVE EFFECTS

The basis of this group of phenomena is that temperature variations vary the electrical resistivity of conductor and semiconductor materials due to the temperature dependency of the concentration and/or mobility of the movable electrical charges inside them (Göpel et al., 1994).

Resistance temperature detector (RTD) is the commonly used term for temperature sensors, the operation of which is based on the positive temperature coefficient of metals (Macklen, 1979). For many metals, the resistivity via temperature characteristic, $\rho(T)$, is approximately linear within a limited range, i.e.:

$$\rho(T) = \rho_o(1 + \alpha\Delta T) \tag{4.1}$$

where ρ_o is the resistivity at a reference temperature, T_o; α is the temperature coefficient of resistance, also called *TCR,* defined as $\Delta\rho/(\rho_o\Delta T)$; and ΔT is the actual temperature difference related to T_o ($\Delta T = T - T_o$). The above phenomenon can be exploited in temperature sensors made of metal wires, and in those made of thin- and thick-film conductor materials. The largest and most reproducible TCR values can be found in materials that are free from impurities and defects. Platinum RTDs are the most known and well-

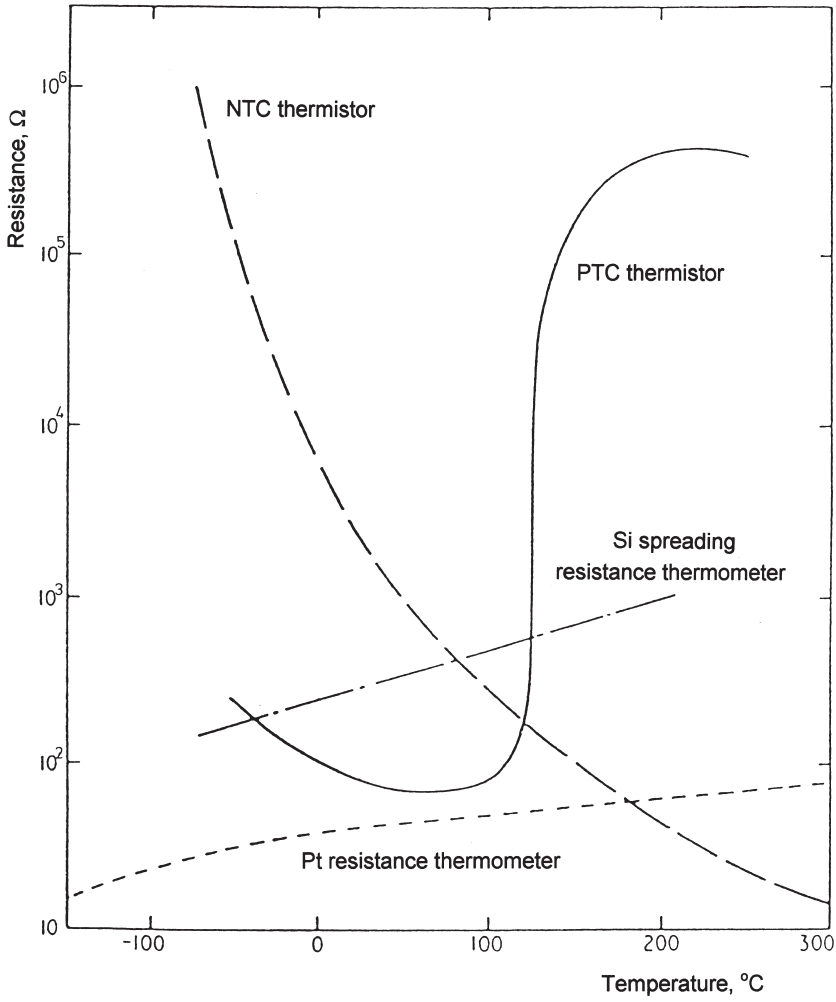

FIGURE 4.1. Typical characteristics of various temperature-dependent resistors.

standardized types, but other metals, such as copper and nickel, are also used in low-cost applications.

The term *thermistor* was introduced for temperature sensitive resistors with large temperature dependencies that were found at transition metal oxides. These simple devices are prepared by ceramic processing technology. Because a negative temperature coefficient of resistance is observed in semiconductor oxides, such as the precisely controlled mixtures of the oxides of Mn, Co, Ni, Cu, and Zn, these sensors were named NTC-thermistors. PTC-thermistors have an opposite characteristic that results from the temperature-dependent electrical properties of grain boundaries in doped piezoelectric (e.g., $BaTiO_3$) ceramic materials. Steep increases of resistance of the latter type make them particularly useful as self-regulating heating elements, current limiting devices, etc. The characteristics of the different temperature-dependent resistor types are compared in Figure 4.1.

The resistivity characteristic of NTC-thermistors can be expressed as follows:

$$\rho(T) = \rho_o \exp(B/T) \tag{4.2}$$

where B is the thermistor constant and assumes values in the range of 1500 K to 6000 K; then the $TCR = -B/T^2$ is typically in the range from -4 to -6%/K. Thus, NTC-thermistors are much more sensitive than RTDs, for which the best values are 0.68%/K for Ni and 0.392%/K for Pt (but the typical value is 0.385%/K for Pt). However, the strong temperature dependency of the *TCR* in thermistors is a feature not appreciated in a lot of applications.

Other temperature-sensitive resistors made of crystalline materials, mainly of silicon, have also been developed. Devices based on the closely linear PTC behavior characteristic for slightly doped silicon were applied in integrated

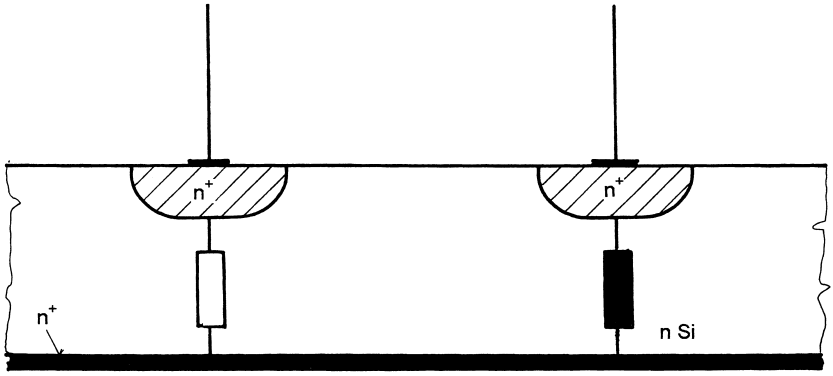

FIGURE 4.2. Schematic structure of the silicon spreading resistor thermometer.

microelectronic circuits. The structure of the spreading resistance thermometer is shown in Figure 4.2. The resistance is practically measured between two strongly doped diffusion islands as two resistor elements between them and the highly doped film on the bottom, as shown in the figure. Because silicon processing is applied, the elements may show very good reproducibility. More about thermal sensors can be found in the literature (Ricolfi and Scholz, 1990).

4.2 THERMOELECTRIC EFFECT

A thermoelement (also called a thermocouple) is a junction of two conducting (metal or semiconductor) materials, A and B, electrically connected at a "hot" point of temperature, T_1, (see Figure 4.3). The nonconnected ends of both legs are kept at another temperature T_0 ("cold" point). In an open circuit, the net current flow through the thermoelement is zero, and a thermoelectric or Seebeck voltage can be observed between the thermocouple leads at the cold point. For small temperature differences, this can be approximated as follows (Göpel et al., 1994):

$$U_s = (\alpha_A - \alpha_B)(T_1 - T_0) = \alpha_{A/B}(T_1 - T_0) \tag{4.3}$$

where α_A and α_B denote the Seebeck coefficients (thermopower or thermoelectric power) of materials A and B. They express specific transport properties determined by the band structure and the carrier transport mechanisms of the materials. U_s is always created in an electrically conducting material when a temperature gradient is maintained along the sample, but it cannot be observed with two legs of the same material for reasons of symmetry. Thermocouple sensors are widely used in practice. They are standardized and many types are available that use precious or base metal wire pairs. The stable ref-

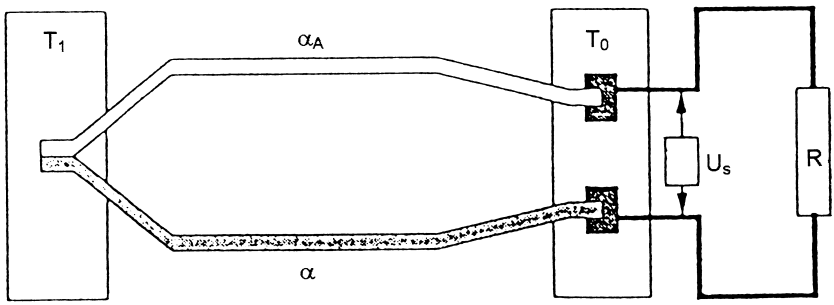

FIGURE 4.3. Schematic representation of the Seebeck effect.

erence temperature of the cold point is maintained by immersing it into a solution with melting ice. Otherwise, the application of compensating electronics is necessary (for compensating the cold point temperature variations caused by the environment). More about thermal sensors can be found in the literature (Ricolfi and Scholz, 1990).

4.3 OTHER THERMOEFFECTS USED IN SENSORS

Since almost all phenomena of nature are temperature dependent, a number of further principles are available for fabricating temperature sensors. The most important effects that are used in practical applications are as follows:

- A *temperature sensitive capacitor* can be made of dielectric materials with strong temperature-dependent permittivity: (BaSrPb)TiO_3-based ferroelectric materials are appropriate for these purposes.
- The *pyroelectric effect* enables an indirect temperature measurement through the thermal radiation emitted by the measurand object; this will be discussed in Section 4.6.
- Semiconductor *pn-junctions* show an analogous effect as thermocouples (Ristic, 1994). The different electron band structures at both sides causes a rectifying behavior of the device. This diode has a temperature-dependent voltage-current characteristic:

$$U = (kT/e) \ln(I/I_0) \tag{4.4}$$

where U is the diode voltage, I its current, k the Boltzmann constant, e the electron charge, and I_0 the reverse current. If the supply is a constant current source, the voltage is a linear function of the absolute temperature. This ideal behavior is only disturbed by the temperature dependency of I_0. This can easily be compensated in integrated circuits because I_0 is a linear function of the junction area. The latter can be multiplied when preparing several diffusion islands with the same geometry in the same silicon substrate. In this way, multi-emitter transistors can easily be prepared with an exact basis-emitter junction area ratio (A_1/A_2). When connecting them as diodes that are driven by the same current (using an analog current mirror, for example), their voltage difference will be independent of the reverse currents, and only the area ratio will appear in the result:

$$\Delta U = U_1 - U_2 = (kT/e) \ln (I_{01}/I_{02}) = (kT/e) \ln (A_1/A_2) \tag{4.5}$$

Several types of temperature-sensing ICs are based on this principle.

More about thermal sensors can be found in the literature (Ricolfi and Scholz, 1990).

4.4 PIEZOELECTRIC EFFECT

Piezoelectric effect is the production of electricity by pressure; more exactly, a polarization change via mechanical strain or stress variation (Kittel, 1981). Practically, it can be measured as a generated voltage between two electrodes. Piezoelectricity occurs only in insulating materials and is manifested by the appearance of charges on the surfaces of a piece of material that is being mechanically deformed. It is easy to see the nature of the basic molecular mechanism involved. The application of stress has the effect of separating the center of gravity of the positive charges from the center of gravity of the negative charges, producing a dipole moment. Clearly, whether or not the effect occurs depends upon the symmetry of the distributions of the positive and negative charges. This restricts the effect so that it can occur only in those material structures that do not have a center of symmetry. For a centro-symmetric crystal, no combination of uniform stresses will produce the necessary separation of the centers of gravity of the charges (Cady, 1946).

It is clear that the converse effect also exists. When an electric field is applied to a piezoelectric crystal, it will strain mechanically. There is a one-to-one correspondence between the piezoelectric effect and its converse. Those materials in which strain produces an electric field will strain when an electric field is applied.

In piezoelectric materials, the electric polarization, P, is related to the mechanical stress, T, or, conversely, the development of a mechanical strain, S, is related to an applied field, E. One can define a piezoelectric coefficient, d, relating polarization to stress and strain to field, respectively, and similarly, d^*, to the converse effect, by (Anderson et al., 1990):

$$d = (\partial P/\partial T)_E \; d^* = (\partial S/\partial E)_T \tag{4.6}$$

where subscript E indicates that the field is held constant and subscript T indicates that the stress is held constant. In other words, the piezoelectric coefficient is given by the rate of change of polarization with stress at a constant field. It can be shown by the laws of thermodynamics that $d = d^*$.

Because the polarization and electric field are vector quantities, and mechanical stress and strain are second-rank tensors, d must be a third-rank tensor. It will consist of twenty-seven elements, but based on the symmetry, only fifteen elements will be independent. How many of these will be nonzero de-

pends on the symmetry of the microstructure of the material in question. An alternative piezoelectric coefficient, g, may also be defined as follows:

$$g = -(\partial E/\partial T)_P \tag{4.7}$$

where the subscript P indicates constant polarization.

Electrical voltage generated by mechanical stress in piezoelectric materials decays due to the charge dissipation. Thus, it increases with applied force but drops to zero when the force remains constant. Voltage drops to a negative peak as the pressure is removed and, subsequently, decays to zero again, as shown in Figure 4.4. That is why piezoelectric effect can be used for dynamic processes but not for static pressure measurements in mechanical sensors.

Among the thirty-two classes of single-crystal materials, eleven possess a center of symmetry and are nonpolar. For these, an applied stress results in symmetric ionic displacements so that there is no net change in dipole moment. The other twenty-one crystal classes are noncentrosymmetric, and twenty of these exhibit a piezoelectric effect. The exception is the cubic system that possesses symmetry characteristics that combine to give no piezoelectric effect. Quartz is a classical example for piezoelectric crystals. Polycrystalline and amorphous materials in which the axes of the dipole moments are randomly oriented show no piezoelectricity. If the axes can be suitably aligned, a piezoelectric polycrystalline ceramic material [e.g., lead-zirconate-titanate (PZT) and $BaTiO_3$] or polymers [polyvinylidene-fluoride (PVDF)] can be produced (Kawai, 1969). The most important parameters of piezoelectric

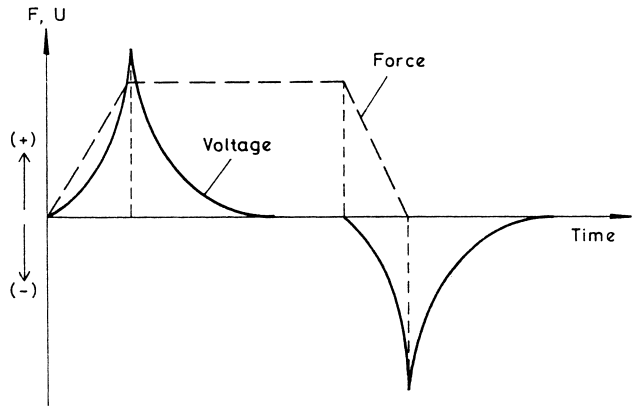

FIGURE 4.4. Typical output signal of piezoelectric devices. (Reproduced with permission from *Polymer Films in Sensor Applications* by G. Harsányi, ©1995, Technomic Publishing Co., Inc., Lancaster, PA, p. 97.)

TABLE 4.1. The Comparison of Piezoelectric Materials. (Reproduced with Permission from Polymer Films in Sensor Applications *by G. Harsányi, ©1995, Technomic Publishing Co., Inc., Lancaster, PA, p. 101.)*

Property	Unit	PVDF	Quartz	PZT	$BaTiO_3$
Density, ρ	10^3 kg/m^3	1.78	2.6	7.5	5.7
Permittivity, ϵ_r	—	12	4.58	1200	1700
$\|d_{31}\|$constant	10^{-12} C/N	23	2.3($\|d_{11}\|$)	110	78
g_{31} constant	10^{-3} Vm/N	216	—	10	5

material examples are compared in Table 4.1. More information about piezoelectricity can be found in the literature (Anderson et al., 1990).

4.5 ELECTRETS IN CAPACITIVE TRANSDUCERS

An electret is a piece of dielectric material that has permanent polarization. If the internal leakage current through the dielectric is small, the polarization remains constant for a long time. By preventing the charge neutralization effect caused by the surrounding gas molecules, for instance, keeping the electret in vacuum, the polarization acts as a built-in voltage between two electrodes. If one electrode of the capacitor is deformed by pressure, the capacitance variation with the built-in voltage induces a measurable voltage variation when connected into a circuit shown in Figure 4.5 (Baker, 1980). This is the operation principle of condenser microphones that would need a high voltage source without the application of electrets (Sessler, 1991).

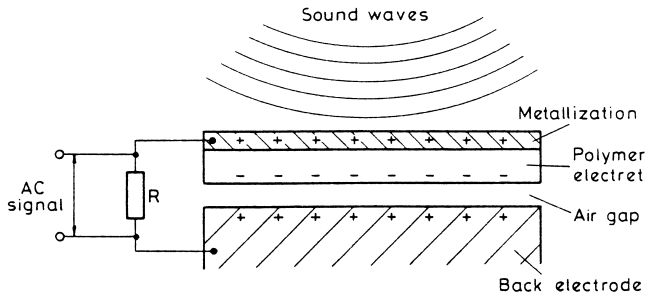

FIGURE 4.5. Operation principle of electret-based acoustic sensors. (Reproduced with permission from *Polymer Films in Sensor Applications* by G. Harsányi, ©1995, Technomic Publishing Co., Inc., Lancaster, PA, p. 104.)

Electrets can be fabricated from insulating materials using a poling process, which may be performed by field-assisted heat annealing or electron injection through corona discharge or electron beam scanning. It has been shown that the conductivity of the electron-penetrated areas rises at charge injection poling methods, but after the process, this conductivity decreases by several orders of magnitude, and the materials would require years for charge redistribution (Gross et al., 1987). The charged particles are closed into conduction traps. Levels of breakdown strength of the dielectric, not the density of trap sites, seem to limit capabilities for charge storage. The persisting behavior of the relative charge density is a function of the material. Polytetrafluorethylene (PTFE) and SiO_2 system traps retain charge indefinitely, whereas those in a number of other materials decay relatively quickly (Baker, 1980). More about electrets can be found in the literature (Baker, 1980; Sessler, 1991).

4.6 PYROELECTRIC EFFECT

When piezoelectric materials are under stress, the centers of gravity of the positive and negative charges are separated, forming an electrostatic dipole and, hence, polarizing the film. In electrets, the centers of gravity of the positive and negative charges are separated, even without applying a stress. These will exhibit spontaneous polarization, which means that there must be permanent electrostatic charge on the surfaces of the film, with one face positive and another negative depending on the direction of the polarization vector. However, the observer would not, in general, be aware of these charges because the atmosphere normally contains sufficient free positive and negative ions to neutralize the free surface charge by being attracted to and adsorbed on the surface (Whatmore, 1986).

Spontaneous polarization will be a strong function of temperature, since the atomic dipole moments vary as the crystal expands or contracts. Heating the crystal tends to desorb the surface neutralizing ions as well as change the polarization, so that a surface charge may then be detected. Thus, the crystal appears to have been charged by heating. This is called the *pyroelectric effect.*

The electric field developed across a pyroelectric crystal can be remarkably large when it is subjected to a small change in temperature. We define a pyroelectric coefficient, p, as the change in flux density, D, in the crystal due to a change in temperature, T, i.e. (Anderson et al., 1990),

$$p = \partial D/\partial T \tag{4.8}$$

Using a capacitor, the pyroelectric voltage signal ΔU is as follows:

$$\Delta U = pd\Delta T/\epsilon_r\epsilon_0 \tag{4.9}$$

where $\epsilon_r\epsilon_0$ is the permittivity, and d is the thickness of the pyroelectric film. When the temperature changes, an excess charge appears on one of the polar faces, and a current will flow in the external circuit. The sense of the current flow depends on the direction of the polarization change. After the initial surge, the current fades exponentially with time and eventually falls to zero until another temperature change comes along; this is very similar to the time-dependent behavior of piezoelectric materials.

Pyroelectric films can be used to detect any radiation that results in a change in temperature of the film but are generally used for infrared detection. Because of its extreme high sensitivity, a temperature rise of less than one-thousandth of a degree can be detected. The detector must be designed so that the heat generated by the radiation does not flow away too quickly. The performance characteristics of the sensors depend on the sensing material, the preparation and geometry of the electrodes, the use of absorbing coatings, the thermal design of the structure, and the nature of the electronic interface as well. Since the output is rate-of-change-dependent, the radiant flux incident upon the sensor must be chopped, pulsed, or otherwise modulated.

Important parameters of the materials are the heat capacity per volume, cth, the heat conductivity, gth, and the penetration depth, l, of the temperature wave in the pyroelectric material at a given modulation frequency (typically 25 Hz). In high accuracy measurements and thermovision applications these parameters have great importance; they influence sensitivity and resolution. Table 4.2 lists the most important properties for some pyroelectric materials (Ploss and Bauer, 1991). More information about pyroelectricity can be found in the literature (Anderson et al., 1990).

TABLE 4.2. Material Data for Common Pyroelectric Materials. (Reproduced with Permission from Polymer Films in Sensor Applications *by G. Harsányi, ©1995, Technomic Publishing Co., Inc., Lancaster, PA, p. 106.)*

Property	PVDF	$NaNO_2$	$LiTaO_3$	TGS*
$p(10^{-4}\ Cm^{-2}K^{-1})$	0.25	0.4	1.8	2.8
Permittivity, ϵ_r	9	4	47	38
c_{th} $(10^6\ Jm^{-3}K^{-1})$	2.3	2.2	3.2	2.3
g_{th} (W/mK)	0.14	2.2	3.9	0.65
l (μm, at 25 Hz)	28	110	90	55

*TGS = Triglycine sulphate

4.7 PIEZORESISTIVE EFFECT

It has been well known for several decades that metal films, semiconductors, and CERMET film resistors are characterized by a resistance variation when mechanical stress and/or strain is applied. This is due to the superposition of two effects: one is the resistivity change versus stress (piezoresistivity) and the other is a pure geometrical effect caused by deformation (geometrical piezoresistivity). More recently, it has been noted that polymer thick-film (PTF) resistors screened and cured on epoxy-glass or polyimide substrates present a notable sensitivity to deformation. If a mechanical stress, T, is induced on a resistor, the resistivity (ρ) change can be expressed as follows:

$$\Delta\rho/\rho = \Pi \cdot T \tag{4.10}$$

where Π is the piezoresistivity coefficient. The behavior of anisotropic single crystals (such as silicon) can be explained using a tensor form of Equation (4.10).

The deformation sensitivity of a resistor can be described with the gauge factor that is defined as the ratio of the fractional change in resistance to the fractional change in geometrical sizes (Prudenziati, 1994):

$$G = (\Delta R/R)/(\Delta l/l) \tag{4.11}$$

where l is the resistor length. If the current is parallel to the strain, the longitudinal G_L, and if the current is perpendicular to the strain, the transverse G_T gauge factors can be defined. For isotropic film resistors, their difference is determined by the Poisson ratio (ν) of the substrate and is independent of the physical properties of the resistor material:

$$G_L\text{-}G_T = 2(1 + \nu) \tag{4.12}$$

In metal film resistors, the change in resistivity is negligible. The basis of operation of a strain gage that consists of a metal alloy deposited onto flexible polymer substrates relies basically on a geometrical effect. The high gauge factor of diffused silicon and CERMET (ceramic-metal composite) thick-film resistors, however, cannot be explained by pure geometrical changes. In silicon and thick-film resistors, the real piezoresistive effect is present, which can be explained by the change of the lattice constant in silicon and by the tunneling of electrons between conductive grains in thick-film composite materials. Table 4.3 gives a comparison of the most important parameters of the different piezoresistors (Forlani and Prudenziati, 1976; Harsányi and Hahn, 1993).

TABLE 4.3 Properties of Piezoresistor Types. (Reproduced with Permission from Polymer Films in Sensor Applications *by G. Harsányi, ©1995, Technomic Publishing Co., Inc., Lancaster, PA, p. 120.)*

Resistor Type	G	TCR (ppm/°C)	Long-term Stability	Relative Cost
Metals	2	20	excellent	high
Thin films	50	0–20	very good	high
Semiconductors	50	1500	good	medium
Thick Films	10	50	very good	medium
PTF	10	500	poor	low

The piezoresistive effect is the basis of operation in the majority of mechanical sensor types, including pressure and acceleration sensors. Compared to the piezoelectric effect, the great advantage of the piezoresistive effect is that static pressure and force measurement can be accurately realized. Moreover, the interference of the pyroelectric effect is not present, however, temperature dependency and long-term stability are important parameters when designing piezoresistive mechanical sensors (Harsányi, 1991).

More information about piezoresistivity in silicon can be found in the book by Göpel et al. (1994), about piezoresistivity in thick films in the book by Prudenziati (1994), and about mechanical sensors in the book by Benedict (1984).

4.8 HALL EFFECT

The Hall effect is widely and conventionally used in several types of magnetic sensors. The basic structure is shown in Figure 4.6. Assuming that $l \gg w$, the carriers of the electric current through the conducting or semiconducting sample will flow parallel to the length at the center of the device. Therefore, an electric field perpendicular to the current direction appears to compensate the Lorentz force acting on the carriers that are moving perpendicular to the magnetic field. The Hall voltage appearing on the Hall electrodes is as follows (Ristic, 1994):

$$U_H = R_H IB/t \tag{4.13}$$

where I is the current, B the magnetic field, t the thickness of the sample, and R_H the Hall constant. The Hall voltage improves for a material with high mobility, low conductivity (e.g., GaAs, InSb), and thin device geometry. More about magnetic sensors can be found in the book by Boll and Overshott (Boll and Overshott, 1989).

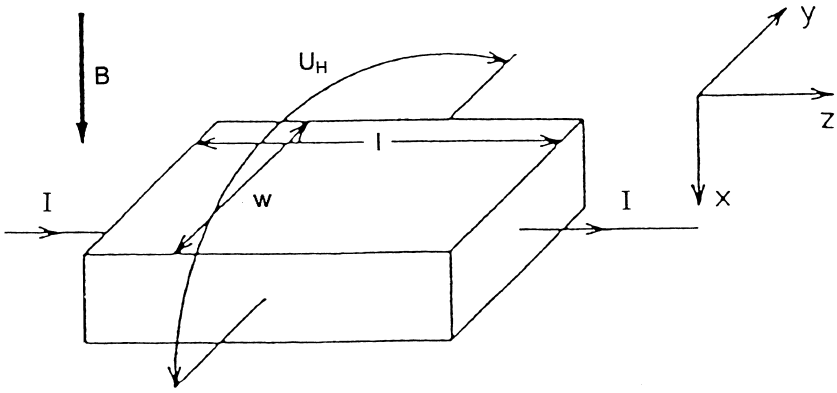

FIGURE 4.6. Schematic representation of the Hall effect.

4.9 FURTHER METHODS OF SENSING MAGNETIC FIELDS

The *magnetoresistive effect* occurs when the resistance of solid-state devices changes with the applied magnetic field (Göpel et al., 1994). There are two causes of the resistance change: change in the resistivity of the material and change in the current path of the magnetic field. In a magnetic sensor, such as a magnetoresistor, both effects contribute to the change in the resistance value. A large change in resistivity requires high mobility, and InSb is the only candidate for such magnetoresistors among semiconductor materials. On the other hand, in ferromagnetic materials, such as Ni-Co and Ni-Fe, the second type of magnetoresistive effect is commonly used because of the spontaneous magnetization of these materials in a relatively low magnetic field. The current path changes according to domain structure redistribution under varying magnetic fields.

Magnetic induction is also an obvious method for sensing a magnetic field. It can be realized by employing simple coils. According to the nature of the effect, however, only changes can be detected, or alternating fields can be measured. More about magnetic sensors can be found in the book by Boll and Overshott (Boll and Overshott, 1989).

4.10 SUPERCONDUCTING QUANTUM INTERFERENCE DEVICE (SQUID)

SQUIDs are the most sensitive devices for sensing magnetic fields; their detection limit is in the femtoTesla range. For a better understanding of the

quantum effect that is the basis of their operation, a short refresher on superconductivity seems to be unavoidable.

The superconducting state is typical for certain conducting materials at cryogenic low temperatures. Its two independent main characteristics are zero resistivity and ideal diamagnetic behavior (when a superconductor material practically excludes the magnetic field). Superconductivity can be reached near zero K in metals, but in high-temperature superconducting (HTS) ceramics, it can be reached near 100K. The great advantage of HTS ceramics is that they are already in the superconductor state when cooled with liquid nitrogen.

The corpuscular explanation of superconductivity is that the electrons are forming Cooper pairs due to the electron-phonon interaction inside the material, and these pairs have integer spin numbers. Thus, they follow the Bose-Einstein statistics instead of the Fermi statistics. The superconductive state can be destroyed not only by temperature elevation, but also by the magnetic field even when induced by the supercurrent itself, if these quantities exceed their critical values.

A special device, a Josephson junction, can be fabricated if a thin insulating layer is formed between two superconductors. Conduction through the insulation is possible by the tunneling of the Cooper pairs; this is the basis of operation. The current-voltage characteristic of the device is very sensitive to the external magnetic field and to high-frequency electromagnetic waves. The critical current density (j_c) of the junction is modulated by the external magnetic flux (Φ) passing through its area:

$$j_c = j_0 \cdot \frac{\left|\sin \frac{\pi \cdot \Phi}{\Phi_0}\right|}{\frac{\pi \cdot \Phi}{\Phi_0}} \tag{4.14a}$$

where j_0 is the value with zero external flux, and Φ_0 is the "fluxon," the quantum of the magnetic flux ($= h/2e$, here h is the Planck constant, and e is the elemental electrical charge). This variation is similar to the Fraunhofer diffraction pattern of light waves passing through a single slit, and this is why the phenomenon is called quantum interference.

A SQUID is a superconducting loop containing one or two Josephson junctions (Wikswo, 1995). A RF (radio frequency) SQUID uses a single junction that is connected into a superconducting loop; a RF current bias is inductively coupled to the SQUID to measure its impedance. A DC SQUID uses a superconducting loop with a pair of Josephson junctions, and a DC current is applied directly to the SQUID to measure the loop impedance [see Figure

5.28(a)]. The overall current (I) of the loop is a quasiperiodic function of the magnetic flux; thus, it is sensitive to magnetic field variations:

$$I = I_{01} \cdot \left| \cos \frac{\pi \cdot \Phi}{\Phi_0} \right| + I_{02} \tag{4.14b}$$

where I_{0i} represent parameters characteristics for the SQUID.

Early SQUIDs applied conventional superconductor-based Josephson junctions such as Nb/Al/AlO_x/Nb structures, while the newer ones apply HTS materials [e.g., $YBa_2Cu_3O_7$ (YBCO) or $Tl_2Ba_2CaCu_2O_8$ (TBCCO)] as thick or thin films deposited onto insulator substrates. More about SQUIDs can be found in the literature (Wikswo, 1995).

4.11 RADIATION INDUCED EFFECTS AND RELATED SENSOR STRUCTURES

The effects of various radiation types (electromagnetic and nuclear), which can be detected by sensors, can be separated into two main groups (Norton, 1982):

- *thermal effects:* the absorption of the energy transmitted by the radiation results in the increase of the temperature of the absorbing object, which enables an indirect detection (e.g., by the use of temperature sensors in bolometers, or of pyroelectric materials in pyrodetectors).
- *quantum effects:* the basis is an energy exchange between the quanta of radiation and the particles inside the sensor structure, which results in measurable changes (e.g., when photons of the radiation pass energy to electrons resulting in an ionization effect in gases or electron-hole generation inside solid-state semiconductors, or other effects)

Thermal effects require indirect transduction mechanisms based on temperature change measurements that are discussed in the previous sections. Quantum effects are different from thermal effects and will be described in this section.

At first, the effects caused by visible light and electromagnetic radiation with wavelengths near the visible ranges [i.e., infrared (IR) and ultraviolet (UV)] will be described. The quantum effect resulting in free movable electrical charge generation is used as a sensing effect in almost all photosensors. The structures of the most important types are shown in Figure 4.7:

- The conventional *photoelectron multiplier (PEM)* is a vacuum tube [see Figure 4.7(a)] applying the photoelectron emission of metal surfaces for

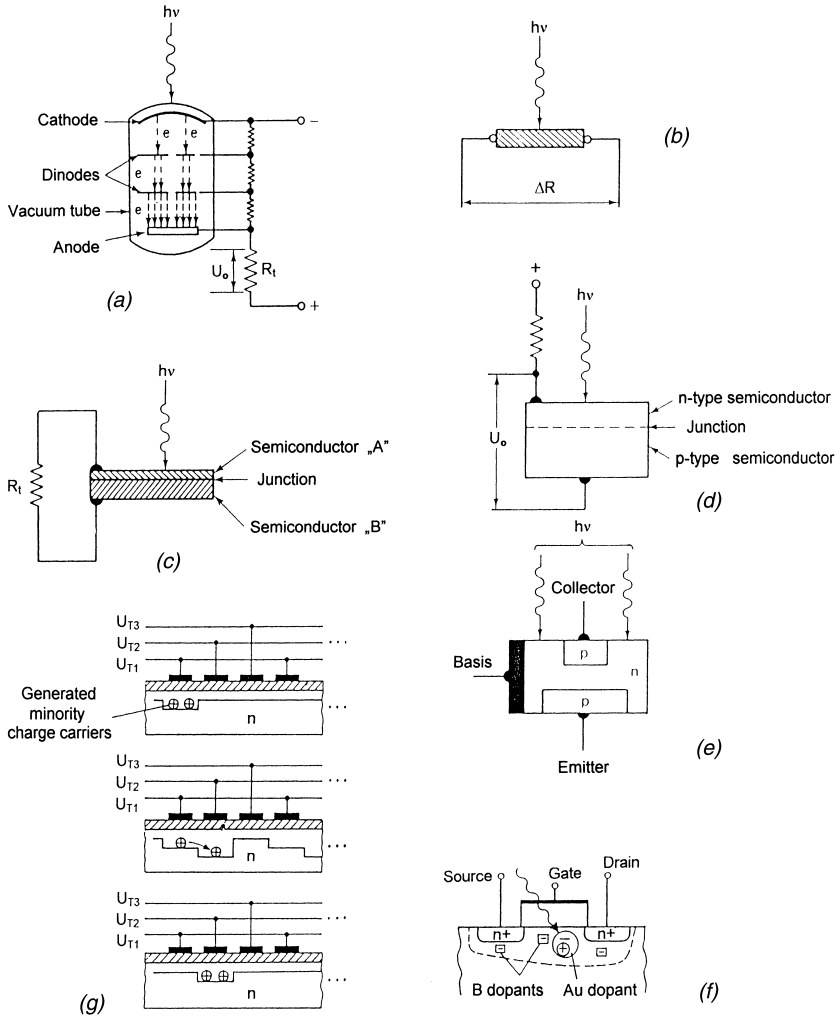

FIGURE 4.7. Basic photosensing effects and related sensor structures: (a) photoelectron multiplier (PEM), (b) photosensitive resistor, (c) photovoltaic cell, (d) photodiode, (e) phototransistor, (f) photosensitive MOSFET, and (g) charge coupled device (CCD) and its charge transfer mechanism.

transduction. Electrons are emitted from the cathode when photons impinge on it. The electrons are ejected from the cathode surface when the energy of the radiation quanta is greater then the work function of the cathode material. In the PEM tube, additional electrodes (dynodes), at subsequently higher positive potential, are located between cathode and

anode so as to amplify the electron current by means of secondary emission from the dynodes. The electrons are collected by the anode and cause a current flow that can be used to produce an output voltage impulse on the load resistor that is connected in series with the anode. Despite its large size and the necessary high voltage, the PEM has unique advantages, such as low noise and great sensitivity.

- *Photoconductive sensors* [photoresistors, see Figure 4.7(b)] are made of semiconducting materials that reduce their resistance in response to increased illumination. This change results from the electron-hole generation that is created by the absorption of the energy of incident photons. Polycrystalline films (e.g., lead salts and InSb), as well as single crystals (such as doped Ge and Si), are used as photoconductor materials. A popular example is the CdS "cell" used in many cameras.
- *Photovoltaic sensors* [see Figure 4.7(c)] are generator-type devices; they require no external excitation power. Their output voltage is a function of the illumination of a junction between two dissimilar materials. The junction acts as a potential barrier across which electron flow is excited by incident photons. Several types of material pairs exhibit the photovoltaic effect, such as Fe-Se, Cu-CuO, and polycrystalline Se-CdO (used in the popular selenium cells). Single-crystal semiconductor photovoltaic cells employing doped Si, Ge, or CdSe use a *pn*-junction as their potential barrier. In a variant of this, the junction is formed by an *n*-type glass (phosphosilicate glass) deposited on a *p*-type single-crystal silicon. The wide variety of available materials enables the creation of photovoltaic cells that are sensitive to various wavelength ranges. InAs-, InSb-, PbSnTe-, and HgCdTe-based cells are sensitive within the IR range and, in order to improve the signal-to-noise ratio, are operated at cryogenic temperatures (typically at 77 K).
- *Photodiodes* [see Figure 4.7(d)] are also based on semiconductor *pn*-junctions. They apply the current-voltage characteristic shift of the device due to the electron-hole generation caused by the absorbed light. The reverse biased current of the diode is measured. The devices have a built-in field that enables them to operate in the photovoltaic cell mode, but they perform better in the photoconductive mode. Photodiodes often apply Si or Ge *pn*-junctions and compound semiconductors with heterojunctions. Devices operated within the visible range are based on compound semiconductors
- *Phototransistors* [see Figure 4.7(e)] are light-sensitive *pnp*- or *npn*-junctions based on photodiodes but they also provide inherent amplification of the photocurrent.
- An intrinsic region (which defines the depletion layer) characterizes the *PIN diodes* between the *p*- and *n*-type regions. Their operation is based

on the excitation of electron-hole pairs in the intrinsic layer, which is caused by photons received at the surface of the *p*-type region. Because the photons are passing through the intrinsic layer generating secondary electron-hole pairs, generation efficiency is improved compared to that of the simple photodiode. The main advantage of PIN diodes is that due to the small reverse biased capacitance, they have an extremely short switching time.

- *Avalanche photodiodes (APDs)* are depletion-layer photodiodes operated with a bias voltage at which electron-hole multiplication will be induced by the avalanche effect. The avalanche effect produces significant amplification of the photocurrent with negligible noise. The operation of these devices is similar to that of the PEM tubes, and they have often been referred to as "silicon avalanche PEMs." They can be integrated with amplifier units.
- *Photosensitive MOS transistors* [see Figure 4.7(f)] can be created by an appropriate doping of the channel region (typically with Au) of a MOS transistor in order to form electron-hole generation centers inside of it. This can be detected as a threshold voltage shift and/or as a channel resistance variation (see Section 3.2).
- *Charge-coupled devices (CCDs)* are advanced sensor elements in image transfer processing (Ristic, 1994). Their structure and charge coupling operation is illustrated by Figure 4.7(g). The charge induced by the incident light can be transferred by an appropriate series of impulses given on the gate electrode system developed on the top of the MIS (metal-insulator-semiconductor) structure. The readout can be performed at a location far from the generation site.

More information about optical sensors can be read in the book by Norton (1982) and in the book by Wagner (Wagner et al., 1992).

Nuclear radiation is the emission of charged and uncharged particles and of electromagnetic radiation from atomic nuclei (Norton, 1982). Charged particles include α- and β-particles, and protons. Uncharged particles are neutrons. Gamma rays and X rays are forms of *nuclear electromagnetic radiation.*

Nuclear electromagnetic radiation photons have many effects similar to light, however, because of their higher energy, they have some specific interactions as well. The most important atomic interactions are illustrated in Figure 4.8 (Kittel, 1981):

- In the *photoelectron effect* [see Figure 4.8(a)], free electrons are generated by the incident radiation, leaving ions behind. That means generation of electron-hole pairs in solid states and ionization in gases. Secondary electromagnetic radiation may also be generated by the redistribution of electrons.

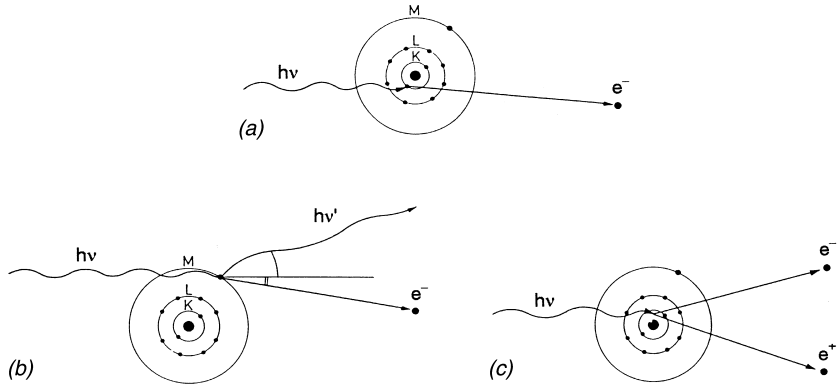

FIGURE 4.8. Corpuscular interaction mechanisms of high-energy (γ- or X-ray) photons scattering on atoms: (a) photoelectric effect, (b) Compton effect, and (c) electron-positron pair generation.

- *Compton scattering* is the elastic scattering of photons on electrons [see Figure 4.8(b)]. The Compton electron is set in motion by interaction with a photon. The energy loss of the photon results in a frequency shift. Also, the direction of movement may change.
- Gamma photons with energies above 1.02 MeV may induce *electron-positron pair generation* when scattering on the internal electromagnetic field of the atoms [see Figure 4.8(c)].

Nuclear particle radiation may result in a number of corpuscular interactions. The phenomenological sensing effects are, however, the same or very similar to those of electromagnetic radiation. They can be distinguished into the following groups (Van der Ziel, 1982):

- *ionization effect:* Incident radiation results in the ionization of gases that can be detected as a current impulse between electrodes in a closed chamber filled with a specially optimized gas mixture. The basic device for detection is called an *ionization chamber. Proportional counters* are operated at voltages high enough for multiplication; thus, the output pulses are proportional to the energy of the incident particle. *Geiger counters* are operated at higher voltages, in the Geiger plateau range, where the collected charge is entirely independent of the amount of initial ionization (Norton, 1982).
- *light emission:* Corpuscular interactions may also cause a secondary light emission. In *fluorescence quenching,* redistribution of the electrons on the outer electron shells of the excited atoms results in the emission of electromagnetic radiation. This phenomenon is used, for example, in X-ray

image amplifier tubes utilized for real-time X-ray imaging in biomedical applications. The incident X rays excite a fluorescent screen and the large area photocathode, which emits electrons due to the photoelectron effect, absorbs the emitted secondary photons. Applying appropriate electron optics allows the image to be transferred onto a monitoring screen. *Scintillation* generally means the emission of light by a photoluminescent material (called phosphor) due to the incidence of ionizing radiation upon the material. It is actually a result of real-time fluorescence excited by photoelectrons. (Compton electrons mean that there is a disturbing effect in scintillating crystals.) This phenomenon is used in scintillation detectors that consist of a scintillation material and a photosensor. PEM is an often-used transducer in scintillation detectors, however, solid-state detectors (SSDs) are preferred in new devices. A number of transducers from the SSD group, ranging from photoconductors to CCDs, have already been applied. Solid scintillation materials are also preferred in these detectors instead of classical scintillation solutions. A conventional scintillation crystal is sodium-iodide (NaI); newer types of scintillation crystals include bismuth-germanate (BGO = $Bi_4Ge_3O_{12}$) (Melcher et al., 1985), cadmium-tungstanate (CWO = $CdWO_4$) (Miyai et al., 1994), and lutetium-orthosilicate (LSO) (Melcher and Schweitzer, 1992). The detectors are often referred to using the crystals' abbreviations. For example, a BGO detector means that it is a scintillation detector using a piece of BGO crystal.

- *Electron-hole generation* in solid-state semiconductors: The effect of electron-hole generation is basically the same as that of the light sensors, but there can be difficulty in reaching the appropriate generation efficiency inside the materials. Both intrinsic Si (*i*-Si) and Ge (HPGe = high purity germanium) single crystals found applications as radiation-sensitive resistors. The advantage of Ge is its better electron-hole pair-generation efficiency, but, due to the rather large dark current, cryogenic operation temperatures should be applied. Certain compound semiconductors have also found applications in nuclear detectors, such as CdTe and CdZnTe. The sensors operated with CdZnTe material are often called CZT detectors. Extrinsic *pn*-junction detectors can also be used. A shallow diffusion *pn*-junction in Si is one of the typical structures. The other is the surface barrier type with an nSi-pSiO_2-Au multilayer structure, where the oxide is a rather thin, almost monomolecular film. The lithium-ion-drifted Si(Li) and Ge(Li) detectors are actually PIN diodes. Lithium-ions that act as high mobility donors (*n*-type dopants) are drifted into a *p*-type material in the presence of a high-electricity field and an elevated temperature (called field-assisted diffusion). The Li ions electrically compensate the acceptor sites, thus, forming an intrinsic region (Rossington

et al., 1993). These devices also should be operated at cryogenic temperatures (at 77 K).

More information about nuclear sensors can be found in the literature (Norton, 1982).

4.12 ADSORPTION AND ABSORPTION OF CHEMICAL SPECIES

A chemical microsensor can be defined as the combination of a physical transducer with a chemically selective thin film. The physical transducer by itself cannot directly detect the analyte molecules in the phase being monitored. Instead, the transducer senses changes in the physical properties of the layer on its surface. It is the sorption of analyte molecules or charged particles from the gas or liquid phase and the resulting modification of the sensed properties of the selective layer that result in the detection of the species in the measurand phase. Thus, the sensor's response is dependent on two conceptually distinct processes, sorption and transduction.

Two types of sorption can be distinguished that are useful for sensing. Adsorption is the collection of species on a surface. In absorption, adsorbed species dissolve in the bulk of the material. Absorption is dependent on the strengths of various fundamental interactions of the absorbed species and the sorbent material. Both processes are reversible, while in chemisorption, a stable new compound is formed on the surface. Thus, chemisorption is irreversible and is not useful for conventional sensor applications. (Affinity biosensors are exceptions, see Section 7.2.) In sensor applications, bulk absorption can collect a higher amount to a sensor surface than surface adsorption, thus offering higher sensitivity. In addition, sensors based on absorption have greater resistance to surface contamination that can degrade the performance of sensors that rely entirely on surface adsorption for their selectivity. On the other hand, adsorption-based sensors offer much better response times (Grate et al., 1995).

The sorbent film may produce several parameter changes:

- The sorbed species alter the overall mass of the film, thus, they also alter the overall mass of the transducer.
- Changes in electrical parameters, such as permittivity and/or resistivity, may occur.
- When charge exchanges are induced, a surface potential may develop.
- Variations in acoustic wave propagation properties may be caused.
- Changes in optical properties can also be imagined, such as refractive index or color changes, etc.

- In certain types of films (mainly polymer), the thickness of the layer may have a measurable variation due to the polymer swelling process.

The interaction between the recognition sites of the sensitive layer and the particles to be detected adjusts the concentration at the surface and in bulk sites. In adsorption and absorption processes, the concentrations within and/or on the sensitive film correspond to the concentration in the analyte after it reaches the thermodynamic equilibrium state. This effect makes it possible to obtain a signal that varies depending on analyte concentration. At adsorption, the surface coverage (the number of adsorbed molecules related to the total number of adsorption sites per unit area) of the component i, Θ_i, can be expressed conventionally by the Langmuir isotherm:

$$\Theta_i = \frac{b_i \cdot p_i}{1 + \sum_j b_j \cdot p_j} \tag{4.15}$$

where p_i represent the partial pressure values of the components that are present, and b_i represent temperature-dependent constants. This equation is somewhat more complicated when the adsorbed molecules dissociate on the surface (Mandelis and Christofides, 1993).

Bulk absorption leads to the enrichment of species in the sensitive film with respect to the gas phase. This may be described by a temperature-dependent equilibrium constant that is denoted as a partition coefficient:

$$K = c_{ab}/c_g \tag{4.16}$$

i.e., the ratio of the concentration of molecules in the film (c_{ab}) and the analyte (c_g).

Surface and bulk contributions may be separated quantitatively if the overall concentration of the molecules is related to the surface area (c_s) and is determined for the sensitive layers with various thicknesses. If the number (N) of ad- and absorbed molecules is determined experimentally by measuring the mass change (Δm) of a quartz microbalance ($N = \Delta m\, N_L/M$), the value of c_s may be calculated as follows:

$$c_s = N/A = \Delta m\, N_L/MA \tag{4.17}$$

where A is the area of the sensitive layer, N_L is the Loschmid number, and M is the molecular weight of the molecules to be detected. For combined ad-

and absorption processes, the concentration c_s is a linear function of the thickness of the layer d:

$$c_s = c_{ad} + dc_{ab} \tag{4.18}$$

Then, surface (c_{ad}) and bulk concentrations (c_{ab}) can be determined from the intercept and the slope in a c_s-d plot, respectively. More information about this topic can be found in the research conducted by Grate, Göpel, and Schierbaum (in Harsányi, 1995).

4.13 SELECTIVE MOLECULAR RECEPTORS

Polymers and supramolecular compounds play an increasing role in selective chemical sensing. They may offer extreme selectivity properties and high flexibility. Two different model systems can demonstrate the basis of selective detection. Polymers, like polysiloxanes, utilize the selective bulk absorption of molecules that corresponds to their permselective properties due to specific built-in organic side chains. Supramolecular compounds, like calixarenes that are bound generally to polymeric surfaces, utilize the incorporation of molecules in cages built of cyclic organic molecules (Schierbaum and Göpel, 1995).

The structure of polysiloxanes consists of a polymeric [RR′Si-O-] "network" with different organic groups R and R′. The geometric structure of the simplest polysiloxane with R=R′=CH_3, i.e., polydimethylsiloxane (PDMS), is well known. At very low temperatures, short-range order forces lead to a helical conformation of the Si-O chain over several atomic distances. However, the geometric structure of the polysiloxane matrix offers a statistical time-dependent structure and, hence, a distribution of recognition "sites" for organic molecules. The sites are formed by the short-range ordering of small intercepts of the RR′Si-O-chains and may turn around an individual solvent molecule [see Figure 4.9(a)].

As a "model system" of supramolecular compounds, we consider calixarenes, which consist of several aromatic rings (in particular, four rings with tertbutyl and isopropyl groups in para-position of the phenolic OH group are considered here) condensed with methylene (-CH_2-) groups to form macrocycles of different sizes [see Figure 4.9(b)]. For this relatively small calix[4]arene molecule, the geometry of the recognition site does not change significantly upon interaction with guest molecules. To a good approximation, this compound has a time-independent structure. Since the "calyx" of calix[4]arenes has a well-defined, but small, size and a limited torsion flexibility of the dihedral angle around the methylene groups, these molecules are

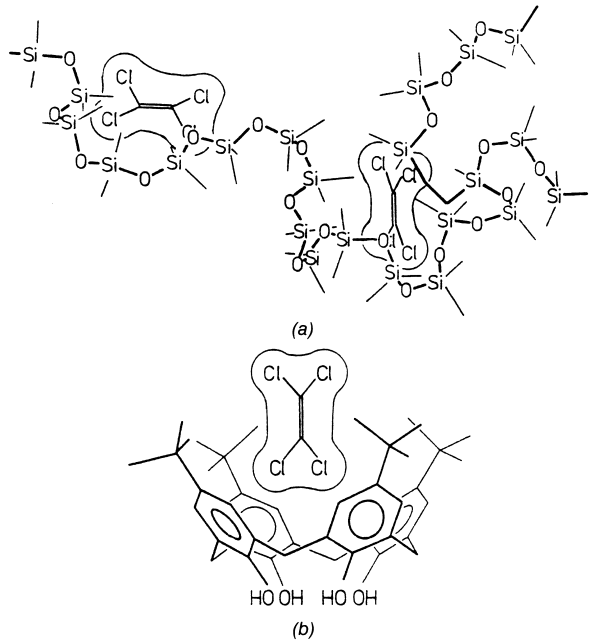

FIGURE 4.9. Examples of selective chemical sensing mechanisms: (a) selective bulk absorption in polysiloxanes and (b) molecular recognition with supramolecular cages of calixarenes (reproduced with permission from "Polymer Films in Sensor Applications" by G. Harsányi ©1995, Technomic Publishing Co., Inc., Lancaster-Basel, p. 153)

expected to exhibit a pronounced shape selectivity for the incorporation of different solvent molecules. More about this topic can be found in the literature (CIBA, 1991).

4.14 PERMEATION THROUGH MEMBRANES

Because the principal function of a polymeric membrane is to act as a variable resistance to the passage of permeating species, its most important characteristics, to which all others must be considered secondary, are permeability and permselectivity. Permeability is a measure of the rate at which a given species permeates a polymeric barrier, and permselectivity is a measure of the rates of two or more species relative to one another. The following considerations are valid mainly for gas permeation, but they can easily be applied for the other process types (Harsányi, 1995).

Permeation is a function of two factors: diffusion and solubility. Because

the solubility of various analytes within a solid membrane generally varies by less than two orders of magnitude, whereas permeability can vary by as many as five orders of magnitude, it is apparent that gas permeation is primarily a diffusion-controlled process.

The phenomenon can be described according to the model shown in Figure 4.10. The two compartments with partial pressures p_1 and p_2 are separated by the membrane. The equilibrium distribution of a vapor between the gas phase and a sorbent polymer is given by the partition coefficient defined by Equation (4.16). Accordingly,

$$p_{1M} = Kp_1 \qquad \text{and} \qquad p_{2M} = Kp_2 \tag{4.19}$$

where p_{iM} represent the partial pressures (concentrations) in boundary regions of the membrane. The particles are transported through the membrane because of the diffusion caused by the concentration difference. The material current density can be expressed according to Fick's law:

$$J/A = D(p_{1\mathrm{M}} - p_{2\mathrm{M}})/t = DK(p_1 - p_2)/t \tag{4.20}$$

where D is the diffusion coefficient, t is the thickness of the membrane, J is the material current, and A is the area of the membrane surface. The permeability constant, P, which is characteristic for a permeant system, can be de-

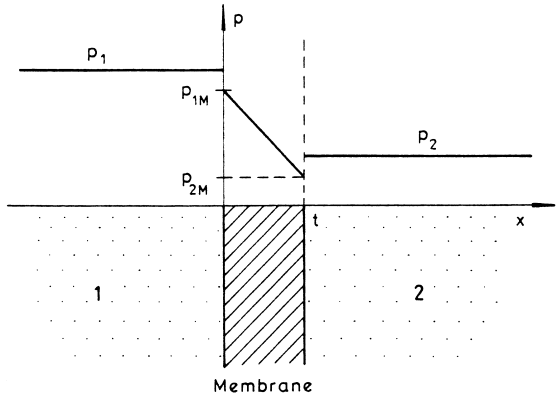

FIGURE 4.10. Schematic model of gas permeation through polymeric membranes. (Reproduced with permission from *Polymer Films in Sensor Applications* by G. Harsányi, ©1995, Technomic Publishing Co., Inc., Lancaster, PA, p. 174.)

fined as the ratio of the flux of the gas or vapor to the concentration gradient across the thickness of the membrane:

$$J/A = P(p_1 - p_2)/t \tag{4.21}$$

thus, it can be expressed with the diffusion and partition coefficients: $P = DK$.

Permselectivity can be defined as a separation factor, α_{AB}, that is, the ratio of permeabilities for components A and B:

$$\alpha_{AB} = P_A/P_B \tag{4.22}$$

More information about this topic is available in the literature (Kesting, 1971).

4.15 ION-SELECTIVE MEMBRANES

Potentiometric ion-selective electrodes are based on the development of a double layer of electrical charges on their surface. For example, in glass pH electrodes, the adsorbed film of H^+ ions and the developed neutralizing charges inside the electrode form the two layers. In thermodynamic equilibrium, the Nernstian-potential development is characteristic of the ionic activity inside the solution (see Section 3.5.1).

In the new highly selective polymer membranes, an ion penetration into the membrane material should be supposed (Armstrong and Horvai, 1995). The ion-membrane interaction has a determining role in the development of the electrode potential. These polymer membranes generally consist of the following compounds:

- A polymer is the basis material (generally PVC).
- Plasticizers primarily provide the required mobility for sufficient fast kinetics of the ion exchange and/or ion extraction at the phase boundary of the membrane and the sample. To some extent, plasticizers may also take part in and influence the stability of the ion/ionophore complex, thus influencing the selectivity pattern of the membrane.
- Ionophores introduce the desired electrochemical properties; they can form complexes with the ion to be sensed selectively. Conventionally, ion-exchanger salts were used for this purpose; currently, neutral ion carrier ligands are preferred.
- A salt of the primary ion must be present for the reversible operation.
- Other compounds on and/or under the membrane, such as supramolecular receptors, permselective films, hydrogels, polyelectrolites, or electroconductive polymers may also be added in order to improve selectivity and stability properties.

The ion/ionophore complexion process is responsible for the double-layer formation and, thus, for the Nernstian electrode potential response. The possible mechanism types are as follows:

- in the case of ion exchangers

$$I_{o1}I_{o2}(M) + I^{+}(W) + C^{-}(W) \Longleftrightarrow I_{o1}{}^{-}I^{+}(M) + I_{o2}{}^{+}(W) + C^{-}(W) \quad (4.23)$$

- using neutral ion carriers

$$L(M) + H_2O(W) + I^{+}(W) \Longleftrightarrow IL^{+}(M) + OH^{-}(M) + H^{+}(W) \quad (4.24)$$

where I is the ion to be detected, C is its counterion in the solution, I_o is the ion exchanger, L is the ligand neutral carrier, and W and M refer to the aqueous and membrane phase, respectively.

In newer ion-selective sensors, the application of neutral ion carriers is preferred. They do not disturb the analyte composition due to the ion extraction and their complexing mechanism is based not only on simple electronegativity but on secondary chemical bonding forces due to their molecular structure as well. Thus, better selectivity properties can be reached. A wide selection also enables the sensing of a variety of simple and complex ion types. More about ion-selective membranes can be found in the research conducted by Armstrong and Horvai [in the book by Harsányi (1995)].

4.16 CHEMICAL-OPTICAL TRANSDUCTION EFFECTS

Fiber-optic sensors are based on a great variety of transduction effects; a complete description of them is not possible here. However, the most important chemical transduction effects can be distinguished in a few well-defined groups (Harsányi, 1995) as follows.

Colorimetric sensors can be built from materials showing color changes for some kind of environmental effect. This can be measured as an absorbance variation of an active film. *Optical ion sensors,* mostly ion optrodes, are based on the ion-concentration-dependent changes of optical properties in thin ion-permeable films. Colorimetric pH sensors can easily be fabricated directly from acid base indicators or from their combination. The indicator dye molecule when protonated is in its acidic form, HI, and is always in equilibrium with its base form, I^{-}, through the process $HI \leftarrow K \rightarrow I^{-} + H^{+}$, where K is the chemical equilibrium constant. According to the definition of pH, the following relationship exists: $pH = pK - \log([HI]/[I^{-}])$, where pK is the negative log-

arithm of the equilibrium constant K, and the angular brackets represent concentrations. Figure 4.11 shows, as an example, the pH-dependent absorbance spectra of phenol red. The largest sensitivity value can be reached near the 540 nm wavelength; thus, the light source LED should be operated around this wavelength. This type of optrode may be operated within the pH range of 6–8. The absorbance [$A = \ln(I_{in}/I_{out})$, I denotes light intensity] via pH characteristic is given in Figure 4.12. Supposing that the absorbance changes are due to the scattering on acid formed dyes, and putting its concentration [I^-] into the Lambert-Beer equation [see Equation (3.9)], their relationship can be expressed as follows:

$$\mathrm{pH} = \mathrm{pK} - \lg[hcl/\ln(I_{be}/I_{ki}) - 1] \tag{4.25}$$

where h is the extinction coefficient, l is the path length inside the medium containing the indicator, and c is the total concentration of the indicator dye

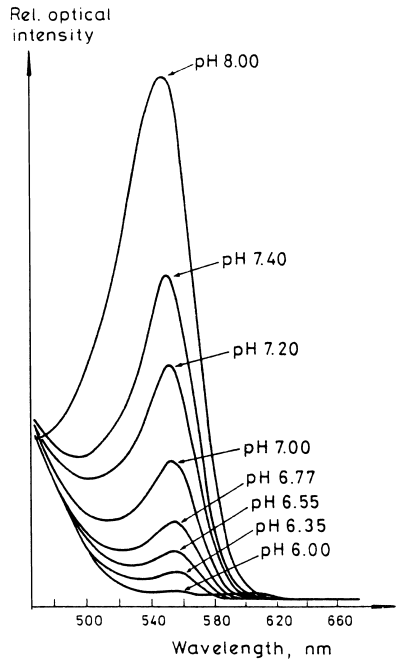

FIGURE 4.11. Absorption spectra of phenol red indicator dye as a function of the pH-value. (Reprinted from *Sensors and Actuators B,* T. Hao, X. Xing and Ch.-Ch. Liu, "A pH Sensor Constructed with Two Types of Optical Fibers: The Configuration and Initial Results," 10, pp. 155–159, ©1993, with permission from Elsevier Science S.A., Lausanne, Switzerland.)

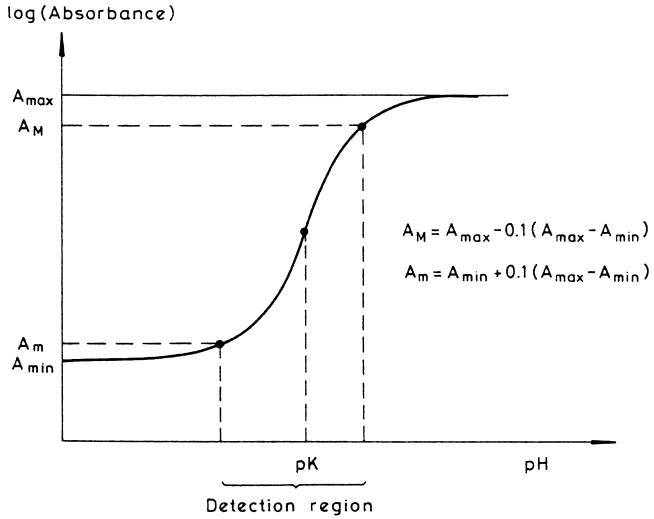

FIGURE 4.12. Typical absorbance-pH characteristic of colorimetric indicators. (Reproduced with permission from *Polymer Films in Sensor Applications* by G. Harsányi, ©1995, Technomic Publishing Co., Inc., Lancaster, PA, p. 201.)

$\{c = ([HI] + [I^-])\}$. The practical meaning of pK is that $pK = (A_M + A_m)/2$, where A_M and A_m are explained in Figure 12.

The most important problems of this type of optrode sensor can be summarized as follows:

- The detection range is quite narrow; in some applications (e.g., in the case of blood pH measurements) this is advantageous, but in others (e.g., in the case of wide gastric pH ranges), it makes the measurements impossible, thus, the application of indicator mixtures is necessary in the latter cases
- Only indicators with reversible operation capabilities can be used.
- Indicator dyes should be immobilized in order to prevent their dissolution; the best approach is chemical (covalent) immobilization which results in absorbance spectra shifts (pK adjustment, see Section 6.1.4).
- The colorimetric change is a direct function of the ion concentration in contrast to the electrodes, the electrode potential of which depends on the ion activity [see Equations (3.4) and (3.5)].

Various types of colorimetric ion optrodes can be produced when both an ion-selective ionophore and a pH indicator are entrapped in a polymer matrix as functional additives. The potential that arises from the complexation of reactive ions (I) with the ionophore (L) in the membrane is compensated by the

coextraction of protons by the indicator (Ind). The process can be illustrated by the following reaction scheme:

$$L(M) + Ind(M) + H_2O + I^-(W) \leftrightarrow LI^-(M) + OH^-(W) + IndH^+(M) \quad (4.26)$$

The ion concentration in the solution is, therefore, correlated with the amount of protons in the membrane and can be detected spectroscopically by the protonation of the indicator. The counterreaction, the deprotonation of a pH indicator entrapped in a polymer matrix, can also be used for the detection of ions:

$$L(M) + Ind^-H^+(M) + I^+(W) \leftrightarrow LI^+(M) + Ind^-(M) + H^+(W) \quad (4.27)$$

Gas and humidity sensors can be operated with acid-base indicators by means of further indirect sensing mechanisms. Currently, direct operation chromoionophores that may follow the concentration of the primary ion by direct color changes without applying any pH indicators are also available.

Fluorescent optrodes utilize the fluorescence quenching of special indicator dyes. In these cases, incident light excites a secondary light emission (see Section 4.11) with a different wavelength. Several sensor types were developed for measuring the partial pressure of molecular oxygen in liquids, for instance, in blood. The fluorescent dye, such as perylene dibutyrate, is absorbed to organic beds contained within a hydrophobic gas permeable membrane, such as porous polyethylene tubing. The dye is excited with blue light (468 nm) and it emits radiation at 514 nm (green). The oxygen partial pressure can be calculated according to the Stern-Volmer equation:

$$pO_2 = A[(I_{blue}/I_{green}) - 1]^m \quad (4.28)$$

where A and m are empirical constants. Fluorescent dyes can also be applied for pH measurements and in other ion-selective optrode types.

Phosphorescence is different from the former effect in that the time decay of the secondary light emission is long enough to allow operation of the optrode even as a light source after the excitation.

The *chemiluminescence* effect can also be used in sensors. The basis of the phenomenon is a catalytic chemical reaction resulting in light emission. It is a generator-type sensing effect and can be operated without applying an external light source. If the reagents are present in high enough concentrations, a continuous light emission can be measured, the intensity of which is a func-

tion of the analyte concentration. The enzyme, if necessary, should be immobilized on the optrode tip. The general reaction scheme is as follows:

$$\text{Reagents} \xrightarrow{\text{enzyme}} \text{Products} + h\nu \tag{4.29}$$

A familiar example of chemiluminescence comes from the firefly, which uses the enzyme luciferase. In the presence of Mg^+ and the substrate luciferin, ATP is utilized in the following reaction (Gautier et al., 1990):

$$\text{ATP} + \text{luciferin} + O_2 \xrightarrow{\text{luciferase}} \text{Products} + \textit{light}\ (560\ nm) \tag{4.30}$$

This is a typical enzymatic reaction that is characteristic for a group of biosensors that will be discussed in Section 7.1.

Light refraction (see Section 3.6) and/or interferometry are obvious ways to build up sensor elements. The refractive index and the geometrical path length determine the optical path length in a given medium. Changes in any of the parameters result in a phase shift, which can be detected by interferometry.

Polysiloxane polymers seem to present these properties and can be used successfully in chemical-sensor applications. Polysiloxanes have been investigated for several years as possible sorbent dielectric films in gas sensors. They are able to alter their permittivity and/or their film thickness when absorbing molecules from the surrounding gases. The close connection between the refractive index (n) and permittivity (ϵ_r) is well known and can be expressed as follows:

$$n^2 = \epsilon_r \tag{4.31}$$

Therefore, the refractive index of the polymeric film varies with the permittivity as the vapor to be detected is absorbed. The Clausius-Mosotti equation,

$$\frac{n^2 - 1}{n^2 + 2} = \frac{4 \cdot \pi}{3} \cdot \frac{\rho}{M} \cdot p_m, \tag{4.32}$$

can be used as an approximation. It can be seen that a variation of the molecular polarizability, p_m, of the density ρ, and/or of the molecular weight M, leads to a variation of the refractive index of the polymer film. Moreover, polysiloxanes may show considerable swelling when they absorb gas molecules; therefore, the films can alter their thickness according to the absorbed amount

of gases, which may also be a useful effect in interferometric sensors (see Section 4.6).

More details about optical transduction effects can be found in the literature (Udd, 1991; Dakin and Culshaw, 1988).

4.17 REFERENCES AND SUPPLEMENTARY READING

Anderson, J. C., Leaver, K. D., Rawlings, R. D. and Alexander, J. M., *Materials Science,* Chapman and Hall, London (1990).

Armstrong, R. D. and Horvai, G., "Polymers in Ion-Sensitive Membranes," in Harsányi, G., *Polymer Films in Sensor Applications,* Technomic Publishing Co., Inc., Lancaster, PA (1995), pp. 182–199.

Baker, W. O., "Polymers in the World of Tomorrow," *Proc. of the Symp. at the 2. Chemical Congress of the North American Continent,* Las Vegas, NV (1980), pp. 165–202.

Benedict, R. P., *Fundamentals of Temperature, Pressure and Flow Measurements,* 3rd Ed., John Wiley & Sons, New York (1984).

Boll, R. and Overshott, K. J., *Sensors: A Comprehensive Survey, Vol. 5, Magnetic Sensors,* John Wiley & Sons, New York (1989).

Cady, W. G., *Piezoelectricity,* McGraw-Hill, New York (1946).

CIBA Foundation Symposium, *Host-Guest Molecular Interactions: From Chemistry to Biology-Symposium, No. 158,* John Wiley & Sons, New York (1991).

Dakin, J. and Culshaw, B. (ed.), *Optical Fiber Sensors: Principles and Components,* Artech House, Boston, MA (1988).

Forlani, F. and Prudenziati, M., "Electrical Conduction by Percolation in Thick Film Resistors," *Electrocomp. Sci. and Techn.* Vol. 3 (1976), p. 77.

Gautier, S. B., Blum, L. J. and Coulet, P. R., "Alternate Determination of ATP and NADH with a Single Bioluminescence-Based Fiber-Optic Sensor, *Sensors and Actuators B,* Vol. 1 (1990), pp. 580–584.

Göpel, W., Hesse, J. and Zemel, J. N. (ed.), *Sensors: A Comprehensive Survey,* Vol.1-6, WILEY-VCH, Weinheim (1994).

Grate, J. W., Abraham, M. H. and McGill, R. A., "Sorbent Polymer Coatings for Chemical Sensors," in Harsányi, G., *Polymer Films in Sensor Applications,* Technomic Publishing Co., Inc., Lancaster, PA (1995), pp. 136–149.

Gross, B., Gerhard-Multhaut, R., Berrassioul, A. and Sessler, G. M., "Electron-Beam Poling of Piezoelectric Polymer Electrets," *J. Appl. Phys.* Vol. 62, No. 4 (1987), pp. 1429–1432.

Harsányi, G., "Polymer Thick-Film Technology: A Possibility to Obtain Very Low Cost Pressure Sensors," *Sensors and Actuators A,* Vol. 25–27 (1991), pp. 853–857.

Harsányi, G., *Polymer Films in Sensor Applications,* Technomic Publishing Co., Inc., Lancaster, PA (1995).

Harsányi, G. and Hahn, E., "Thick-Film Pressure Sensors," *Mechatronics,* Vol. 3, No. 2 (1993), pp. 167–171.

Kawai, H., "The Piezoelectricity of Polyvinylidene Fluoride," *Japan J. Appl. Phys.,* Vol. 8 (1969), pp. 975–976.

Kesting, R. E., *Synthetic Polymeric Membranes,* McGraw-Hill, New York (1971).

Kittel, C., *Introduction to Solid State Physics,* John Wiley & Sons, New York (1981).

Macklen, E. D., *Thermistors,* Electrochemical Publications, Ayr (1979).

Mandelis, A. and Christofides, C., *Solid State Gas Sensor Devices,* John Wiley & Sons, New York (1993).

Melcher, C. L. and Schweitzer, J. S., "Ceruim-Doped Lutetium Orthosilicate: A Fast, Efficient New Scintillator," *IEEE Transactions on Nuclear Science,* Vol. 39 (1992), pp. 502–504.

Melcher, C. L., Schweitzer, J. S. and Liberman, A., "Temperature Dependence of Fluorescence Decay Time and Emission Spectrum of Bismuth Germanate," *IEEE Transactions on Nuclear Science,* Vol. 32 (1985), pp. 529–532.

Miyai, H., Kawasaki, S., Kitaguchi, H. and Izumi, S., "Response of Silicon Detector for High Energy X-ray Computed Tomography," *IEEE Transactions on Nuclear Science,* Vol. 41 (1994), pp. 999–1003.

Norton, H. N., *Sensor and Analyzer Handbook,* Prentice Hall, Englewood Cliffs, NJ (1982).

Ploss, B. and Bauer, S., "Characterization of Materials for Integrated Pyroelectric Sensors," *Sensors and Actuators A,* Vol. 25–27 (1991), pp. 407–411.

Prudenziati, M., *Thick Film Sensors,* Elsevier Science, Amsterdam (1994).

Ricolfi, T. and Scholz, J., *Sensors: A Comprehensive Survey, Vol. 4, Thermal Sensors,* John Wiley & Sons, New York (1990).

Ristic, L., *Sensor Technology and Devices,* Artech House, Boston, MA (1994).

Rossington, C. S., Fine, P. M. and Madden, N. W., "Large Area, Low Capacitance Si(Li) Detectors for High Rate X-ray Applications," *IEEE Transactions on Nuclear Science,* Vol. 40 (1993), p. 354.

Schierbaum, K. D. and Göpel, W., "Selective Chemical Sensing: Molecular Recognition with Polymeric Layers and Cage Compounds," in Harsányi, G., *Polymer Films in Sensor Applications,* Technomic Publishing Co., Inc., Lancaster, PA (1995), pp. 149–172.

Sessler, G. M., "Acoustic Sensors," *Sensors and Actuators A,* Vol. 25–27 (1991), pp. 323–330.

Udd, E., *Fiber Optic Sensors: An Introduction for Engineers and Scientists,* John Wiley & Sons, New York (1991).

Van der Ziel, A., *Solid State Physical Electronics,* Prentice Hall, Englewood Cliffs, NJ (1982).

Wagner, E., Danliker, R. and Spenner, K., *Sensors: A Comprehensive Survey, Vol. 6, Optical Sensors,* John Wiley & Sons, New York (1992).

Whatmore, R. W., "Pyroelectric Devices and Materials," *Rep. Prog. Phys.,* Vol. 49 (1986), pp. 1335–1386.

Wikswo, J. P., Jr., "SQUID Magnetometers for Biomagnetism and Nondestructive Testing: Important Questions and Initial Answers," *IEEE Transactions on Applied Superconductivity,* Vol. 5, No. 2 (1995), pp. 74–81.

CHAPTER 5

Physical Sensors and Their Applications in Biomedicine

This chapter deals with physical sensors and their applications in biomedical measuring devices, in artificial organs, and in small personal and clinical, and large diagnostic appliances. Our approach is to provide a technical description of the sensor elements and their application problems. The basics of diagnostic and medical imaging techniques and their physiological relations are not discussed here.

5.1 MEASURING TEMPERATURE

Temperature is one of the most closely controlled variables of the human body. Its regulatory system is extremely efficient and capable of maintaining interior body temperature within a range of ± 0.5°C. The inner (core) temperature is almost independent of the exterior environment, even when exposed to extreme conditions; it is about 37°C for a healthy person. As in any regulated system, thermal control is based on a feedback mechanism. It must include a reference (a substance needed to determine the "set point"), temperature sensing elements (warm and cold receptors located in the skin), actuators (the organs capable of generating or losing heat: muscles, skin, lungs, etc.), and a central controlling module (the hypothalamus). The nature of the reference temperature is presently not clear. One hypothesis (Fraden and Bochkov, 1976) suggests that the structure of water may determine the reference temperature. Structural changes are reflected in the specific heat curve of water, which has a minimum value near 37°C.

There are several distinct areas of interest in medical thermometry that are pursued using different methods:

- Body (near-core) temperature measurement is a venerable, routine diagnostic method. Fever is a result of toxic substances and viral and bacterial diseases that affect the hypothalamus.
- Skin or surface temperature reflects the condition of subcutaneous tissues. Surface temperature distribution measurement, applying thermal imaging equipment, can be used for detecting tumors, especially breast tumors, that exhibit slightly elevated temperatures (hyperthermia) in the surrounding tissues. On the other hand, reduced big-toe temperature (hypothermia) is a good early indicator of shock in anesthesiology.
- Blood temperature is almost equal to the core temperature. Its measurement is performed intravascularly; this is almost always obtained with other measurements by using multisensor catheters. The role of the temperature sensor often is the temperature compensation of other sensor signals.

Basics of temperature measurements are summarized in the literature (Fraden, 1991).

5.1.1 Measuring Core Temperature

Because skin temperature cannot directly be correlated with interior body temperature, *body (core) temperature* measurement is traditionally performed inside a body cavity: orally, rectally, or under the arm. These measured cavity temperatures may vary from the "true" core temperature depending on a number of physiological and environmental effects. An old and traditional device used for body temperature measurement is the mercury thermometer that does not contain sensors (see Chapter 1). Its drawbacks are slow operation and difficult reading and registration of the result; furthermore, it can easily be broken and poison the environment. However, its application is widespread because it is a low-cost device.

Microelectronics and related modern mounting processes of the electronics technology enabled the production of low-cost electronic thermometers with digital displays to replace mercury thermometers. Their application is already widespread. They generally contain diodes as temperature-sensing elements with a special package design that can assure small thermal capacity and good thermal conductivity to the environment. They have relatively short response times and good visible display units, but they require the use of batteries. More complicated versions for clinical use may also contain intelligent functions, such as storage and readout facilities for computer data processing. Long-life batteries enable up to a three-year operation.

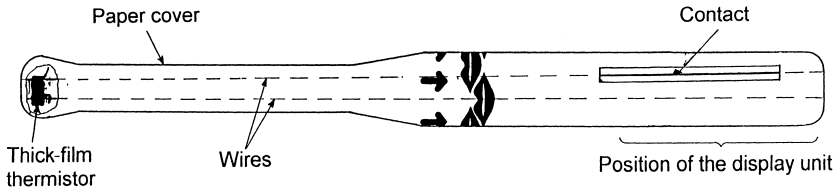

FIGURE 5.1. Structure of a disposable oral thermometer.

Nowadays, very low-cost, disposable oral thermometers are available for clinical use (see Figure 5.1) This type of thermometer consists of a small-size thick-film thermistor and two wires between two appropriately shaped and impregnated paper pieces that are attached. The contact area can be pushed into the display unit during measurement. The application of thermistors avoids polarity problems. A limiting requirement is the interchangeability of the disposable elements. On the other hand, long-term operation is not needed; thus, the low-cost packaging solution demonstrated here is appropriate.

All contact measurement methods discussed above require a significant degree of patient cooperation, which is not always the case in medical practice, especially when dealing with babies and unconscious patients. Although skin temperature varies from the core value and exact measurement is not possible when using simple surface contact, temperature variations can be monitored continuously. For such purposes, simple meandrous copper resistor thermometers can be used that are etched from a flexible printed wiring board (PWB) copper cladding (see Figure 5.2). Other electrodes, for example for ECG, may also be integrated onto the same flexible PWB substrate and the whole structure can be fixed onto the body by means of an elastic belt. The system was developed for a baby monitoring system to prevent sudden infant death (Hubin et al., 1993).

All *contact methods* have disadvantages in that the measured temperature varies from the "true" core temperature. One can measure various values by

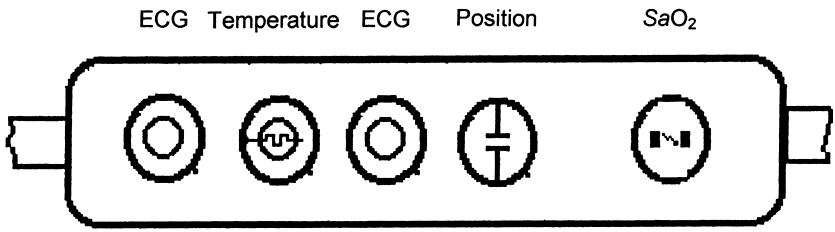

FIGURE 5.2. Resistor thermometer and ECG electrodes on a flexible printed wiring board substrate. (Reproduced with permission after Hubin et al. from *Proceedings SENSOR 93,* Vol. I.)

choosing different measurement sites. Results also depend on physical and mental activities of the patient and environmental conditions. While perspiring, skin temperature is considerably decreased. Oral temperatures can be affected by respiration, food, or speech. Underarm measurement time may be relatively long due to a poor coupling between the probe and dry skin.

Ideally, the probe should be positioned in a body cavity that is not affected by the mentioned interferences and is reasonably clean and easily accessible. Close proximity to the hypothalamus is also preferred. The auditory canal is a near perfect cavity to use to obtain for body temperature measurements. Tympanic membrane temperature is the most accurate approximation of body core temperature. In addition, the ear canal acts as an ideal black object in the term of radiation. Measuring its emitted infrared radiation intensity, temperature can be calculated. The block diagram of an ear thermometer is shown in Figure 5.3 (Fraden, 1991). This version is based on a pyroelectric sensor. Thermal radiation flux from the auditory canal is channeled by the optical waveguide toward the pyroelectric sensor. When pressing the start button, the shutter opens momentarily, exposing the sensor to thermal radiation and replacing the radiation coming from the shutter itself. An ambient temperature sensor element is behind the shutter. The radiation reaches the sensor where it is converted into electric current impulse due to the pyroelectric effect (see Section 4.6). A current-to-voltage converter feeds its output voltage into the multiplexer (MUX) and then into the A/D converter that also reads the ambient temperature sensor signal. Calculation of the temperature of the radiating element continues in the microprocessor. The sensor element has a dual struc-

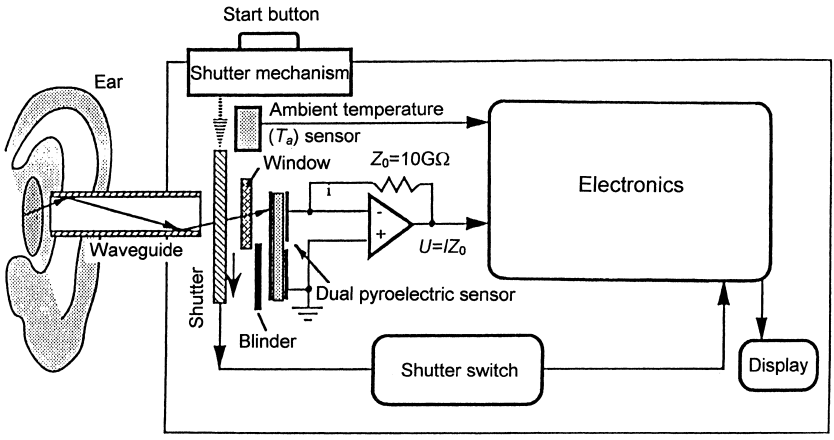

FIGURE 5.3. Block diagram of a pyroelectric radiation ear thermometer. (Reprinted after Fraden, 1991, p. 546, courtesy of Marcel Dekker, NY.)

ture to compensate the pyroelectric signals caused by ambient temperature changes. Ceramic- and polymer-based sensor elements have been used within these types of appliances that have been available on the market since 1986 for clinical and personal use. The obvious disadvantage of pyroelectric sensors is the necessity of employing moving elements. Thermopile sensors have also been used in radiation thermometers. These are sensors consisting of thin, alternating layers of metals acting as serially connected thermocouples. A heat absorbing black layer is deposited above the hot points, while the cold points are kept at the ambient temperature. A multiplied thermovoltage can be measured at the output, which is a function of radiation impinging the absorbent film.

Telemetry temperature measuring systems also became available; they were especially designed for animals (Sugiura et al., 1991), but recently are also used in human applications, e.g., for astronauts. NASA developed an ingestible temperature-monitoring capsule for this purpose. The epoxy shell capsule covered with an outer silicone coat contains a miniature battery, a communication coil, PWB and hybrid circuit assemblies on ceramic substrates, and the temperature sensing element: a resonator crystal oscillating at a temperature-dependent frequency.

5.1.2 Surface Temperature Mapping

Surface (skin) temperature distribution can be determined by thermal imaging using mainly infrared cameras. A thermograph is essentially a picture taken in the thermal radiation spectral range and converted into the visible range for observation and analysis. Using digital picture processing, isotherm lines can also be displayed.

Design of a high-performance electronic infrared camera is usually based on an array of bandgap semiconductor (e.g., HgCdTe) sensors housed in a liquid-nitrogen-filled Dewar enclosure. The sensors are shielded from visible light by an infrared-only transparent window (Si or Ge). At room temperatures, self-radiation of the sensor elements is enough to generate photoelectron-hole pairs; thus, the dark current is extremely high. To get a reasonably better sensitivity and signal-to-noise ratio, cryogenic operation is necessary.

A thermal imaging camera operating at room temperature can be built using pyroelectric materials. The structure of the pyroelectric vidicon (PEV) is shown in Figure 5.4. The photocatode of a conventional vidicon camera is replaced by a pyroelectric film that generates electrical charge superimposed on the thermal image. The face of the receiving tube is an infrared transmitting window. Imaging radiation impinges on the pyroelectric film and an electron beam reads out the charge created. The charge density is then displayed simultaneously with the scanning. The disadvantages of PEV are its compli-

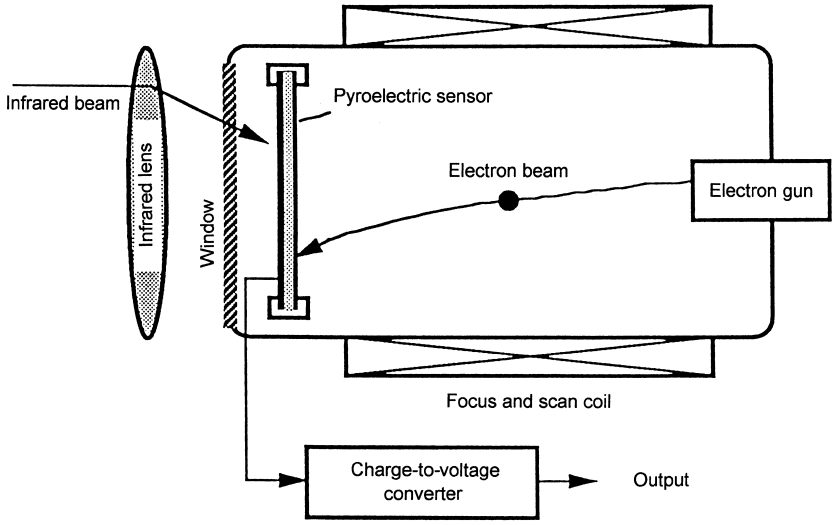

FIGURE 5.4. Structure of the pyroelectric vidicon camera. (Reprinted after Fraden, 1991, p. 523, courtesy of Marcel Dekker, NY.)

cated and large structure sensitive to mechanical effects due to the piezoelectric behavior.

Because the use of CCDs is widespread in cameras, their application in thermal imaging is also desirable. Cooled infrared cameras have been designed recently using platinum silicide gate CCDs. Their application has, however, not overcome the cooling problem. Typical pixel numbers are 640×480.

Increased need for thermal imaging has accelerated the development of solid-state uncooled mosaic sensor arrays. One approach is the fabrication of *pyroelectric detector arrays* on the surfaces of silicon chips. Cross-talk problems become more difficult to overcome with miniaturization; PVDF seems to be a good pyroelectric material within these structures because of its low thermal conductivity (see Table 4.2). In Figure 5.5(a), the typical realization of a sensor array using a PVDF film on the silicon IC surface is presented. Its circuit connection is illustrated by Figure 5.5(b) (von Münch and Thiemann, 1991). A *p*-well CMOS process with aluminum gates (see Section 2.1) is used. New technology for integrating high-value gate resistors as *p*n-junctions operated at zero bias has also been developed.

The sensors are coupled to an impedance-matching preamplifier with a MOSFET input. A bias resistor for each element is useful in order to eliminate the influence of temperature variations of the whole detector. This resistor is also necessary for adjusting the operating point of the MOSFETs. Special attention has to be paid to these resistors. The basic requirement is that

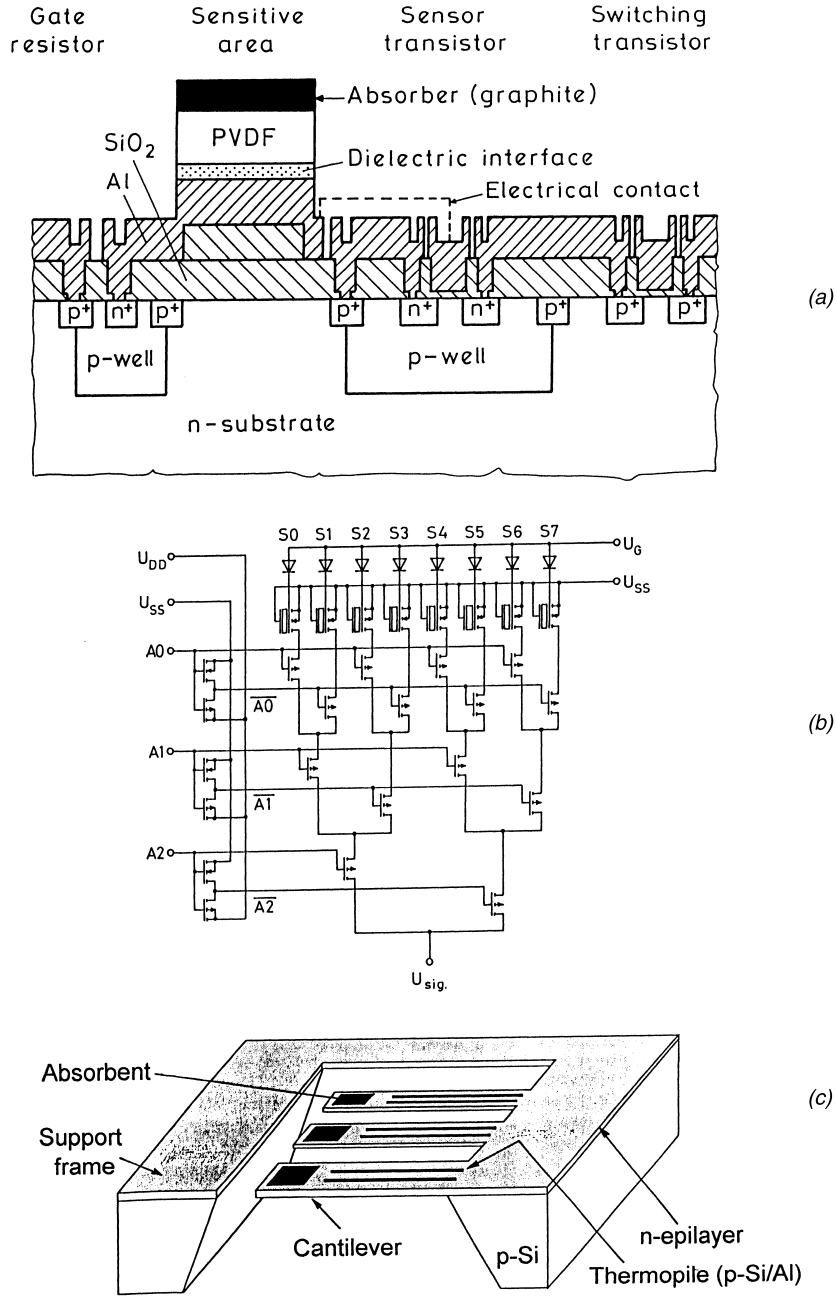

FIGURE 5.5. Noncooled integrated infrared detector arrays realized on a silicon substrate: (a) cross section and (b) circuit diagram of the pyroelectric sensor array, and (c) sensor array based on silicon micromachining [(a) and (b) are reprinted from *Sensors and Actuators A,* W. von Münch and U. Thiemann, "Pyroelectric Detector Array with PVDF on Silicon Integrated Circuit," 25–27, pp. 167–172, ©1991, with permission from Elsevier Science S.A., Lausanne, Switzerland.)

the electrical time constant of each sensor element must exceed the inverse of the chopper frequency (which is necessary for operating the pyroelectric elements continuously), while the chopper frequency must exceed the thermal time constant of the system. Using a chopper frequency of 10 Hz and a sensor capacitance of 10 pF, this leads to a resistance value in the 10 GΩ range. It is evident that conventional diffused silicon resistors cannot achieve this value. In order to be compatible with the CMOS process, the gate resistor is realized as a *pn*-junction in a separate *p*-well.

The thick oxide layer reduces parasitic capacitance and heat conduction. The sensors are further improved by sputtering a thick oxide under the PVDF film. A 25 μm-thick PVDF film was used as a pyroelectric material. The upper side was coated with a thin IR-absorbent conducting film of graphite, which also serves as the common counterelectrode for all sensors. The sensor electrodes were formed from the contact metallization on the silicon chip.

The use of integrated *pn*-junctions as gate resistors makes it possible to polarize the pyroelectric layer on the chip without damaging the gate oxide film of the sensor MOSFETs. This is done by operating the diode in a forward direction, thus reducing the resistance of the junction by several decades. The transfer function at 10 Hz is about 850 V/W, the cross-talk between adjacent pixels in the low frequency range is about 0.3×10^{-3}.

Several similar structures for building linear and small (3×3 size) arrays, have been designed in the past few years that are very small compared to the optical imaging arrays with 512×512 pixels (von Münch et al., 1993). However, the advantages of pyropolymer detectors and the great progress made in their development in the last five years indicate that larger arrays may be expected in the near future.

Another charge coupling and readout possibility is the application of charge coupling devices (CCDs) in combination with pyroelectric materials. An infrared imaging sensor with 64×32 infrared-sensitive MOS gates has been developed by combining several types of pyroelectric materials on Si-CCDs (Okuyama et al., 1990).

The necessary chopping of pyroelectric detectors and the cryogenic operation of quantum detectors can be avoided by using silicon micromachined detector arrays. A typical example is shown in Figure 5.5(c). This infrared sensor array is based on thermopiles consisting of *p*-Si/Al thermoelements. Cantilever beams made by anisotropic etching of silicon (see Section 2.1) suspend the individual thermopiles. The supporting rim acts as a heat sink, keeping the thermopile cool points at a constant temperature, while the hot points at the cantilever edges are heated by the incident infrared radiation impinging on the absorbent material (Ristic, 1984).

Other approaches have been developed for uncooled micromachined silicon IR imaging devices. The bimaterial cantilever system is highly sensitive.

The cantilevers made by silicon micromachining operate like bimetal devices; their thermal movement can be recorded by capacitive position measurement. Potential applications include inexpensive infrared cameras.

A similar technology is the application of micromachined suspended microbolometers: polysilicon resistors covered by absorber material. A 327 × 245 microbolometer array with compatible CMOS circuitry has been developed recently (White et al., 1998).

Another possibility for thermal imaging is based on *microwave emission mapping.* Since any object radiates electromagnetic waves over a theoretically infinite bandwidth, detection in the radio-frequency range is also possible. Within the cm wavelength ranges, microwave power is proportional to the object's temperature. In the microwave scanner, emitted energy is focused through a large elliptical reflector into the horn of a radiometer, and the detected power is displayed according to the scanning. Temperature and spatial resolutions are about 0.1°C and 1 cm, respectively, when detecting the 3 cm wavelength emission. In contrast to infrared thermal scanners, this method allows noninvasive imaging to subcutaneous depths of several centimeters (Fraden, 1991).

5.1.3 Invasive Temperature Measurements

Invasive temperature measurements (mostly intravascular blood) can be realized with catheters. Small-diameter wire thermocouples, miniature thermistors, and microchip *pn*-junctions will be mentioned here. Because these types of sensors are generally combined with other catheter measurements as secondary applications, they will be discussed later.

Special attention should be given to fiber-optic invasive temperature measurements that can be applied in combination with the use of optical fiber catheters. The excited state phosphorescence lifetime of alexandrite crystals can be used to monitor temperature in the physiological range with an accuracy of 0.2°C. The crystal is excited by pulsed laser light, creating Fourier transform of the response impulses; the intensities of given frequency harmonics are temperature dependent (Alcala et al., 1995). Another approach is to employ temperature-dependent spectral transmission in special glasses that provide temperature-dependent transmissions at given frequency ranges that can be used for temperature measurements. They are, however, temperature independent at other frequencies and can be used for other sensing purposes when the device is designed as a simple transparent element. Thus, it can be connected serially to other fiber-optic sensors (Wolthuis et al., 1993).

Optical-fiber thermometers, due to their electrical isolation and immunity from electromagnetic interference, are particularly suitable for inducing controlled heating of biological tissues, for example, when using microwave or

RF hyperthermia for cancer treatment. The use of conventional temperature sensors (thermocouple or thermistors) can perturb the incident electromagnetic field and lead to localized heating spots or sensing errors (Harmer and Scheggi, 1989). The main measurement requirement is resolution of 0.1°C over a range of a few degrees (35°C to 50°C). Several practical solutions have been developed from which a few examples are mentioned as follows.

Thermographic phosphors with a temperature-dependent fluorescence emission are well known, and fiber-optic temperature sensors operating by means of this effect are commercially available. Mainly rear-earth phosphor mixtures were used conventionally. A newer technique uses the measurement of fluorescence decay times of magnesium fluorogermanate phosphor (Wickersheim, 1987).

Another well-established technique employed for temperature sensors is based on the light absorption of semiconductors. Since the energy gap defining the absorption cutoff characteristics shows a negative temperature coefficient for most semiconductors, the light from a suitably chosen source in the band-edge region will be strongly amplitude modulated by temperature. A sensor of this type has been engineered for a clinical hyperthermia system consisting of a small GaAs prism as the sensing element and a GaAlAs LED source. The temperature-dependent photoluminescence of crystalline GaAs has also been used as a sensing principle (Harmer and Scheggi, 1989).

5.2 OTHER APPLICATIONS OF TEMPERATURE SENSORS

Temperature sensors can be used for measuring not only temperature but also a number of other physical parameters. They are often applied in calorimetric (see Section 3.4) flow sensors, i.e., for measuring blood or respiratory airflow. A few examples are demonstrated in this section.

5.2.1 Skin Blood-Flow Sensor

The measurement of thermal conductivity is obviously based on temperature sensors. The thermal distribution around a heat source depends on the thermal conductivity of the surrounding medium. By placing temperature sensors in fixed positions around the source, variations of the thermal conductivity can be followed. Thermal conductivity is defined by the following equation:

$$j_{\text{th}} = -K \cdot \text{grad}\, T\,(r) \tag{5.1}$$

where j_{th} is the thermal current density, $T\,(r)$ is the temperature distribution, and K is the thermal conductivity with the practical dimension of mW/cm°C.

Skin blood flow (SBF) or skin perfusion is a complex phenomenon that occurs in capillaries. In perfused tissue, thermal conductivity depends not only on the thermal conductivity of the tissue materials, but also on the heat convection transferred by the blood flow in capillaries. Thus, thermal conductivity of the skin can vary within a wide range; its minimum value, 2.5 mW/cm°C, is characteristic for null blood flow, and its maximum value, 10 mW/cm°C, is typical for vasodilatation. SBF measurements are important diagnostic tools when studying the vascularization of skin that has been burnt or operated on, and, since SBF is related to brain activity, vigilance status and emotional response may be monitored.

Figure 5.6 shows the cross-sectional view of a miniature *SBF sensor* called "Hematron" (Dittmar et al., 1992), which is based on thermal conductivity measurements. The transducer consists of a disc (25 mm in diameter, 4 mm in thickness) that is fixed to the skin with double-sided adhesive tape. A flat heater with a very low thermal inertia a 2 μm-thick constantan resistor on a polyamide substrate, is located in the central part of the sensor element, in close contact with the skin. The difference between the temperatures of the center and the periphery of the sensor is measured by a thermopile consisting of sixteen copper-constantan thermocouples. The circular layout of the transducer avoids any influence due to the direction of blood flow. The temperature of the central part is regulated by a PID (proportional-integral-derivative) controller to ensure a constant (2°C) temperature difference, which is measured by the thermopile. This requires the application of a heating power that varies with the skin blood flow. The sensor could be calibrated using refer-

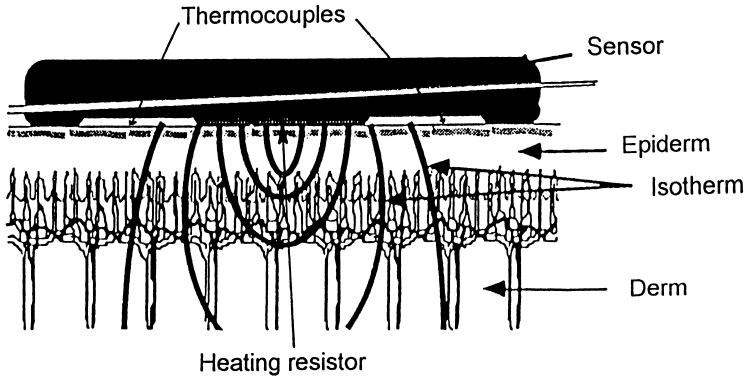

FIGURE 5.6. Cross section of the skin blood-flow (SBF) sensor with an isotherm system generated in the skin. (Reprinted from *Sensors and Actuators B,* A. Dittmar, T. Pauchard, G. Delhomme and E. Vernet-Maury, "A Thermal Conductivity Sensor for the Measurement of Skin Blood Flow," 7, pp. 327–331, ©1992, with permission from Elsevier Science S.A., Lausanne, Switzerland.)

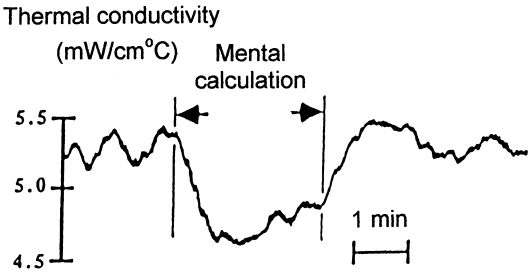

FIGURE 5.7. Effect of mental calculation on skin blood flow (36-year-old male, ambient temperature 24°C, sensor on left hand). (Reprinted from *Sensors and Actuators B,* A. Dittmar, T. Pauchard, G. Delhomme and E. Vernet-Maury, "A Thermal Conductivity Sensor for the Measurement of Skin Blood Flow," 7, pp. 327–331,. ©1992, with permission from Elsevier Science S.A., Lausanne, Switzerland.)

ence materials. Figure 5.7 illustrates an interesting example: the effect of mental calculation on skin blood flow.

5.2.2 Hot-Film Anemometry for Measuring Blood Flow

Measuring blood-flow velocity and/or flow rate in the heart and large vessels is an important diagnostic tool for monitoring the cardiovascular system. One way of measuring velocity and flow rate is to apply a *hot-film anemometer* on a catheter tip (Yamaguchi, 1989). The method is based on the heat transfer from a small body placed in the fluid flow. The sensing element is a small thin-film or wire-wound Pt or Ni thermoresistive element (see Section 4.1) connected to a bridge circuit (Figure 5.8) for the generation of heat by electrical current. A servoamplifier feeds back the error voltage of the bridge circuit so that the resistance of the sensor, which is a function of the temperature, is kept constant. This principle is called constant temperature anemometry (CTA). Heat loss varies with the flow velocity of the surrounding medium; thus, the bridge voltage necessary to keep the sensitive element at a constant temperature follows velocity variations. The sensor system generally has nonlinear characteristics. The resistor material should be covered by a thin insulating film, usually quartz, that does not interfere significantly with heat transfer. The method can easily be used to obtain invasive blood-flow measurements. The sensing resistor element is mounted onto a catheter tip with a typical diameter of 0.5 mm.

This method has several disadvantages:

- Catheterization of the large inner vessels is rather complicated.
- The general problem with invasive techniques is that sterilization recently became undesirable due to the possibility of transmitting HIV. Thus, dis-

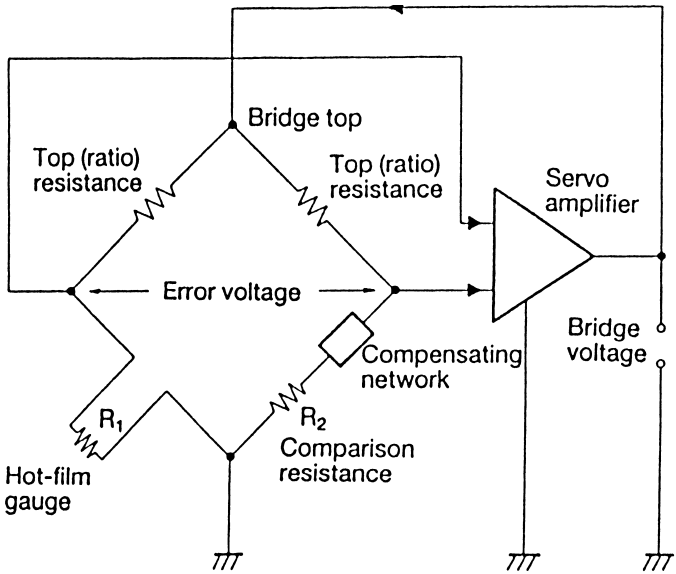

FIGURE 5.8. Schematic circuit diagram of the constant temperature hot-film anemometer used for blood-flow measurements. [Reprinted with permission from T. Yamaguchi, "Blood Flow Measurement with the Hot-Film Anemometer, " in M. Sugawara, F. Kajiya, A. Kitabatake and H. Matsuo (ed), *Blood Flow in the Heart and Large Vessels,* pp. 187–188, Figure 13.1, ©1989, Springer-Verlag, New York/Berlin.]

posable invasive elements are preferred, which makes the use of accurate but costly Pt resistors impractical.

- The operation of the sensor strongly depends on the consistency of blood; for the exact calculation of blood-flow velocity, the hematocrit value and the plasma total protein content must be taken into consideration.

These disadvantages explain the primary reasons why other, mainly noninvasive, methods are becoming widespread for obtaining blood-flow measurements. Some of these methods will be discussed later. More about blood-flow measurements can be found in the literature (Webster et al., 1997).

5.2.3 Respiratory Flow Monitoring by Hot-Film Anemometry

Hot wire anemometers are used for obtaining *respiratory flow measurements,* especially when using anesthesia and mechanical ventilation. Silicon processing enables small, integrated resistor bridges to be placed into the respiratory system (van Putten et al., 1997). A bidirectional flow vector sensor

was employed recently on a silicon chip consisting of two Wheatstone bridges. Two resistors of the bridge vary in the airflow. This bridge is driven by a constant current, while the other bridge is heated so that the voltage across the measurement bridge remains constant. The output follows the heating voltage variations. The measurement range is from -1 to $+1$ l/s with a response time less than 60 ms.

Respiratory frequency can be measured by using the *nasal thermistor technique:* a simple, unheated miniature (1 mm diameter) bead-type thermistor is mounted on a plastic crocodile clip that can be attached to one of the patients' nostrils with the thermistor placed in the nose (Storck et al., 1996). The expired air passes over the sensor and heats it, altering its resistance so that this change can be used to measure a periodical signal. Thin- and thick-film thermistors integrated on specially shaped flexible substrates have also been used as infant respiratory sensors (Neuman et al., 1994).

More information about respiratory measurements can be found in the literature (Webster et. al., 1997).

5.3 MECHANICAL SENSORS IN BIOMEDICINE

Mechanical sensors are mainly used for measuring and/or monitoring force and pressure, as well as mechanical impulses and waves, including the detection of sound.

5.3.1 Noninvasive Blood Pressure Measurements

Blood pressure measurement appliances are among the oldest diagnostic tools. Arterial blood pressure measurement is conventionally performed using the Korotkoff technique by means of mercurial or aneroid sphygmomanometers. A latex bag inside a Velcro cuff is fixed onto the arm and is subsequently pumped to compress the vessels until the bloodstream is stopped. During the slow cuff deflation, one has to listen to the Korotkoff sound (the arterial pressure-wave propagation caused by the heartbeats) in the arteries of the arm using a stethoscope. The sounds can be heard when the changing pressure of the cuff is between the systolic and diastolic values. The application of the stethoscope can be replaced by using a piezoelectric capacitor sensor inside the cuff close to one of the arteries so that it gives electrical voltage impulses according to the heartbeat. However, the pressure itself is still measured by manometers.

The application of low-cost, silicon-based piezoresistive pressure sensors brought a real breakthrough to blood pressure measurement techniques. The battery-operated, digital-display electronic appliances based on pressure sen-

sors are able not only to measure the static pressure but also using an appropriate electronic filtering process, to detect the pressure waves caused by the Korotkoff effect as well. This is the *oscillometric measurement* method. Pulse rate and systolic and diastolic pressure values are displayed. Cuff inflation and deflation are performed and controlled automatically. The miniaturization of the electronics enabled the development of wrist and finger appliances. Finger monitors have great importance since portable blood pressure monitors recently became part of the personal care market. Digital data processing and storage are essential when collecting blood pressure values over a longer period: the ambulatory blood pressure monitoring (ABPM) technique became an important tool in the pharmacological treatment of high-blood-pressure patients, because a single measurement provides poor information.

Piezoresistive silicon pressure sensors employ resistors as sensing elements, diffused or implanted into the surface region of a membrane made by anisotropic etching (see Section 2.1). The typical layout and circuit diagram is illustrated in Figure 5.9, while the cross section of the structure is shown in Figure 5.10(a). A pressure difference between both sides of the membrane causes its deformation. Due to the piezoresistive effect (see Section 4.7), the resistors follow the deformation with resistance changes; two resistors increase and two decrease, resulting in a multiplied effect in the Wheatstone-bridge configuration. The resistance changes, ΔR_i, can be expressed as follows:

$$\Delta R_i/R_i = GKp/Ea \tag{5.2}$$

where G is the gauge factor, E is the Young's modulus of the membrane, a is its thickness, and K is constant depending exclusively on the geometrical sizes. The output voltage of the bridge, U, related to the supply, U_0, is:

$$U/U_0 = GKp/Ea \tag{5.3}$$

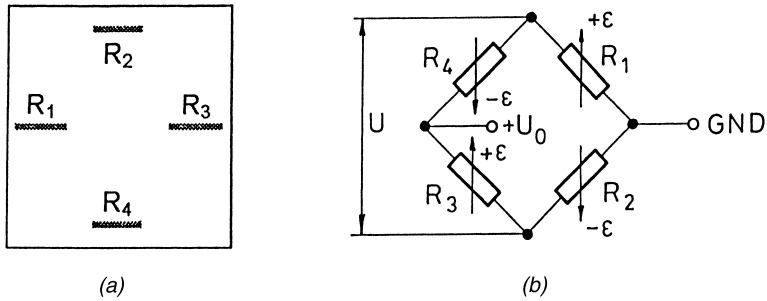

FIGURE 5.9. (a) Typical resistor layout structure and (b) circuit connection of the piezoresistive pressure sensor membranes.

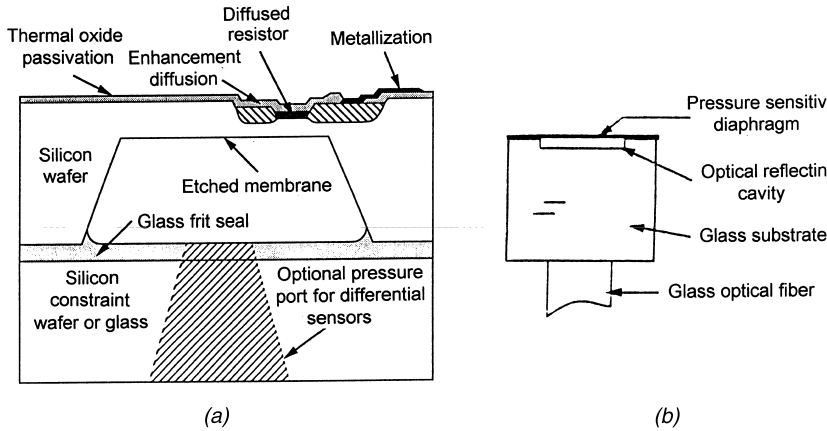

FIGURE 5.10. Pressure sensor structures based on silicon diaphragms: (a) piezoresistive and (b) optical fiber version. [Reprinted with permission: (b) from R. Wolthuis, G. Mitchell, J. Hartl and E. Saaski, "Development of a Dual Function Sensor System for Measuring Pressure and Temperature at the Tip of a Single Optical Fiber," *IEEE Transactions on Biomedical Engineering,* Vol. 40, No. 3, pp. 298–302, ©1993, IEEE.]

The linearity of the sensor depends on the uniformity of the resistance values and deformations; thus, the bridge must be exactly balanced and the resistors must be well positioned. The temperature drift of the zero output is determined by the TCR tracking of the resistors, while the temperature dependency of the sensitivity is determined mainly by the temperature coefficient of the gauge factor (TCGF). The bridge balance adjustment is generally made by external potentiometers or by laser trimming. An analog compensation of the temperature dependency can be achieved by connecting appropriate temperature-dependent resistors between the bridge and the power supply. Digital temperature compensation can be realized by measuring the chip substrate temperature with a simple integrated *pn*-junction temperature sensor element (see Section 4.3). The pressure sensor chip is generally mounted onto another silicon or glass substrate, as shown in Figure 5.10(a), in order to minimize the stresses due to the thermal expansion mismatch between the silicon chip and the packaging materials.

5.3.2 Hemodynamic Invasive Blood Pressure Sensors

The application of miniature silicon pressure sensors enables the practical realization of *invasive blood pressure monitoring,* when the time dependency of hemodynamic pressure impulses that are generated by the heartbeats can continuously be followed. One approach is to package the pressure sensor chip

in a sterilizable plastic housing called a dome. A cannula is installed into one of the arteries, and a pipe transmits the blood pressure from this to the dome and the pressure sensor membrane. In some solutions, an intermediate membrane is mounted between the blood and the sensor chip, and the cavity between them is filled with silicon oil. Thus, blood clotting and protein formation occurs not on the sensor chip but on the intermediate membrane that can be replaced periodically. Another advantage of this version is that bioelectric interferences from the sensor chip can be isolated. Table 5.1 summarizes the parameters of several commercially available cannula-dome physiological pressure sensors (one example is demonstrated in Appendix 1).

Catheter (invasive) blood pressure measurements are sometimes desired to collect information from special locations of the body, for example, to obtain intrauterine and intracardial pressure measurements. For these purposes, silicon processing offers great advantages: the pressure sensor, the temperature sensor, and the signal processing circuit can be integrated onto a single miniature silicon chip with typical measurements of 5 mm x 1 mm x 15 μm that can be mounted directly onto a catheter tip. In this case, the silicon chip is in direct contact with blood. Because the relative pressure measurement is not possible, a closed cavity with a reference pressure should be formed between the anisotropically etched silicon chip and the glass substrate to achieve an absolute pressure measurement (Otter et al., 1991). A sensitivity of 1 mV/V/mmHg was achieved with a temperature coefficient of offset less than 0.5 mV/°C.

Ultraminiaturized piezoresistive pressure sensor chips with sizes of 0.5 × 0.5 × 2.3 mm for catheter applications were also developed using surface mi-

TABLE 5.1. Most Important Parameters of Physiological Pressure Sensor Examples.

Manufacturer, type	AME[1] AE 840	HIPOT[2]
Pressure range	−10...+ 40 kPa (−75...+ 300 mmHg)	−2.666...+ 40 kPa (−20...+ 300 mmHg)
Sensitivity	5 μV/V/0,1333 kPa	200 μV/V/0,1333 kPa
Maximum supply voltage	15 V	15 V
Bridge resistance	1 kΩ	1 kΩ
Nonlinearity and hysteresis	max. 1% FSO	max. 0.5% FSO
Zero balance	max. 1% FSO	max. 2% FSO
Thermal sensitivity shift	0.1%/°C	0.15%/°C
Thermal zero shift	max. 0.02 kPa/°C	max. 0.02 kPa/°C
Operating temp. range	−20...+ 100°C	−20...+ 100°C
Isolation resistance	min. 50 MΩ	min. 103 MΩ

[1]AME—Aksjeselskapet, Horten, Norway
[2]HIPOT-RDG, Senternej, Slovenia

cromachining (Lisec et al., 1996). In this processing, an LPCVD polysilicon film is deposited onto a sacrificial layer that is etched to form a polysilicon bridge or membrane. A sensitivity of 20 μV/V/0.1333 kPa could be realized with this sensor. A picture in Appendix 2 shows the sensor chip.

Fiber-optic pressure sensors were also fabricated for catheter blood pressure measurements. One example is shown in Figure 5.10(b) (Wolthuis et al., 1993). The sensor consists of an optical reflecting cavity etched onto one face of a glass substrate. The optical reflecting cavity is evacuated and then covered and sealed with a thin, pressure-sensitive diaphragm made of single-crystal silicon. As pressure above the sensor changes, the diaphragm deflects and changes the cavity depth. Thus, the pressure modulates the reflected light intensity. The cubic-shaped sensor has a dimension of 300 μm. It provides an accuracy of 0.1333 kPa (1 mmHg) within the range of −2.666 . . .+40 kPa (−20...+300 mmHg). Because of its construction and the materials used, the sensor exhibits essentially zero hysteresis.

More about blood pressure measurements can be found in the literature (Webster et al., 1997; Geddes and Baker, 1989).

5.3.3 Mechanical Sensors in Spirometry

Another important application field of pressure sensors is in *respiratory flow measurement.* Conventional pneumotachograph instruments operate with the Fleisch tube that measures the pressure difference across a grid as a function of the flow (Kacmarek et al., 1993). If the flow-resistance (R_f) of the grid is known, the flow rate (v) can be calculated from the pressure difference (Δp): $v = \Delta p/R_f$. Nowadays, such instruments employ silicon-based miniature pressure sensors for measuring the pressure difference. Turbine flow, respiratory flow testing systems are also available on the market.

An *optical fiber pressure transducer* was also developed *for use in the upper airways* to prevent obstructive sleep apnea syndrome (OSAS). A total of seven transducers were thought to be necessary: one at the tip of the catheter placed into the esophagus to measure pressure in the chest, and six arrayed over 20 mm intervals to measure the pressure from the back of the nose to just above the larynx (Goodyer et al., 1996). The design of the transducer uses a series of three optical fibers, one emitting and two receiving, the combination of the two receiving optical fibers is used to reduce effects of light loss: a bend radius of 50 mm is typical for insertion into the nasopharynx. The transducer's transduction element is a silicone gel coated with reflective titanium dioxide; the meniscus deforms under pressure and modulates the intensity of light reflected back into the receiving optical fibers. The transducer has a resolution of 10 Pa over the range ±5 kPa; the diameter of a single transducer element is 0.94 mm.

Flow measurements in *anesthesia and respiratory function analysis* can be performed with mechanical sensors other than pressure transducers. If there is a tube with airflow outside of the body, many possibilities are realizable among the conventional flow-rate measurement methods. One example is the *turbine flow meter* that measures the number of rotations of a turbine wheel placed inside the flowing medium (Doebelin, 1990). Another approach is to use the *vortex shedding flow meter.* If a fluid (liquid or gas) flows around an obstacle, it creates vortices behind it. Above a certain velocity, uniform vortices are shed alternately from either side of the obstacle. The vortex shedding frequency is proportional to the flow velocity. Vortices create local pressure variations at the bluff body that can be detected by piezoelectric capacitors, for example. The output is an AC signal with a frequency proportional to the velocity of the flow. Supposing a respiratory function analysis system, the total number of counts is proportional to the total volume that is the vital capacity.

More information about flow measurements can be found in the literature (Webster et al., 1997).

5.3.4 Sensors for Pressure Pulses and Movement

A wide variety of mechanical sensors are based on the piezoelectric effect of the PVDF polymer, which can be applied for detecting pressure impulses or movements.

Figure 5.11 shows the structure of the piezopolymer finger *pulse and breathing wave sensor* (Chen et al., 1990). Pulse sensing is a convenient and efficient way of acquiring important physiological information concerning the cardiovascular system. Finger pulse pickups can be employed in systems that measure blood pressure, heart rate, and blood flow. The sensor shown in Figure 11 can pick up breathing waves simultaneously with pulse waves. It has a U-shaped structure, and its open side can be closed with Velcro. In this way, the sensor can conveniently and comfortably be fixed in the right position on the finger. For the purpose of enhancing the sensor's immunity to electric interferences, a hybrid buffer electronic system incorporating high-impedance FETs is affixed to it. The pulse-wave signal is sent through the buffer to the signal-processing electronics. The PVDF film is in direct contact with the finger; therefore, its metallized surfaces have to be shielded on both sides with thin metallized protecting polymer films and sealed with highly insulating silicone rubber to avoid damage to the surface electrodes through friction and sweat erosion. Separation of pulse and breathing waves is possible through electronic low- and high-pass filtering, respectively. From recordings generated by the PVDF finger pulse sensor, not only the informative pulse wave and respiration wave can be extracted, but also meaningful information con-

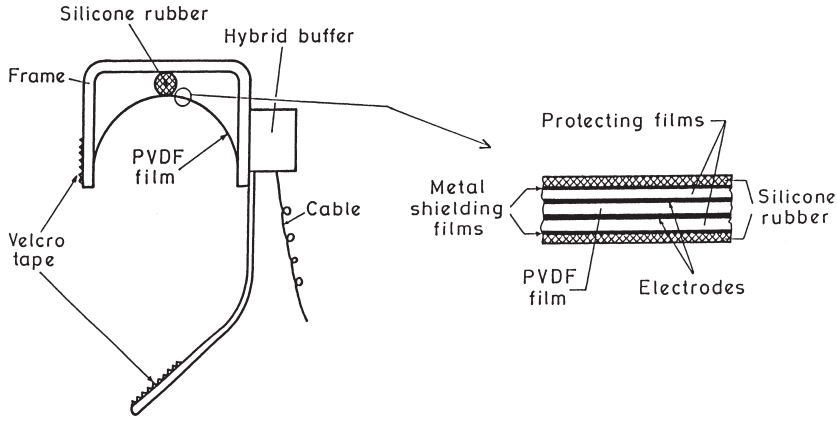

FIGURE 5.11. Structure of the piezopolymer-based finger pulse and breathing wave sensor. (Reprinted from *Sensors and Actuators A,* Y. Chen, L. Wang and W. Ko, "A Piezopolymer Finger Pulse and Breathing Wave Sensor," 21–23, pp. 879–882, ©1990, with permission from Elsevier Science S.A., Lausanne, Switzerland.)

cerning the local microcirculation condition of the measured finger can be obtained.

Piezofilms are used in a variety of medical monitoring systems. One of the most important areas is in the application of apnea sensors in *baby monitoring systems.* A sheet of piezopolymer film placed under the baby's mattress picks up respiration and heartbeat of the child by way of slight center-of-gravity shifts. The sensitive part of the film can also be attached to an elastic belt that is then fixed onto the baby's chest. If an apnea occurs, alarms in the monitor system are activated, waking the child and the parents (Halvorsen, 1988).

A piezopolymer-based sensor was also developed for service in a *portable fetal heart rate (FHR) monitor* that will permit an expectant mother to perform the fetal nonstress test, a standard predelivery test, in her home (Zuckerwar et al., 1993). Several piezopolymer-based capacitive sensor elements were mounted in an array on a belt worn by the mother. The sensor layout and signal processing design conforms to the distinctive features of the fetal heart tone, namely, the acoustic signature, frequency spectrum, signal amplitude, and localization. The components of the sensor serve to fulfill five functions: signal detection, acceleration cancellation, acoustical isolation, electrical shielding, and electrical isolation of the mother. Seven hexagon-shaped twin-capacitor cells separated by a Ni plate were mounted onto the belt to form another hexagon with their centers and with the seventh hexagon in the center of the latter. Two copper-coated Kapton foils completely surround the sensor elements to assure electrical shielding. A silicon rubber coating pro-

vides electrical isolation. Conventional microphones can also be used to monitor fetal heart rate.

Strain gauges are applied mainly for *measuring joint angle variations.* Finger and other joint angular displacement measurements are important during physico-therapy treatments in order to receive quantitative feedback about any changes. Such sensors can be fabricated using the strain gauge principle: a narrow, metal film is deposited on one surface of a thin, flexible substrate such as polyimide to form a strain gauge (Neuman et al., 1994). By flexing the structure so that the strain gauge is on the convex surface, the deformation causes the strain gauge to be extended, and its resistance will change. For small deformations, the change in the resistance will be proportional to the angle over which it is fixed, according to the piezoresistive effect. For practical applications, several strain gauges are applied and connected to form a resistor bridge, similar to the pressure sensor configuration discussed previously. For example, finger joint angular displacement measuring units were fabricated by placing the strain gauges in a flexible tube sewn to a tightly fitting glove, so that the sensor spans the finger joint to be measured. Overall errors are 2° over a range of angles of 0–105°.

A compliant strain-gauge-based *abdominal infant respiration sensor* was also developed that consists of a corrugated polyester or polyimide substrate with a thin-film strain gauge pattern deposited on one surface (Neuman et al., 1994). The function of this sensor is similar to that of the angle sensor described in the previous paragraph. The gold film patterned on the convex portions of the corrugations is wide and contributes only a small portion of the total resistance. On the other hand, a narrow strip is patterned on the concave portions of the corrugations, and it is these strips that contribute the majority of the resistance. The corrugations make this sensor compliant so that it can easily be extended by applying a small tensile force between its ends. This tensile force causes the structure to elongate as the corrugations flatten. The narrow portions of the gold film in the concave regions of the corrugated substrate will experience a tension that remains within the elastic limits of the gold film, but, nevertheless, elongates it. Thus, the electrical resistance of these portions of film will increase as the sensor is stretched, thereby increasing the overall resistance. The contribution of the convex portions can be neglected. The sensor is used on infants by stretching it slightly and then taping each end to the abdomen. As the infant inhales, the sensor is stretched, and as the infant exhales, the elastic recoil of the corrugations brings the sensor back to its original configuration. The changes in electrical resistance are converted to voltage variations. The advantage of the corrugated structure is that the infant does not need to put any extra effort into breathing compared to using stretched belts. Also, skin irritations are minimized.

5.3.5 Measuring Internal Ocular Pressure

Another important application field of miniature silicon-based mechanical sensors may be *intraocular pressure measurement (IOP)* in ophthalmoscopy in order to diagnose the eye disease open-angle glaucoma (Bergveld, 1994). Normal intraocular pressures are in the range of 1.33–2 kPa (10–15 mmHg), while a pressure over 2.8 kPa (21 mmHg) may indicate the mentioned disease. The internal pressure (p) in a sphere can simply be calculated by measuring the necessary force (F) that can flatten a certain area (A) of the sphere: $p = F/A$. Two correction terms have to be introduced, one due to the cornea stiffness and the other resulting from shear forces due to the cornea tear film. Both correction terms cancel each other if the flattened area has a diameter of 3.06 mm. The Goldmann tonometer is based on this principle. It measures the force by which a glass plate is pressed against the anesthetized cornea until the desired deformation is adjusted. The edges of the applanation can be observed by means of a slit-lamp microscope because the anesthetizing fluid is made fluorescent. By measuring the corresponding force, the IOP can be calculated. Another approach is the Mackay-Marg method in which a fixed 5 mm-diameter footplate containing a small pressure sensor in the center is applied. When pressing it against the eyeball, a pressure versus time curve can be recorded that shows a typical dip in the value of IOP. It can be proved that at a sufficient applanation, the disturbing forces act only on the footplate and not on the pressure sensor, however, the result is strongly dependent on the distance between the edge of applanation and the pressure sensor. If the dip does not exist on the curve, the measurement should be repeated. Thus, a simultaneous applanation measurement would be desirable to avoid false or unsuccessful measurements.

For the improvement of IOP measurements, a combined Goldmann Mackay-Marg tonometer was developed that employs not only miniature silicon-based pressure and force sensors, but also a silicon applanation sensor designed especially for tonometer purposes (Bergveld, 1994). The applanation sensor and its application are illustrated in Figure 5.12. The sensor consists of a silicon substrate of 6.3 $\times$ 6.3 mm that contains four meandrous diffused resistor arrays with a number of resistor elements with meandrous contacts at the resistor nodes. The resistors are shaped around a plunger, which is located in the center as shown in Figure 5.12(a). The sensor is covered by a Mylar® (DuPont) foil that is coated with a thin gold layer at the side that faces the sensor surface. The foil is separated from the sensor by a polyimide spacer as shown in Figure 5.12(b). The center plunger, produced by anisotropic etching of silicon, provides the coupling with the attached pressure sensor. When the applanation sensor is pressed against the eye globe, the Mylar® foil with its gold film contacts a certain area as a function of the

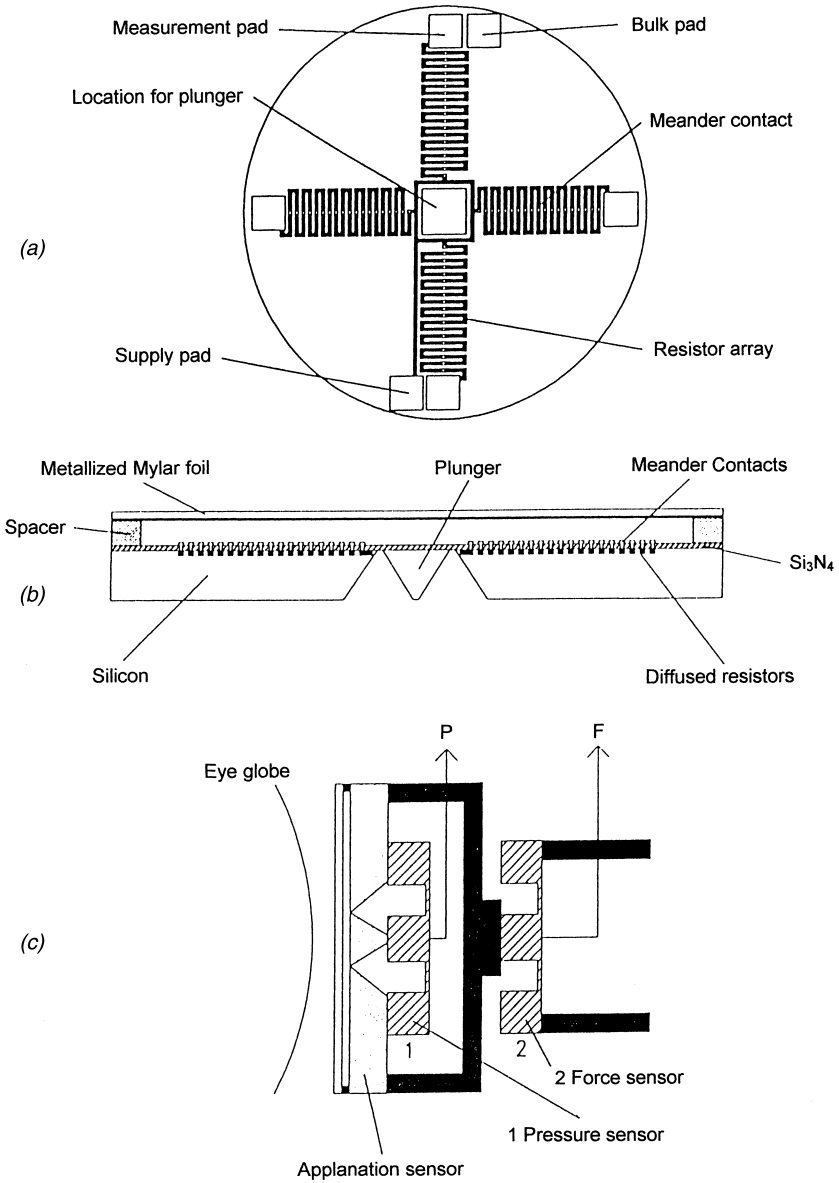

FIGURE 5.12. Structure and application of the applanation sensor used in tonometers: (a) resistor array layout on its surface, (b) cross-sectional view, and (c) applying it in a tonometer by combining with a pressure (1) and a force (2) measuring sensor. (Reprinted from *Sensors and Actuators A,* P. Bergveld, "The Merit of Using Silicon for the Development of Hearing Aid Mcrophones and Intraocular Pressure Sensors," 41–42, pp. 223–229, ©1994, with permission from Elsevier Science S.A., Lausanne, Switzerland.)

applied force; thus, short-circuiting the meander resistor arrays within that area. By measuring the resistance values that reflect the size and eccentricity of the flattened area, its diameter and distance from the nearest edge can be calculated. A resolution of 60 μm could be achieved with this sensor. By attaching two silicon pressure sensors to the applanation sensor, as shown in the configuration of Figure 5.12(c), the pressure and the force measurements can be obtained simultaneously; thus, both measurement methods can be applied.

5.3.6 Acoustic Sensors in Hearing Aids

Hearing aid appliances are a special biomedical application field of acoustic sensors. The sensor elements are miniature microphones designed especially for this purpose. Modern hearing aid appliances consist of one unit that can be fixed into the auditory canal. It contains the microphone with preamplifier, a signal processing unit, and a power amplifier with a loudspeaker. The newest techniques of electronics packaging are applied to minimize the size, such as combining flip-chip and wire bonding techniques. The microphone is always of the electret type (see Section 4.5) due to its high sensitivity and built-in electric field. Due to its capacitive nature, the microphone capsule needs to contain the preamplifier as well. Since noise reduction can most effectively be achieved in the first stage, microphone elements should be integrated with preamplifiers. A typical hybrid integrated version based on a ceramic substrate is illustrated in Figure 5.13(a) (Baker, 1980).

Silicon micromachining enables the integration of mechanical parts with preamplifiers. Efficiency can also be improved by integrating several microphone elements onto the same chip. A silicon-based microphone structure is shown in Figure 5.13(b) (Voorthuyzen et al., 1989). The sensor applies electron-beam-charged PTFE (polytetrafluoroethylene) electret deposited onto the bottom surface of the cavities and patterned by plasma etching prior to the poling process. A Mylar® (DuPont) foil, metallized on one side, was applied as a diaphragm. The silicon substrate was shaped by anisotropic etching. The sensitivity of the device is (applying a 200 V electret, without amplification) 25 mV/Pa, the maximum frequency is 15 kHz. Newer silicon-based capacitive microphones were also developed by surface micromachining based on the sacrificial layer technique. They employ SiO_2 and Si_3N_4 layers as electrets and diaphragms, respectively. The processing is generally CMOS compatible; thus, the power consumption can also be minimized by applying CMOS preamplifiers (Bergveld, 1994). The new generation of hearing aids consists of a single chip with nerve stimulating electrodes. This may replace the role of the eardrum. Its nerve-stimulating principle is similar to that of the artificial retina.

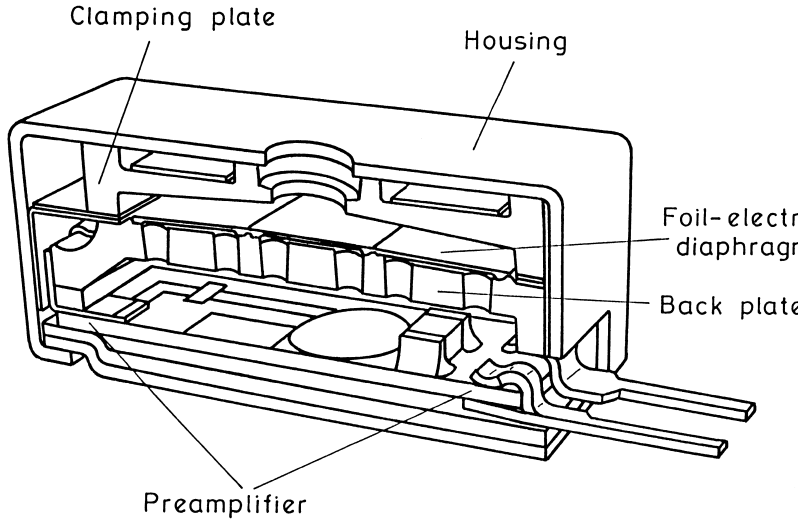

(a)

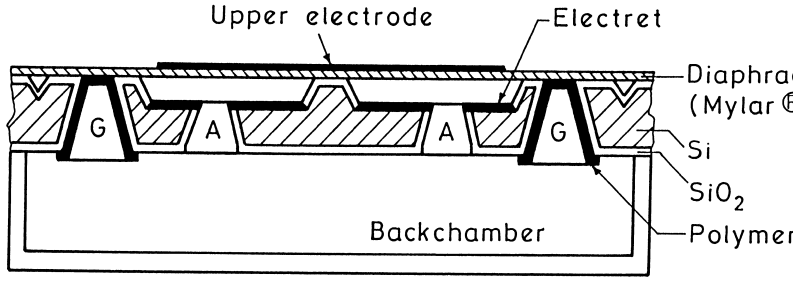

(b)

FIGURE 5.13. Miniature microphone structures for hearing aid appliances: (a) hybrid integrated and (b) silicon micromachined based versions (A = acoustic hole, G = hole for gluing). [Reproduced with permission: (a) from W. O. Baker, "Polymers in the World of Tomorrow," *Proc. of the Symp. at the 2. Chemical Congress of the North American Continent,* Las Vegas, 1980, pp. 165–202, ©1980, American Chemical Society; (b) from J. A. Voorthuyzen, P. Bergveld and A. J. Sprenkels, "Semiconductor-Based Electret Sensors for Sound and Pressure," *IEEE Transactions on Electrical Insulation,* EI-24, pp. 267–276, ©1989, IEEE.]

5.4 SENSORS IN ULTRASOUND IMAGING

Ultrasound imaging (echography or sonography) is one of the most important and still growing diagnostic tools in use today. Its great advantage is that it uses nonnuclear radiation; thus, the danger of genetic or somatic damages is prevented. State-of-the-art ultrasonic scanners offer real-time gray-scale images of anatomical detail with millimeter spatial resolution superimposed on a color map of Doppler blood-flow information. Complex diagnostic imaging is possible: several organs can be investigated simultaneously. The greatest limit of the technique is that organs filled with air (e.g., lungs) cause total reflection of waves that appear as nontransparent shadows in the image.

Ultrasound energy has the ability to propagate through soft biological tissues and suffer only a moderate attenuation in its passage. The basis of imaging is the fact that at an interface between two acoustically different types of tissue, ultrasound waves will be partly reflected and partly transmitted. The reflected waves can be detected and used as an indication of the position of the interface by measuring the reflected wave impulse time-of-flight times. Together with knowledge of the propagation velocity, the distance of the interface can be calculated. The reflected intensity depends on the acoustic impedance difference between the two media on both sides of the interface (the acoustic impedance is the product of the mass density and the ultrasound wave propagation velocity).

Clinical applications of ultrasonic imaging are expanding as the operating frequency increases. The conventional frequency ranges from 1 to 10 MHz that corresponds to a wavelength range of 0.15–1.5 mm in water. The attenuation increases, thus, the penetration depth decreases with higher frequencies, however, the resolution will be improved. In some cases, such as ophthalmoscopy, ultrasound measurements at frequencies above 15 MHz are employed. Peripheral organs, such as skin, arteries, and veins of the digits, are amenable to ultrasound measurements at frequencies up to 40 or 50 MHz (Payne, 1985).

The most important part of ultrasound imaging appliances is the transducer that emits and detects ultrasound waves. The alternating signal of an electronic impulse generator will be converted into pressure waves by means of a piezoelectric (see Section 4.4) capacitor (called a transmitter). The same capacitor detects the echo waves, converting their energy into alternating voltage signals (the receiver mode) through the reverse piezoelectric effect. Thus, the piezoelectric transducer launches and detects ultrasound wave pulses in alternating periods (pulse-echo operation mode).

5.4.1 Ultrasound Imaging Modes

The first and simplest ultrasound imaging systems applied the *A-mode (amplitude modulation)* imaging illustrated in Figure 5.14(a) (Payne, 1985): echo

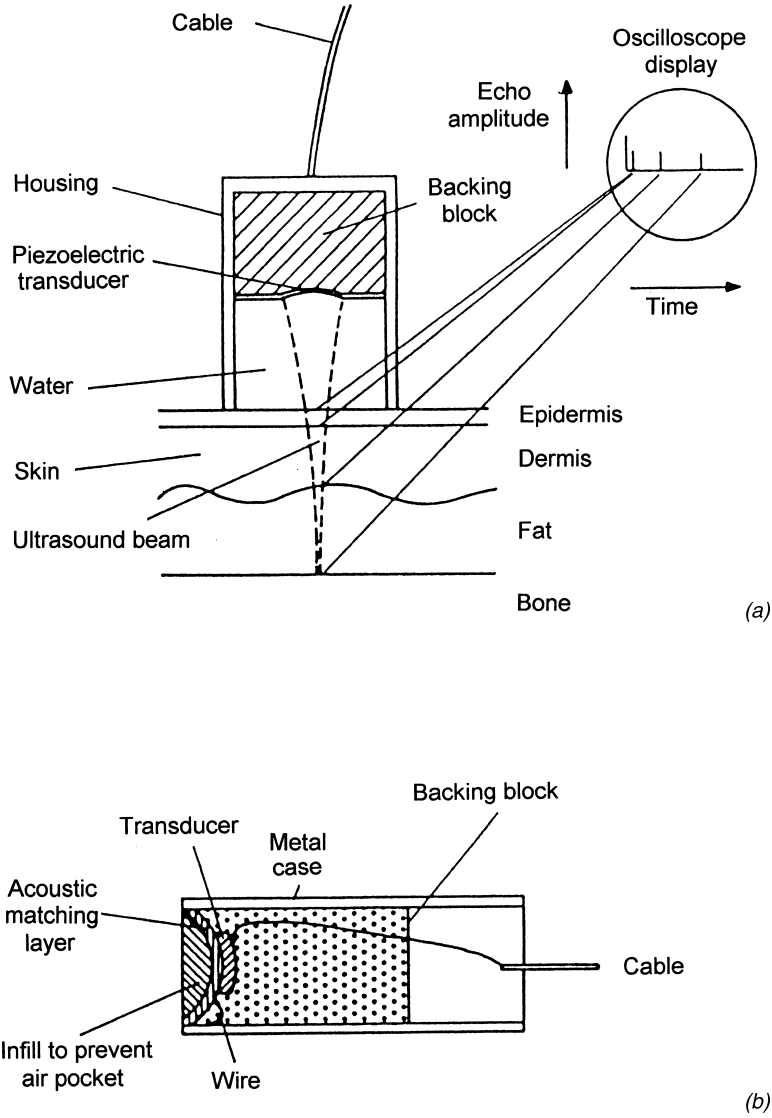

FIGURE 5.14. Illustration of A-mode ultrasound imaging: (a) principle and (b) transducer construction. (Reproduced with permission from P. A. Payne, "Medical and Industrial Applications of High Resolution Ultrasound," *Journal of Physics E, Scientific Instruments,* Vol. 18, pp. 465–473, ©1985, IOP Publishing Ltd.)

impulse amplitude heights are displayed as a function of time-of-flight which corresponds to the deepness of the reflection.

In *B-mode (brightness modulation)* imaging, all echo impulses are represented by a pixel on the display, and the brightness corresponds to the amplitude of the echo. To get a two-dimensional cross-sectional image, an appropriate scanning of the desired cross section is necessary. Several scanning methods are illustrated in Figure 5.15 (von Ramm and Smith, 1983). Two-dimensional images are produced in a *sequential linear array scanner,* consisting of a number (typically 128 to 512) of individual transducer elements, by transmitting on each of the array elements (or small group of elements) and receiving the echo information with the same elements for each B-mode line in the final display. These sequences of image formation result in a rectangular image format as illustrated in Figure 5.15(a). *Mechanical sector arrays* used in early stages include one or more piston transducers that are rocked or rotated about a fixed axis by means of an electric motor [see Figure 5.15(b)]. Individual B-mode lines are scanned radially from a common origin corresponding to the center of rotation.

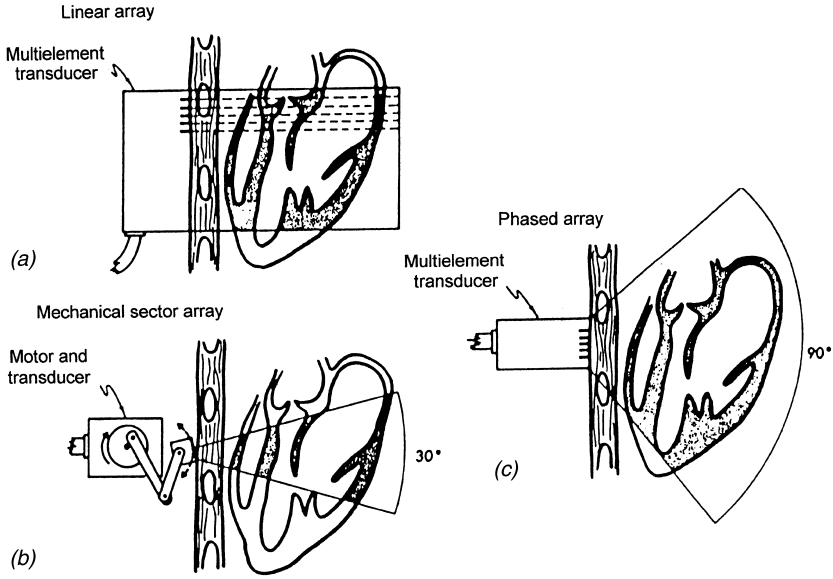

FIGURE 5.15. Scanning methods in B-mode ultrasound imaging: (a) sequential linear array scanner, (b) mechanical sector scanner, and (c) phased array sector scanner. (Reproduced with permission from O. T. von Ramm and S. W. Smith, "Beam Steering with Linear Arrays," *IEEE Transactions on Biomedical Engineering,* Vol. 30, No. 8, pp. 438–452, ©1983, IEEE.)

Phased array scanners are the most sophisticated real-time systems. They utilize a small array transducer with a length of 1–3 cm and a composition of 64–256 elements. They produce images by rapidly steering the acoustic beam through the target organ by electronic rather than mechanical means. In contrast to the sequential linear array scanners, all of the array elements in a phased array system are utilized in producing each of the individual B-mode lines that comprise the final two-dimensional image. While the pitch size (the raster of the array elements) should be greater than $\lambda/2$ (λ is the wavelength) at the linear array in order to minimize the cross talk, it must be smaller than $\lambda/2$ at phased arrays because the wave interference effect is utilized for steering. The method by which a linear array may be excited to produce a wave front that propagates at any desired azimuth angle is illustrated in Figure 5.16 (von Ramm and Smith, 1983). The direction of propagation of the effective wave front is directly related to the excitation time sequence of the array elements. Focusing can also be realized by an appropriate excitation schedule, as shown in Figure 5.16(b). Rapid two-dimensional B-mode imaging known

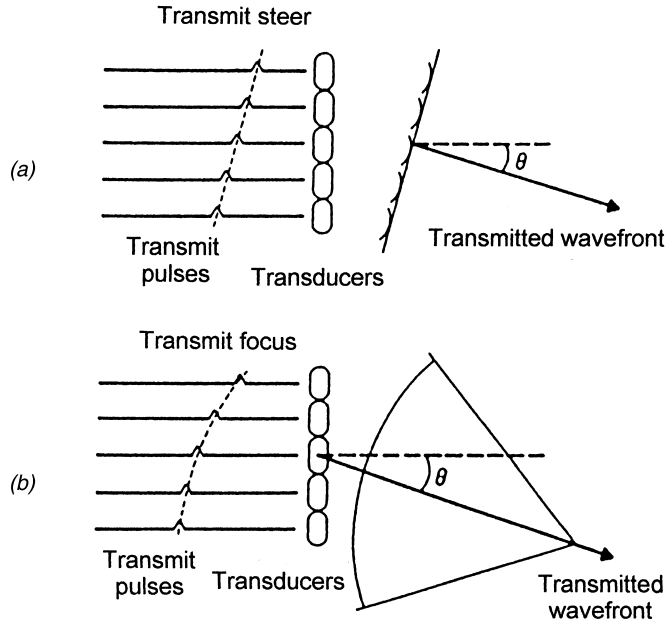

FIGURE 5.16. Wave generation with a phased array system: (a) transmit steering and (b) focusing. (Reproduced with permission from O. T. von Ramm and S. W. Smith, "Beam Steering with Linear Arrays," *IEEE Transactions on Biomedical Engineering,* Vol. 30, No. 8, pp. 438–452, ©1983, IEEE.)

as "real-time scanning" enables visualization of moving targets within the body.

M-mode (movement mode) imaging uses a standard A-mode instrument. The pixel elements are rendered together according to the distance of reflection (Shung et al., 1992): the horizontal or x-axis is driven by a relatively slow ramp sweeping (representing the time axis), while the y-axis indicates the distance of echo. M-mode display is useful for mapping the movement of moving objects such as mitral valve in the heart, etc.

C-mode or (constant depth mode) instrumentation is very similar to that of B-mode. However, unlike B-mode, where one dimension of the display is inferred from the time-of-flight information of the ultrasonic pulse, the scanning plane is fixed at a constant depth, and the two-dimensional mapping of reflection intensity is displayed. This type of imaging has not been found useful in clinical diagnosis, but it occupies an important position in acoustic microscopy.

5.4.2 Ultrasound Transducers and Arrays

The typical cross section of a single ultrasound transducer (transmitter-receiver) element fabricated for A-mode operation is shown in Figure 5.14(b). Focusing can be achieved by applying bowl-shaped or disc-shaped transducers with acoustic lenses. The role of the matching material is to assure a low reflection from the body surface. Conventional transducers applied piezoelectric ceramic materials, such as $BaTiO_3$, PZT, and lead metaniobate. Recently, much attention has focused on the use of piezoelectric polymer (PVDF) material. Its acoustic impedance matches that of water and of biological tissues, hence, removing the need for matching layers. The easy fabrication of the material enables the production of linear or two-dimensional (2D) transducer arrays, as well as their integration with preamplifier circuit elements, which can result in better signal-to-noise ratio and smaller cross talk. A number of other factors will also be involved when applying this material, such as the low-cost and the achievable broad bandwidth. The disadvantages of PVDF are that it has a low transmitting constant, and its dielectric loss is large. One of the most promising frontiers in transducer technology is the development of piezoelectric 1–3 composite materials consisting of small-diameter PZT rods embedded in a low-density polymer. By varying the volume ratios and rod sizes, the properties can be adjusted to their desired values. One of the most important disadvantages is the complicated and, therefore, high-cost fabrication of the material (Shung and Zipparo, 1996).

Modern B-mode ultrasound imaging almost entirely applies multielement transducers. Figure 5.17(a) shows the structure of a sixteen-channel linear transducer array (Granz, 1986). The common electrode of the piezoelectric

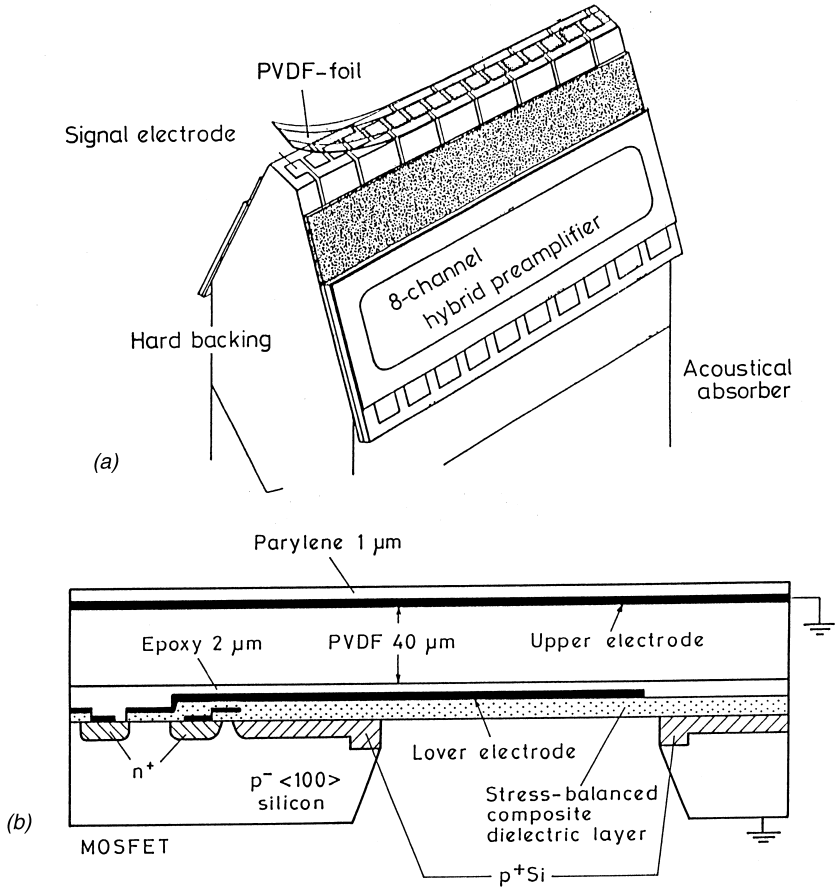

FIGURE 5.17. Integrated ultrasound transducer structures with PVDF: (a) linear hybrid array and (b) one cell of a silicon-based version (POSFET). [Reproduced with permission: (a) from B. Granz, "Ultraschall-Empfangsarray aus dem piezoelektrischen Polymer PVDF," *NTG-Fachberichte, Sensoren - Technologie und Anwendung, Bad Neuheim,* pp. 264–270, ©1986, VDE-Verlag GmbH; (b) from *Sensors and Actuators A,* J. H. Mo, L. Anrew, L. Robinson, F. L. Terry, Jr., D. W. Fitting and P. L. Carson, "Improvement of Integrated Ultrasonic Transducer Sensitivity," 21–23, pp. 679–682, ©1990, with permission from Elsevier Science S.A., Lausanne, Switzerland,]

transducer capacitor elements is on the surface of the PVDF polymer foil, while the individual signal electrodes are on the substrate connected with alternating wires to both sides. The signal conditioning is performed by two eight-channel hybrid integrated MOSFET-input amplifier units. The resolution is limited by the size of the array elements and the lateral ultrasound

spreading inside the piezoelectric material and the substrate. The application of PVDF is favorable from the latter point of view.

Linear arrays can be focused and steered in only one plane—the azimuth plane. A lens is used in the elevation plane, perpendicular to the imaging plane, to focus, and this determines the slice thickness of the imaging plane. Because of the broadened beamwidth in the near field and beyond the focal zone, contrast resolution degrades in these regions. This problem can be alleviated by using multidimensional (1.5D or 2D) arrays (Shung and Zipparo, 1996). A few rows of linear arrays comprise 1.5D arrays. The use of additional rows in the elevation plane is limited to provide a dynamic focus, similar to that described in connection with Figure 5.16(b). Focusing in the elevation plane allows a reduction in slice thickness and, thus, an improvement in the image quality over a larger depth of view.

The ultimate ultrasonic scanners, which should be capable of producing real-time images in 3D, necessitate real 2D arrays with a large number of linear array rows. Annular arrays with concentric, ring-shaped transducer elements have also been used to achieve biplane focusing. With appropriate dynamic processing, focusing throughout the field of view can be attained. However, this type of probe cannot provide beam steering; mechanical steering has to be used to generate 2D images (Shung et al., 1992).

Recently, miniature two-dimensional integrated ultrasound sensor arrays based on silicon micromachining have been developed. The structure of a single individual cell is shown in Figure 5.17(b) (Mo et al., 1990). The metallized piezoelectric foil is attached to the surface of the silicon chip that contains a thin diaphragm made by anisotropic etching. The input MOS transistor of the preamplifier unit is integrated close to the diaphragm; its gate electrode is directly connected to the piezoelectric capacitor. The operation is based on the sound-pressure-induced modulation of the drain current in the field effect transistor. The device is often called POSFET (Piezopolymer Oxide Semiconductor FET). The structure assures a number of advantages for ultrasound imaging. It employs the mentioned advantages of PVDF. The thin diaphragm can pick up the sound-pressure-induced deformations with a high efficiency; the thin silicon substrate assures low lateral propagation, and thus, a low-level cross talk between adjacent array elements; the integration of the preamplifier improves the signal-to-noise ratio; and the small cell size gives good resolution. Not only linear arrays, but also 2D-matrices, can be realized, which enables the three-dimensional imaging technique. Its disadvantage is that the direct connection between the capacitor and the field effect transistor prevents transmitter operation. The transmitter can be operated either by disconnecting the preamplifier electronically during transmission or by controlling the transmitter and receiver elements separately. Both solutions result in more complicated cell structures. The device performs at about a 1 mV/Pa sensitivity and at a 1.6 kPa lower detection limit.

5.4.3 Doppler-Sonography for Blood-Flow Measurements

With a suitable choice of wavelength, ultrasound may be scattered from moving structures such as red blood cells (Atkinson and Woodcock, 1982). It is possible with ultrasound to measure the velocity of red blood cells and deduce the *velocity of blood flow in arteries and veins.* To do this, the well-known Doppler technique is employed, the principle of which is illustrated in Figure 5.18 (*Doppler sonography*). In the duplex transducer, two piezoelectric elements work together: one only in transmitter mode, the other only in receiver mode. The transmitter generates monochromatic ultrasound waves, and the receiver detects the frequency shift of the reflected sound waves scattered from the moving blood cells. Supposing a small angle between the incident and reflected directions, the connection of the velocity (v) and frequency shift (Δf) can be expressed as follows:

$$\Delta f \approx -(2v/\lambda) \cdot \cos\phi \tag{5.4}$$

where λ is the wavelength and ϕ is the angle between the incident radiation and the direction of flow. The frequency shift can easily be monitored by electronic mixing.

Doppler sonography has recently become the most important tool for non-invasive blood flow measurements. CW (continuous wave) Doppler blood-flow detectors operate by means of continuous sinusoidal excitation. The frequency difference calibrated for flow velocity can be displayed or transformed by a loudspeaker into an audio output. Such appliances are available on the market with various interchangeable, pencil-like probes that are operated with different frequencies, generally, one is used for examining vessels near the skin, another for intermediate or deep vessels, and a third for fetal heartbeat monitoring. Angle adaptors can be used for holding the probe at a fixed degree.

Simple CW Doppler systems are unable to distinguish the source of the echoes. This may be a serious problem when there are overlapping vessels. In pulse-mode wave (PW) operation, sinusoidal ultrasound pulses are excited while time-of-flight and frequency shift are simultaneously monitored. Combined with dynamic scanning, a blood flow velocity map can be displayed according to the cross section of the vessel. CW Doppler imaging systems can also be operated based on similar principles such as C-mode scanning. Duplex Doppler imaging appliances, which combine B-mode real-time imaging with Doppler flowmetry, provide unique possibilities unattainable with other imaging modalities. Color Doppler imaging techniques involve displaying the conventional cross-sectional gray-scale B-mode view superimposed on a color blood-flow velocity map. Because a discussion of further details of ultrasound

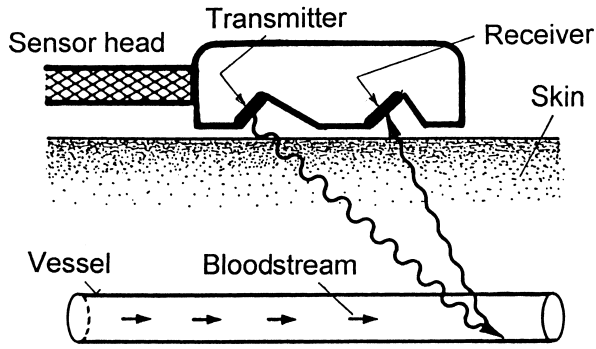

FIGURE 5.18. Principle of the Doppler blood-flow measurement.

imaging is beyond the scope of this book, we refer to the literature (Shung et al., 1992; Webster et al., 1997).

Invasive catheter echography and Doppler sonography also became available with the introduction of PVDF- and silicon-based miniature transducers.

5.5 DETECTORS IN RADIOLOGY

5.5.1 X-ray Imaging with Sensors

X-ray radiation is the oldest and most widely used noninvasive medical imaging tool in radiological diagnostics. In classical X-ray diagnostics, visible images are produced on X-ray-sensitive film or are displayed on a fluorescent screen. When displaying these images on a fluorescent screen, X-ray image amplifiers enable a direct image display. Incident X rays impinge on the surface of a fluorescent (generally CsI) screen from which secondary, visible photons are emitted (Shung et al., 1992). These photons excite photoelectrons from the photocathode of a vacuum tube that, by means of appropriate electron optics, can be used to obtain a real-time visible image on a display screen located on the opposite side of the same vacuum tube. By combining the X-ray amplifier with image dividers and video cameras, real-time monitoring and image and motion storage become available. Modern teleradiology makes it possible for digital imaging equipment to be used to store, send, and view X-ray images. Digital image processing tools, such as background subtraction, smoothing, windowing, zooming, etc., enable improved image quality; thus, details that may be hidden during normal image viewing can be recognized. Another advantage is that patients may be exposed to lower doses of X-ray radiation. The possibilities of the X-ray-amplifier/TV-chain system are

limited by the complicated multiplied signal transduction (X ray → visible light → photoelectron → visible light → electron → A/D conversion) that results in the deterioration of resolution and signal-to-noise ratio. Thus, the most important tools of future teleradiology should be X-ray sensor arrays that enable direct image digitalization.

One approach for producing *X-ray images by sensor arrays* is to use X-ray CCDs that are covered by fluorescent materials, "phosphors." The most notable problem with these sensors is that since X rays cannot be handled by lenses as can visible light, the image they produce is much smaller than that needed in general applications. Therefore, the first application of these sensors was in dental radiography: making x-ray images of teeth. Also, conventional X-ray mammography systems using large-area (49 mm × 85 mm) CCD detectors became available recently. For larger images, NASA researchers applied a new mosaic scanner technique with CCD chips arranged as shown in Figure 5.19 (Jalink, 1995). In this mosaic scanning, a checkerboard of CCDs

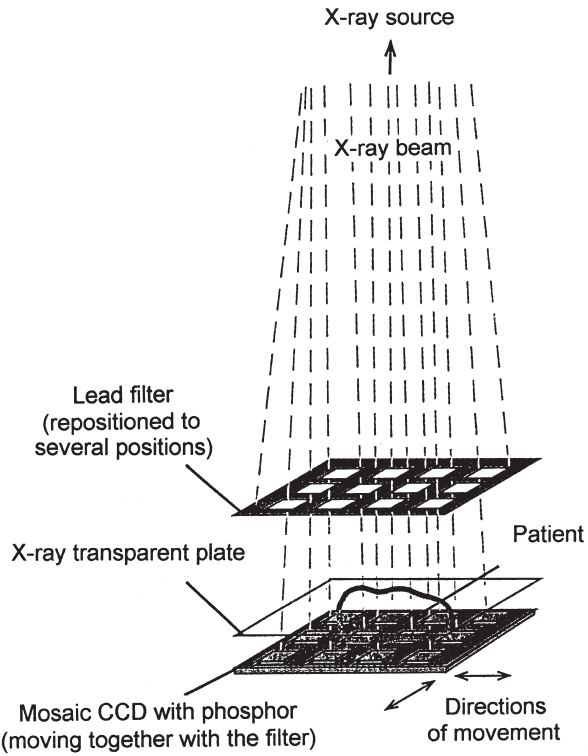

FIGURE 5.19. X-ray image formation using CCD mosaic (Jalink, 1995).

quickly acquires an image several times in different positions, eliminating "dead stripes." The movement is tracked by an appropriate lead-collimator system placed between the X-ray source and the patient. The mosaic images formed in each position are then recombined by a computer that produces a composite. The prototype can prepare images with a size of only 5.08 × 5.08 cm (2″ square) with a resolution that enables the recognition of precancerous tissue spots with the size of 0.1 mm diameter.

According to another approach called the *optically coupled CCD X-ray imaging system,* X rays are impinged into a fluorescent screen and the image produced is then transferred onto the surface of an individual CCD by optical lenses (Liu et al., 1994). The resolution is worse than that of the previously mentioned system, but allows for large moving pictures to be viewed in real time and processed digitally. To overcome the problem of resolution, the applied photosensor array elements should be fabricated directly on the surface of the scintillation screen, called a *flat-panel imager* (Antonuk et al., 1992). One array element consists of a hydrogenated amorphous silicon (a-Si:H) thin-film-based photodiode and a thin-film field effect transistor fabricated by CVD. As transparent electrodes, indium-tin-oxide thin films were applied. The biggest drawback to this solution is that a large number of array elements must be used in order to achieve good resolution and large-area image transfer. The yield of the processing drastically drops with an increase in the area and pixel number. One solution is to seamlessly tile amorphous silicon photodiode TFT (thin-film transistor) arrays for very large area X-ray image sensors (Powell et al., 1998). Four standard arrays are cut parallel to the bus bars, in the space between the bus bar and the preceding pixel electrode. The four subarrays are then rotated by 90°, with respect to their neighbors, and butted together. By doing this, the seam between each tile would have no bus bar, and the pixel pitch between neighboring tiles could be reproduced with an acceptable alignment tolerance of the tiles. A 192 × 192 pixel array with a 200 μm pitch has demonstrated the feasibility of the method.

A new invention, the combination of collimated X-ray scanning and the so-called "Charpak" detector, a multicomponent proportional counter (see Section 4.11) array, is illustrated in Figure 5.20 (Kalifa, 1995). The proportional multiwire chamber is a gas (a mix of xenon and CO_2) ionization particle detector. On the inside, there is an alignment of copper wires, ten microns in diameter, that are pulled tight like the weave of fabric on a loom. The axis of each wire faces the X-ray source, 1.3 m away. The wires measure five centimeters and are separated from one another by 1.2 mm. Cathodes are set up on each side of the wire layout. Each wire is connected to an amplifier, a selection component, and a counter. The chamber/electronic-counting unit is supported by an arm with the X-ray tube fitted onto its other end. A finely collimated X-ray beam scans the patient's body during the examination. The

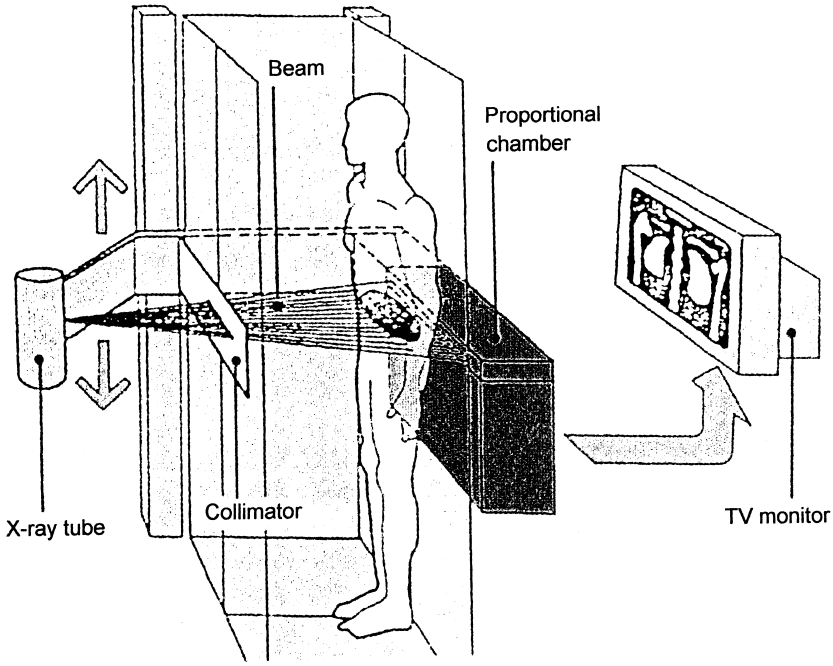

FIGURE 5.20. X-ray image formation using Charpak detector and X-ray scanning. (Reproduced from G. Kalifa, "New System Slashes X-ray Radiation Hazards," *Biophotonics International,* July/August 1995, pp. 18–19, with permission of Prof. Gabriel Kalifa, Service de Radiologie, Hopital Saint-Vincent-de-Paul, Paris, France.)

detector records a line every 30 ms and stores it in the computer's memory bank. The lines are than processed and displayed on the computer's screen. The spatial resolution of the system is 0.6×0.6 mm. Its further advantage is that it delivers 100 times fewer X-rays (!) than existing radiology systems. The reason for this is a more efficient detector component and less radiation scattered by the collimator system. Besides lowering irradiation, eliminating scattered radiation improves data quality; a weak contrast is no longer lost in the background noise.

5.2.2 X-ray Sensors in Computed Tomography

It is doubtless that X-ray *computed tomography (CT)* was the greatest invention in the history of X-ray radiology (the 1979 Nobel Prize was awarded to the investors, Hounfield and Cormack). The method relies on the newest results of nuclear technology, electronics (radiation detection, amplification, noise reduction, X-ray scanning), and digital signal processing. Images are

made not parallel to the axis of the human body, but perpendicular to it, enabling cross-sectional views to be prepared. The basic idea, independent of the practical appliance considerations, is that the collimated X-ray bundle sweeps the body transversely and the penetrated radiation intensity profile versus angle is measured by the detector array located on the opposite side of the body (see Figure 5.21). The X-ray source moves around the object, making intensity profiles in a number of positions that are then processed by the computer. One pixel brightness of the cross-sectional view is set proportionally to the sum of all intensity values measured with source-pixel-detector straight coincidence. By making several cross-sectional views, three-dimensional images can be prepared using a *morphometer.* The exposition time of one cross-sectional image is 1–25 s. This relatively long image preparation time limited the first applications of the method to investigations of the skull, brain, and motionless tumors. Tomography of moving organs, like the heart, only recently became a reality. The ultra-fast CT (UFCT) can prepare 15–20 individual cross-sectional images in seconds, simultaneously (Song et al., 1994).

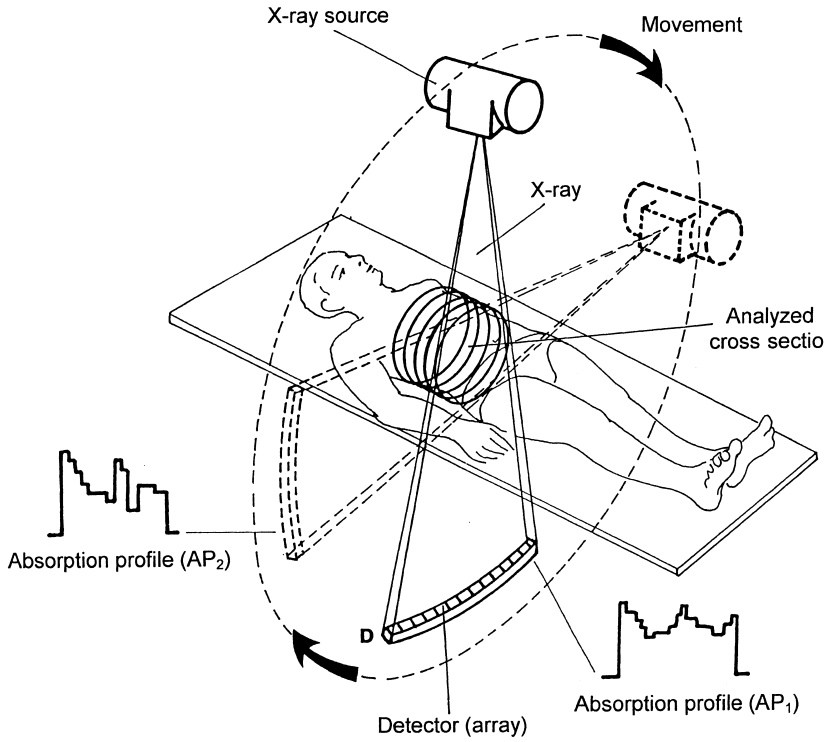

FIGURE 5.21. Principle of X-ray computed tomography.

Conventional X-ray computed tomography detectors are photoelectron multipliers (PEMs) combined with collimators and scintillation crystals (see Figure 5.22), such as NaI, BGO, CWO, or LSO (see Section 4.11). PEMs offer several unique advantages in image processing over newer solid state detectors (SSDs) including low noise, high speed, and a detection limit as low as one photon. Their disadvantages include the large size, the sensitivity to mechanical and electromagnetic interferences, and the necessity of a stable high voltage for operation. One possibility considered for overcoming these disadvantages is to use large-area silicon PIN photodiodes and APDs (Holl et al., 1995) in scintillation detectors instead of PEMs (see Section 4.11). A severe restriction on the use of silicon diode scintillation readout comes from the high noise level. Newer low-noise APDs seem to overcome this problem. Currently, commercial CT appliances utilize BGO or CWO crystals combined with large-area silicon APDs. The main disadvantage of these detectors is the limited resolution.

A direct operation (nonscintillation) metal-sandwiched silicon solid-state detector (Si-SSD) is illustrated in Figure 5.23. The direct electron-hole generation caused by the incident X ray cannot be applied because of the small scattering efficiency inside silicon. Therefore, the collimated incident X ray is scattered first within a metal slab that produces secondary photons that penetrate one of the silicon detectors. These are diodes facing the slab, in the depletion layer of which electron-hole pairs are generated. The metal slab improves the probability of interaction with the X-ray beam in comparison with the silicon (Miyai et al., 1994).

High-purity germanium (HPGe) detectors assure better scattering efficiency. Amorphous Ge (a-Ge) deposited on high-purity Ge crystals by sputtering fol-

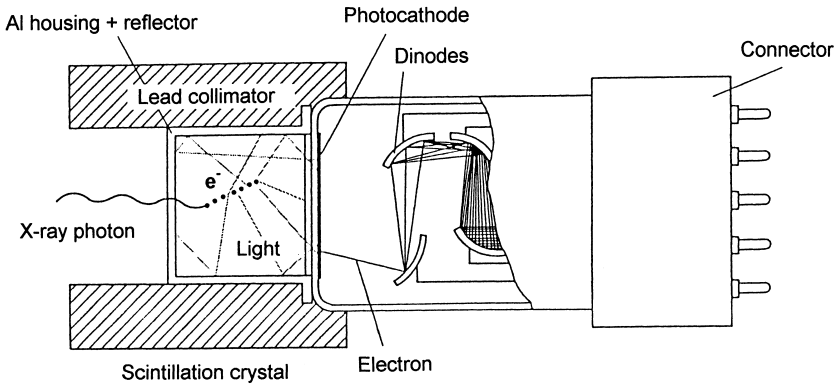

FIGURE 5.22. Structure of the classical X-ray detector used in CT—photo-electron multiplier with scintillator crystal and collimator.

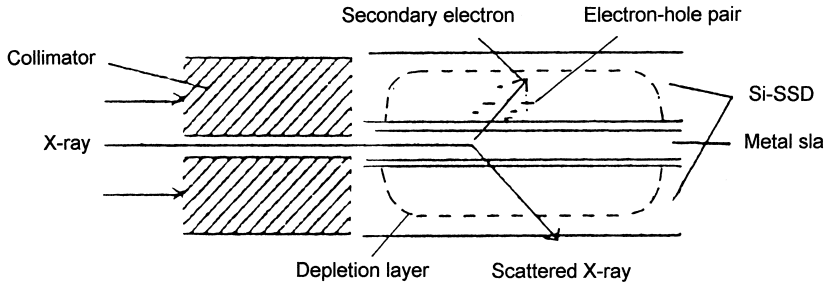

FIGURE 5.23. Structure of the metal-slab sandwich silicon solid-state X-ray detector. (Reproduced with permission from H. Miyai, S. Kawasaki, H. Kitaguchi and S. Izumi, "Response of Silicon Detector for High Energy X-ray Computed Tomography," *IEEE Transactions on Nuclear Science,* Vol. 41, No. 4, pp. 999–1003, ©1994, IEEE.)

lowed by metallization forms low-leakage-current blocking contacts suitable for radiation detector array applications, as shown in Figure 5.24 (Luke et al., 1994). The lateral resistance between the contact areas is larger by six orders of magnitude than that of the bottom contact, which forms the actual detector-resistor element. For noise reduction, a cryogenic operation at the temperature of 77 K should be assured.

Compton X-ray backscatter imaging (CBI) does not use the transmitted X-rays, but instead uses those scattered by the organs due to the Compton effect (see Section 4.11). This new method can noninvasively map displacement and velocity patterns on the epicardial surface with a high degree of spatial and temporal precision. The same X-ray detectors can be used here as in the CT described previously (Herr et al., 1994).

5.5.3 Detectors in Nuclear Radiology

Nuclear radiology uses nuclear radiation for imaging. The *in vivo* method is performed by delivering radioactive isotopes (e.g., $^{99}Tc^{m}$, ^{123}I) into the body of the patient, the time-dependent distribution of which is followed by measuring γ-radiation intensity. The conventional *scintigraphic* equipment applied a single detector; the distribution image was composed from step-by-step intensity measurements. Later, the Anger-(γ)-camera was used for such purposes, enabling real-time 2D distribution imaging. This imaging device consists of a collimator system, a large-area NaI scintillator crystal, and a photoelectron multiplier (PEM) array. Modern angiography employs position-sensitive PEMs (PSPEMs). PSPEM unifies the PEM array into a single vacuum tube containing a large-area common photocathode, a mesh system of dinode arrays, and a multiwire anode array consisting of a number of electri-

cally independent wires in both x and y directions. Coordinates of the scintillation can be determined using appropriate readout electronics. A pulse height analyzer circuit makes it possible to determine the energy of the absorbed photons individually. New generation gamma cameras employ semiconductor solid-state sensor arrays that are operated either cryogenically (Ge) or at room temperature (CdTe, Si).

Modern nuclear radiology applies the tomographic imaging technique. In *single photon emission computer tomography (SPECT),* similar to angiography, the emitted γ-radiation intensity is measured in various directions. A γ-camera rotates around the object, taking measurements in a number of positions. Cross-sectional images are produced in a manner similar to conventional X-ray CT imaging. Several cross-sectional images can be produced simultaneously. The resolution of the method is in the "cm" range.

Figure 5.25 shows the idea of a real-time SPECT imaging system that does not apply moving parts (Singh et al., 1989). The central ring of a multi-ring SPECT instrument consists of eight cameras with a divergent-hole collimator on each camera to obtain a field of view that totally encompasses the central circle-shaped cross-sectional area. Each camera consists of a NaI scintillator and a position-sensitive PEM tube. Thus, various directions are rendered to show scintillation positions at the PEM.

The concept of electronic collimation has also been developed, which can be realized mainly with semiconductor detectors. Typically, cryogenically cooled germanium and room-temperature operable silicon and cadmium-zinc-telluride (CZT) semiconductor detector arrays have been applied to replace PEMs (Singh et al., 1995). Semiconductors have superior energy resolution and a fast response time of about 10^{-9} sec. However, their application in nuclear radiology is limited due to cost and noise problems. Using modern

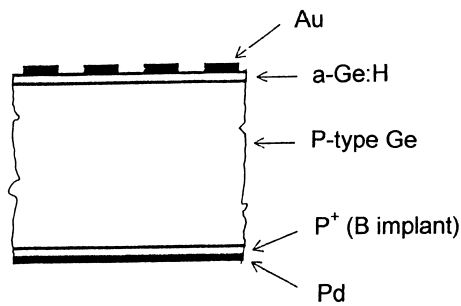

FIGURE 5.24. Structure of the X-ray detector array fabricated on a high-purity Ge crystal. (Reproduced with permission from P. N. Luke, R. H. Pehl and F. A. Dilmanian, "A 140-Element Ge Detector Fabricated with Amorphous Ge- Blocking Contacts," *IEEE Transactions on Nuclear Science,* Vol. 41, No. 4, pp. 976–981, ©1994, IEEE.)

SPECT imaging techniques, resolution is already in the range of a few millimeters. The main limitation of the method is that the transmission attenuation of the γ-rays passing through the body is unknown, thus, correction is impossible.

Positron emission tomography (PET) employs ultra-short lifetime positron (β^+) sources, like ^{11}C, ^{13}N, ^{15}O, and ^{18}F isotopes, that can easily bind to the organic molecules of living cells (Shung et al., 1992). The emitted positrons scatter with high efficiency on electrons that are present in all molecules of living cells, and the positron-electron annihilation results in two γ-photons having equal energies (511 keV each) and opposite term velocity vectors. The basic element of the PET system is a pair of γ-detectors in 180° position in coincident operation; thus, a positron absorption is registered only if both detectors simultaneously give impulses. This coincidence measurement provides unique possibilities for noise reduction and for designating the direction of positron absorption. Some transmission attenuation compensation is also pos-

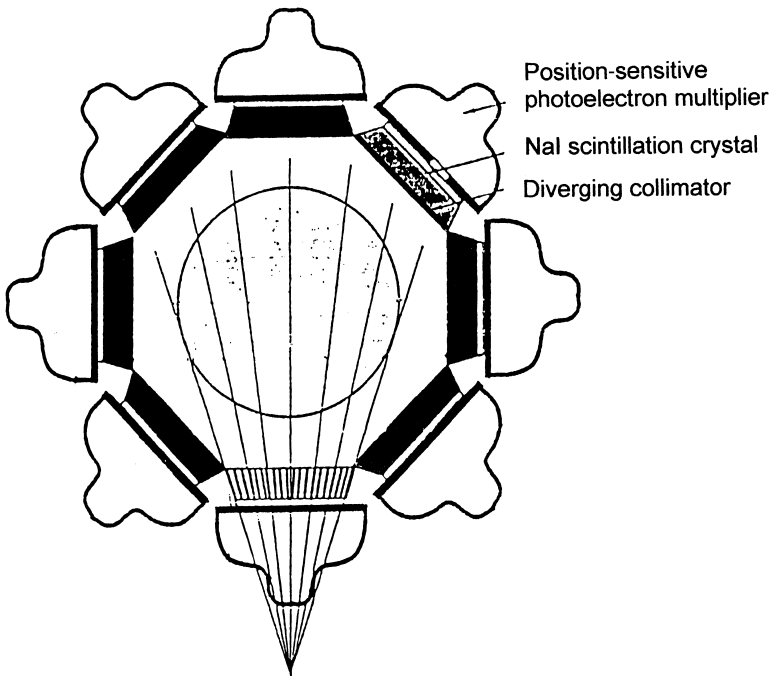

FIGURE 5.25. Central ring of a real-time SPECT system. (Reproduced with permission from M. Singh, R. Leahy, R. Brechner and X. Yan, "Design and Imaging Studies of a Position Sensitive Photomultiplier Based Dynamic SPECT System," *IEEE Transactions on Nuclear Science,* Vol. 36, No. 1, p. 1132, ©1989 IEEE.)

sible since the exact original energy of the γ-photons is known. Although PET is not a competitor of conventional X-ray tomography in terms of resolution, real-time imaging of dynamic processes is possible. Due to its application, metabolic processes during brain and heart operations were investigated and special scientific inventions became available. Radiation exposure to the patient is minimal, since the isotopes have short half-lives of 2–20 min. This is also, however, the main limitation of the method—it must be settled near a cyclotron in order to have short-lifetime radioactive-isotope sources continuously on site. Because of this limitation, PET is a tool of scientific research, rather than a method of everyday medical diagnostics. However, it is currently the most developed imaging technique. Since the spatial and time resolutions are mainly dependent on the detectors, their development is the focus of PET research efforts. The resolution of 5–7 mm, that was typical for the first PET systems, has been reduced to under the mm size (McIntyre et al., 1995). A few detector examples are demonstrated as follows.

For three-dimensional real-time imaging, detector blocks should be arranged circularly around the object. A typical arrangement is illustrated in Figure 5.26(a) (Rajeswaran et al., 1992), while the structure of an individual block is shown in Figure 5.26.b (Cutler and Hoffman, 1994). The detector module is fabricated from a scintillation crystal segmented into an array and coupled to a PSPEM. Typically, BGO or LSO scintillation crystals are applied instead of NaI because of their higher absorption, thus, there is greater interaction efficiency with high-energy γ-photons. Annihilation event direction can be determined by identifying the scintillating segment by the position-sensitive PEM.

The block design used in most PET systems suffers from several drawbacks that may limit their application in high-resolution imaging appliances. First, mispositioning is possible resulting from the cross talk inside the PEM tube, which becomes more serious with size reduction. Densely packed, fine-grained crystal arrangements cannot directly be coupled to PEM tubes. A bundle of optical fibers is generally applied between the tubes, enabling one-to-one coupling of scintillation crystal and multianode PEM segments (McIntyre et al., 1995). The greatest problem is the bigger size of the overall apparatus. The real size reduction may be achieved by combining scintillation crystals with semiconductor APDs or PIN diodes, the application of which is in the development stage because of the noise problems mentioned previously (Schmelz et al., 1995; Moses et al., 1995).

Another problem of the scintillation PET systems is that only about 44% of the 511 keV gamma rays interact photoelectrically; thus, many of the detected events are scattered in the block. The block detector has no way of discriminating between photoelectric events and events that undergo one or more Compton scatters. Compton electrons may also generate secondary scintilla-

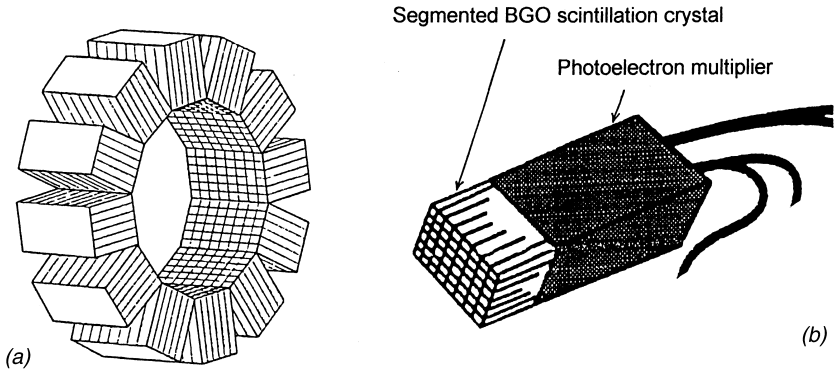

FIGURE 5.26. PET system consisting of detector blocks: (a) arrangement of the blocks and (b) typical structure of an individual detector block. [Reproduced with permission: (a) from S. Rajeswaran, D. L. Bailey, S. P. Hume, D. W. Townsend, A. Geissbühler, J. Young and T. Jones, "2-D and 3-D Imaging of Small Animals and the Human Radial Artery with a High Resolution Detector for PET," *IEEE Transactions on Medical Imaging,* Vol. 11, No. 3, p. 386, ©1992, IEEE; (b) from P. D. Cutler and E. J. Hoffman, "Use of Digital Front-End Electronics for Optimization of a Modular PET Detector," *IEEE Transactions on Medical Imaging,* Vol. 13, No. 2, p. 408, ©1994, IEEE.]

tion in adjacent crystal segments resulting in cross talk. Photoelectron events have, however, a well-defined penetration depth with a narrow tolerance. The real solution for a better crystal-PEM coupling and for distinguishing photoelectron and Compton-type scintillation would be to measure interaction depth and identify the scintillating crystal element.

The combination of position-sensitive photodiodes with a BGO-PEM detector is shown in Figure 5.27 (Derenzo et al., 1989). Figure 5.27(b) shows the layout of the position-sensitive photodiode that has one common electrode, while the other consists of two triangular twin segments. Each segment was connected to separate charge amplifiers and filter circuits. The sum of the outputs represents the energy deposited in the crystal, while their ratio corresponds to the center of intensity of the photons along the length of the photodiode. The detector module consists of three (or more) optically isolated BGO crystals attached to a single PEM tube, which provides fast timing pulse for the block. Each crystal is also individually coupled to a position-sensitive photodiode that identifies the crystal that stopped the annihilation photon and determines the depth of interaction in order to distinguish photoelectron and Compton scintillation effects. This type of detector can be operated at room temperature.

In another solution, the two LSO-PSPEM detector elements of the pair are aligned perpendicularly. One detector is the imaging detector (sensing the direction of event), and the other is the coincidence and penetration depth detector (Vaquero et al., 1998).

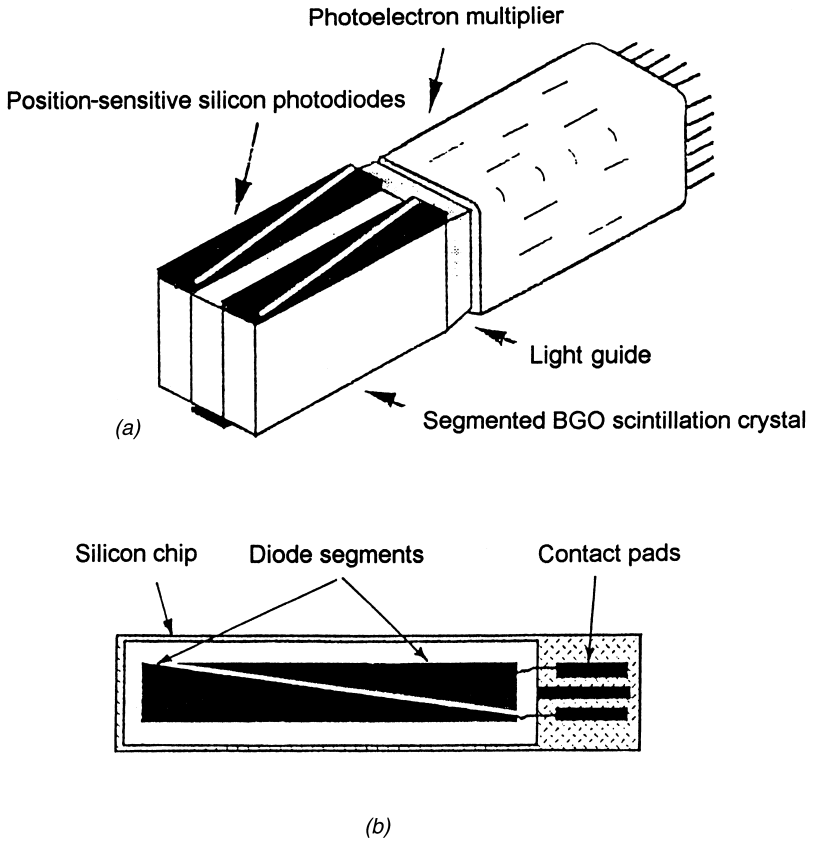

FIGURE 5.27. Position-sensitive scintillation detector block: (a) structure and (b) layout of the position-sensor photodiode. (Reproduced with permission from S. E. Derenzo, W. W. Moses, H. G. Jackson, B. T. Turko, J. L. Cahoon, A. B. Geyer and T. Vuletich, "Initial Characterization of a Position-Sensitive Photodiode/BGO Detector for PET," *IEEE Transactions on Nuclear Science,* Vol. 36, No. 1, pp. 1084–1089, ©1994, IEEE.)

A different approach was developed for measuring the depth of interaction (McIntyre et al., 1995). This approach employs plastic scintillator blocks that have much larger interaction depths. In contrast with crystals, only Compton scattering occurs in them. Two optical fiber bundle systems measure the axial and radial positions of the penetration depth. Therefore, the mechanical and electronic constructions are rather complicated.

5.5.4 Other Applications of Nuclear Detectors

Radioactive labeling of proteins, lipids, and carbohydrates is a very important technique of *in vitro radiology* for identifying, isolating, and investigat-

ing their properties and receptor binding assays (see Section 7.2.2). In such procedures, the preferred radiolabel is often tritium, because it does not interfere with the normal conformal structure of the proteins. Tritium atoms emit β-particles, the detection of which usually requires the destructive and time-consuming manipulation of the samples and their placement into the scintillating fluid. If the spatial resolution inside the samples must be preserved, the two-dimensional distribution pattern of the labeling source is conventionally measured using X-ray film. This approach requires an exposure period ranging from several days to a month.

A novel technology was developed using a specially designed large area, monolithic APD array that records the tritium activity distribution at each point within the field of view. The 1 mm^2 array elements exhibited 27% detection efficiency with low cross talk (Gordon et al., 1994).

The last, very important application field of radiation sensors in radiology is the field of *personal dosimeters* that can perform continuous monitoring, displaying, data storage, and alarm signal generation, if necessary (Izumi et al., 1989). The name-badge-size appliances are compatible in geometrical measurements and practical use with conventional indicators, and they apply low-cost Si-SSDs (the noise is not very important here) and low-power CMOS circuitry operated by button-size batteries (Moreno et al, 1995).

5.6 BIOMEDICAL APPLICATIONS OF MAGNETIC FIELD SENSORS

5.6.1 Nuclear Magnetic Resonance Imaging

The most important, but not unique, application of magnetic field sensing is the medical *nuclear magnetic resonance imaging (NMR or MRI)* technique. The basis of the method is the phenomenon that nuclei in an external magnetic field (B) can only be excited at definite frequencies (ω) that can be expressed by the Larmor equation:

$$\omega = \gamma B \tag{5.5}$$

where γ is the gyromagnetic ratio characteristic of the type of nuclei. According to a mechanistically developed model, this frequency is equal to the frequency of precession rotation of nuclei. Conventional MRI is based on ^1H nuclei (protons) (γ = 42.6 MHz/Tesla); thus, the distribution and bonding state of tissue fluid is the basis of the image contrast. Other types of MRI techniques have become available for practical applications that apply ele-

ments other than H, such as ^{23}Na (γ = 11.3 MHz/Tesla) or ^{31}P nuclei (γ = 17.2 MHz/Tesla).

Under normal conditions, the nuclei precess with the same frequency, but in randomized phase. As a consequence, the rotating magnetic moments generate radio signals that cannot be detected. If they are conditioned with a short radio signal at the same frequency as they are precessing, they begin to radiate a signal with a magnitude that is a function of the number of spinning nuclei (spin density) and the strength of the imposed magnetic field. The physical mechanism responsible for the image's production is a consequence of Equation (5.5). If the imposed field is not uniform along the sample, than the resonant frequency is different in each section. A magnetic field that varies with spatial variation is known as a gradient and can be applied during or after the excitation process. If a gradient is energized during the excitation pulse parallel to the high constant magnetic field (denoted z-axis), only those nuclei that satisfy the Larmor equation for the particular frequency of excitation will be affected. This phenomenon, known as selective excitation, is used to identify the location and orientation of the image plane. The ability to select slice information gives the z gradient the name "slice selection gradient." By changing the center frequency of RF excitation pulse and the bandwidth, the slice position and slice thickness can be changed.

Similarly, x and y gradients are used in combination with different RF pulses to encode and read out (decode) spatial information from the image plane. An important phenomenon is that spin alignments and spinning phases can be ordered by appropriate pulse sequences. The "phase encoding gradient" pulse is applied after ordering the spinning phases, and just before a RF impulse. Nuclei along the axis of the gradient will rotate with different frequencies. Switching out the gradient field, they will rotate again with the same frequency, but with different phases. Thus, phase encoding of the nuclei has been performed according to the rows of the slice. Each time an excitation pulse is sent out, the value of the encoding gradient may be changed, until the entire distance is covered. The third gradient, the frequency or readout gradient, is applied when echo radiation is emitted by the nuclei to divide the rows into pixels by encoding the columns of the slice with different answer frequencies. The image itself is generated from a set of echo pulse data, each member of which is uniquely associated with a particular encoding gradient and readout gradient. After the data are collected, a double Fourier transformation is applied to convert time to frequency and phase, which maps the x, y coordinates with the Larmor equation.

The value of each pixel is related to the amplitude of the echo signal from a given location. The signal intensity varies with time in a fashion that can be described in terms of the relaxation phenomena. There are two different relaxation processes that affect the magnetic resonance signal: T_1, the longitu-

dinal or spin-lattice relaxation time, and T_2, known as the spin-spin relaxation time. The influence of the parameters on the signal is described by the Bloch equation:

$$I \sim N(\mathrm{H}) \cdot [1 - \exp(-T_R/T_1)] \cdot \exp(-T_E/T_2) \tag{5.6}$$

where N(H) is the spin density, T_R is the pulse repetition time, and T_E is the echo time. Thus, conventional images represent a complicated convolution of intrinsic relaxation time parameters. Using appropriate pulse sequences, simultaneous T_1 and T_2 mode imaging can be realized, and further images may be obtained by mathematical processing of the images (O'Donnell et al., 1986). A more detailed description of image processing is beyond the scope of this book, so we refer to the literature (Shung et al., 1992).

Clearly, the signal is a function of the number of nuclei that have been excited in a given volume element (voxel). This is a function of the volume excited and the spin density. The voxel size is a function of the slice thickness and image pixel dimensions. Big voxel sizes will generate more nuclei and so improve the signal-to-noise ratio, but will destroy the spatial resolution at the same time. If a given excitation pulse sequence is repeated at the same encoding gradient setting, an improvement in the signal-to-noise ratio can be achieved by averaging. The price paid for this is the multiplied scan time, which also increases the data acquisition time.

The great advantage of MRI is its ability to produce image pixels from direct measurements without applying ionizing radiation. Since NMR spectroscopy is a well-known method in chemical analysis, it also has the potential for getting physiological and biochemical information noninvasively. The spatial resolution is 1–2 mm, and the slice thickness is 5–20 mm. Data acquisition time depends strongly on the task. It ranges from seconds to several minutes, although the scanning time is in the ms range.

The most important part of the MRI instrument is a large magnet that provides a constant, homogenous magnetic field of 0.1–1.5 T along the patient's body. Superconducting electromagnets are now the industry standard for this purpose. Low-field (0.05–0.3 T) permanent magnets are also attractive because of their low cost. Generally, several other coils assure the gradient fields, the RF excitations, and the detection of echo signals. The same RF coil may be used to transmit and to receive the RF signal, but in many cases, it would be desirable to have a separate coil to receive the signal. This solution allows for a geometric configuration of individual coils that are optimized for transmission and reception, respectively.

A number of RF coil designs, including the solenoid, the multiple-turn solenoid, the "birdcage" coil, and the saddle coil, have been used in MRI sys-

tems (Partain et al., 1988). The noise floor of conventional MRI systems is determined by the receiver coil noise for low-frequency imaging and a small field of view. The signal-to-noise ratio can be increased by reducing the coil noise. The thermal noise of a conventional copper coil can be lowered by decreasing its operating temperature. Whole-body receiver coils are generally operated with cryogenic cooling at liquid nitrogen temperatures (Hall et al., 1988). Even liquid-helium-cooled superconducting RF coils in combination with DC SQUID (see Section 4.10) amplifiers have been developed for MRI at 0.01 T (Seton et al., 1995).

Nowadays, planar inductors called "surface coils" are used in the "receiver only" mode in combination with a large-body transmission RF coil to get more information from few details with high resolution and improved signal-to-noise ratio. Surface coils are most often used for imaging the knee, shoulder, neck, spine, and eye. The application of high-temperature superconductor (HTS) materials has gained great importance in this field. Superconducting receiver coils of HTS materials can be operated with liquid nitrogen, where they can show extremely low noise levels in the RF range as a result of their low AC resistance. The problems stem from the processing of HTS materials because wire production is still under development. Surface coils can, however, easily be fabricated by means of thin- or thick-film technologies (Withers et al., 1993). HTS materials may also be applied in other areas, such as *magnetic resonance microimaging (MRMI)* (Black et al., 1944), where small-size film-type planar coils can be applied, and in *sodium MRI,* where low noise is an important consideration (Miller et al., 1996). They are also widely used in the field of *in vivo* NMR spectroscopy.

A multilayer thin-film TBCCO superconducting receiver coil sputtered onto $LaAlO_3$ substrate and patterned by ion milling for sodium MRI purposes was investigated recently (Miller et al., 1996). The coil design consists of single planar coil inductor elements with interdigital capacitors between the turns of the inductor to avoid crossover complications associated with the fabrication of a multilevel structure. The signal-to-noise ratio was improved by a factor of ten by using the HTS coil instead of a room temperature copper coil. The imaging of sodium nuclei holds enormous potential as a diagnostic tool in distinguishing normal and damaged tissue. Sodium MRI has shown advantages over conventional hydrogen MRI in the early detection of certain brain disorders.

Capacitive coupling was also used between thin-film YBCO coil elements deposited onto the same type of substrates to determine LC resonators for MRMI purposes at 7 T (Black et al., 1994). The signal-to-noise ratio was improved by a factor of 10–30 relative to a copper coil operated at room temperature.

5.6.2 Sensors for Recording Biomagnetism

The unrivaled ability of SQUID magnetometers (see Section 4.10) to measure weak magnetic fields associated with physiological and pathological activity in the human body initiated a new field of research that is gaining significant interest in laboratory and clinical use. The widest scientific and commercial interests have concentrated on *magnetoencephalography (MEG),* and, hence, this is the area with the most active instrumentation development. In electrical activity of the brain, currents in the nerve dendrites induce magnetic fields that are measurable outside of the surface of the scalp. Impressive results have been achieved in three-dimensional localization of epileptic foci. In *magnetocardiography (MCG),* magnetic fields produced by ionic currents in the heart are recorded outside of the body. Multichannel MCG systems relying on SQUID arrays may provide additional information beyond that recorded by the less expensive conventional electrocardiogram (ECG) (Numminen et al., 1995). Biomagnetic signals have also been detected from a number of organs, and the abbreviations have been formed accordingly, like MOG (magnetooculogram), MGG (magnetogastrogram), MMG (magnetomyogram), MNG (magnetoneurogram), F-MEG (fetal MEG), F-MCG (fetal MCG), etc. The strength of these signals can be as low as a few tens of femtoTeslas (1 fT = 10^{-15}T) that should be measured in environments with a noise level of 10^8 fT.

A SQUID magnetometer is a superconducting loop containing one or two Josephson junctions (see Section 4.10) (Wikswo, 1995). It is connected with the external world by means of a superconducting "flux transformer." This consists of a closed loop of two coils—the detection coil senses the external field, while the other, the input coil, is tightly coupled to the SQUID. When applying thin- or thick-film SQUIDs, both the SQUID and the input coil are deposited onto the same substrate [see Figure 5.28(a) and (b)]. A flux transformer is used because the detection coil can be shaped to best suit the experimental requirements. First of all, with large-area detector coils, the magnetic field can be multiplied; thus, the lower detection limit may be extended. On the other hand, the ambient magnetic noise can be compensated for by using an appropriate detector coil design so that shielded room operation is not necessary. The basic idea is that magnetic fields originating from distant sources can be handled as homogenous ones. Their effects can be compensated by splitting the conventional single coil ["type 1" shown in Figure 5.28(c), called a magnetometer] into subcoils having opposite turns (Romani, 1984). Figure 5.28(c) demonstrates a number of coils developed for this purpose. A "type 2" detection coil is called a first-order gradiometer, as it senses only the first derivative of the field and higher order. A second-order gradiometer coil is demonstrated as "type 3" in Figure 5.28(c) First-order gra-

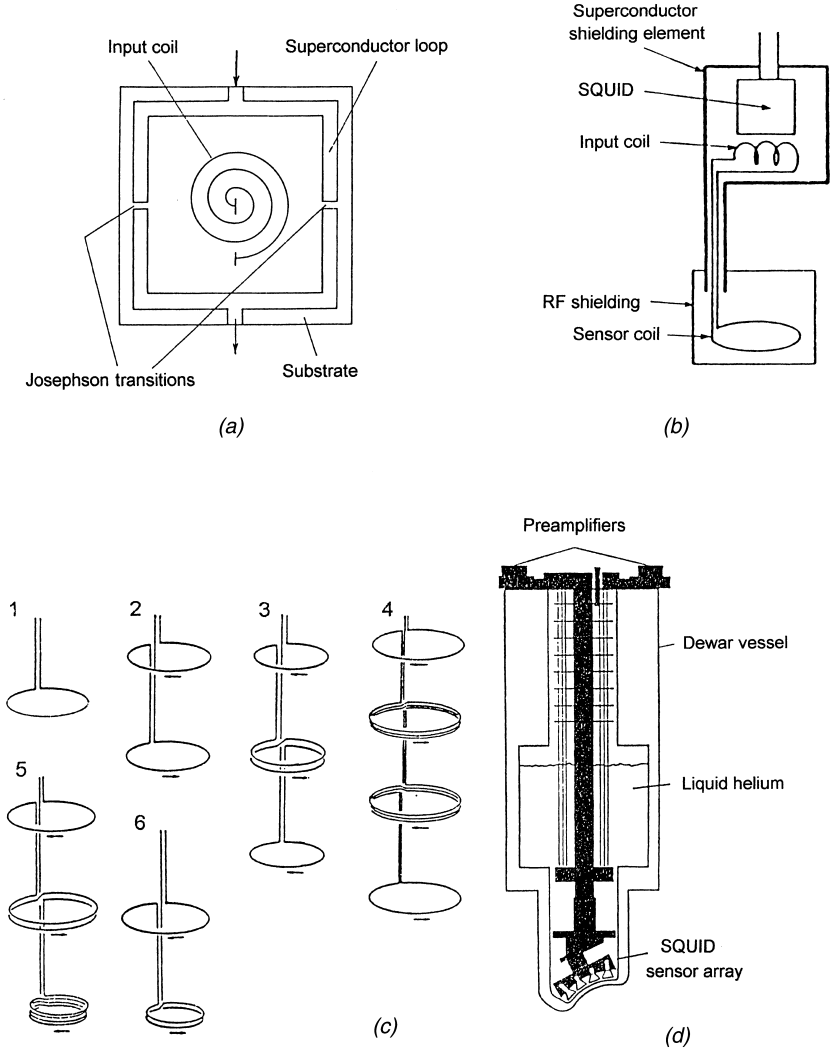

FIGURE 5.28. Detector chamber and its components for measuring biomagnetism: (a) schematic structure of the SQUID, (b) its connection with a flux transformer, (c) magnetometer (1) and gradiometer (2–6) detector coils, and (d) design of a multichannel detector chamber. [Reproduced with permission: (b) and (c) from G. L. Romani, "Biomagnetism: An Application of SQUID Sensors to Medicine and Physiology," *Physica B + C,* Vol. 126, pp. 70–81, ©1984, Elsevier Science-NL, Amsterdam, The Netherlands; (d) from J. Numminen, S. Ahlfors, R. Ilmoniemi, J. Montonen and J. Nenonen, "Transformation of Multichannel Magnetocardiographic Signals to Standard Grid Form," *IEEE Transactions on Biomedical Engineering,* Vol. 42, No. 1, pp. 72–81, ©1995, IEEE.)

diometers can be used in a weakly shielded environment, while second- or higher-order gradiometers are successfully run in many laboratories and clinics. The disadvantage of their application is that the source of the biomagnetic signals should be placed as close as possible to the lowest coil of the gradiometer. The other "penalty" to be paid is the reduced sensitivity of the detector coils. The overall system is schematically shown in Figure 5.28(d) (Numminen et al., 1995). A superconducting assembly consisting of an array of SQUIDs and flux transformers is located inside the tail of a superinsulated fiberglass dewar and is kept cold at liquid He temperature. HTS material-based systems can be operated at liquid nitrogen temperature. Using single-channel systems, data acquisition time may take hours. This time could be reduced by several orders of magnitude by using multichannel detector arrays consisting of twenty-four or more elements.

5.6.3 Magnetic Backprojection Imaging

Magnetic field sensors can also be used for imaging the vascular lumen. Conventional modalities used for the diagnosis of vascular disease include ultrasound and Doppler flow imaging, X-ray angiography, and MRI with their rather complicated and high-cost equipment. A new approach to vascular characterization, *magnetic backprojection imaging (MBI),* in contrast to other magnetic imaging techniques, uses inexpensive, readily available Hall sensors (see Section 4.8) (Hong and Fox, 1995). The basis of the technique is that human blood plasma contains many ionic compounds; thus, its resistivity is about 0.7 Ωm, which is much smaller than that of the vessel wall with a typical resistivity of 140–200 Ωm. Therefore, blood vessels act as electrical conductors surrounded with insulating tissues. Layered atherosclerotic plaques exhibit a high resistivity of 600–1600 Ωm. If a current is injected or coupled into the bloodstream in a minimally invasive way using a needle-type electrode, or in a potentially noninvasive way using capacitive coupling, the direction of the current flow will follow the central direction of the vascular lumen. Plaque buildup usually blocks a part of the lumen, and thereby changes the direction of the bloodstream, leading to detectable change in current flow direction. As is well known, an electrical current flow excites a magnetic field. From the measurement of this magnetic field, it is possible to estimate the current source distribution that generates it. By an appropriate choice of current, the magnetic field is strong enough to be able to measure it using Hall sensors. The output of a Hall sensor can be used in a backprojection to reconstruct the centroid of the blood flow and, thus, to localize the plaque region. Hall detectors can also measure constant magnetic fields. The technique cannot detect an exactly symmetric narrowing of blood vessels, but this is not typical in practice. The sensitivity and signal-to-noise ratio can be modified with the injected cur-

rent. The resistivity of the blood can also be lowered by injecting physiological saline solution into the vessel.

5.7 FURTHER APPLICATIONS OF PHYSICAL SENSORS

A number of applications of physical sensors are discussed in this section that are beyond the scope of the previous sections.

5.7.1 Electrodynamic Sensors for Blood-Flow Rate

One very important field is *flow measurement,* especially important is determining *bloodstream flow rate.*

Several methods for blood-flow measurement and for vessel lumen imaging were discussed previously, e.g., the skin blood-flow sensor, hot-wire anemometry, Doppler sonography, special versions of MRI, and MBI (see Sections 5.2, 5.4, and 5.6). Another catheter-based *invasive blood-flow measurement* method is the electrodynamic flow-rate measurement. Similar to MBI, it relies on the ionic conductivity of blood, but there is no need for an external current. If a convection current of electrical charges flows through a magnetic field perpendicular to the current-flow direction, the Lorentz force deflects the movement of the charged particles until the developed electrical field compensates for this effect (as was discussed in connection with the Hall sensor in Section 4.8). If a pair of electrodes in a distance of l are placed into the flow of charged particles perpendicularly both on the direction of flow and the magnetic field, an electrical voltage (U) can be measured, the value of which is proportional to the flow velocity (v):

$$U = Blv \tag{5.7}$$

where B is the magnetic field. In practical arrangements, the electrodes are placed onto both sides of a slot made at the catheter tip; a small magnet is fixed next to the tip, the axis of which is perpendicular both to the axis of the catheter and to the slot. The exact measurement needs a temperature compensation and an adjustment according to the actual blood composition (Yamaguchi, 1989).

5.7.2 Sensors in Ophthalmoscopy

Recent advances in electro-optics based partly on *photo sensors* have led to a number of new methods in *ophthalmic imaging* that use electronic detection of light. For example, in the conventional optical system for fundus

imaging, which illuminates and then images an extended area of fundus, a CCD array can replace photographic film. However, in newer techniques, images are formed by scanning a focused laser spot across the fundus while collecting the reflected light with a single detector. In a *scanning laser ophthalmoscope (SLO),* images of the retina with micrometer spatial resolution are constructed in this way. With automatic focusing, the depth of the retina can also be measured, and cross-sectional images can be constructed; this is the basis of *scanning laser tomography (SLT). Scanning laser polarimetry (SLP)* employs linearly polarized light that, traversing the retinal nerve fiber layer, becomes elliptically polarized because of the birefringence of the retina. Using appropriate polarizer-analyzer arrangements, a quantitative image of fundus retardation can be delivered (Knighton, 1995).

The technique of *optical coherence tomography (OCT)* provides a micron-scale resolution cross-sectional image from the overall eyeball, not only from the retina (Hee et al., 1995). OCT is similar to B-scan ultrasonic imaging (see Section 5.4), except that image contrast relies on differences in optical rather than acoustical backscattering characteristics of the tissue. Low-coherence interferometry is used to resolve the positions of reflective or optical backscattering sites within the sample. This method is illustrated in Figure 5.29. The

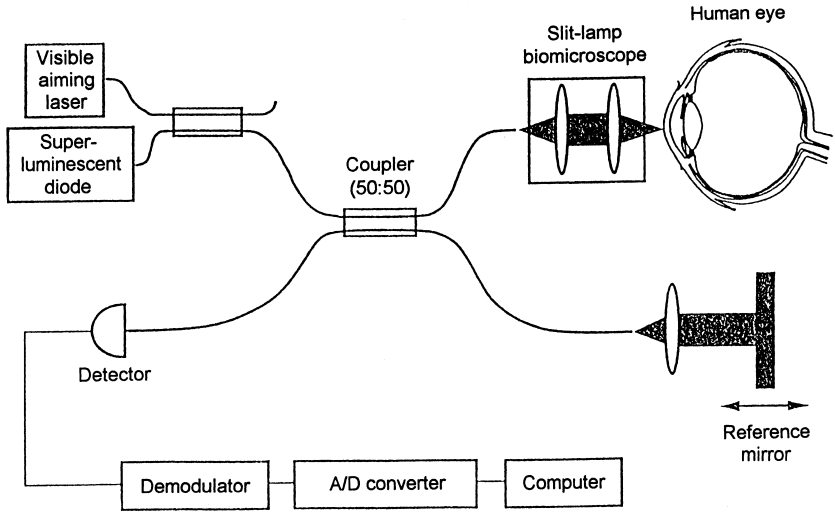

FIGURE 5.29. Schematic diagram of optical coherence tomography instrumentation. (Reproduced with permission from M. R. Hee, J. A. Izatt, E. A. Swanson, D. Huang, J. S. Schuman, C. P. Lin, C. A. Puliafito and J. G. Fujimoto, "Optical Coherence Tomography for Ophthalmic Imaging," *IEEE Engineering in Medicine and Biology,* January/February, p. 67, ©1995, IEEE.)

broad bandwidth, low-coherence (14 μm) light from a superluminescent diode source is coupled into a fiber-optic Michelson interferometer. The 843-nm-wavelength light is divided at a 50/50% fiber beam splitter into reference and sample paths. Light retroreflected from a variable-distance reference mirror is recombined in the beam splitter with light backscattered from the patient's eye. Coherent interference between the reference and sample beams is detected by a silicon photodiode, followed by signal processing electronics and computer data acquisition. Heterodyne detection provides sensitivity to weakly backscattered light exceeding 95 dB. A coherent interference signal is evident at the detector only when the reference arm distance matches the optical length of a reflective path through the eye to within the source coherence length. A longitudinal profile of reflectivity versus depth into the sample is obtained by rapidly translating the reference arm mirror and synchronously recording the magnitude of the resulting interference signal. Two-dimensional images are created by a sequence of uniaxial scans while scanning the probe beam across the sample. Pixels are pointed out by the probe beam and reference mirror positions; their value is modulated by the detector output. The axial resolution is determined by the coherence length of the source.

5.7.3 Artificial Retina

Sensors applied in *artificial organs* seem to be a topic of science fiction, however, research results assure that they will be realistic in the near future. Hearing aids were discussed in Section 5.3; a few additional examples as follow.

The first example is an artificial silicon retina, a smart sensor array with signal processing circuitry modeled after the vertebrate retina. Its eventual application will be as a sensor input to an implanted cortical stimulation array for sightless persons. Conventional cameras do not model such functions as light adaptation and lateral inhibition found in the vertebrate retina, which are also desirable in an artificial retina. An extensive parallel signal processing circuitry is necessary to mimic such functions as real-time spatial filtering (lateral inhibition) and temporal filtering (light and dark adaptations) of optical signals from an array of highly sensitive photosensors (Christensen et al., 1994). A 3D architecture was developed as shown in Figure 5.30(a), with sensors and signal processing VLSI (very large-scale integrated) circuitry fabricated on different planes in the structure. It is built with silicon wafers that are fabricated with through-wafer interconnects; the individual silicon wafers are connected using solder bump (bump grid array, flip chip) technology. This solution eliminates the trade-off between sensitivity and circuitry complexity, because the sensors and the signal processing circuitry do not compete for the same silicon surface area. Both photodiode array and CCD technologies were

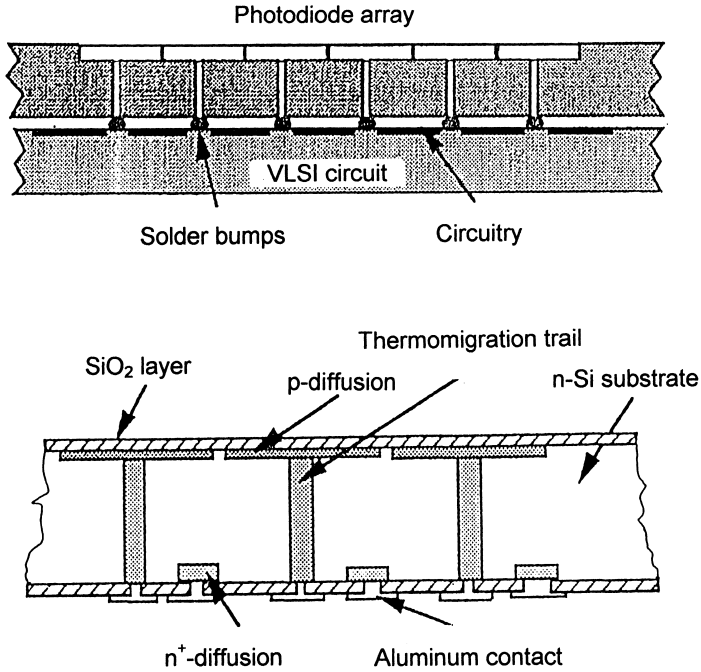

FIGURE 5.30. Schematic structure of the "artificial retina": (a) its three-dimensional architecture and (b) the cross section of the photodiode-array chip. (Reproduced with permission from D. Christensen, T. Johansson and D. Petelenz, "Biosensor Development at the University of Utah," *IEEE Engineering in Medicine and Biology,* June/July, pp. 388–395. ©1994, IEEE.)

developed for the sensor chip, the former is illustrated in Figure 5.30(b). The photodiodes are *pn*-junction devices formed by boron diffusion into the *n*-type silicon substrate (see Section 2.1). In practical arrangement, the size of each of the 100 photodiodes is 300 $\times$ 300 μm, separated from each other by 25-μm spacing strips. The photosensitive side of the array is referred to as the "front side" of the system.

The interconnects between the front side and the back side are thermomigrated trails made using the temperature gradient zone melting process. This is a high-temperature process where a thermal gradient is produced across the silicon wafer, causing aluminum, deposited and patterned photolithographically on the surface of the wafer, to migrate through the wafer as an Al-Si alloy droplet. This leaves behind a highly conductive trail of *p*-doped silicon. These highly conductive trails connect the photodiodes to the aluminum pads on the backside. The average diameter of the thermomigration trails is 80 μm. Additional n^+ islands provide an ohmic contact to the substrate.

5.7.4 Tactile Sensors for Artificial Limbs

Another application field is in the use of *tactile sensors in artificial limbs,* mainly in hands. The situation is somewhat easier here than in the artificial retina because there is no need for cortical stimulation. Self-organized movement functions can be built in with simple regulation feedback, such as the adjustment of the forces to be applied according to the shape, surface roughness, and hardness of the object to be handled. Since the problem has been studied for many years in robotics, the results can be adapted into artificial hands for human applications. In this field, there is no need for exact pressure and force measurement. It is more necessary to detect the distribution and direction pattern of forces, called the tactile image. When an object has to be manipulated, process control data concerning the orientation and shape of the object can only be deduced from the tactile image. This requires not only appropriate control units but also efficient tactile sensors that measure the local distribution of forces on the fingertips of the gripper. This can be achieved by integrating many small-force transducers in the gripping area.

Figure 5.31 shows various practical solutions for tactile image sensors. The devices use a solid rigid substrate to support a force-sensitive elastic polymer layer, which is the active film and gives an electrical signal through a kind of transduction mechanism. The signal-detecting circuitry can be hybridized alongside the device on the supporting substrate.

There are a lot of elastic polymer tactile sensors based on the following sensing effects: piezoresistive, optical waveguide, magnetic, capacitive, piezoelectric, and ultrasound.

Figure 5.31(a) shows the basic structure of a conductive composite polymer rubber-based piezoresistive tactile sensor (Wolffenbuttel and Regtien, 1991). The elastic rubber layer is a carbon- or silver-loaded polymer composite. Tactile forces imply a localized condensation of conductive particles; thus, the conductivity between two adjacent electrodes increases. Also, the pressure-dependent contact resistance between the conductive rubber layer and contact electrodes can be used. Disadvantages of this sensor include the nonlinear change of resistance and the cross talk caused by the lateral stiffness of the rubber, which limits the spatial resolution to a few millimeters.

Figure 5.31(b) shows an optical tactile transducer that conducts trapped light in a transparent plate under an elastic layer, using the condition of total internal reflection (Wolffenbuttel and Regtien, 1991). Low-intensity light leaves the plate, and a uniformly black area is seen from the bottom, monitored by a phototransistor array, until the elastic polymer film is brought into contact with the transparent layer as a consequence of tactile forces. Diffuse reflection, rather than total internal reflection, takes place, and illuminated areas ap-

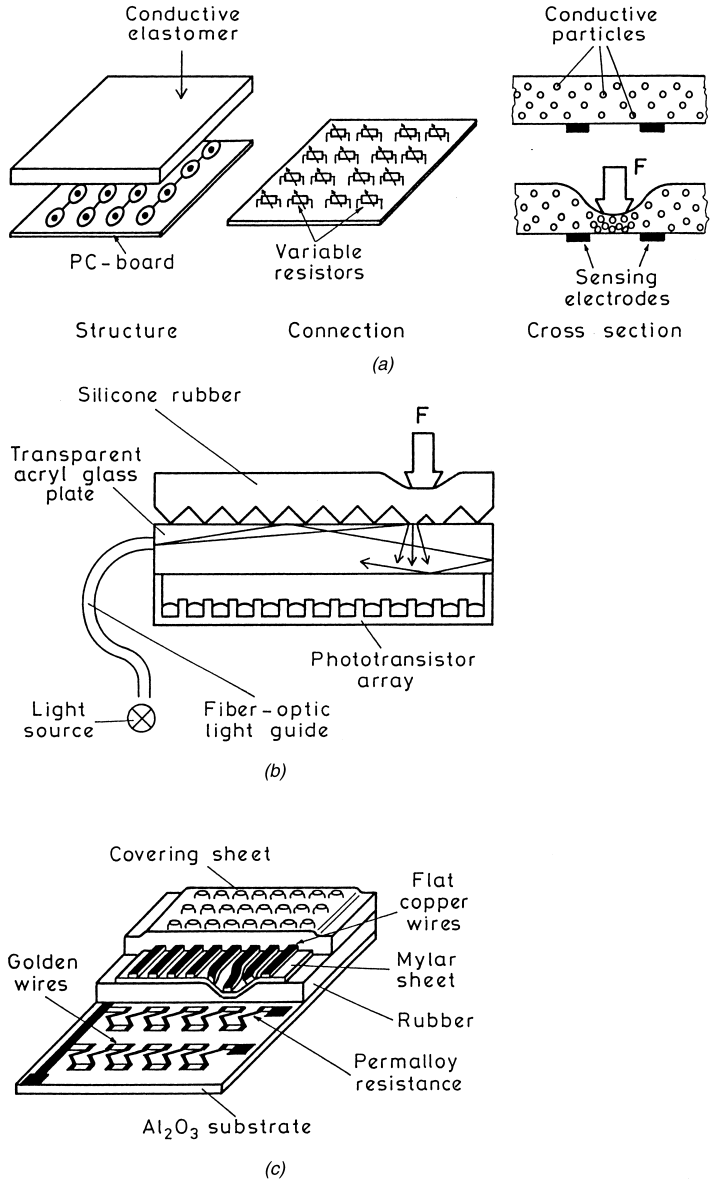

FIGURE 5.31. Rubber- and polymer-based tactile sensors using various transduction mechanisms: (a) piezoresistive, (b) optical, (c) magnetoresistive, (d) capacitive, (e) piezoelectric, and (f) ultrasound echo types [Reproduced with permission: (a,b,c) from M. R. Wolffenbuttel and P. P. L. Regtien, "Polysilicon Bridges for the Realization of Tactile Sensors," *Sensors and Actuators A,* 25-27, pp. 257–264, ©1991, Elsevier Science S.A., Lausanne, Switzerland.

(continued)

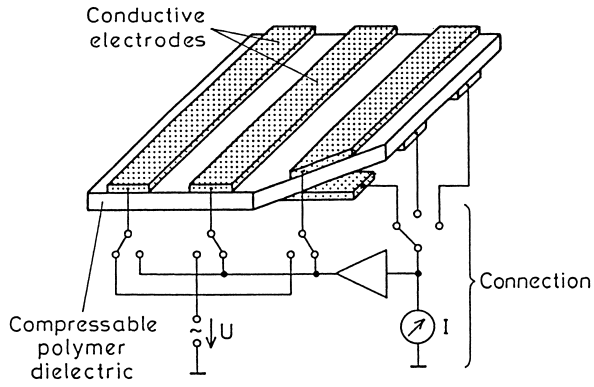

(d)

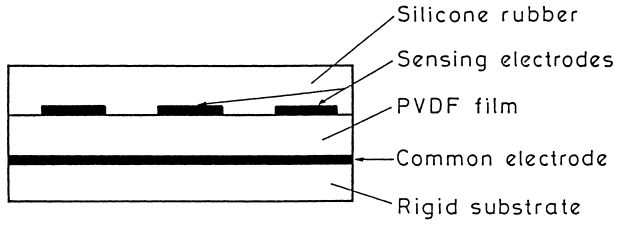

(e)

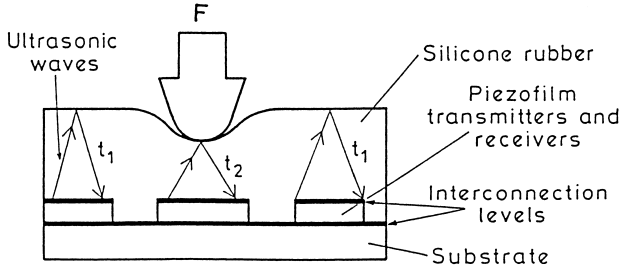

(f)

FIGURE 5.31 (Continued). (d) from J. Seekircher. and B. Hoffmann, "Improved Tactile Sensors," *IFAC-Symposium on Robot Control,* U. Rembold (ed.), VDI-VDA (GMA), Düsseldorf, pp. 20.1–20.5 Karlsruhe, 1988.]

pear where the object touches the sensor. The large spatial resolution is the major advantage, and the limited dynamics is the main drawback of this type.

Figure 5.31(c) shows the complex structure of a magnetoresistive tactile sensor, the operation of which is based on the magnetic field-dependent resistivity of Permalloy layers (Wolffenbuttel and Regtien, 1991). The sensor is composed of a matrix of resistive Permalloy strips on an alumina ceramic substrate covered with an elastic polymer or rubber skin with flat copper wires on top of it. The resistance of each Permalloy strip is sensitive to changes in the strength of the magnetic field, which is induced by the flat copper wires. Tactile forces modulate the localized magnetic field, which is measured with a row-by-row sampling of the network. The required complex mechanical construction limits the minimal size of each element to a few millimeters.

Figure 5.31(d) shows the schematic structure and connection of the capacitive tactile sensor (Seekircher and Hoffmann, 1988). This sensor applies an elastic polymer mat as a dielectric; the electrode bars are shaded. The deformation of the elastic material changes the distance between two parallel capacitor plates, and it can be measured as a change of capacitance. Using the matrix structure shown in Figure 5.31(d), this capacitive method permits the arrangement of many sensors on a small area. The insertion of a dielectric and elastic mat between the electrode bars leads to a tactile sensor. Each intersection of electrodes forms a transducer. The electronic circuitry selects a sensor element and prevents the measurement from being affected by neighboring elements. The greatest problem of this type of sensor is that the absolute change of capacitance is very small. Assuming a sensor area of 4 mm^2, a thickness of the dielectric of 30 μm, a relative permittivity of 5, and a large deformation with a thickness change in the order of 10%, the resulting change of capacitance is 0.6pF. Accepting an error less than 1 %, a resolution of 6fF is required. Enhancement of the sensitivity can be achieved when embedding conductive particles in the dielectric layer. The conductive particles decrease the effective distance between the electrodes and, therefore, effect a higher capacitance and a higher absolute sensitivity of the sensor. It is necessary to coat the conductive particles with a thin insulating film to avoid short circuiting between the electrodes. Good results can be achieved using Al_2O_3-coated aluminum fillings, though the hysteresis is increased.

Piezoelectric tactile sensors are constructed from polyvinylidene fluoride (PVDF) film material that generates localized charge at the surface when it is subjected to mechanical stresses. Figure 5.31(e) shows the typical structure of piezoelectric tactile sensors using metallized PVDF foil (Chatigny, 1988; Harsányi, 1995). The shape of the top electrode can vary according to the application; circular dots, squares, and bars can also be used. PVDF has a large piezoelectric effect (see Section 4.4), good linearity, and low hysteresis with respect to elastomers. However, charge leakage through internal resistances

prevents the formation of an image of static tactile forces. Piezoelectric transducers are most often used with charge amplifiers so that the output voltage signal is proportional to the measured stress. According to the finite insulation resistance and amplifier input bias currents, the electrical charge is changed during storage and amplification; thus, the measurement is falsified. By integration, the error increases during the time of measurement. Consequently, a pure static measurement cannot be performed. The application is restricted to situations in which a workpiece has to be quickly gripped, transported, and positioned. In addition, PVDF also possesses pyroelectric (see Section 4.6) properties; thus, the layers are sensitive to changes and gradients in temperature. Therefore, a temperature difference between the workpiece and the gripper causes a measuring error. In a sensor area of 4 mm^2, a temperature change of 0.15 K generates a charge equivalent to a force of 1N. Therefore, the application of heat insulation (using a silicone rubber cover layer) and filtering is necessary.

Piezopolymer films can also be used in an ultrasonic tactile sensor configuration (Chatigny, 1988; Harsányi, 1995). Pieces of piezo film are placed on the bottom of the transducer with a section of silicone rubber on the top of them [see Figure 5.31(f)]. Ultrasonic pulses are transmitted by the piezo films, which bounce off the rubber-air interface and return. The time of flight of the pulses can be determined. Where the rubber is compressed, the time of flight decreases. With a known modulus for the rubber, even the applied force can be determined.

Silicon integrated tactile image sensors became more and more important recently. They apply the former effects with an integrated CMOS signal conditioning circuitry. Silicon-based piezoresistive tactile sensors have also been applied for finger/mounted applications in hand rehabilitation devices (Beebe et al., 1998).

5.7.5 Pick-Ups for Bioelectrical Measurements

According to the definition, sensors perform transduction that means some kind of conversion (see Section 1.1). Thus, simple electrodes picking up electric signals are not handled as sensors. There are a number of diagnostic and research methods in biomedicine, however, where electrical signals generated by various organs and by the nerve system are analyzed [e.g., electrocardiograph (ECG), electroencephalograph (EEG), nerve recorders, etc.]. For scaling down and preventing skin lesion problems, various modern microelectrode types have been fabricated for these purposes, using mainly the fabrication methods of sensorics. Since these microelectrode types are discussed with sensors in the technical literature, a few examples are given below.

The greatest disadvantage of conventional ECG electrodes is their large size

that is inapplicable for monitoring neonates. Skin irritations and false recordings can often occur even with small metal electrodes. On the other hand, they are opaque to X-rays and, thus, have to be removed during X-ray analysis. Biopotential electrodes made by thick-film and thin-film technology (see Section 2.3) have been realized in order to avoid these problems. These electrodes are small, flexible, and almost transparent for X rays. Several electrodes can be integrated onto the same flexible substrate (see Figure 5.2). Skin irritations may occur after a much longer period of monitoring than with conventional electrodes (Neuman et al., 1994).

Integrated circuit and silicon micromachining technologies (see Section 2.1) have been used to produce multichannel recording and to stimulate microprobes for use in a variety of electrophysiological applications, such as cortical and peripheral nerve recording (Najafi, 1994), as well as regenerating nerve injuries (Kovacs, 1991). The basic structure of a silicon microprobe is shown in Figure 5.32 (Najafi, 1994). The probe consists of a precisely micromachined silicon substrate that supports an array of thin-film conductors. These conductors interconnect the recording/stimulating sites along the shank of the probe, with signal processing circuitry located at the rear of the substrate. The conductors are insulated above and below, with openings defined photolithographically at the sites and the output pads. Typical needle sizes are in the range of 25–150 μm. The fabrication sequence is shown in Figure 5.32(b). After the *p*-diffusion process, a multilayer thin-film interconnection system is deposited onto the oxidized wafer. The *p*-type region will be the support substrate. Finally, the needle is etched from the wafer removing the *n*-type material using selective etchants. The needle tip is fabricated by anisotropic etching. The sandwich needle should behave as a mechanically stress-free composite structure.

Recently, sharp tips made by silicon anisotropic etching have gained special interest in *atomic force microscopy (AFM),* which has great potential in imaging biological samples such as cells, large biostructures, and even molecular thin-films of DNA and proteins (Diaspro and Rolandi, 1997). Its great advantage, compared to conventional electron microscopy, is that AFM operates in air or liquid, allowing biostructures to be studied in conditions very close to their natural environment, at a typical resolution between 1 and 10 nanometers. The basic element of the appliance is its tip, the physical probe, placed at the end of a cantilever, that scans the sample along the x-y directions. The cantilever deflects as a function of the tip-sample interaction due to mutual attractive-repulsive forces. The detectable displacements of the cantilever are in the order of fractions of a nanometer due to forces in the order of nanonewtons. A laser-based optical system is typically used to sense and amplify these displacements, and it is possible to detect both vertical and torsional displacements of the probe. A feedback loop, based on the signal of

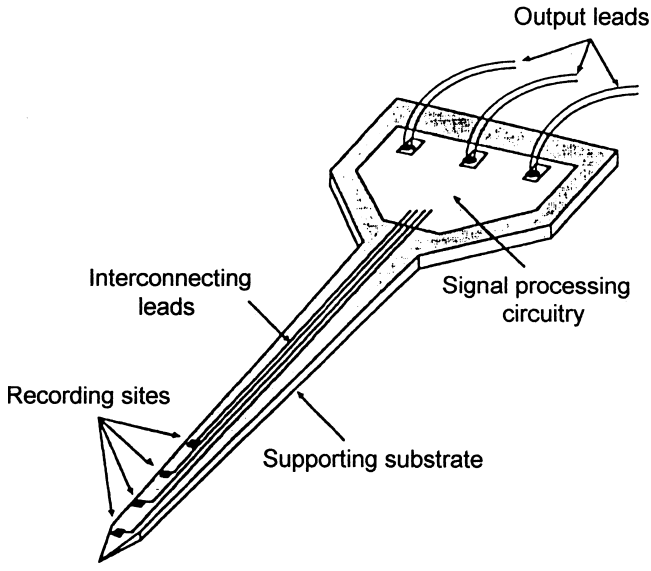

(a)

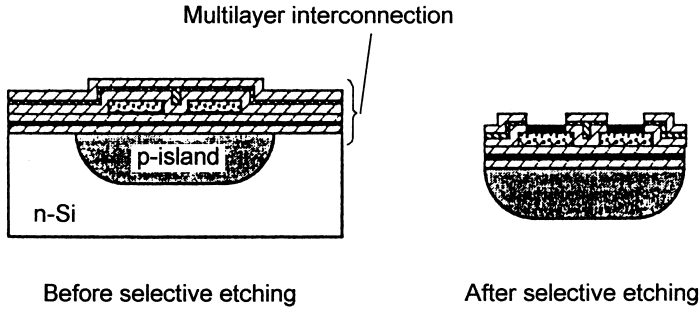

(b)

FIGURE 5.32. Typical multichannel silicon microprobe for neural recording: (a) structure and (b) fabrication sequence. (Reproduced with permission from K. Najafi, "Solid State Microsensors for Cortical Nerve Recordings," *IEEE Engineering in Medicine and Biology,* June/July, pp. 375–387, ©1994, IEEE.)

the photodiode, can adjust the distance between the surface of the sample and the tip, depending on the acquisition mode. All movements of the sample are realized by means of a piezoelectric actuator, that ensures very precise changes in position along the x-y axes. An important aspect of the actual research in the field is due to the fact that the tips can be made selectively sensitive to the presence of specific molecules by adsorbing receptor molecules on their surfaces. This discussion leads to the topic of biosensors, covered in Chapter 7.

5.7.6 Microwave Tomography

Microwave tomography has been considered for more than a decade as a potential biomedical imaging technique to complement other existing modalities using X-rays, ultrasound, and magnetic resonance. This interest follows from the sensitivity of microwaves to the type of tissue and to several physical and physiological factors such as temperature, solute concentration, and blood-flow rate, as revealed by large contrasts in complex permittivity. Consequently, microwave images are expected to provide information on the distribution of such parameters, with applications in diagnostic and functional imaging. Several microwave-imaging prototypes have been developed using the 2.45-GHz excitation frequency. The detectors applied include the planar microwave camera, the cylindrical scanner, the chirp radar system, the four-transmit channel/four-receive channel system, and the circular tomographic system. Most of these prototypes were designed for qualitative reconstruction algorithms such as filtered backprojection and diffraction tomography. Planar microwave cameras have successfully been applied in diffraction tomography for hyperthermia analysis (Franchois et al., 1998).

5.8 REFERENCES

Alcala, R. J., Liao, S. C. and Zeng, J., "Real Time Frequency Domain Fiberoptic Temperature Sensor," *IEEE Transactions on Biomedical Engineering,* Vol. 42, No. 5 (1995), pp. 471–476.

Antonuk, L. E., Yorkston, J., Huang, W., Boudry, J., Morton, E. J., Longo, M. J. and Street, R. A., "Radiation Response Characteristics of Amorphous Silicon Arrays for Megavoltage Radiotherapy Imaging," *IEEE Transactions on Nuclear Science,* Vol. 39, No. 4 (1992), p. 1069.

Atkinson, P. and Woodcock, J. P., *Doppler Ultrasound and its use in Clinical Measurement,* Academic Press, San Diego (1982).

Baker, W. O., "Polymers in the World of Tomorrow," *Proc. of the Symp. at the 2. Chemical Congress of the North American Continent,* Las Vegas, NV (1980), pp. 165–202.

Beebe, D. J., Denton, D. D., Radwin, R. G. and Webster, J. G., "A Silicon-Based Tactile Sensor for Finger-Mounted Applications," *IEEE Transactions on Biomedical Engineering,* Vol. 45, No. 2 (1998), pp. 151–159.

Bergveld, P., "The Merit of Using Silicon for the Development of Hearing Aid Microphones and Intraocular Pressure Sensors," *Sensors and Actuators A,* Vol. 41–42, (1994), pp. 223–229.

Black, R. D., Roemer, P. B. and Mueller, O. M., "Electronics for a High Temperature Superconducting Receiver System for Magnetic Resonance Microimaging," *IEEE Transactions on Biomedical Engineering,* Vol. 41, No. 2 (1994), pp. 195–197.

Chatigny, J. V., "Piezofilm—Ein Sensorik Basismaterial," Reprint from *Elektroniker,* No. 7 (1988), pp. 39–46.

Chen, Y., Wang, L. and Ko, W., "A Piezopolymer Finger Pulse and Breathing Wave Sensor," *Sensors and Actuators A,* Vol. 21–23 (1990), pp. 879–882.

Christensen, D. A., *Ultrasonic Bioinstrumentation,* John Wiley & Sons, New York (1988).

Christensen, D., Johansson, T. and Petelenz, D., "Biosensor Development at the University of Utah," *IEEE Engineering in Medicine and Biology,* June/July (1994), pp. 388–395.

Cutler, P. D. and Hoffman, E. J., "Use of Digital Front-end Electronics for Optimization of a Modular PET Detector," *IEEE Transactions on Medical Imaging,* Vol. 13, No. 2 (1994), p. 408.

Derenzo, S. E., Moses, W. W., Jackson, H. G., Turko, B. T., Cahoon, J. L., Geyer, A. B. and Vuletich, T., "Initial Characterization of a Position-sensitive Photodiode/BGO Detector for PET," *IEEE Transactions on Nuclear Science,* Vol. 36, No. 1 (1989), pp. 1084–1089.

Diaspro, A. and Rolandi, R., "Atomic Force Microscopy (From the Guest Editors)," *IEEE Engineering in Medicine and Biology,* March/April (1997), pp. 26–27.

Dittmar, A., Pauchard, T., Delhomme, G. and Vernet-Maury, E., "A Thermal Conductivity Sensor for the Measurement of Skin Blood Flow," *Sensors and Actuators B,* Vol. 7 (1992), pp. 327–331.

Doebelin, E. O., *Measurement Systems, Application and Design,* McGraw-Hill, New York (1990).

Fraden, J., "Noncontact Temperature Measurements in Medicine," in *Bioinstrumentation and Biosensors* (ed. Wise, D., L.), Marcel Dekker, New York (1991), pp. 511–549.

Fraden, J. and Bochkov, V., "Water Structure as a Temperature Sensor," (in Russian), *Chemistry and Life, USSR Acad. Sci.,* 9 (1976), pp. 80–82.

Franchois, A., Joisel, A., Pichot, C. and Bolomey, J. C., "Quantitative Microwave Imaging with a 2.45-GHz Planar Microwave Camera," *IEEE Transactions on Medical Imaging,* Vol. 17, No. 4 (1998), pp. 550–561.

Geddes, L. A. and Baker, L. E., *Principles of Applied Biomedical Instrumentation,* 3rd ed., John Wiley & Sons, New York (1989).

Goodyer, P. D., Fothergill, J. C., Jones, N. B. and Hanning, C. D., "The Design of an Optical Fiber Transducer for Use in the Upper Airways," *IEEE Transactions on Biomedical Engineering,* Vol. 43, No. 6 (1996), pp. 600–606.

Gordon, J. S., Farrell, R., Daley, K. and Oakes, C. E., "Solid State Tritium Detector for Biomedical Applications," *IEEE Transactions on Nuclear Science,* Vol. 41, No. 4 (1994), pp. 1494–1499.

Granz, B., "Ultraschall-Empfangsarray aus dem Piezoelektrischen Polymer PVDF," (Ultrasound Detector Array Made of Piezoelectric Polymer PVDF) *NTG-Fachberichte, Sensoren - Technologie und Anwendung,* Bad Neuheim (1986), pp. 264–270.

Hall, A. S., Barnard, B., McArthur, P., Gilderdale, D. J., Young, I. R. and Bydder, G. M., "Investigation of a Whole-Body Receiver Coil Operating at Liquid Nitrogen Temperatures," *Magn. Reson. Med.,* Vol. 7 (1988), p. 230.

Halvorsen, D. L., "Piezo Electric Polymers in Sensing Applications," *Congress Proc. Sensor '88,* Nünrberg (1988), pp. 29–44.

Harmer, A. and Scheggi, A., "Chemical, Biochemical, and Medical Sensors," in *Optical Fiber Sensors: Systems and Applications* (eds. Culshaw, B. and Dankin, J.), Artech House, Boston, MA (1989).

Harsányi, G., *Polymer Films in Sensor Applications,* Technomic Publishing Co., Inc., Lancaster, PA (1995).

Hee, M. R., Izatt, J. A., Swanson, E. A., Huang, D., Schuman, J. S., Lin, C. P., Puliafito, C. A. and Fujimoto, J. G., "Optical Coherence Tomography for Ophthalmic Imaging," *IEEE Engineering in Medicine and Biology,* January/February (1995), pp. 67–75.

Herr, M. D., McInerney, J. J., Lamser, D. G. and Copenhaver, G. L., "A Flying Spot X-ray System for Compton Backscatter Imaging," *IEEE Transactions on Medical Imaging,* Vol. 13, No. 3 (1994), p. 461.

Holl, I., Lorentz, E., Natkaniez, S., Renker, D., Schmelz, C. and Schwartz, B., "Some Studies of Avalanche Photodiode Readout of Fast Scintillators," *IEEE Transactions on Nuclear Science,* Vol. 42, No. 4 (1995), p. 351.

Hong, H. and Fox, M. D., "Magnetic Backprojection Imaging of the Vascular Lumen," *IEEE Transactions on Biomedical Engineering,* Vol. 42, No. 1 (1995), pp. 102–108.

Hubin, M., Sabor, J. and Hassani, M., "Multisensor Intelligent System for Infant Monitoring," *Proceedings Sensor 93* (1993), Nünrberg, pp. 179–185.

Izumi, S., Kitaguchi, H., Mitani, S. and Kikuchi, H., "A Computerized Personal Dosimeter with an IC Card," *IEEE Transactions on Nuclear Science,* Vol. 36, No. 1 (1989), pp. 1150–1153.

Jalink, A., "NASA CCD System Helps Detect Breast Cancer," *Biophotonics International,* July/August (1995), pp. 19–20.

Kacmarek, R. M., Hess, D. and Stoller, J. K., *Monitoring in Respiratory Care,* C.V. Mosby, St. Louis, MO (1993).

Kalifa, G. "New System Slashes X-ray Radiation Hazards," *Biophotonics International,* July/August (1995), pp. 18–19.

Knighton, R. W., "Quantitative Reflectometry of the Ocular Fundus," *IEEE Engineering in Medicine and Biology,* January/February (1995), pp. 43–51.

Kovacs, G. T. A., "Regeneration Microelectrode Arrays for Direct Interface to Nerves," *Proc. of 1991 Int. Conf. on Solid State Sensors and Actuators (Transducers 91),* San Francisco, CA (1991), pp. 116–119.

Lisec, T., Kreutzer, M. and Wagner, B., "Surface Micromachined Piezoresistive Pressure Sensors with Step-Type Bent and Flat Membrane Structures," *IEEE Transactions on Electron Devices,* Vol. 43, No. 9 (1996), pp. 1547–1552.

Liu, H., Karellas, A., Moore, S. C., Harris, L. J. and D'Orsi, C. J., "Lesion Detectability Considerations for an Optically-Coupled CCD X-ray Imaging System," *IEEE Transactions on Nuclear Science,* Vol. 41, No. 4 (1994), p. 1506.

Luke, P. N., Pehl, R. H. and Dilmanian, F. A., "A 140-Element Ge Detector Fabricated with Amorphous Ge-Blocking Contacts," *IEEE Transactions on Nuclear Science,* Vol. 41, No. 4 (1994), pp. 976–981.

McIntyre, J. A., Allen, R. D., Aguiar, J. and Paulson, J. T., "A Positron Emission Tomograph Designed for $^{3}/_{4}$ mm Resolution," *IEEE Transactions on Nuclear Science,* Vol. 42, No. 4 (1995), pp. 1102–1106.

Miller, J. R., Zhang, K., Ma, Q. Y., Mun, I. K., Jung, K. J., Katz, J., Face, D. W. and Kounz, D. J., "Superconducting Receiver Coils for Sodium Magnetic Resonance Imaging," *IEEE Transactions on Biomedical Engineering,* Vol. 43, No. 12 (1996), pp. 1197–1199.

Miyai, H., Kawasaki, S., Kitaguchi, H. and Izumi, S., "Response of Silicon Detector for High

Energy X-ray Computed Tomography," *IEEE Transactions on Nuclear Science,* Vol. 41, No. 4 (1994), pp. 999–1003.

Mo, J. H., Anrew, L., Robinson, L., Terry, F. L. Jr., Fitting, D. W. and Carson, P. L., "Improvement of Integrated Ultrasonic Transducer Sensitivity," *Sensors and Actuators A,* Vol. 21–23 (1990), pp. 679–682.

Moreno, E. G., Iniguez, B., Roca, M., Segura, J. and Sureda, S., "CMOS Radiation Sensor with Binary Output," *IEEE Transactions on Nuclear Science,* Vol. 42, No. 3 (1995), pp. 174–178.

Moses, W. W., Derenzo, S. E., Melcher, C. L. and Manente, R. A., "A Room Temperature LSO/PIN Photodiode PET Detector Module That Measures Depth of Interaction," *IEEE Transactions on Nuclear Science,* Vol. 42, No. 4 (1995), pp. 1085–1089.

Najafi, K., "Solid State Microsensors for Cortical Nerve Recordings," *IEEE Engineering in Medicine and Biology,* June/July (1994), pp. 375–387.

Neuman, M. R., Buck, R. P., Cosofret, V. V., Lindner, E. and Liu, C. C., "Fabricating Biomedical Sensors with Thin-Film Technology," *IEEE Engineering in Medicine and Biology,* June/July (1994), pp. 409–419.

Numminen, J., Ahlfors, S., Ilmoniemi, R., Montonen, J. and Nenonen, J., "Transformation of Multichannel Magnetocardiographic Signals to Standard Grid Form," *IEEE Transactions on Biomedical Engineering,* Vol. 42, No. 1 (1995), pp. 72–81.

O'Donnell, M., Gore, J. C. and Adams, W. J., "Toward an Automated Analysis System for Nuclear Magnetic Imaging. I. Efficient Pulse Sequences for Simultaneous T_1-T_2 Imaging. II. Initial Segmentation Algorithm," *Medical Physics,* Vol. 13, No. 2 (1986), pp. 182–190, and No. 3, pp. 293–297.

Okuyama, M., Togami, Y., Taniguchi, H., Hamakawa, Y., Kumita, M. and Denda, M., "Basic Characteristics of an Infrared CCD with Pyroelectric Gate," *Sensors and Actuators A,* Vol. 21–23 (1990), pp. 465–468.

Otter, D., Ansermet, S. and Werner, C., "A Monolithic Compensated Silicon Pressure Transducer with Temperature Output for Biomedical Applications," *Sensors and Actuators B,* Vol. 4 (1991), pp. 251–255.

Partain, C. L., Price, R. R., Patton, J. A., Kulkarni, M. V. and James, A. E., Jr., *Magnetic Resonance Imaging,* W.B. Saunders, Philadelphia (1988).

Payne, P. A., "Medical and Industrial Applications of High Resolution Ultrasound," *Journal of Physics E, Scientific Instruments,* Vol. 18 (1985), pp. 465–473.

Powell, M. J., Hughes, J. R., Bird, N. C., Glasse, C. and King, T. R., "Seamless Tiling of Amorphous Silicon Photodiode-TFT Arrays for Very Large Area X-ray Image Sensors," *IEEE Transactions on Medical Imaging,* Vol. 17, No. 6 (1998), pp. 1080–1083.

Rajeswaran, S., Bailey, D. L., Hume, S. P., Townsend, D. W., Geissbühler, A., Young, J. and Jones, T., "2-D and 3-D Imaging of Small Animals and the Human Radial Artery with a High Resolution Detector for PET," *IEEE Transactions on Medical Imaging,* Vol. 11, No. 3 (1992), p. 386.

Ristic, L., *Sensor Technology and Devices,* Artech House, Boston, MA (1994).

Romani, G. L., "Biomagnetism: An Application of SQUID Sensors to Medicine and Physiology," *Physica B+C,* Vol. 126 (1984), pp. 70–81.

Schmelz, C., Bradbury, S. M., Holl, I., Lorentz, E., Renker, D. and Ziegler, S., "Feasibility Study of an Avalanche Photodiode Readout for a High Resolution PET with nsec Time Resolution," *IEEE Transactions on Nuclear Science,* Vol. 42, No. 4 (1995), pp. 1080–1084.

Seekircher, J. and Hoffmann, B., "Improved Tactile Sensors," *IFAC-Symposium on Robot Control,* Karlsruhe (ed. U. Rembold), VDI-VDA (GMA), Düsseldorf, (1988), pp. 20.1–20.5.

Seton, H. C., Bussel, D. M. and Hutchison, J. M. S., "A Liquid Helium-Cooled RF Coil and DC SQUID Amplifier for MRI at 0.01 T," *Proc. Soc. Magn. Reson.* Vol. 2 (1995), p. 959.

Shung, K. K. and Zipparo, M., "Ultrasonic Transducers and Arrays," *IEEE Engineering in Medicine and Biology,* Nov./Dec. (1996), pp. 20–30.

Shung, K. K., Smith, M. B. and Tsui, B. W. M., *Principles of Medical Imaging,* Academic Press, San Diego (1992).

Singh, M., Doty, F. P., Friesenhahn, S. J. and Butler, J. F., "Feasibility of Using Cadmium-Zinc-Telluride Detectors in Electronically Collimated SPECT," *IEEE Transactions on Nuclear Science,* Vol. 42, No. 4 (1995), pp. 1139–1146.

Singh, M., Leahy, R., Brechner, R. and Yan, X., "Design and Imaging Studies of a Position Sensitive Photomultiplier Based Dynamic SPECT System," *IEEE Transactions on Nuclear Science,* Vol. 36, No. 1 (1989), p. 1132.

Song, S. M., Leahy, R. M., Boyd, D. P., Brundage, B. H. and Napel, S., "Determining Cardiac Velocity Fields and Intraventicular Pressure Distribution from a Sequence of Ultrafast CT Cardiac Images," *IEEE Transactions on Medical Imaging,* Vol. 13, No. 2 (1994), p. 386.

Storck, K., Karlsson, M., Ask, P. and Loyd, D., "Heat Transfer Evaluation of the Nasal Thermistor Technique," *IEEE Transactions on Biomedical Engineering,* Vol. 43, No. 12 (1996), pp. 1187–1191.

Sugiura, T., Mizushina, S., Yoshimura, K. and Harada, Y., "Microcomputer-Based Telemetry System for Heart Rate and Blood Temperature in Dogs," in *Bioinstrumentation and Biosensors* (ed. Wise, D. L.), Marcel Dekker, New York (1991), pp. 551–567.

van Putten, M. J. A. M., van Putten, M. H. P. M., van Putten, A. F. P., Pompe, J. C. and Bruining, H. A., "A Silicon Bidirectional Flow Sensor for Measuring Respiratory Flow," *IEEE Transactions on Biomedical Engineering,* Vol. 44, No. 2 (1997), pp. 205–208.

Vaquero, J. J., Seidel, J., Siegel, S., Gandler, W. R. and Green, M. V., "Performance Characteristics of a Compact Position-Sensitive LSO Detector Module," *IEEE Transactions on Medical Imaging,* Vol. 17, No. 6 (1998), pp. 967–978.

von Münch, W. and Thiemann, U., "Pyroelectric Detector Array with PVDF on Silicon Integrated Circuit," *Sensors and Actuators A,* Vol. 25–27 (1991), pp. 167–172.

von Münch, W., Nägele, M., Wöhl, G., Ploss, B. and Ruppel, W., "A 3x3 Pyroelectric Detector Array with Improved Sensor Technology," *Proc. of Eurosensors VII. Conf.,* Budapest, Hungary (1993), p. 335.

von Ramm, O. T. and Smith, S. W., "Beam Steering with Linear Arrays," *IEEE Transactions on Biomedical Engineering,* Vol. 30, No. 8 (1983), pp. 438–452.

Voorthuyzen, J. A., Bergveld, P. and Sprenkels, A. J., "Semiconductor-Based Electret Sensors for Sound and Pressure," *IEEE Transactions on Electrical Insulation,* Vol. 24 (1989), pp. 267–276.

Webster, J. G., Neuman, M. R., Olson, W. H., Peura, R. A., Primiano, F. P., Siedband, M. P. and Wheeler, L. A., *Medical Instrumentation: Application and Design,* 3rd ed., John Wiley & Sons, New York (1997).

White, T., Butler, N. and Murphy, R., "An Uncooled IR Sensor with Digital Focal Plane Array, Low Cost Microbolometer Technology Applications Could Improve Diagnostic Approaches," *IEEE Engineering in Medicine and Biology,* July/August (1998), pp. 60–65.

Wickersheim, K. A., "A New Fiberoptic Thermometry System for Use in Medical Hyperthermia," *Proc. SPIE, 713: Optical Fibers in Medicine II,* (ed. Katzir, A.), (1987), pp. 150–157.

Wikswo, J. P. Jr., "SQUID Magnetometers for Biomagnetism and Nondestructive Testing: Important Questions and Initial Answers," *IEEE Transactions on Applied Superconductivity,* Vol. 5, No. 2 (1995), p. 74.

Withers, R. S., Liang, G. C., Cole, B. F. and Johansson, M., "Thin-Film HTS Probe Coils for Magnetic Resonance Imaging," *IEEE Transactions on Applied Superconductivity,* Vol. 3 (1993), pp. 2450–2453.

Wolffenbuttel, M. R. and Regtien, P. P. L., "Polysilicon Bridges for the Realization of Tactile Sensors," *Sensors and Actuators A,* Vol. 25–27 (1991), pp. 257–264.

Wolthuis, R., Mitchell, G., Hartl, J. and Saaski, E., "Development of a Dual Function Sensor System for Measuring Pressure and Temperature at the Tip of a Single Optical Fiber," *IEEE Transactions on Biomedical Engineering,* Vol. 40, No. 3 (1993), pp. 298–302.

Yamaguchi, T., "Blood Flow Measurement with the Hot-Film Anemometer, " in *Blood Flow in the Heart and Large Vessels* (ed. Sugawara, M., Kajiya, F., Kitabatake, A. and Matsuo, H.), Springer-Verlag, New York/Berlin (1989), pp. 187–188.

Zuckerwar, A. J., Pretlow, R. A., Stoughton, J. W. and Baker, D. A., "Development of a Piezopolymer Pressure Sensor for a Portable Fetal Heart Rate Monitor," *IEEE Transactions on Biomedical Engineering,* Vol. 40, No. 9 (1993), pp. 963–969.

CHAPTER 6

Sensors for Measuring Chemical Quantities in Biomedicine

The largest group of chemical (not bio-!) sensors for measuring concentrations of various analytes in biomedicine are applied for *in vivo* or *ex vivo* monitoring of blood components, such as dissolved oxygen and CO_2 partial pressure, pH, and concentration of ionic compounds. The oxygen saturation of blood hemoglobin is monitored by physical sensors (photosensors) using the methods of oximetry, which are different from those of dissolved blood oxygen measurements. Although the majority of sensors are applied for blood analysis, their use in monitoring secretions (e.g., gastric acid, sweat, etc.) is also becoming more and more important. Since there is no reason to have continuous monitoring of urine, the application of sensors for determining urine compound concentrations has no practical interest.

Beyond the following description, further details about chemical sensors applied in biomedicine can be found in the literature (Göpel et al., 1991; Fraser, 1997; Spichiger-Keller, 1998; Diamond, 1998).

6.1 SENSORS FOR MONITORING BLOOD GASES AND PH

Arterial blood gas analysis is one of the most frequently requested tests performed on critically ill patients both in the operating room and in the intensive care unit. The partial pressures of oxygen and carbon dioxide (pO_2 and pCO_2) in arterial blood, as well as pH, are determined to provide physicians with information about respiratory and metabolic imbalances as reflected by the adequacy of blood-oxygenation and CO_2 elimination. With frequent measurement of blood gas parameters, the physician can correct these imbalances by adjusting mechanical ventilation or the ventilation gas composition or by administering pharmacological agents. Blood gas measurements are particu-

larly important in prematurely born (preterm) babies that are vulnerable to respiratory illnesses because of immaturity of the lungs or an inadequately developed mechanism for the control of breathing. If the arterial pO_2 falls to a low level for only a short period of time, brain damage or even death may follow. If, on the other hand, the arterial pO_2 goes too high as a result of the administration of oxygen, damage to the eyes, which can result in blindness, may occur. Moreover, rupture of blood vessels in the brain can happen as a consequence of fluctuations in cerebral blood flow caused partly by changes in pCO_2. The third parameter, the value of pH, provides information about the general state of metabolism.

The technique of individual blood samples only gives information at one point in time, a snapshot of what is happening. It is known that large variations in blood gas levels can occur over the course of a few minutes. Traditional and new small bedside analyzers have the same shortcomings, including loss of patient blood each time a test is requested and errors as well as loss of time when transferring the blood sample from the patient to the analyzer. The ideal blood analyzer should allow continuous and accurate measurement that can only be realized by means of sensors. Continuous *in vivo* blood monitoring can be performed either invasively or noninvasively and requires data collection directly from the body. *Ex vivo* sensors are used to monitor blood samples that are continuously taken from the body by means of a catheter or cannula system.

Before starting with a detailed description, the background of blood gas transport and some related definitions will be provided.

Oxygen is carried in blood in two forms: oxygen chemically combined with hemoglobin (Hb) as oxyhemoglobin (HbO_2) and oxygen physically dissolved in the plasma. Under normal physiological conditions, every 100 ml of blood contains 18.5 ml oxygen to form (HbO_2) and 0.5 ml oxygen is in the physical solution. The degree to which it is chemically combined with Hb is most commonly expressed as blood oxygen saturation and is defined with the following expression:

$$SO_2 = (HbO_2)/(Hb + HbO_2) \tag{6.1}$$

It is generally given as a percentage. Normally, arterial blood saturation (SaO_2) fluctuates around 98%, while venous blood saturation (SvO_2) is approximately 75%. These definitions assume that no other hemoglobin species (e.g., combined with CO) are present in the blood.

Arterial pO_2 and SaO_2 are good indicators of blood oxygenation. Their relationship is given by the dissociation curves shown in Figure 6.1 (Parker, 1987). It is obvious that the relationship can be handled only with the exact measurement of blood pH. There are, however, a number of other factors, any

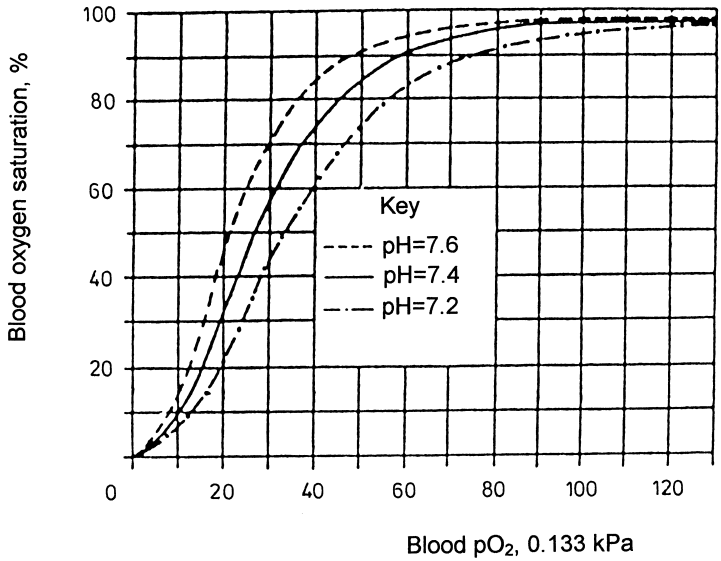

FIGURE 6.1. Blood oxygen saturation and oxygen tension relationships. (Reproduced with permission from D. Parker, "Sensors for Monitoring Blood Gases in Intensive Care," *J. Phys. E: Sci. Instrum.,* Vol. 20 (1987), pp. 1103–1112, IOP Publishing Ltd., Bristol, UK.)

one of which can lead to a displacement of the dissociation curve. In the saturation ranges, the derivation of real SaO_2 from the value calculated using pO_2 is likely to give large errors; thus, the direct measurement of SaO_2 should be preferred. On the other hand, patients breathing 100% oxygen will have a pO_2 over 66.6 kPa (500 mmHg), though pO_2 values cannot be derived from SaO_2 measurements over 16 kPa (120 mmHg). Therefore, the direct measurement of pO_2 values is desirable in anesthesia, for patients with artificial ventilation, and for babies in incubators. To conclude, ideally, both parameters should be monitored directly.

CO_2 is carried by the blood in a dissolved state and combined with Hb and plasma proteins as carbamino compounds. The normal pCO_2 of arterial blood is about 5.3 kPa (40 mmHg), whereas that of venous blood is about 6 kPa (45 mmHg).

Normal physiological pH fluctuates between 7.0 and 7.4. The generally accepted measurement range is rather narrow (6.8–7.8), but high precision (0.01) is needed. It is estimated that sensor-measured pO_2 and pCO_2 values that are within 5–10 % of blood gas analyzer values, and pH measurements that agree to within 0.02–0.04 pH units will lead to equivalent clinical treatment decisions.

TABLE 6.1. Required Specifications of Blood Gas and pH Sensors. (Reproduced with Permission from B. R. Soller, "Design of Intravascular Fiber Optic Blood Gas Sensors," IEEE Engineering in Medicine and Biology, June/July (1994), pp. 327–335, ©1994, IEEE.)

	pO_2	pH	pCO_2
Measurement range	4–80 kPa (30–600 mmHg)	6.8–7.8	2.7–13.3 kPa (20–100 mmHg)
Resolution	0.133 kPa (4–20) (1 mmHg) 0.667 kPa (20–40) (5 mmHg) 1.333 kPa (40–80) (10 mmHg)	0.01	0.133 kPa (1 mmHg)
Temperature range	20–40°C	20–40°C	20–40°C
Stability (/72 hours)	<1.066 kPa	<0.03	<0.8 kPa
Response time	<3 min	<3 min	<3 min
Insensitivity for	anesthetic gases, pH, pCO_2	anesthetic gases, pO_2, pCO_2	anesthetic gases, pH, pO_2

Blood gas and pH measurement is a serious challenge for sensorics. The most important technical requirements are summarized in Table 6.1 (Soller, 1994). A few further requirements include sterilizability, rapid and easy calibration, low cost and disposability (especially for intravascular elements), biocompatibility (thromboresistant and nontoxic), and fitting possibility in 20 gauge (0.024 in) catheters without compromising arterial pressure measurements.

6.1.1 Operation Principles of Electrochemical Cells

A general description about electrochemical cell sensors was given in Section 3.5. The special structures and operation principles of electrochemical pH, pO_2, and pCO_2 sensors are briefly summarized here.

The structure and operation of pH sensitive potentiometric glass and polymer membrane electrodes have been discussed in Sections 3.5 and 4.15. The basis of a pH-dependent Nernstian electrode potential measurable on these electrodes is the selective and reversible H^+ ion adsorption onto special composition glass surfaces, as well as a complex formation with ionophores within polymer membranes. Metal/metal-oxide electrodes can also be used for pH measurements. If the electrochemical oxidation of metal is reversible, a pH-dependent electrode potential will develop as a consequence of the following chemical reaction:

$$M_xO_y + 2y(e^- + H^+) \Longleftrightarrow xM + yH_2O. \tag{6.2}$$

The situation is much more complicated if the metal can appear with several valency numbers in its oxides, but this is out of the scope of this discussion.

Dissolved oxygen concentration (partial pressure) can be measured by means of the Clark amperometric sensor (Clark, 1958). The general structure is illustrated in Figure 6.2 in such a case, when the reference and counter-electrodes are not separated (see Section 3.5.2). The anode is the reference Ag/AgCl electrode. The cathode is generally made of platinum or gold (sometimes silver or graphite), and the electrolyte solution usually contains potassium chloride with a buffering agent. The whole electrochemical cell is separated from the sample liquid with a diffusion membrane that is permeable to oxygen but impermeable to water, ions, proteins, and blood cells. The most commonly used membrane materials are PTFE, polyethylene, and polypropylene. The cathode reaction is the basis of operation. According to the reaction

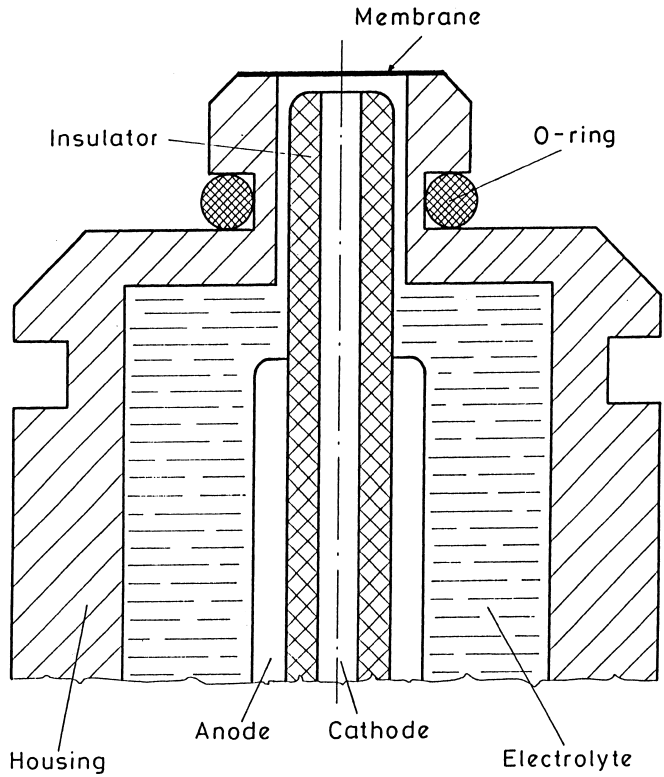

FIGURE 6.2. Structure of the Clark oxygen sensor. (Reproduced with permission from G. Harsányi, *Polymer Films in Sensor Applications,* ©1995, Technomic Publishing Co., Inc., Lancaster, PA, p. 332.)

model currently accepted, the reduction of dissolved oxygen molecules proceeds via a two-electron pathway with the intermediate formation of hydrogen peroxide:

$$O_2 + 2H_2O + 2e^- \Longrightarrow H_2O_2 + 2OH^- \tag{6.3a}$$

$$H_2O_2 + 2e^- \Longrightarrow 2OH^- \tag{6.3b}$$

The cathode is usually polarized at about −700 mV with respect to the reference electrode so that the sensor operates in the diffusion controlled limiting current region; thus, the cell current is, theoretically, a linear function of the external oxygen concentration (see Section 3.5.2).

For the measurement of pCO_2, the Stow-Severinghaus potentiometric electrode can be used (Severinghaus and Bradely, 1958). This is a glass pH electrode covered by a membrane freely permeable to carbon dioxide molecules but impermeable to water, hydrogen ions (H^+), and bicarbonate ions (HCO_3^-). A sodium-bicarbonate ($NaHCO_3$) layer is placed between the pH electrode and the membrane. CO_2 molecules diffuse through the membrane to equilibrate with the electrolyte through the following reactions:

$$CO_2 + H_2O \Longleftrightarrow H_2CO_3 \Longleftrightarrow H^+ + HCO_3^- \tag{6.4}$$

In equilibrium, the pH value corresponds to the pCO_2:

$$pH = \text{constant} - \log pCO_2 \tag{6.5}$$

Thus, the glass electrode measures the external pCO_2 indirectly.

Another sensing principle has also been proposed recently, which is based on the determination of the ion formation as described by Equation (6.4) (Varlan and Sansen, 1997). That means a conductimetric sensor would be placed in the closed cavity. The advantage is simplicity; there would be only two electrodes in the closed chamber.

6.1.2 Invasive Electrochemical Sensors

The invasive (intravascular) application of electrochemical sensors for blood gas and pH measurement seems easy to perform, since only electrodes (coated wires) have to be placed into the vessels. The practical problem arises because not only a single electrode, but also electrode pairs or even whole electrochemical cells must be catheterized. Three main approaches may be distinguished in connection with the invasive application of sensors:

- miniature membrane-covered cylindrical-shaped electrochemical cells on catheter tips for *in vivo* monitoring

- electrochemical cells mounted into sample-taking cannula/catheter/dome systems for *ex vivo* applications
- miniaturized silicon sensors made by the processing methods of microelectronics and micromachining that are mounted either onto catheter tips or into cannula/catheter/dome systems

The primary device of pH measurements is the glass electrode; catheter-size versions have been produced using pH-sensitive soda-lime-glass covered Pt wires. Their main drawback, the possibility of breakage of glass, is the reason for searching for other solutions. An antimony/antimony-oxide electrode may also be applied (Buerk, 1993). Its operation relies on the following anodic electrochemical reaction:

$$2Sb + 3H_2O \rightleftharpoons Sb_2O_3 + 6e^- + 6H^+ \tag{6.6}$$

Thus, the Ag/AgCl reference electrode has to be connected as a cathode, resulting in the following reaction:

$$O_2 + 4H^+ + 4e^- \rightleftharpoons 2H_2O \tag{6.7}$$

This also describes the main shortcoming of the system since the electromotive force of the cell depends on the dissolved oxygen concentration that results in a disturbing cross-sensitivity in blood. With multisensor applications, the error can be compensated. Indium and palladium-oxide electrodes can be operated without this problem; however, their multiple valency results in complicated pH-dependent characteristics.

Today, the most widely applied potentiometric pH sensors are solid-state electrodes covered by ion-selective polymer membranes, mainly plasticized PVC or silicone rubber with a tri-n-dodecyl-amine ionophore additive that is a neutral ion carrier, enabling the selective and reversible complex formation with H^+ ions.

Silicon-based pH-sensitive ISFETs (see Section 3.2) can be fabricated by employing either SiO_2/Si_3N_4 or ion-selective PVC membrane gate-insulating layers. By selecting an appropriate inert cover material, REFETs can also be fabricated. The realizable small size obtained by integrating them onto the same chip enables their application on catheter tips.

Figure 6.3 shows the cross-section of a miniature pH-sensitive membrane electrode fabricated by thin-film processing (Keplinger et al., 1993). The gold or platinum metallization and the Si_3N_4 insulating layer were deposited onto the substrate by sputtering. The electrochemically deposited polypyrrol film (see Section 2.4) serves as a buffering film for charge exchange in electrochemical processes, temporarily absorbing reaction products and, thus, pre-

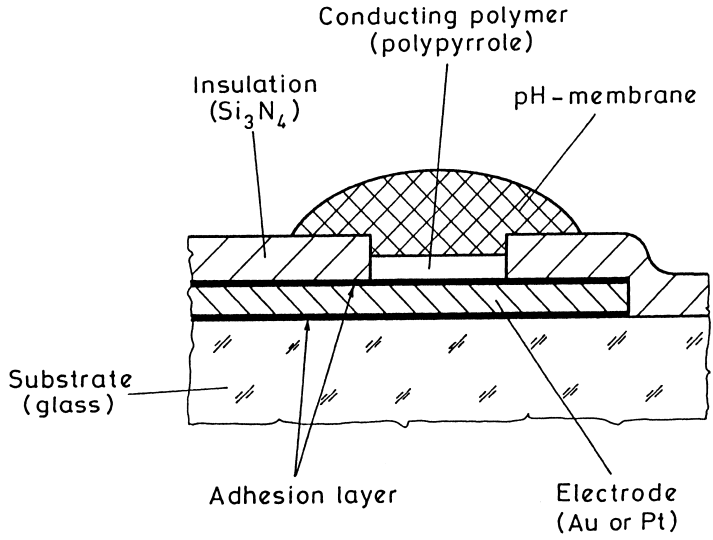

FIGURE 6.3. Structure of a thin-film pH-sensitive electrode (Keplinger et al., 1993).

venting the system from the detachment of the ion-selective PVC membrane and from the resultant potential error.

Sensors for measuring blood pO_2 are almost exclusively based on the Clark principle. Figure 6.4 shows several catheter-tip sensors fabricated for practical applications (Rolfe, 1994). Type "a" employs liquid electrolyte closed into a cell that is covered by a polyethylene membrane. The refreshing necessity of the electrolyte is the largest shortcoming of this arrangement. Newer types ("b" and "c") contain the basis salt of the electrolyte in dry solid powder form between the surface of the electrodes and the plasticized PVC membrane. The catheters should assure the possibility of taking blood samples—this is the reason for using two-lumen catheters [see Figure 6.4(b)]. The membrane must allow water molecules to diffuse through it from blood into the electrolyte region, thereby, dissolving the powder and forming a liquid electrolyte layer. Type "b" uses a thimble cathode pushed over the tip of the catheter, with a hole at the anode location. Type "c" has a simpler structure. A cathode wire is insulated from and surrounded by an Ag/AgCl reference electrode, however, the appropriate insulation of the electrodes means more serious requirements for the applied insulating materials. Polyethylene membrane has a good permeability to oxygen and is impermeable to water. PTFE has even better permselectivity and is mechanically resistant. The best permselectivity (see Section 4.14) can be achieved with silicone rubber, but its flexibility can cause potential shifts. Types "b" and "c" need water vapor permeable membranes;

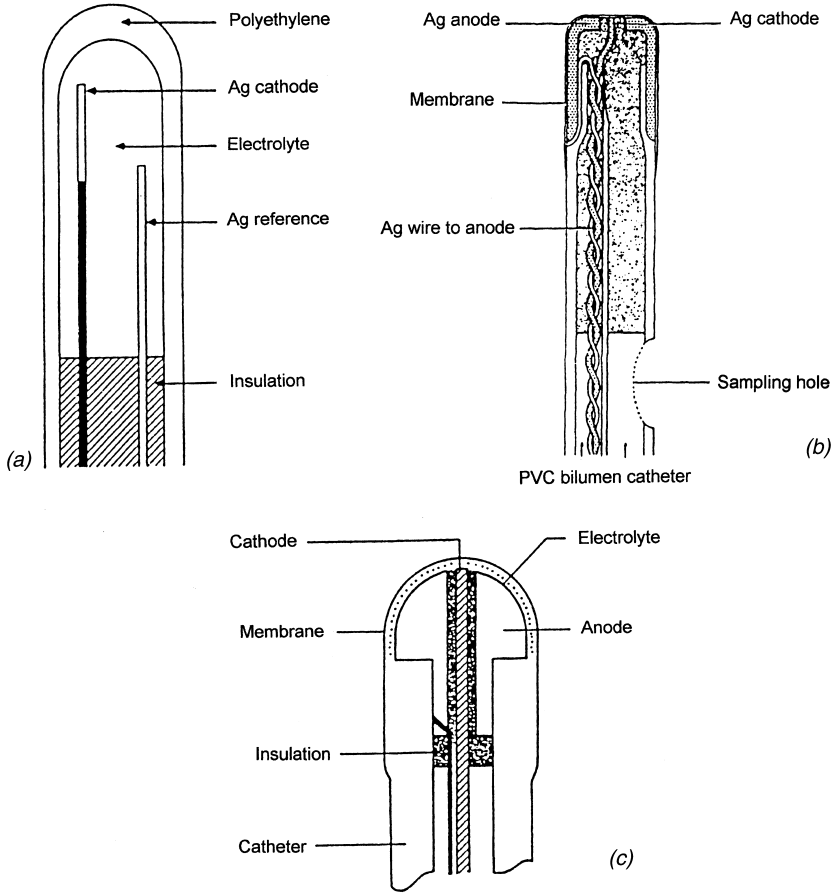

FIGURE 6.4. Conventional Clark blood oxygen sensors for catheter tip applications. (Reproduced with permission from P. Rolfe, "Intra-Vascular Oxygen Sensors for Neonatal Monitoring," *IEEE Engineering in Medicine and Biology,* June/July (1994), pp. 336–346, ©1994, IEEE.)

this is the reason for applying plasticized PVC, the further advantage of which is that it is possible to adjust its flexural properties quite easily. However, a significant disadvantage is that it generally has high water absorption, so it swells and thickens during *in vivo* use. The problems have partially been overcome by using polyurethane.

All types of electrochemical cells demonstrated in Figure 6.4 employ silver cathode, first of all, because of cost reduction (for more details see Appendix 6). Tests on various cathode materials have shown that the best results can be expected from gold. Platinum is less favorable, but its advantage is the

possibility of preparing hermetic metal-glass bonding; thus, platinum cathodes can be insulated well with good insulation glasses. Graphite cathode is inexpensive, but it has relatively high negative polarization voltage (< -1 V) and large instability. The greatest disadvantage of silver cathodes is their instability due to electrochemical corrosion and migration of silver that can even cause short circuit formation and/or electrode consumption (Harsányi, 1995a; Cha et al., 1990; see also Appendix 6). A saturated solution electrolyte can decrease the possibility of latter effects. Generally, KCl solution is used as an electrolyte. Salt crystallization on electrode surfaces due to water evaporation may also result in disturbances. Water evaporation can be decreased by means of further Na or K salt (phosphate, nitrate, or bicarbonate) additives.

Another promising approach for cost reduction, instead of replacing gold or platinum with silver, is the application of thin- and thick-film processing. The main problem of these solutions is the anodic reaction of H_2O_2 that is developed at the cathode [see Equation (6.3a)]. This leads to the consumption of the Ag/AgCl electrode by its dissolution. This can be reduced by increasing the spacing between the electrodes, which also represents the limits of scaling down (Harsányi et al., 1994, see also Appendix 6).

Figure 6.5 shows the structure of a Clark sensor that is fabricated by means of silicon micromachining and thin-film processing and employs liquid electrolyte (Suzuki et al., 1993). Its sizes enable catheter tip application. A glass substrate with a silver working electrode, gold counterelectrode, and Ag/AgCl reference electrode is bonded to a silicon substrate by field-assisted bonding at 250°C by applying -1200 V to the glass substrate against the silicon substrate in nitrogen atmosphere. The silicon substrate has anisotropically etched "V" grooves to provide small cavities to accommodate an electrolyte solution. Because the electrochemical reactions are localized in a very small amount of electrolyte, electrochemical cross talk between the electrodes must be eliminated. Therefore, the container grooves are etched only over each electrode area, and they are connected by long narrow grooves. The oxygen-permeable membrane, made of poly(fluoroethylene propylene) PFEP, was affixed thermally to the silicon substrate over an etched-through cavity above the working electrode. The electrolyte was incorporated by dipping the whole chip into the electrolyte solution within a centrifuge tube, placing it into a chamber, and evacuating. The channel system was closed by a droplet of silicone rubber that can easily be removed for electrolyte refreshing. The response of the miniature amperometric sensor was about 30 nA/ppm O_2, with an average response time of 30 sec and an almost zero residual current. The stable operation period of the sensor was 10 h.

Figure 6.6 shows a silicon-based Clark sensor fabricated compatibly with integrated circuit processing; thus, the ISFETs and the circuitry components

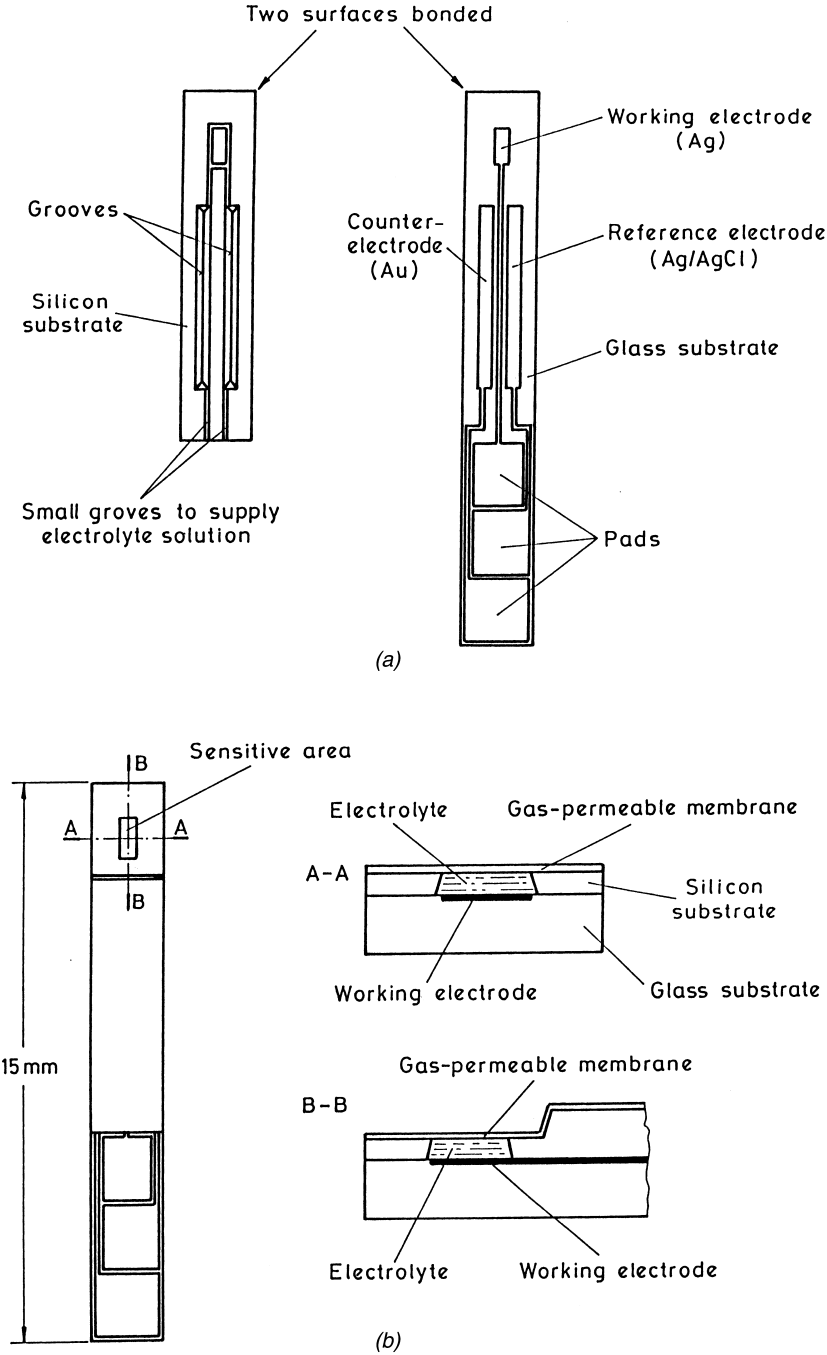

FIGURE 6.5. Structure of the micromachined Clark oxygen sensor: (a) the two parts of the sensor and (b) the complete structure. (Reprinted with permission from H. Suzuki, A. Sugama and N. Kokima, "Micromachined Clark Oxygen Electrode," *Sensors and Actuators B,* 10, pp. 91–98, ©1993, Elsevier Science S.A., Lausanne, Switzerland.)

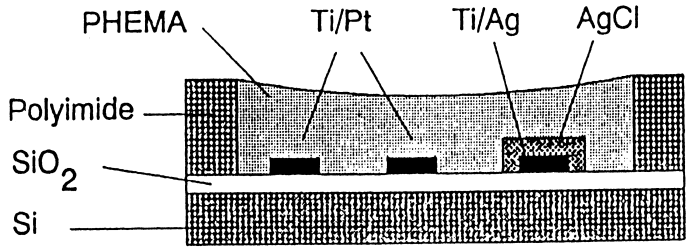

FIGURE 6.6. Schematic cross section of the thin-film Clark sensor. (Reproduced with permission from W. Gumbrecht, W. Schelter, B. Montag, J. A. H. Bos, E. P. Eijking and B. Lachmann, "Monitoring of Blood pO_2 with a Thin-Film Amperometric Sensor," *Proc. of 1991 Int. Conf. on Solid State Sensors and Actuators (Transducers '91),* San Francisco, CA, pp. 85–87. ©1991, IEEE.)

can be integrated onto the same silicon substrate (Gumbrecht et al., 1991). The sensor consists of a planar thin-film three-electrode system with two platinum electrodes and an Ag/AgCl reference electrode. Evaporated titanium layers were used to obtain good adhesion to the SiO_2. The silver was partly converted to chloride by chemical chloridization. A 30 μm thick photosensitive polyimide layer was deposited and patterned photolithographically to form a micropool above the electrode arrangement. Finally, the micropool was filled with a PHEMA [poly(hydroxiethyl methacrylate)] hydrogel. This is permeable to oxygen molecules and small ions, but protects the Pt working electrode from proteins that adhere to and poison the surface. The water content of the hydrophilic PHEMA membrane can vary within a wide range; thus, it acts both as electrolyte and as membrane. Another construction was also fabricated using a poly(vinyl alcohol) electrolyte buffer and a silicone rubber permselective membrane.

Very similar problems have to be solved when fabricating pCO_2 sensors for blood gas measurements. The most important differences are as follows:

- The cathode is a pH electrode.
- The electrolyte is generally $NaHCO_3$.
- Potentiometric or conductimetric measurement has to be applied.
- The applicable membrane material is PTFE or silicone rubber.

Practical forms of potentiometric devices are discussed in connection with transcutaneous and combined sensor types (see Sections 6.1.3 and 6.1.6).

A novel sensing principle has been proposed recently that is based on the revealing of an ion formation as described by Equation (6.4) (Varlan and Sansen, 1997). That means that there is a conductometric sensor in the closed cavity. The advantage is the simplicity; there are only two electrodes in the closed chamber. The silicon micromachined sensor involves two planar elec-

trodes housed in a micromachined chamber formed between a silicon and a glass substrate, as was shown in connection with pressure sensors (see Section 5.3.1). The cavity was filled with deionized water and was connected with the chemical environment via a sieve etched from the silicon and covered with a polymeric membrane.

The other approach of invasive blood analysis, instead of using microelectrodes and microelectronic sensors on catheter tips, is *ex vivo* measurement. Here, a cannula or a two-lumen catheter with a blood flow-through cell is applied to obtain blood samples, enabling the operation of larger sensors nonintravascularly (Schelter et al., 1992). Figure 6.4(b) shows a two-lumen catheter enabling catheter tip sensor mounting and blood sample taking.

6.1.3 Transcutaneous Electrochemical Sensors

Although intravascular monitoring remains an important part of intensive care, catheterization of arteries has some risks, especially for newborn babies. This is one of the reasons, which has led to the advent and rapid growth of noninvasive blood gas monitoring. The transcutaneous technique has a lot of interest, enabling blood gas measurements through the skin.

Human skin is practically impermeable for gas molecules at normal conditions. Baumberger and Goodfriend revealed in 1951, however, that if skin temperature is increased, it might behave as a semipermeable membrane. Near 45°C, pO_2 measured at the surface can approach the arterial value quite closely. The estimation of arterial pO_2 and pCO_2 based on this noninvasive method is called the *transcutaneous technique.* The sensor elements are Clark- and Stow-Severinghaus (see Section 6.1.1) electrochemical cells equipped with heating elements and temperature sensors that enable an operation within a well-controlled narrow temperature range.

A good estimation of arterial blood gas parameters is based on the correct choice of skin temperature (Huch et al., 1972). Heating the skin causes several effects to be considered at pO_2 measurements:

- Vasodilatation of dermal capillaries occurs, thereby "arterializing" the capillary blood.
- A rightward shift of the oxyhemoglobin dissociation curve takes place; i.e., pO_2 increases at the sensor site.
- An increase of oxygen diffusion both through the stratum corneum of the skin and through the polymer membrane of the sensor will also occur.
- The increased speed tissue metabolism increases the oxygen consumption resulting in a drop of pO_2.
- The overall operation of the electrochemical cell is strongly temperature dependent.

According to empirical results, phenomena that cause a virtual change in pO_2 at the sensor site may balance each other's effect by an appropriate choice of temperature. A sensor temperature of 43.5 ± 0.5°C has been found to be optimum for reliable monitoring of arterial pO_2, ensuring a good correlation between values measured by transcutaneous and invasive methods, respectively. However, the temperature fluctuation of the sensor element must not exceed 0°C.

Figure 6.7 shows the structure of a conventional transcutaneous pO_2 sensor (Parker, 1987). This is a specially designed Clark oxygen sensor, in which a miniature heater coil is incorporated to maintain the skin at the necessary temperature. The temperature control is enabled by a thermistor. A second thermistor acts as a safety cutout to prevent the sensor from overheating in case of a primary thermistor malfunction. The three-element cathode consists of 20 μm platinum wires fused into glass and surrounded by an Ag/AgCl an-

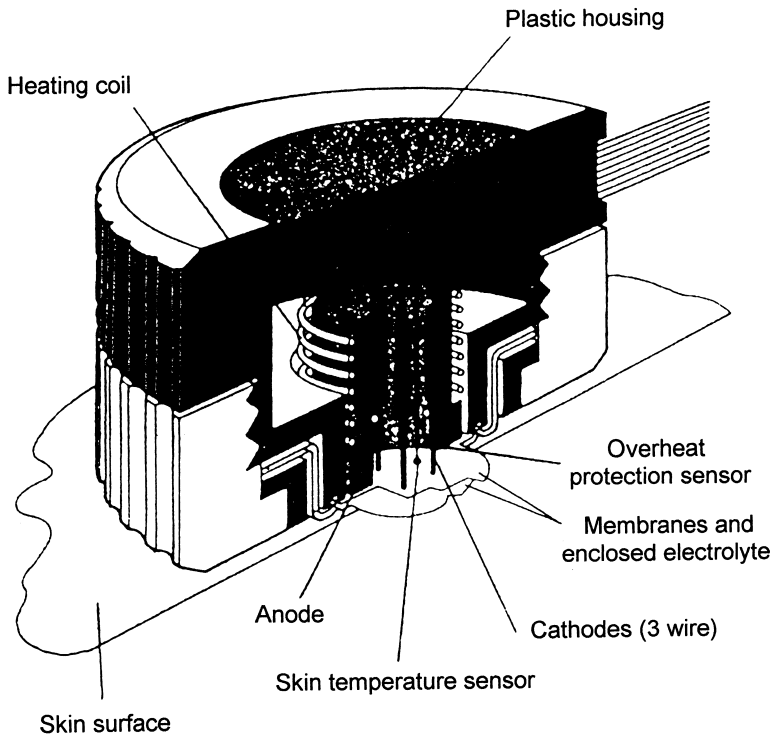

FIGURE 6.7. Structure of a transcutaneous blood pO_2 sensor. (Reproduced with permission from D. Parker, "Sensors for Monitoring Blood Gases in Intensive Care," *J. Phys. E: Sci. Instrum.,* Vol. 20, pp. 1103–1112, ©1987, IOP Publishing Ltd., Bristol, UK.)

ode. The electrolyte is contained by a 25 μm thick PTFE membrane. Attachment of the sensor to the skin is performed by applying double-sided adhesive tape to achieve a gas-tight seal around the circumference of the sensor. The typical current output of such a sensor is in the range of nanoamperes at a pO_2 of 20 kPa (150 mmHg).

The biggest problem with conventional transcutaneous sensors is that they have a very complicated structure; a number of miniaturized elements must be integrated into a small device. They are generally expensive because of the difficult mounting process and the application of bulk precious metal electrodes.

Potential advantages obtainable through the microfabrication of electrochemical biomedical sensors include reduced size, reduced sample volume, fast response, and reduced cost because of the minimal precious metal consumption of the film electrodes. In addition, it should be possible to produce a highly uniform and well-defined microstructure of the electrode surface area using microelectronic technology. However, a lot of special problems have to be solved and complications may arise as the size of the electrodes and interelectrode distances are reduced (see Section 6.1.2).

A new transcutaneous pO_2 sensor structure is presented in Figure 6.8 (Harsányi, 1995b), which is based on the multilayer ceramic technology that is used in the fabrication of high-density electronic interconnection systems. The electrodes are made using thick-film technology with small amounts of precious metals. The heating element is an integrated thick-film resistor, and a *pn*-junction is used for temperature sensing. The disc-shaped ceramic sensor body has a groove at the edge for packaging purposes and a deep cavity in its center for the temperature sensor chip. The sensor chip should be as close to the skin surface as possible for accurate temperature control. A diode chip is used for temperature-sensing purposes. The horseshoe-shaped heating resistor is screen printed and fired on the top of the ceramic body using a common thick-film processing technique. It consists of several segments to give more freedom for heating.

The sensing electrode was fabricated of thick-film gold paste. The Ag film for the Ag/AgCl reference electrode was also formed by the thick-film technique before being electrochemically chloridized in a 0.1 M HCl solution. The total surface area of this Ag/AgCl electrode is 0.7 cm^2, while the area of the Au electrode is 1.77 mm^2. The ceramic body was molded into a plastic package. The PTFE membrane with a thickness of 10 μm was fastened with a mounting ring to the surface of the sensor, as shown in the cross section in Figure 6.8(b). A conventional KCl solution with a buffering agent was used as the electrolyte. A thin disc-shaped cellophane foil was placed between the electrodes and the membrane as a spacer. The application of multilayer wiring helps to make an appropriate electrode separation necessary to reduce the pick-

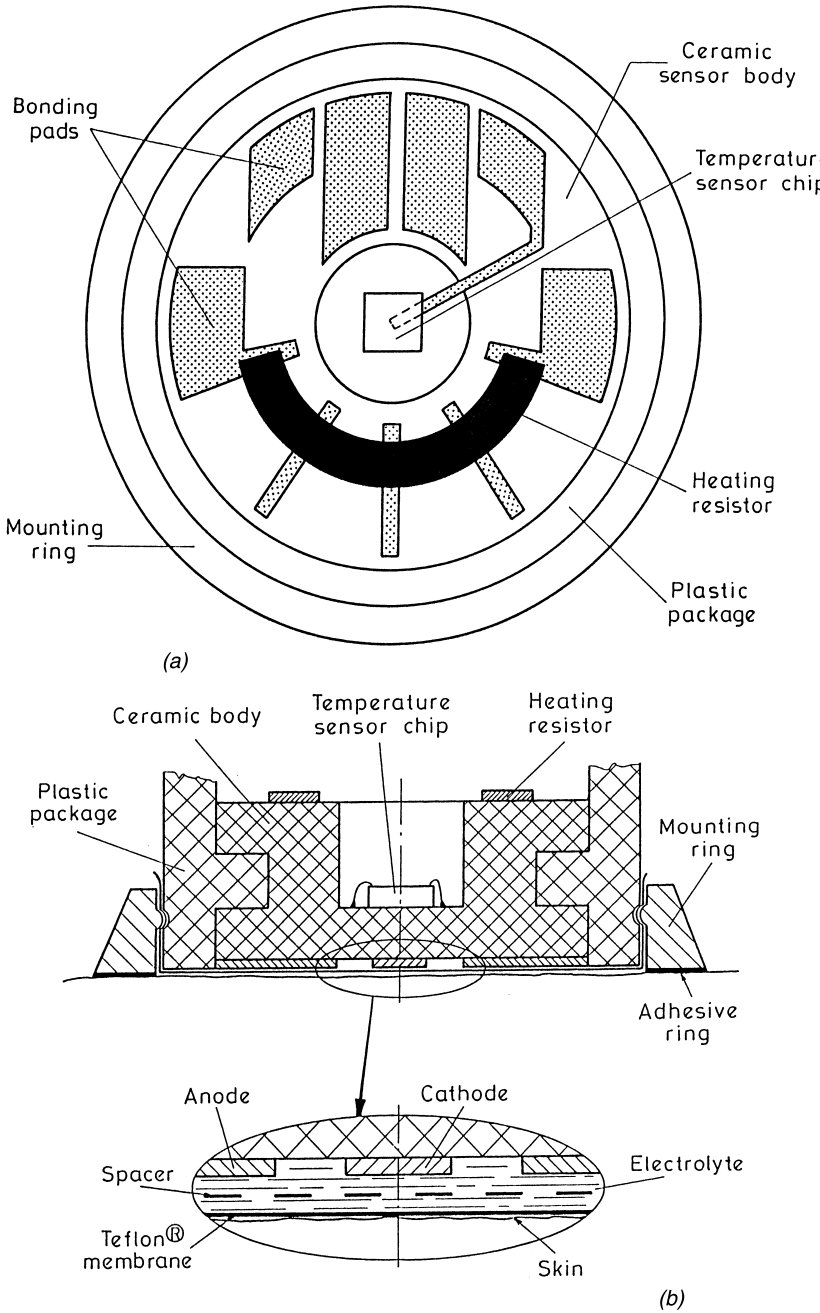

FIGURE 6.8. Structure of the ceramic transcutaneous blood O_2 sensor: (a) top view and (b) cross section. (Reproduced with permission from G. Harsànyi, *Polymer Films in Sensor Applications,* ©1995, Technomic Publishing Co., Inc., Lancaster, PA, p. 378.)

up of the hydrogen peroxide intermediate, causing electrochemical cross talk and electrode consumption (see Section 6.1.1). (This problem arises in connection with film sensors, as the conventional sensors apply bulk wire electrodes.) Some photos of the sensor structure are shown in Appendix 3.

The transcutaneous pCO_2 measurement relies on a similar technique. It is performed by means of heated Stowe-Severinghaus electrochemical sensors. Although the measurement technique is very similar, the transcutaneous estimation of blood pCO_2 differs in theory from that of pO_2 measurements, since there is no balance-of-errors possibility; all of the effects of heating (decreased solubility, increased speed metabolism, increased diffusion) result in the increase of the measured *(tc)*pCO_2 compared to the real arterial pCO_2 value. Their connection can be expressed by the following equation:

$$(tc)pCO_2 = m \cdot pCO_2 + c \tag{6.8}$$

where $m = 1.22$ and $c = 6.6$—empirical values appear to have gained a general acceptance, however, they might be somewhat dependent on sensor size and shape.

A recent trend is to use a single sensor for both gases. The schematic cross section of such a combined transcutaneous sensor is shown in Figure 6.9 (Parker, 1987). It uses the same 0.6 M/l $NaHCO_3$/ethylene glycol electrolyte for the pO_2 and pCO_2 measurements and has a common reference electrode and polymer diffusion membrane. The cathode is a 25 μm diameter platinum wire, and the pH-sensitive glass electrode for CO_2 measurements using the Stow-Severinghaus method is 2–3 mm in diameter. The schematic cross section also shows the heater coil and the temperature-controlling thermistor. The diffusion membrane is held in position by a PTFE ring, and the outer annulus is for attachment to the skin by means of a double-sided adhesive disc.

The combined sensor is essentially a pCO_2 sensor with a cathode incorporated in it to measure pO_2. It is essential to limit the production of hydroxyl ions by the cathode so that the pCO_2 measurement is not affected by a change in the pH of the electrolyte. It can be shown that at a typical cathode current of 3nA, the maximum average change in the electrolyte will be less than 5×10^{-5} pH/h, which will not affect the pCO_2 readings. Figure 6.9(b) shows the typical characteristics of this type of combined sensor.

A newer approach is the application of pH-ISFETs instead of electrodes. A novel miniature transcutaneous pCO_2 sensor was developed recently using a pH-ISFET, a conventional Ag/AgCl electrode, a hydrogel gate-membrane containing 0.1 M/l $NaHCO_3$ electrolyte, a heater coil, and a *pn*-junction temperature sensor (Jinghong et al., 1995). The whole structure is covered with a CO_2 gas permeable membrane. The sensor's measurement range is 0.53–40 kPa (4–300 mmHg) with a response time less than 2 min.

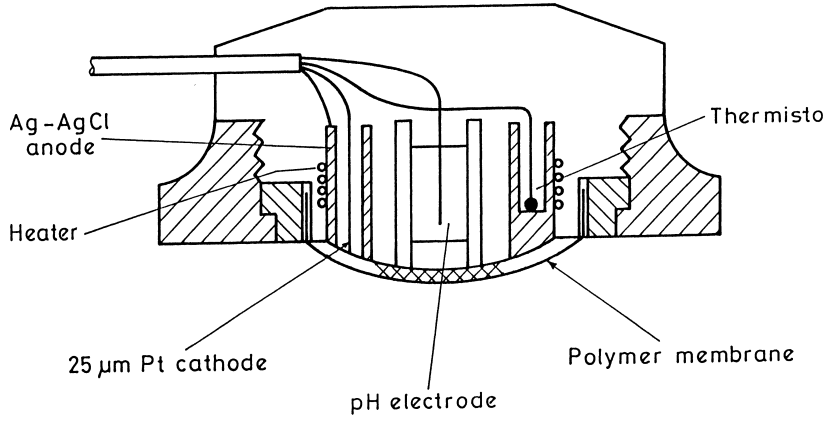

(a)

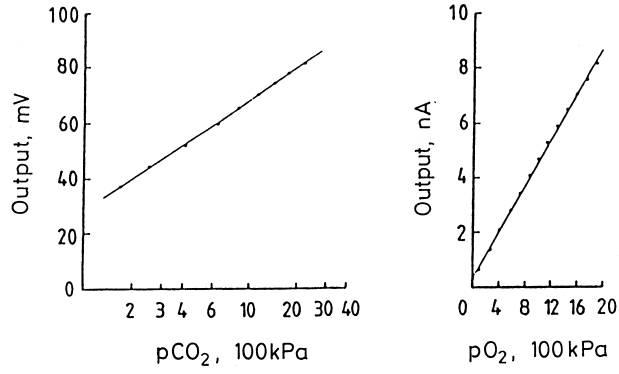

(b)

FIGURE 6.9. A combined pO_2/pCO_2 transcutaneous sensor: (a) its schematic structure and (b) its typical characteristics. (Reproduced with permission from D. Parker, "Sensors for Monitoring Blood Gases in Intensive Care," *J. Phys. E: Sci. Instrum.*, Vol. 20, pp. 1103–1112, ©1987, IOP Publishing Ltd., Bristol, UK.)

6.1.4 Optical Fiber Sensors

Optical fiber sensors for blood gas and pH monitoring enable invasive, generally intravascular, measurements and have an optrode-type structure (see Section 3.6). There are single-fiber and multiple-fiber arrangements. In a single-fiber optrode, the incident and outcoming light has to be separated by means of a beam splitter. In indicator-mediated sensors, the absorbance is

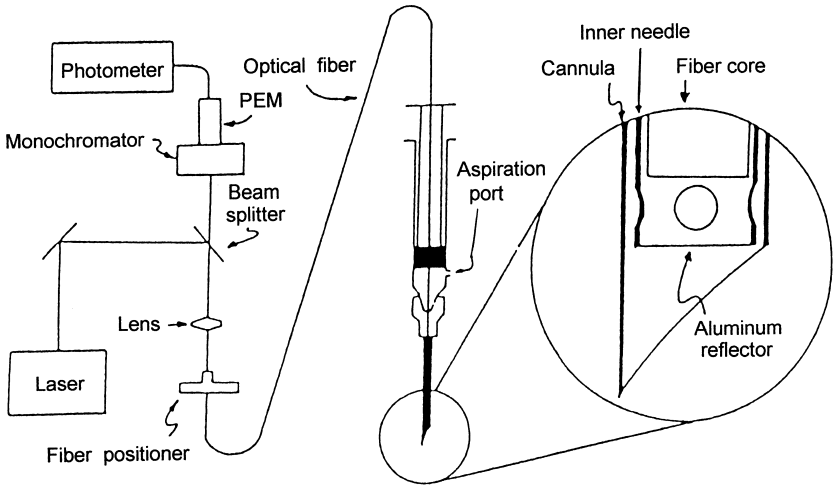

FIGURE 6.10. Schematic structure of single-fiber catheter absorbance measurements and associated instrumentation. (Reproduced with permission from O. S. Wolfbeis, "Biomedical Application of Fiber Optic Chemical Sensors," *Int. Journal of Optoel.,* Vol. 6, No. 5, pp. 425–441, ©1991, Taylor & Francis, London, UK.)

measured; therefore, the reflection from the fiber tip should be increased by using reflective surfaces, as shown in Figure 6.10. In fluorescent optrodes, a secondary light emission is excited; thus, the reflection of the primary light should be prevented. Figure 6.10 demonstrates a single-fiber arrangement. Conventional measurement setups employed monochromatic laser sources and a photoelectron-multiplier for detection. Currently, the low-cost appliances generally operate with LED sources and photodiode detectors. Figure 6.11 demonstrates the typical structure of a double-fiber, reflection-mode optrode catheter (Wolfbeis, 1991).

Optrodes for measuring blood pO_2 are generally based on fluorescent quenching (see Section 4.16) of oxygen-sensitive fluorescent dyes such as perylene-dibutyrate (Soller, 1994). The excited light intensity can be described by the Stern-Volmer equation [see Equation (4.28)]. Neglecting the nonlinearity from the nonunit extension, the measurable intensity is as follows:

$$I = I_o /(1 + k \cdot pO_2) \tag{6.9}$$

where I_o is the fluorescent emission intensity in the absence of the quencher. This relationship results in a nonconstant sensitivity (S) for oxygen:

$$S = dI/dpO_2 = kI_o/(1 + k \cdot pO_2)^2 \tag{6.10}$$

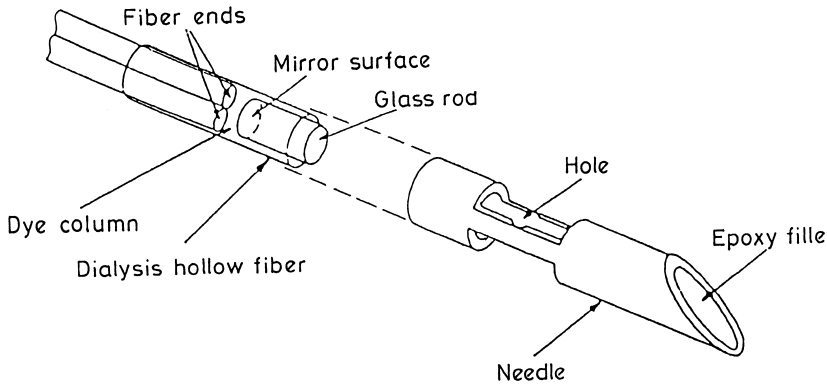

FIGURE 6.11. Typical structure of a double-fiber optrode for intravascular measurements. (Reproduced with permission from O. S. Wolfbeis, "Biomedical Application of Fiber Optic Chemical Sensors," *Int. Journal of Optoel.,* Vol. 6, No. 5, pp. 425–441, ©1991, Taylor & Francis, London, UK.)

Figure 6.12 is a plot of normalized sensitivity as a function of pO_2. The best sensitivity is achieved in the region of 4 to 20 kPa (30–150 mmHg), but drops off considerably at higher levels, making it difficult to resolve small changes when the oxygen partial pressure is greater than 26.6 kPa (200 mmHg).

The fluorescent dye can be entrapped in a polystyrene membrane, for instance, and kept in position at the fiber end with porous polyethylene tubing. The greatest problem of the measurement is the interference of anesthetic agents; narcotic halothane acts in the same manner as oxygen in fluorescent quenching. A method has been worked out applying two sensors with different susceptibilities to quenching by oxygen and halothane, giving two independent signals that could be converted into oxygen and halothane partial pressures (Wolfbeis, 1991). Further efforts have been reported (see Section 4.16) about phosphorescence quenching of metalloporphyrins and terbium complexes used in blood oxygen optrodes (Papkovsky, 1993; Soller, 1994). Ru-based fluorescent dye complexes have shown especially good lifetimes and stability (Colvin et al., 1996).

Optical-fiber blood pH sensors are mostly reflection optrodes based on acid-base indicator dyes. Their behavior can be described by Equation (4.25). The absorbance is measured generally at two wavelengths, at one with the maximum pH dependence, and at another that is insensitive to pH and can be used as a reference. The sensor signal (J) can be expressed as follows:

$$J = J_0 \cdot e^{-hcl(10^{(\mathrm{pK}-\mathrm{pH})}+1)} \tag{6.11}$$

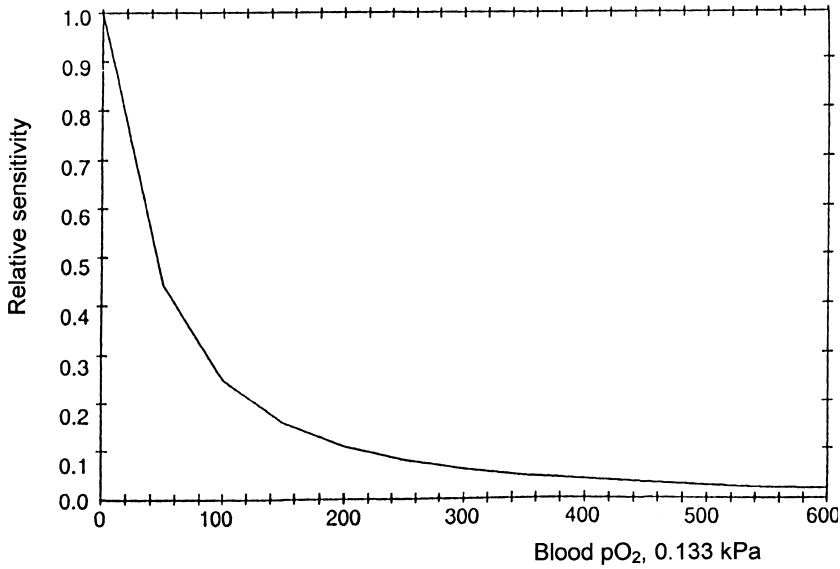

FIGURE 6.12. Sensitivity plot of a fluorescent blood oxygen optrode as a function of pO_2. (Reproduced with permission from B. R. Soller, "Design of Intravascular Fiber Optic Blood Gas Sensors," *IEEE Engineering in Medicine and Biology,* June/July, pp. 327–335. ©1994, IEEE.)

where (J_0) is the signal produced when no base form of the dye is present, and the other symbols are the same as in Equation (4.25). This shows that the sensor properties depend on inherent properties of the dye material (h, pK) and the manufacturing processes used to make the sensor (c, l). Blood pH measurements have to be performed in a narrow range with high accuracy (see Table 6.1). One of the most effective ways to achieve resolution goals is to optimize the pK of the dye material. Figure 6.13 shows the normalized response of a pH optrode for three different values of pK (Soller, 1994). When the pK of the dye is at the center of the range to be measured, 7.4 in the case of blood pH, the maximum sensitivity will be achieved.

The first blood pH optrodes employed phenol red (see Figure 4.11) indicator dye, copolymerized with acrylamide, and a cellulose membrane. Although phenol red has a pK of 7.9 in aqueous solutions, its value was lowered to 7.57 inside the polymer bed. Similar phenomena were found with various indicator types. Thus, pH sensors could be designed with excellent resolution over the entire pH range by "tuning" the pK of the sensing material. This can be accomplished by properly choosing a functional group to be attached to the absorbing portion of the dye molecule or by immobilizing it into a polymer matrix with appropriate ionic characteristics. In this way, a pH

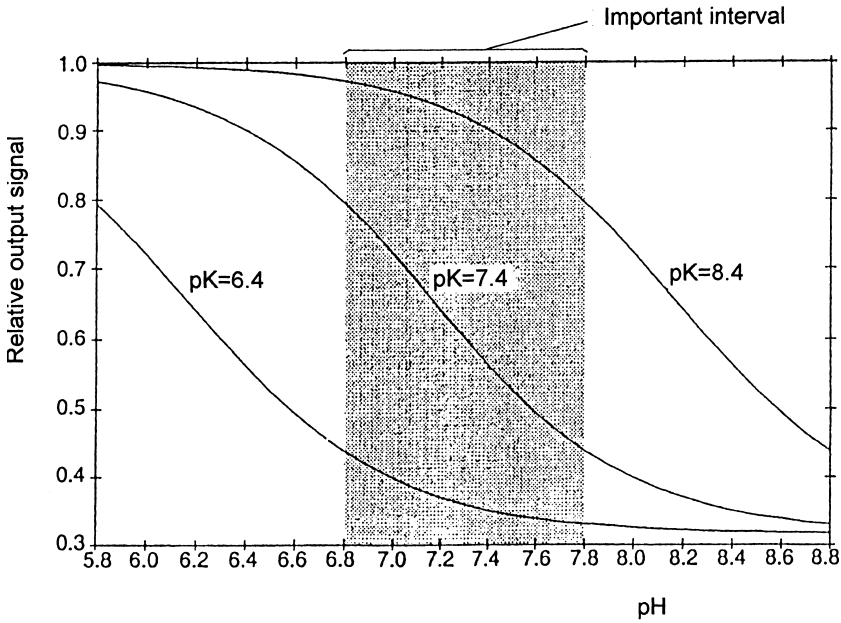

FIGURE 6.13. Characteristics of absorption-based pH sensors with various pK values. (Reproduced with permission from B. R. Soller, "Design of Intravascular Fiber Optic Blood Gas Sensors," *IEEE Engineering in Medicine and Biology,* June/July, pp. 327–335, ©1994, IEEE.)

sensor with phenol red was realized for the physiological detection range with an accuracy of 0.01 and with a temperature coefficient of 0.017 pH units/°C (Peterson et al., 1980).

Fluorescence-based pH sensors have also been fabricated using the pH-dependent excitation spectra of hydroxy-pyrene-trisulfonic (HTPS) acid (Wolfbeis et al., 1983). The excitation/emission spectra are shown in Figure 6.14 (Leiner and Hartmann, 1993). The deprotonated form of HTPS bound to cellulose can be excited at 475 nm to give a fluorescence emission at 530 nm. The intensity of the latter is a function of the pH. The acid form of the dye can be excited at 410 nm to give fluorescence emission from the same band as the base form. When excited at the isoemissive wavelength of 428 nm, a pH-independent fluorescent signal is obtained that can be used for reference purposes.

Additional fluorescent indicator dyes include fluoresceinamine and dichloro-fluorescein. pH sensors were also fabricated using colorimetric and fluorescent indicator dyes.

Most fiber-optic sensors for measuring pCO_2 use the same approach as the

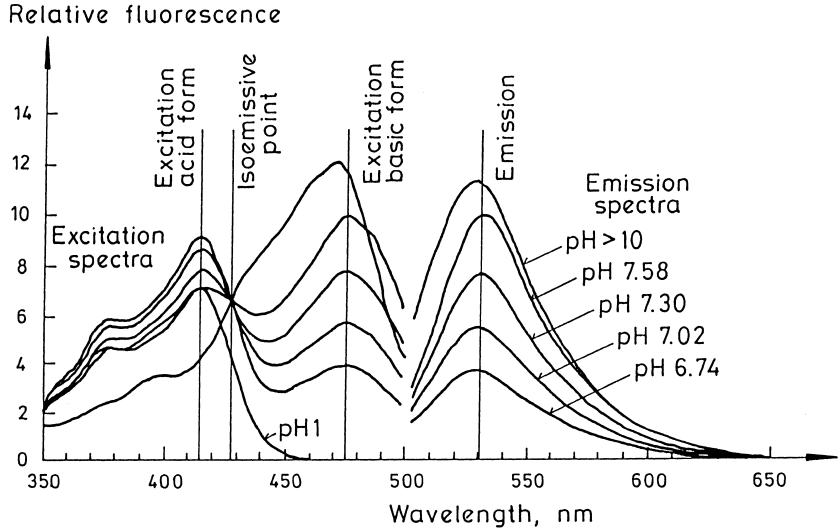

FIGURE 6.14. pH-dependent absorption and emission spectra of a fluorescent optrode with HTPS dye. (Reprinted with permission from M. J. P. Leiner and P. Hartmann, "Theory and Practice in Optical pH Sensing," *Sensors and Actuators B,* 11, pp. 281–289, ©1993, Elsevier Science S.A., Lausanne, Switzerland.)

electrodes—a pH sensor is placed in contact with an internal solution of bicarbonate ion and is separated from the environment by a gas-permeable membrane such as silicone rubber or a copolymer of dimethylsiloxane. Absorption optrodes with phenol red and fluorescence-based optrodes applying dichlorofluorescein have been developed. The key for optimizing pCO_2 sensor design is to control the internal bicarbonate ion concentration. Figure 6.15 shows the pH-pCO_2 plot of the sensor for several bicarbonate ion concentrations (Soller et al., 1994). The graph shows that the resolution of the sensor does not change as a function of bicarbonate ion concentration. In order to achieve the desired pCO_2 resolution of 0.133 kPa (1 mmHg), the pH sensor must have a resolution of 0.009 pH units. However, the internal bicarbonate ion concentration determines the range of the pH response. To take advantage of the pH sensor designed to measure blood pH, the bicarbonate ion concentration should be chosen so that the internal pH varies between 6.8 and 7.8. As shown in Figure 6.15, a bicarbonate concentration of 0.035 M/l produces a pH response in the desired range. The bicarbonate may be soaked into the pH-dye layer or may be placed into a separate chamber, resulting in multimembrane optrode structures. It is important to maintain a constant bicarbonate ion concentration; therefore, water evaporation should be prevented. Thus, sensors are stored in an aqueous buffer that can than also serve as one of the calibration solutions.

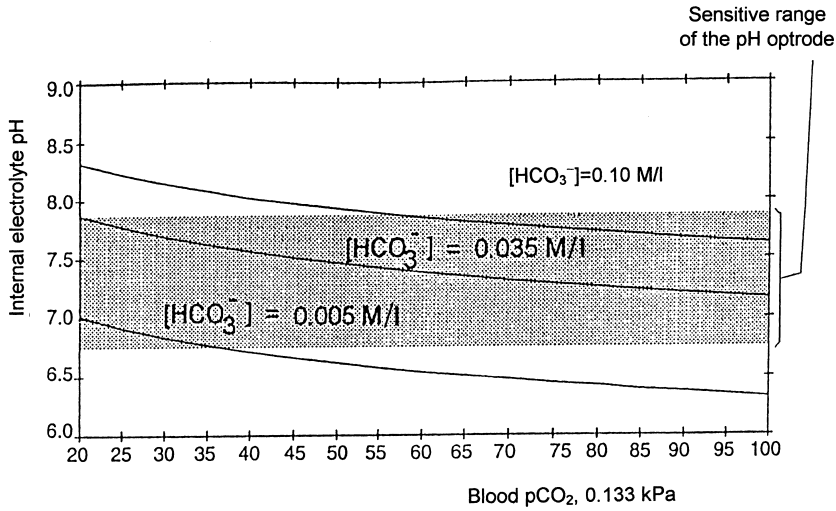

FIGURE 6.15. Internal pH characteristics of pCO_2 sensors with various internal bicarbonate ion concentrations. (Reproduced with permission from B. R. Soller, "Design of Intravascular Fiber Optic Blood Gas Sensors," *IEEE Engineering in Medicine and Biology,* June/July, pp. 327–335, ©1994, IEEE.)

6.1.5 Other Techniques

In this section, those blood gas and pH measurement methods are surveyed, in which the analysis itself is made outside of the body. One group of these techniques does not apply real signal-transducer sensor elements. The common properties of them are as follows:

- The analysis is made using one of the classical analytical methods.
- The "sensor" of the system is practically only a sample-taking unit.

Although these techniques do not apply real sensors according to the definition in Section 1.1, they must be mentioned here in connection with biomedical measurements. A detailed description of the mentioned analytical methods is, however, beyond the scope of this book.

Gas chromatography and mass spectrometry have been applied for blood gas measurements. The actual sensor takes and removes a gas sample "from the blood" in these methods. The greatest advantages of their applications are that the stability problems of electrochemical and fiber-optic sensors are avoided, and several gas compounds can be analyzed simultaneously (not only O_2 and CO_2, but N_2, and anesthetic gas as well). The price for that is the use

of a more complicated and more expensive analytical instrument and sample-taking system.

Indwelling catheters can be applied intravascularly to remove a gas sample from the blood, utilizing a carrier gas or vacuum and feeding the sample to an external gas chromatograph or mass spectrometer for analysis. Figure 6.16 shows a gas chromatograph blood gas "sensor" based on a closed-tipped two-lumen intra-arterial catheter (Mendelson, 1991). The blood gases diffuse into the lumen of the catheter and approach an equilibrium concentration with the carrier gas contained in the lumen. After equilibrium is achieved, which takes a few minutes, a bolus of the gas content in the lumen is delivered to the gas chromatograph for separation and analysis. Helium gas is delivered from the analyzer through the outer annular supply line in the catheter, and is then drawn back with the sample into the analyzer through the central return tube. Silicone rubber is used as the gas permeable membrane.

The continuous analysis of gases in blood by means of mass spectrometry has also been realized. A gas sample is drawn using a vacuum in this case. The probe consists of an evacuated cannula with a gas permeable membrane supported mechanically by some suitable means at its tip, such as a porous sintered plug or a perforated hypodermic tube, as shown in Figure 6.17 (Rolfe, 1994). Gases diffuse from the blood through the membrane into the evacu-

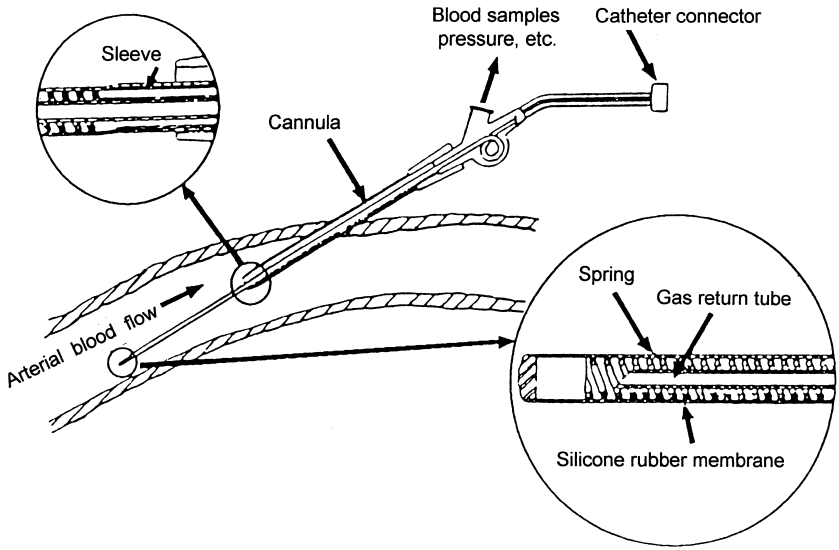

FIGURE 6.16. Indwelling blood gas catheter for gas chromatography. (Reprinted after Mendelson, 1991, p. 260, courtesy of Marcel Dekker Inc, New York.)

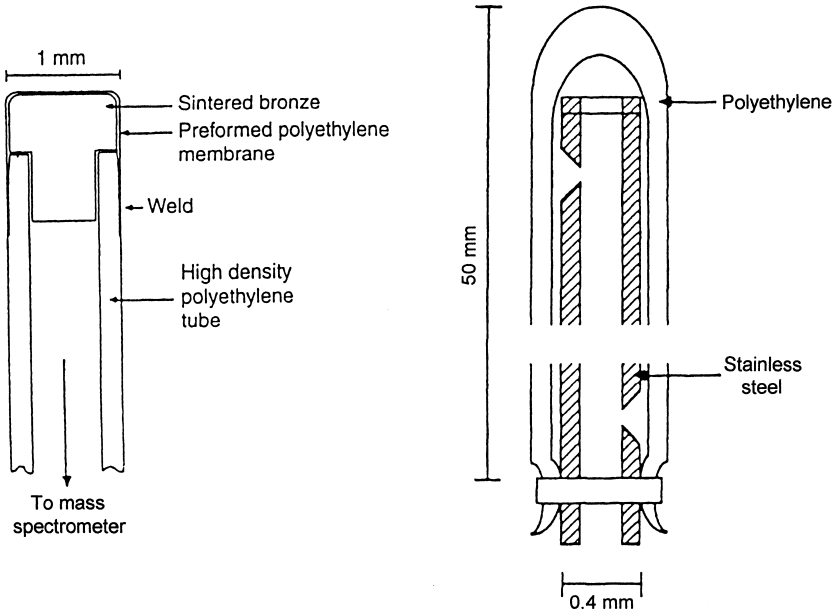

FIGURE 6.17. Examples of blood gas sample-taking probes for mass spectrometry. (Reproduced with permission from P. Rolfe, "Intra-Vascular Oxygen Sensors for Neonatal Monitoring," *IEEE Engineering in Medicine and Biology,* June/July, pp. 336–346, ©1994, IEEE.)

ated space and then migrate along the connecting tube to the mass spectrometer inlet, and, hence, to the analysis chamber.

Transcutaneous solutions for mass spectrometry have also been developed as shown in Figure 6.18 (Mendelson, 1991). The "sensor" consists of a small stainless-steel chamber with a porous metallic substrate across its open face. A membrane is placed across the substrate and sealed to the skin with a double-sided, self-adhesive ring. Gases collected in the chamber pass by a vacuum pump along a gas-impermeable tube into the ion source of the mass spectrometer. The back of the sensor contains a heating coil and a thermistor for controlling the temperature of the sensor. The major drawbacks are the possibility of gas leaks at the skin surface and the relatively slow response time.

Ex vivo blood gas and pH measurements can also be realized using optical fiber sensors. Figure 6.19 shows an interesting device design that can be applied in a flow-through cell of an extracorporeal blood circuit (Wolfbeis, 1991). Two permeable membranes separate the bloodstream from the sensor chemistry placed on the disposable sensor element that is connected to the fiber-optic cable. An electrical contact is also included for temperature measurement using a thermistor. The disposable sensor element can be changed without

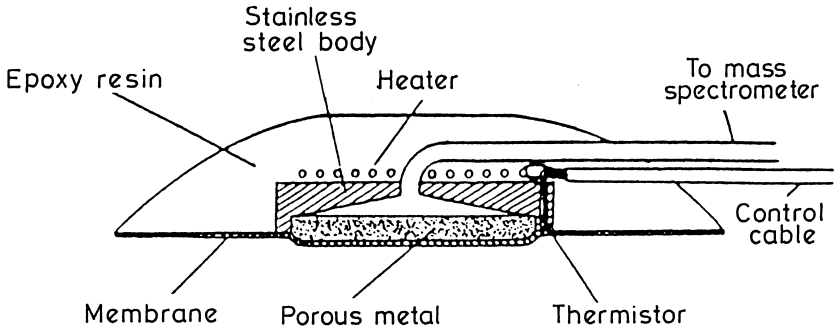

FIGURE 6.18. Cross-sectional diagram of a typical transcutaneous mass spectrometer probe. (Reprinted after Mendelson, 1991, p. 273, courtesy of Marcel Dekker Inc., New York.)

removing the extracorporeal loop from the patient—only the bloodstream has to be stopped for a while. The optical fiber bundle is mounted onto another part, which cannot be changed. Such an instrument can be developed, in which the unstable parts that contain the indicators and membrane, and are in contact with blood during the operation, are disposable without changing any other parts, such as the fibers and the thermistor. The flow-through cell and tubes are also separate components that may be sterilizable or disposable.

6.1.6 Combined Sensors

A few examples of combined multisensors have already been demonstrated in the previous sections (see Sections 6.1.3 and 6.1.5). Multisensors are capable of simultaneous monitoring of several parameters including pO_2, pCO_2, pH, and temperature. This has great importance, especially in biomedical applications, for the following reasons:

- All four parameters are physiologically important.
- Gas sensors are sensitive for pH; thus, the measurement of pH enables the compensation of this effect.
- All sensors are temperature dependent, the compensation of which requires the application of temperature sensors.

Miniaturization is especially important when producing catheter tip sensors. The following approaches are available:

- building up compound electrochemical sensors using multielectrode systems
- integrating multiple sensors into silicon substrates
- building up multioptrodes using optical-fiber bundles

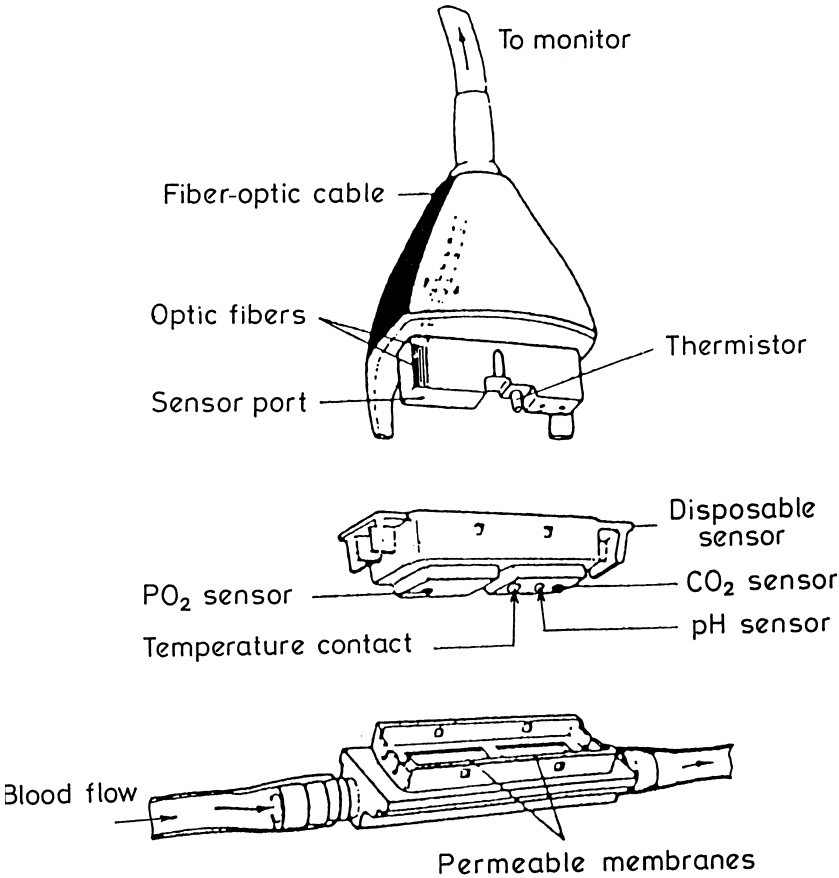

FIGURE 6.19. Extracorporeal fiber-optic blood gas sensor. (Reproduced with permission from O. S. Wolfbeis, "Biomedical Application of Fiber Optic Chemical Sensors," *Int. Journal of Optoel.,* Vol. 6, No. 5 pp. 425–441, ©1991, Taylor & Francis, London, UK.)

The example in Figure 6.20 demonstrates how three different sensor types can be integrated into the same silicon substrate using compatible processing sequences (Tsukada et al., 1990). The combined sensor consists of a Clark pO_2 sensor with a Pt sensing electrode, a Stow-Severinghaus pCO_2 sensor with a Si_3N_4-gate pH-ISFET, and a pH sensor ISFET. Both gas sensors apply poly(vinyl alcohol) film for soaking the electrolyte: the KCl solution at the pO_2 sensor and the NaCl-$NaHCO_3$ solution at the pCO_2 sensor, respectively. The gate membrane of the pH-ISFET is also Si_3N_4. Using plasticized PVC membranes with various ionophores, several ion-selective ISFETs can also be integrated onto the same chip.

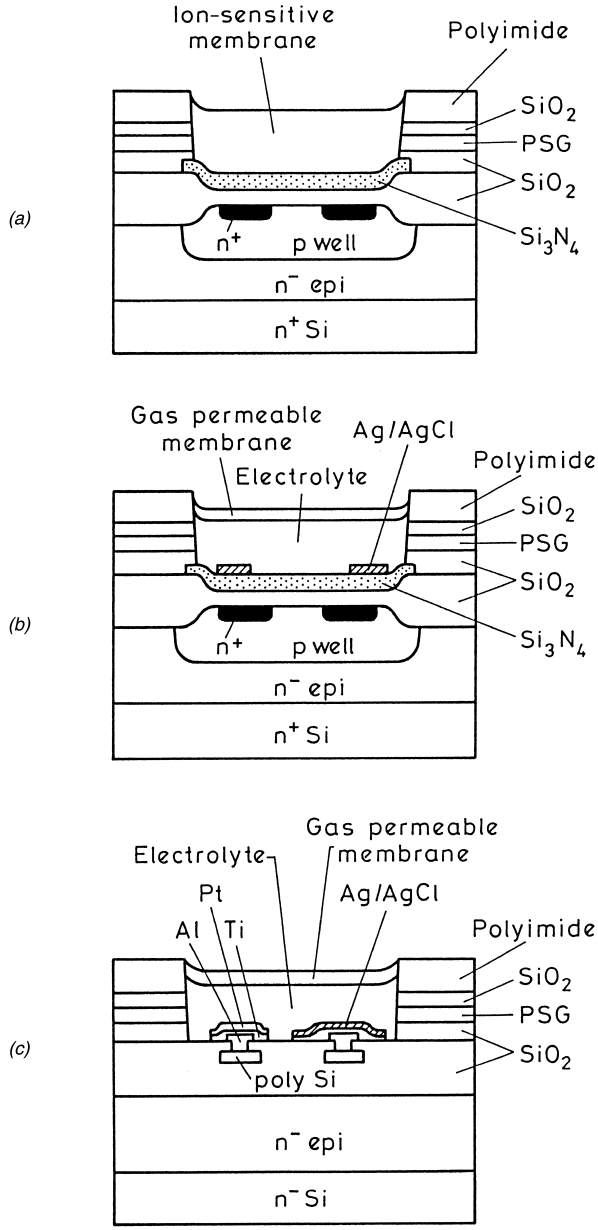

FIGURE 6.20. Cross-sectional structure of the elements in an integrated chemical sensor: (a) ISFET, (b) pCO_2 sensor, and (c) pO_2 sensor. (Reproduced with permission from K. Tsukada, Y. Miyahara, Y. Shibata and H. Miyagi, "An Integrated Chemical Sensor with Multiple Ion and Gas Sensors," *Sensors and Actuators B,* 2, pp. 291–295, ©1990, Elsevier Science S.A., Lausanne, Switzerland.)

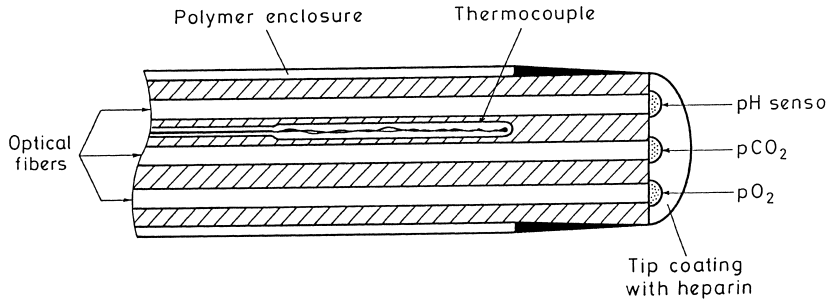

FIGURE 6.21. Triple-fiber optrode sensor for blood monitoring. (Reproduced with permission from O. S. Wolfbeis, "Biomedical Application of Fiber Optic Chemical Sensors," *Int. Journal of Optoel.,* Vol. 6, No. 5, pp. 425–441, ©1991, Taylor & Francis, London, UK.)

The fiber-optic approach is advantageous in intravascular measurements because it offers a way for sensor miniaturization so that even a fiber bundle can be introduced into the radial artery of a patient through a catheter. One example is shown in Figure 6.21 (Wolfbeis, 1991). The working chemistries of the three sensors are placed at the tip of the three fibers, while a thermocouple gives a direct reading of the sensor temperature at the tip. The issue of thrombogenicity has been addressed by designing a smooth tip surface and by covalently immobilizing heparin on the surface.

In an interesting new solution, the sensors are incorporated onto an ophthalmoscope, providing the sensors' data at the same time as an image (Alcock and Turner, 1994). The device comprises an array of small fibers, each in contact with part of a chemically sensitive membrane covering the tip of the bundle, effecting an array of sensors via the pixels (see Figure 6.22).

Hybrid intravascular sensors have also become possible, using optical sensing of pH and pCO_2 combined with temperature measurement and electrochemical sensing of pCO_2.

6.2 OPTICAL OXIMETRY

Optical oximeter devices measure oxygen saturation (SO_2) of blood or tissue by exploiting the differences between the absorption spectra of organic compounds transporting oxygen, such as hemoglobin (Hb) and cytochrome aa_3. Oximetry is a technique for measuring a chemical-to-optical transduction effect without applying special indicator dyes. Here the dye is within the analyte. Although, as a result, the sensor elements are physical sensors (e.g., photodiodes), the discussion of this method fits into this chapter.

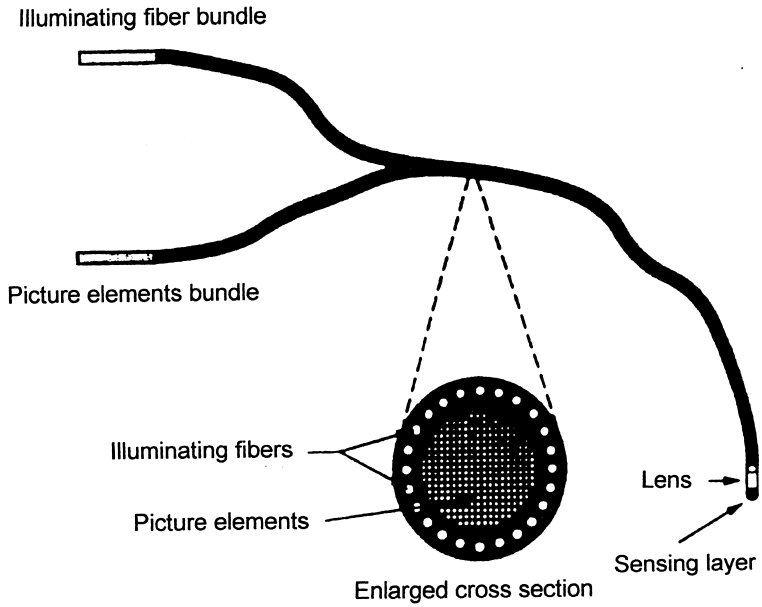

FIGURE 6.22. Design of an imaging/sensing fiber bundle system. (Reproduced with permission from S. J. Alcock and A. P. F. Turner, "Continuous Analyte Monitoring to Aid Clinical Practice," *IEEE Engineering in Medicine and Biology,* June/July, pp. 319–326, ©1994, IEEE.)

6.2.1 Theoretical Bases of Blood Oximetry

Most oximeter sensors and appliances determine blood oxygen saturation [see Equation (6.1)], based on the different absorption (extinction) spectra of Hb and HbO_2, as demonstrated in Figure 6.23 (Parker, 1987). This is actually the cause of the different colors of arterial and venous blood. The measurement employs a minimum of two different wavelengths—one in the red range (generally around 660 nm) and another in the infrared range (between 805 and 1000 nm). The extinction coefficient is the same for Hb and HbO_2 at 805 nm, so that this (isobestic) wavelength can serve as a reference.

In *reflection mode oximetry,* backscattered light from the specimen is sampled at two different wavelengths (λ_1 and λ_2), and the oxygen saturation is estimated with the reflectance [$R = \ln (I_0/I_r)$, where I_0 is the incident and I_r is the reflected intensity] ratio, according to the following expression:

$$SO_2 = A - B \cdot [\, R(\lambda_1)/R(\lambda_2)] \tag{6.12}$$

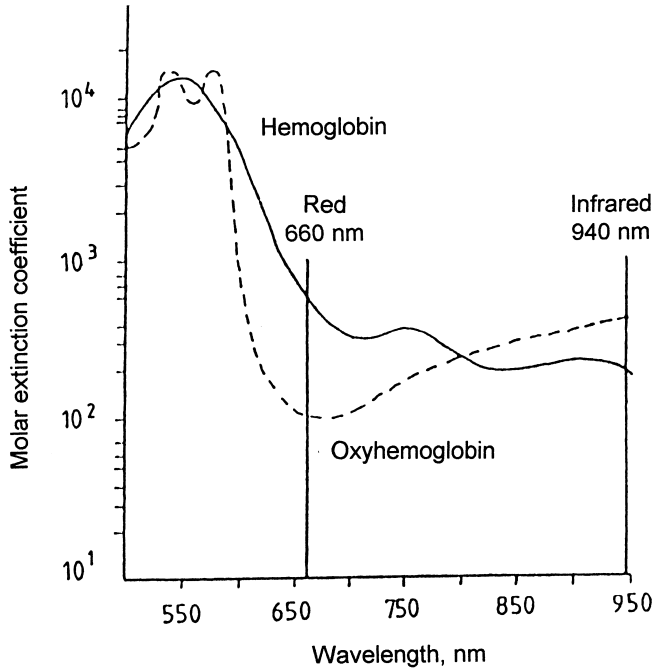

FIGURE 6.23. Absorption spectra of hemoglobin and oxyhemoglobin. (Reproduced with permission from D. Parker, "Sensors for Monitoring Blood Gases in Intensive Care," *J. Phys. E: Sci. Instrum.,* Vol. 20, pp. 1103–1112, ©1987, IOP Publishing Ltd., Bristol, UK.)

where A and B are empirical constants. Although the nonlinearity of scattering can be neglected in practice, the constants are, of course, dependent on the volume ratio of red blood cells, thus, the hematocrit. To compensate this effect, the measurement is generally made on three wavelengths (Wolfbeis, 1991).

In *transmission oximetry,* the absorption of the transmitted light is analyzed. According to the definition of optical density (d):

$$d = \ln (I_0/I_t) \tag{6.13}$$

where I_0 is the incident and I_t is the transmitted light intensity. Applying the Lambert-Beer equation for a blood sample (see Equation 3.9) we get the following:

$$d = l\,[h(\mathrm{Hb})C(\mathrm{Hb}) + h(\mathrm{HbO_2})C(\mathrm{HbO_2})\,] \tag{6.14}$$

where C is the concentration, and h is the extinction coefficient of the differ-

ent compounds, while l is the optical path length. The expression supposes the linear contribution of the various compounds to the overall absorption. By performing density measurements on two different wavelengths (λ_1 and λ_2), the concentrations [C(Hb) and $C(HbO_2)$] can be determined from two linear equations, knowing the extinction coefficients [$h(\lambda_1,HbO_2)$, $h(\lambda_2,HbO_2)$, $h(\lambda_1,Hb)$, $h(\lambda_2,Hb)$] and the optical path length (l). The oxygen saturation (SO_2), however, can be calculated without knowing the exact value of l (Takatani and Ling, 1994):

$$C(\text{Hb}) = [h(\lambda_2,\text{Hb})d(\lambda_1) - h(\lambda_1,\text{Hb})d(\lambda_2)]/l \cdot [h(\lambda_1,HbO_2)h(\lambda_2,\text{Hb}) - h(\lambda_2,HbO_2)h(\lambda_1,\text{Hb})] \quad (6.15a)$$

$$C(HbO_2) = [h(\lambda_2,HbO_2)d(\lambda_1) - h(\lambda_1,HbO_2)d(\lambda_2)]/l \cdot [h(\lambda_1,\text{Hb})h(\lambda_2,HbO_2) - h(\lambda_2,\text{Hb})h(\lambda_1,HbO_2)] \quad (6.15b)$$

$$SO_2 = C(HbO_2)/[C(\text{Hb}) + C(HbO_2)] \quad (6.15c)$$

Because of the complicated absorption and scattering processes in blood, these results are often not accurate enough for practical applications. Measurements are then made on three or more different wavelengths, and the oxygen saturation is calculated from the measured densities according to the following equation that is a more general form of Equation (6.15) (Mendelson, 1991):

$$SO_2 = \frac{a_0 + \sum_i a_i \cdot d(\lambda_i)}{b_0 + \sum_i b_i \cdot d(\lambda_i)} \quad (6.16)$$

where a_i and b_i are constants that can be determined empirically on a diverse range of subjects breathing varying O_2 concentrations.

At first, the technique of oximetry was used for the analysis of blood samples. Nowadays, sensors and analyzer systems enabling continuous *in vivo* monitoring are the focus of interest.

6.2.2 Invasive Oximetry

For intravascular oximetry, plain optical fibers are used to guide the light signal inside the vessel and the light reflected from red blood cells back to the light detector. In estimating SO_2, usually the reflectances at two wavelengths, one in the red and the other in the near-infrared range, are used with

the empirical relation given by Equation (6.12). According to the location of the measurement, arterial and venous saturation can be measured separately.

The oximeter, the block diagram of which is shown in Figure 6.24, employs two different LEDs as light sources driven on alternate half-cycles of the clock pulse (Wolfbeis, 1991). Light from the LEDs is tightly coupled into a branch of fibers. Reflected light is coupled to a photodiode, amplified and delivered to the sample-and-hold circuit that reads the pulse heights whose ratio is computed and displayed. The typical operation frequency of the system is 200 Hz. The empirical parameters can be set for the computations during an *in vitro* calibration. With an appropriate calibration, the accuracy of the system was found in the range of 1%.

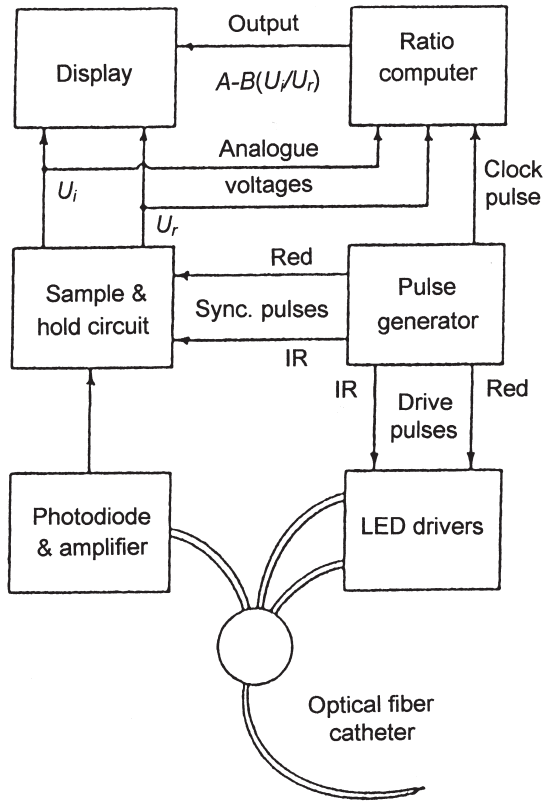

FIGURE 6.24. Schematic block diagram of the intravascular optical fiber oximeter. (Reproduced with permission from O. S. Wolfbeis, "Biomedical Application of Fiber Optic Chemical Sensors," *Int. Journal of Optoel.,* Vol. 6, No. 5, pp. 425–441, ©1991, Taylor & Francis, London, UK.)

One of the disadvantages of the fiber-optic oximeter is that damage to optical fibers results in severe measurement error. In order to circumvent this shortcoming, catheter-tip oximeters using hybrid miniature sensors have also been developed, as shown in Figure 6.25. The smart sensor elements, the red and infrared LEDs, the photodiodes, and the preamplifier chips are mounted in a planar arrangement onto the same substrate (Takatani and Ling, 1994).

6.2.3 Noninvasive Ear Oximetry

Because of the mentioned problems and risks of catheterization, methods of noninvasive oximetry have been developed extensively. Noninvasive oximetry is practically tissue oximetry. Tissue is a complicated medium in which blood vessels, both artery and vein, are distributed nonhomogeneously. Because their distribution is unknown, the analysis of optical processes in tissue is rather complex. The ear oximeter developed first by Hewlett Packard has acquired some clinical success (Mendelson, 1991). The operation principle and block diagram of the instrumentation is illustrated in Figure 6.26. A high-intensity tungsten lamp generates a broad spectrum of light. Eight narrow-band interference filters are mounted on a rotating wheel that intercepts the light path sequentially to provide a source of wavelength selection. These filtered light beam pulses enter a fiber-optic cable that carries them to the ear. A second fiber-optic cable guides the light pulses transmitted through the ear back to the instrument for detection and analysis. To measure arterial blood saturation ($Sa\mathrm{O}_2$), the ear probe is attached to the pinna of the ear after the ear has been rubbed briskly for about 20 s in order to increase local blood flow. A temperature-controlled heater within the probe maintains the temperature at 41°C, causing a local increase of blood flow and blood "arterialization" after the probe has been properly positioned on the ear. The computation circuits derive $Sa\mathrm{O}_2$ using Equation (6.16). The accuracy of the

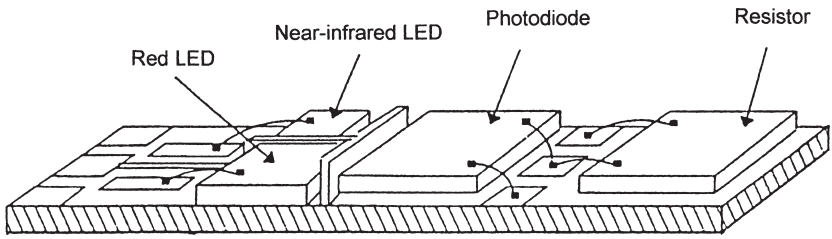

FIGURE 6.25. Catheter-tip hybrid circuit oximeter sensor. (Reproduced with permission from S. Takatani and J. Ling, "Optical Oximetry Sensors for Whole Blood and Tissue," *IEEE Engineering in Medicine and Biology,* June/July, pp. 347–357, ©1994, IEEE.)

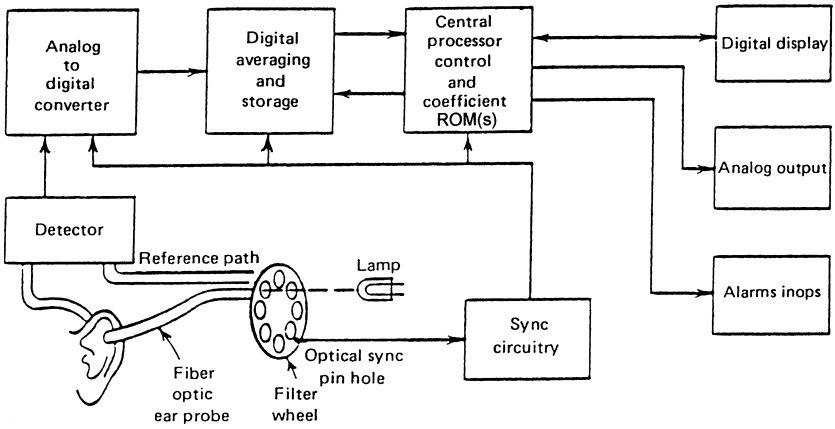

FIGURE 6.26. Simplified diagram of a typical ear oximeter. (Hewlett Packard product, reprinted after Mendelson, 1991, p. 268, courtesy of Marcel Dekker Inc., New York.)

measurement was found to be better than 2.5% saturation regardless of skin color and ear thickness. According to another computation method, the subtraction of the bloodless tissue attenuation is made that can be measured by compressing the ear using a transparent pressure capsule that is initially inflated to a pressure that exceeds the arterial blood pressure, thus, rendering the ear pinna practically bloodless. Main shortcomings of the method include discomfort for patients caused by heating and pressure on the ear and the relatively large weight of the optical cable that is a particular disadvantage in monitoring neonates and premature infants.

6.2.4 Pulse Oximetry

Pulse oximetry is a noninvasive determination of blood SaO_2 that solves the problems of ear oximetry. The basis of the technique is to measure the change in light transmitted through the skin that occurs as a result of arterial pulsation. The signal varies with pulsating changes in tissue blood volume, as shown by the plethysmographic diagram in Figure 6.27 (Mendelson, 1991). It is assumed that the change in light transmitted through tissue during the inflow phase of the cardiac cycle (i.e., systole) is caused solely by the arterial blood, there is no pulse from the surrounding tissue, and the pulse of venous blood is normally insignificant. Consequently, the pulsating component of the optical signal has to be measured. The optical signal is usually sampled at two wavelengths, one in the red (e.g., at 660 nm) and another in the infrared region (e.g., at the isobestic 805 nm or at 940 nm). A conventional linear re-

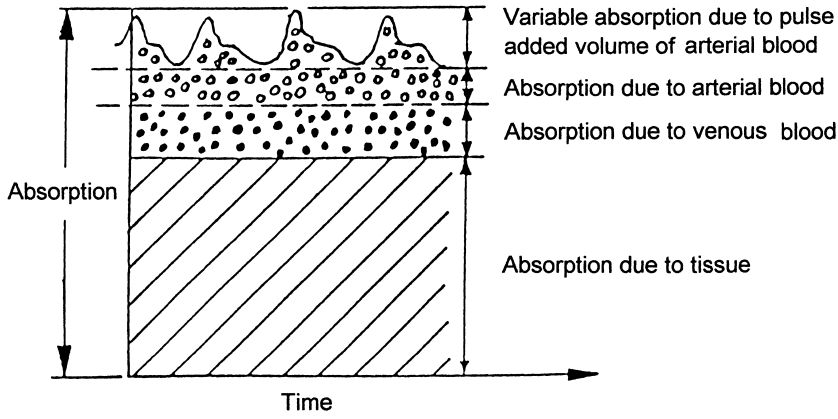

FIGURE 6.27. Variations in light attenuation by tissue illustrating the rhythmic effect of arterial pulsation. (Reprinted after Mendelson, 1991, p. 268, courtesy of Marcel Dekker Inc., New York.)

gression according to Equation (6.12) is applied to obtain arterial saturation. $Sa\mathrm{O}_2$ measured by pulse oximetry is often marked as $Sp\mathrm{O}_2$. Most pulse oximeters are of the transmission type, where forward-scattered light through the fingertip or the earlobe is analyzed. Reflection pulse oximeters have also been developed, with more general applicability to any portion of the body, such as the forehead, cheek, calf, and thigh. However, in comparison to transmission, reflection pulse oximeters have poorer signal-to-noise ratio.

Figure 6.28 shows a planar-structure reflection hybrid sensor (Mendelson, 1991). The hermetically sealed metal-glass package with a transparent cover/lid contains an interconnection system on a ceramic substrate, four LEDs, and six large-area photodiodes around them that enables the averaging of the spatial differences. The LEDs and photodiodes are optically shielded from each other. The metal package is molded into a plastic housing.

New $Sp\mathrm{O}_2$ measurement appliances employ only two LEDs and a single photodiode on ceramic substrates in a variety of sensor heads for several applications. These include the adult finger glove, pediatric finger glove, and neonatal foot strap and earlobe clip, combined with a single measurement appliance (Kästle et. al., 1997). The relationship between the ratio of the plethysmographic amplitudes measured in red and infrared regions, respectively, and $Sa\mathrm{O}_2$ is shown in Figure 6.29.

Since pulse oximeters rely on adequate arterial pulsation, a significant reduction in peripheral vascular pulsation, such as in hypotension, vasoconstriction, or hypothermia, can produce a signal too small to be processed reliably by the oximeter. Furthermore, motion artifacts can cause erroneous

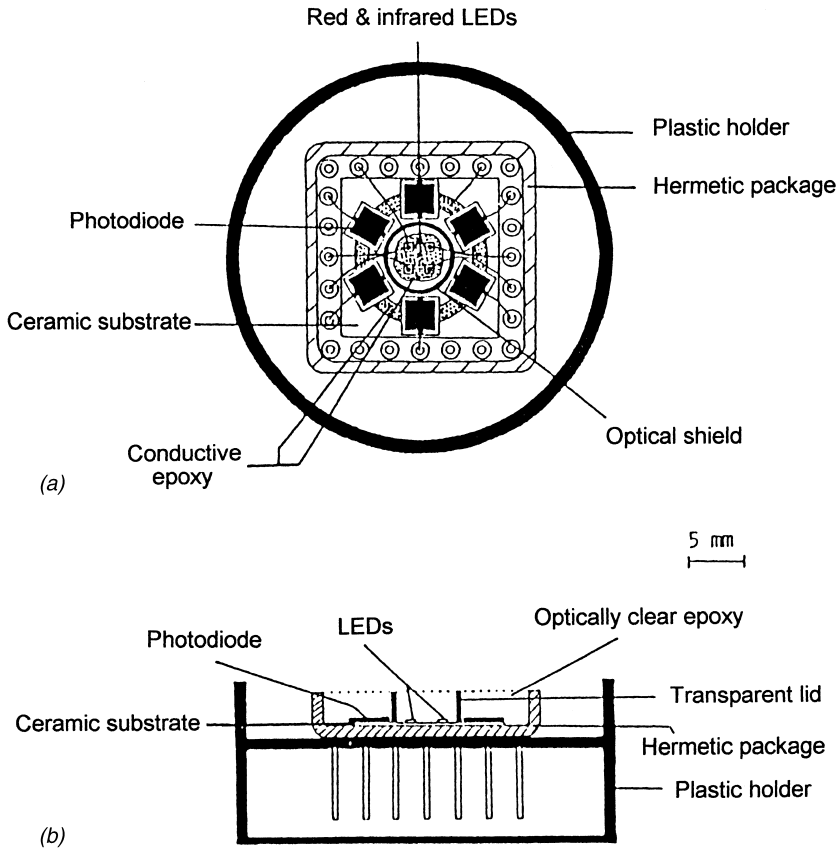

FIGURE 6.28. Noninvasive reflection oximeter sensor. (Reprinted after Mendelson, 1991, p. 271, courtesy of Marcel Dekker Inc., New York.)

readings. Practically, these artifacts are reduced by digital processing of analog signals and averaging of the measured values over several seconds before they are displayed. The interference from electrosurgical units and high-density light sources such as surgical lamps, in addition to various compounds possibly present in blood, such as intravenous dyes, can cause inaccurate readings. Even when considering the many sources of errors, the accuracy of pulse oximetry is sufficient for many clinical applications. Most manufacturers claim that their instruments are accurate to within 2% saturation in the range between 70 and 100%.

Despite the mentioned limitations, pulse oximetry is becoming the most popular and useful technique of blood oxygen measurement and monitoring. Recently, it has been recommended as a standard of care for basic intraoper-

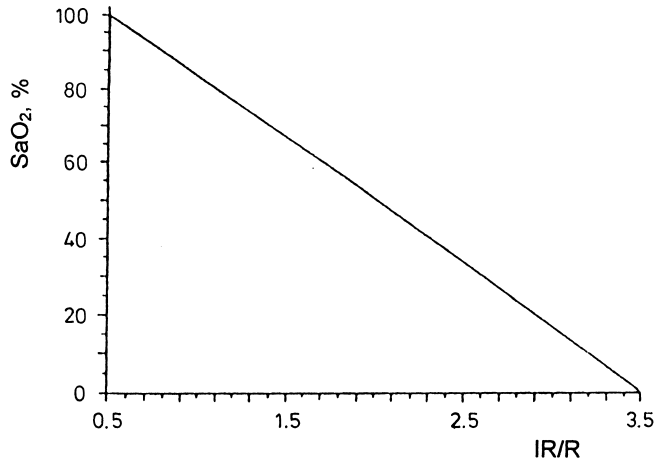

FIGURE 6.29. Relationship between the ratio of the plethysmographic amplitudes in red and infrared regions and oxygen saturation. (Reproduced with permission from D. Parker, "Sensors for Monitoring Blood Gases in Intensive Care," *J. Phys. E: Sci. Instrum.,* Vol. 20, pp. 1103–1112, ©1987, IOP Publishing Ltd., Bristol, UK.)

ative and neonatal monitoring. This is due to its major advantages in comparison with all other methods used for measuring blood oxygenation:

- It is a noninvasive technique.
- It enables the direct determination of $Sa\mathrm{O}_2$ with good accuracy.
- It is not necessary to heat up the skin.
- There is no need for complicated computing and calibration processes.
- The sensors can easily and quickly be attached, and the measurement takes only a short time.
- The sensor elements do not contain any parts that need to be refreshed (such as electrolytes and/or membranes); thus, a stable long-term operation is assured.

6.2.5 Other Oximetry Methods

Cytochrome aa_3 (cytochrome oxidase) is the terminal enzyme of the mitochrondrial respiratory chain and catalyzes approximately 90% of all O_2 utilization in the body. This enzyme is of particular importance in monitoring oxidative metabolism because it donates electrons to O_2. Therefore, the redox state of cytochrome aa_3 is believed to be an indicator of intracellular O_2 sufficiency. In the oxidized state, this enzyme exhibits a distinctive absorption band in the 820 to 870 nm region of the spectra. This band disappears upon

reduction when O_2 delivery is compromised. Since Hb and HbO_2 also absorb in this spectral region, multiple wavelengths and the application of appropriate algorithms are required to eliminate this interference (Mendelson, 1991).

Noninvasive *cerebral oxygenation monitoring* can be performed by cytochrome aa_3 oximetry using three GaAlAs laser diode light sources with peak emission wavelengths between 760 and 904 nm. The light is guided to the subject's forehead by an optical fiber, while the backscattered light from the brain is collected by another optical fiber located a few centimeters lateral from the incident entry beam. By using a third fiber close to the entry to collect backscattered light only from the bone, a differential measurement can be performed to minimize the effects on the skull, and deep-layer brain tissue information can be obtained in this way (Takatani and Ling, 1994). Time-resolved spectroscopy can also be applied to get information from deep-layer tissues. The basis of this technique is that the excitation is made with pulses with very narrow durations (picosecond order), and the backscattered pulse waveforms are analyzed. The depth of information can be estimated in this way. Multiple detectors can be placed to focus at specific depths in tissue, yielding a *three-dimensional mapping of the oxygen* field of tissue. Time-resolved spectroscopy is becoming important in neonatal cerebral monitoring.

Choroidal eye oximetry can be performed with special noninvasive tools by shining a multiple-wavelength light beam into the eye and measuring the amount of light that is backscattered from the ocular fundus using a special fundus camera. Blood oxygen saturation is computed applying the usual methods of oximetry. Since choroidal blood is characteristic of the blood supply to the brain, this is an indirect method of brain oximetry.

6.3 OTHER APPLICATIONS OF CHEMICAL SENSORS

Those sensor types and application possibilities that could not be involved in previous parts of this chapter are surveyed in this section. The following groups can be distinguished:

- monitoring ionic compounds in blood and other secretions
- determining pH and pO_2 of the inner eyelid
- pH monitoring in gastric acid
- tissue pH and pO_2 measurements and mapping
- miscellaneous gas sensor applications

6.3.1 Ionic Compounds in Blood and Other Secretions

Of great importance in blood compound monitoring are a number of ion concentrations (i.e., Na^+, K^+, Ca^{2+}, Mg^{2+}, NH_4^+, Cl^-), the monitoring of

which can be solved by means of ion-selective sensors. Ion-selective electrodes for catheter-tip applications can be built up using precious metal wires covered by plasticized PVC membranes with ion-selective neutral carriers (see Section 4.15). With a reference electrode, potentiometric measurement can be realized, similar to pH electrodes (see Section 6.1.2). A recent approach is the application of thin- and thick-film multilayer electrode systems and integrated ISFETs for multisensors and also with signal processing circuitry on the same chip or substrate.

Figure 6.30 demonstrates the structure of a rather complicated thin-film ion-selective electrode for Na^+/K^+ (Keplinger et al., 1990). Metal layers were evaporated on glass substrates and shaped by photolithography. The internal reference electrode was established by the following metal multilayer sequence: Ti/Au/Ag/AgCl. The Ag layer was chemically chloridized. The insulating layer is a PECVD-Si_3N_4 film; the salt layer was evaporated and structured by liftoff technique. It acts as an internal solid electrolyte. Finally, the

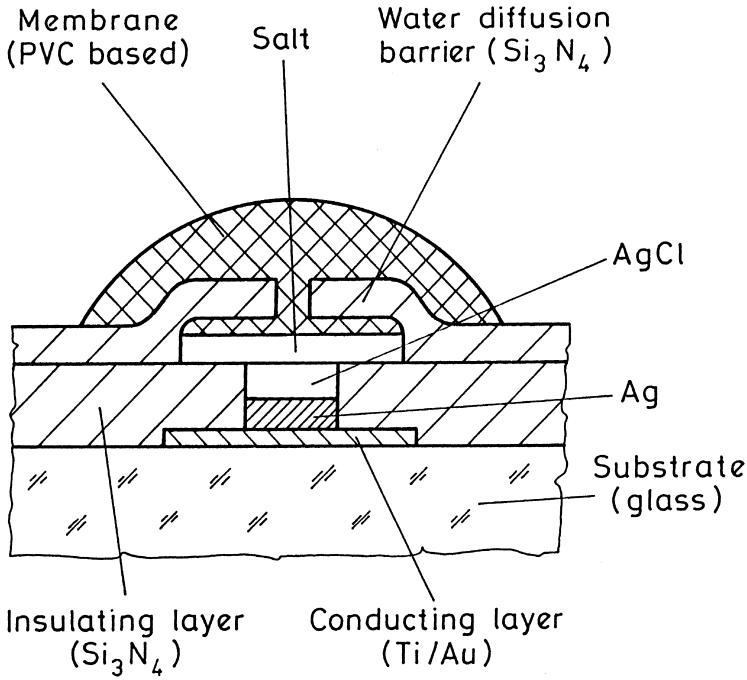

FIGURE 6.30. Cross section of the thin-film ion-selective device with a water diffusion barrier. (Reproduced with permission from F. Keplinger, R. Glatz, A. Jachimowicz, G. Urban, F. Kohl, F. Olcaytug and O. J. Prohaska, "Thin-Film Ion-Selective Sensors Based on Neutral Carrier Membranes," *Sensors and Actuators B,* 1, pp. 272–274, ©1990, Elsevier Science S.A., Lausanne, Switzerland.)

structure was coated with the ion-selective membrane. For potassium electrodes, a composition of PVC-dioctyl-sebacate with valinomycin ionophore was chosen and for the sodium electrode, a PVC-nitrophenyl-octyl-ether with Na^+-ionophore was chosen. To enhance the long-term stability, an additional silicon nitride layer with a small aperture was introduced to limit the water transport across the membrane in order to obtain a longer lifetime (at least three days). The potential change is about 100 mV when the ion concentration is changed from 1 mM/l to 0.1 M/l.

Figure 6.31 shows an integrated micro-multi-ion sensor using platinum gate ISFETs with several polymeric membranes (Tsukada et al., 1991). It consists of two kinds of ion sensors (K^+- and Na^+-ISFETs) and two CMOS unity gain buffers, as shown in the circuit diagram of Figure 6.31(a). The ISFETs are buffered by high-impedance amplifiers. The configuration gives a linear dependence between the ion-selective membrane potential and the output voltage. The schematic structure of the cross section is shown in Figure 6.31(b). In the chemically active area, the ion-selective membranes were formed on Pt/Ti/Al multilayer electrodes that are connected to NMOS gates. The platinum film was used as a protective layer against ion migration and hydration, and Ti was used as an adhesion layer. They were patterned with a liftoff process. The SiO_2 and phospho-silicate-glass were used as passivation films. Finally, a polyimide layer was deposited and patterned photolithographically to form a well. The ion-selective membranes consisted of PVC, ionophore, plasticizer, and additives. Almost ideal Nernstian sensitivities [49mV/decade at 25°C, see Equation (3.4)] have been detected with good selectivity factors ($\lg S_{ij} < -2$).

Ion-selective sensors may have applications not only in monitoring blood compounds, but also in analyzing other secretions. For example, an integrated probe for sweat analysis is mentioned here (Bezegh et al., 1987, 1988). Sweat, as a body fluid, can yield useful clinical information. One of the few viable sweat tests is the determination of chloride for diagnosis of cystic fibrosis. Although the concentration in sweat may vary within a wide range according to many circumstances, the local concentration measured *in situ* may have useful information. A solid-state integrated differential probe based on Na^+/Cl^- ISFETs was used to determine the concentration of sodium chloride in sweat. The two silicon chips were attached to a flexible printed wiring substrate. Then, a blank membrane containing only the PVC polymer and plasticizer was applied as a continuous coating to the device surface. The electrochemical selectivity was introduced by doping this membrane with electroactive ingredients (ionophores). In practice, this was performed by dropping ionophores selectively onto the surface of the membrane. The device was attached to the surface of the skin, like the transcutaneous probes (see Section 6.1.3). The difference between the two transistor currents was measured as a function of the

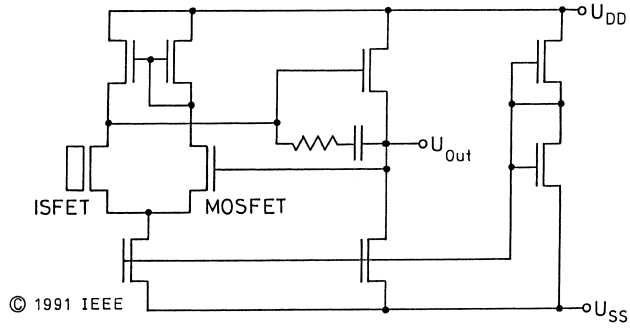

(a)

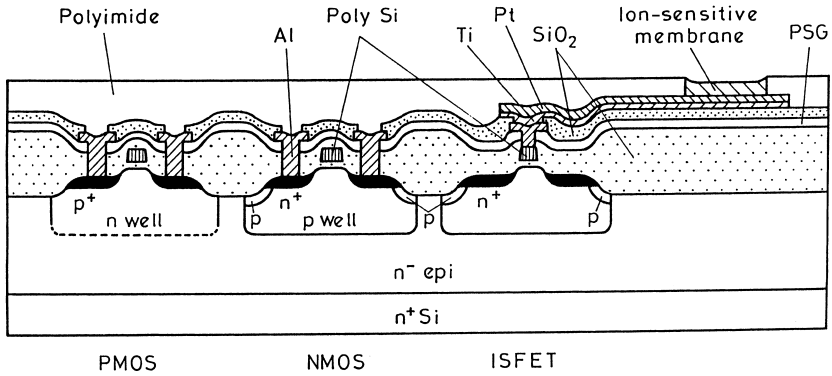

(b)

FIGURE 6.31. Circuit diagram (a) and cross-sectional structure (b) of the integrated ISFET. (Reproduced with permission from K. Tsukada, Y. Miyahara, Y. Shibata and H. Miyagi, "An Integrated Micro Multi-Ion Sensor Using Platinum-Gate Field-Effect Transistors," *Proc. Conf. Solid State Sensors and Actuators, Transducers '91,* San Francisco, CA, pp. 218–221, (c)1991, IEEE.)

NaCl concentration. The total amount of liquid required for the measurement is 0.3 μl, which is small, compared to the 80 μl needed for conventional chloride titration. Pictures of the sensor are shown in Appendix 4.

6.3.2 Chemical Parameters of the Inner Eyelid

The eyelid sensor takes advantage of the unique function of the capillary bed in the palpebral conjunctiva, which is perfused by the internal carotid artery that supplies O_2 to the avascular cornea during sleep. The conjunctival

oxygen sensor is essentially a miniaturized unheated version of a Clark-type pO_2 electrode mounted in an oval ophthalmic conformer ring as shown in Figure 6.32 (Mendelson, 1991). The conformer ring, which is made of a plastic biocompatible material [PMMA, poly(methyl methacrylate)], is contoured to the shape of the sclera so that normal vision is not obstructed, and free eye movement can be maintained. The inner eyelid is also a potential site for monitoring blood pH and SaO_2. Fiber-optic pH sensors and pH-ISFETs with a miniature reference electrode have demonstrated the possibility of pH monitoring, while oxygen saturation can be measured by a miniature reflectance oximeter sensor. The primary limited applications of these sensor types to date have been in emergency and critical care medicine.

6.3.3 Monitoring pH in Gastric Acid

The ambulatory *monitoring of pH in the upper gastrointestinal tract* is increasingly used for diagnostic and research purposes. That field represents a further application of inorganic component sensing beyond blood monitoring. Gastric acid measurements are currently performed with integrated glass and antimony electrodes. A severe drawback of these electrodes may be encountered if several sensors must be installed in the gastroesophageal tract.

A new construction using ISFETs is shown in Figure 6.33 that permits the realization of multiple mounting on a single catheter (Thybaud et al., 1990). It consists of several types of polymers; however, the ISFET itself is not

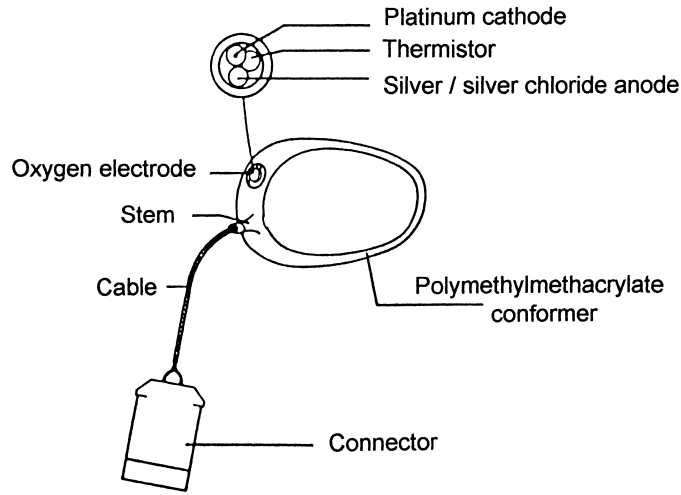

FIGURE 6.32. Diagram of the eyelid sensor. (Reprinted after Mendelson, 1991, p. 274, courtesy of Marcel Dekker Inc., New York.)

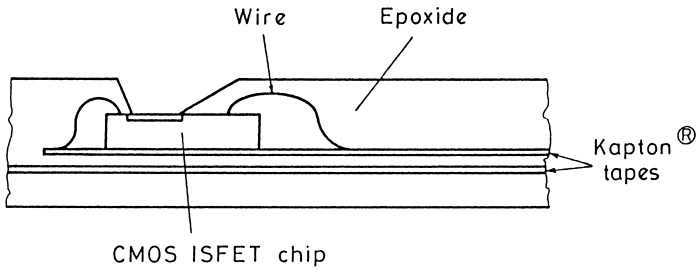

FIGURE 6.33. Structure of the gastric pH catheter. (Reproduced with permission from L. Thybaud, C. Depeursinge and D. Rouiller, "Use of ISFETs for 24 h pH Monitoring in the Gastroesophageal Tract," *Sensors and Actuators B,* 1, pp. 485–482, ©1990, Elsevier Science S.A., Lausanne, Switzerland.)

polymer-based. The gastric probe is composed of a supple PVC catheter in which the ISFETs are mounted on a floppy substrate of Kapton®. The passivating film is an epoxy. The reference electrode is also installed at the catheter tip. The very small dimensions of the ISFET chips allow several ion-sensitive sensors to be mounted on a single catheter. Such multi-ISFET probes are expected to be very useful in the study of gastroesophageal reflux that affects numerous people. The whole measuring system enables the 24 h ambulatory monitoring of pH and other ion concentrations in the gastrointestinal tract.

Another obvious approach to prepare gastric catheters is to use optrode probes. The major inconveniences of optical pH sensors are their narrow pH range (maximum pH 3) and their decreasing precision when the difference between the measured pH and the pK of immobilized dye is increased (see Figure 4.12). The pH determination in blood is facilitated because the range is narrow (pH 7.0–7.5, see Section 6.1). Medical applications concerning gastric diagnostics need measurements in a large pH range from 0.9 to 7.7. Two possibilities are able to mitigate these disadvantages—either use a dye having several pK values as demonstrated with thymol blue for acid and basic media, or apply a more general solution such as the co-immobilization of several dyes. Figure 6.34 (Boisde et al., 1991) shows typical characteristics of a four-indicator-based pH optrode. The dye shows a different behavior in solution and is grafted into a PVI [poly(*N*-vinylimide-azole)] bed. Although the curve consists of two almost linear zones with different sensitivities, it enables pH determination in the range of 0–12.

6.3.4 Measuring and Mapping Tissue pH/pO_2

The direct measurement of tissue pH and pO_2 with minimal damage to the cells or to the microcirculation in the tissue represents a serious challenge for

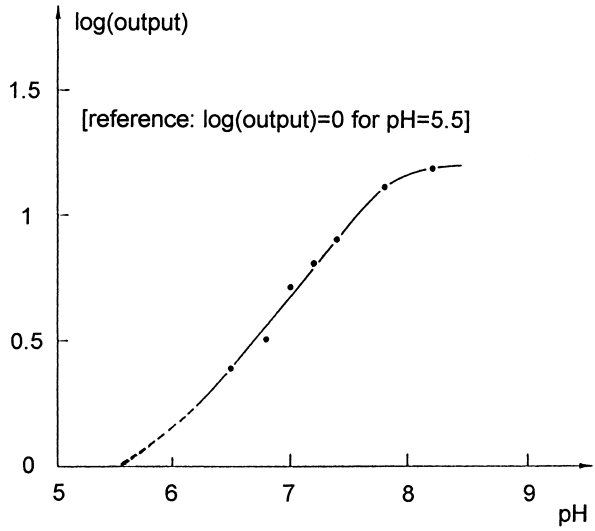

FIGURE 6.34. Characteristics of a four-dye optrode system. (Reproduced with permission from G. Boisde, F. Blanc and X. Machuron-Mandard, "pH Measurements with Dyes Co-immobilization on Optrodes: Principles and Associated Instrumentation," *Int. Journal of Optoel.,* Vol. 6, No. 5, pp. 407–423, ©1991, Taylor & Francis, London, UK.)

sensors. These micromeasurements are still mostly a part of laboratory research and do not belong to everyday clinical practice. They can be applied in monitoring the brain, heart, and muscle metabolism and ischemia.

For practical measurements, microelectrodes are used with tip sizes in the range of living cell dimensions. These sizes are much smaller than required by conventional vessel catheters. Generally, compound glass-metal electrodes are fabricated using various techniques of glass processing and metallurgy, such as glass pulling, mechanical and chemical polishing, grinding, chemical- and electrochemical-etch beveling, etc. Without providing a detailed discussion about preparation methods, the structure of various pH and pO_2 microelectrodes are shown in Figures 6.35 and 6.36 (Buerk, 1993). The first-generation microelectrodes employed open-tip glass or metal electrodes with the smallest possible tip sizes (typically in the range of 10 μm for glass and less than 1 μm for metal types) and a separate reference electrode [see Figures 6.35(a) and 6.36(a)]. Impurities could shift the characteristics of these types of electrodes after a few periods of use and after the refreshing etch processes altered the tip geometry. Recessed-tip electrodes [see Figures 6.35(b) and 6.36(b)] offered a significant improvement. First, an open-tip microelectrode was prepared and then inserted into an insulating glass micropipette. One drawback of this design was a longer time response due to the increased

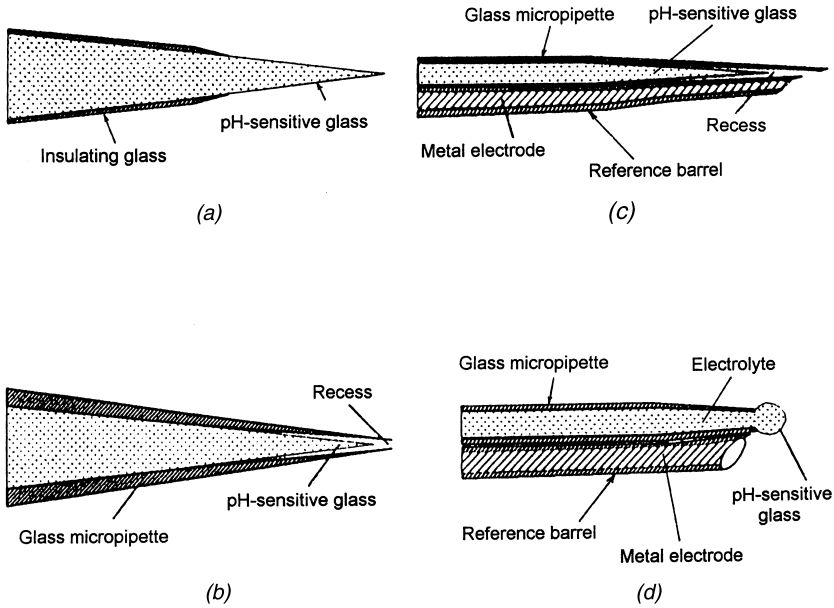

FIGURE 6.35. Typical structure of tissue-pH microelectrodes: (a) open tip, (b) recessed tip, and (c)–(d) double-barrel types. (Used with permission from D. G. Buerk, *Biosensors, Theory and Applications,* p. 98 ©1993, Technomic Publishing Co., Inc., Lancaster, PA.)

diffusion distance from the tip to the transducer surface. The common shortcoming of all of these types was that the measured electromotive force was interfered with by the cell membrane potential if an intracellular measurement was made with the reference electrode external to the cell. The double-barrel design [shown in Figures 6.35(c, d) and 6.36(c, d)] combines the recessed type with a second barrel that is used as a reference electrode. Generally, it contains an Ag/AgCl electrode, and the barrel is filled with physiological saline. The two micropipette tips are fused together by local heating and pressure. Practical tip measurements are in the range of 10–35 μm. The newest electrochemical microelectrode types are based on silicon micromachining, and their structure is very similar to that of the electrical biopotential pickup electrodes (see Figure 5.32).

Extremely fine probes have already been developed that can be used to map out detailed surface features. In scanning electrochemical microscopy, a three-dimensional representation of a region is made by systematically sweeping the probe across the sample. The fine tip of an electrochemical transducer is moved in small increments by a computer-controlled translation element. Figure 6.37 shows an example of the electrochemical scanning technique applied to pO_2 measurements over a pair of blood vessels in the retina of a cat eye

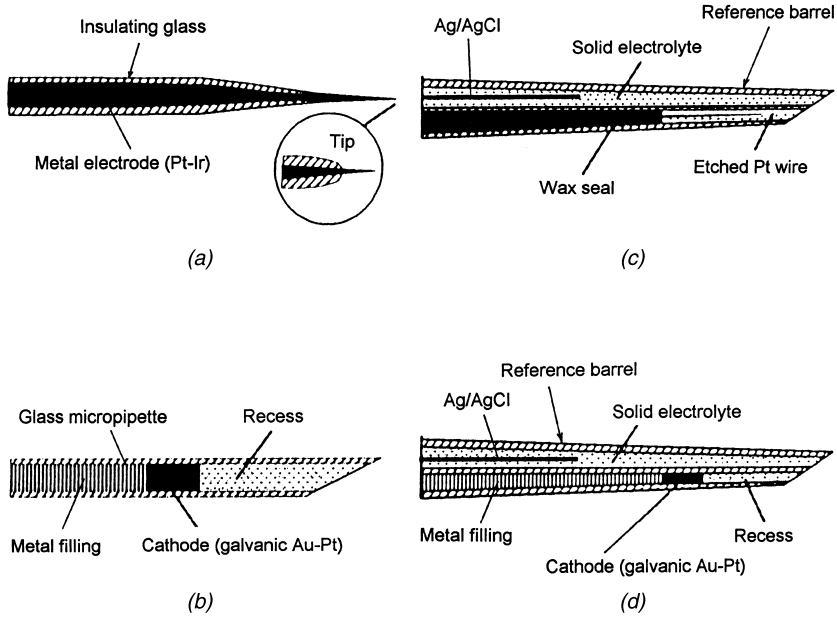

FIGURE 6.36. Typical structure of tissue-pO_2 microelectrodes: (a) open tip, (b) recessed tip, and (c)–(d) double-barrel types. (Used with permission from D. G. Buerk *Biosensors, Theory and Applications,* p. 102 ©1993, Technomic Publishing Co., Inc., Lancaster, PA.)

(Buerk, 1993). It is well demonstrated that the artery is leaking oxygen into the vitreous humor, while the vein is picking up oxygen. The distribution corresponds to their positions. The resolution depends on the diameter of the scanning tip and the distance from the tip to the sample. (Of course, there are practical limitations on how close the probe can be placed to the surface, particularly if it is irregular or is moving.)

Electrochemical mapping can be simplified by means of electrode arrays. One example for oxygen mapping is shown in Figure 6.38 (from Buerk, 1993, originally designed by Morita and Shimizu, 1989). It is actually a bundle of carbon fibers embedded into an epoxy bed, forming a recessed microhole array. The carbon fibers were electroplated with platinum.

Silicon microfabrication with electron-beam lithography and/or reactive ion etching (RIE) is a promising approach to preparing microelectrode arrays. Figure 6.39 shows a band of ultramicroelectrodes, the microstep electrodes on a $Si\text{-}SiO_2$ substrate (Samuelsson et al, 1991). A thin film of adhesion promoter Cr and a subsequent film of Au or Pt were deposited by RF sputtering for the electrode (see Section 2.3). The insulating Si_3N_4 was deposited by plasma CVD (see Section 2.1) and patterned, subsequently, by photolithography and

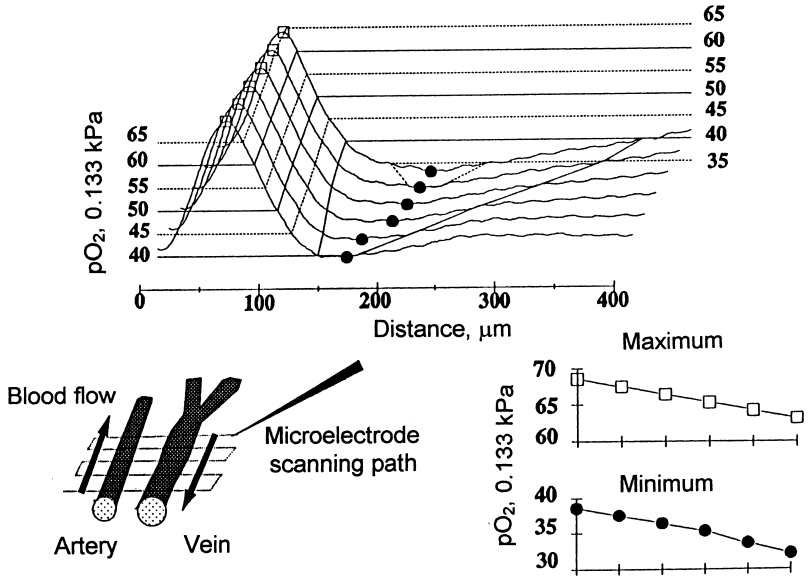

FIGURE 6.37. Example of electrochemical scanning microscopy applied to O_2 measurements over a pair of blood vessels in the retina of a cat eye. (Used with permission from D. G. Buerk, *Biosensors, Theory and Applications,* p. 197, ©1993, Technomic Publishing Co., Inc., Lancaster, PA.)

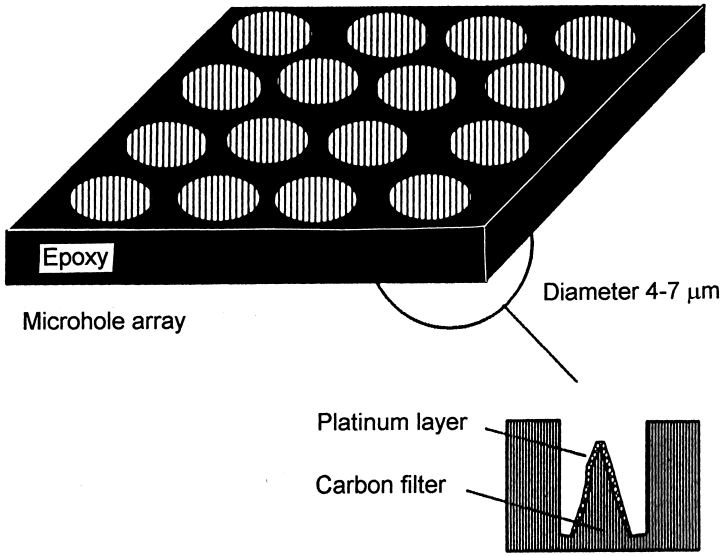

FIGURE 6.38. Microhole array with recessed Pt/carbon fiber cathodes for O_2 measurement. (Used with permission from D. G. Buerk, *Biosensors, Theory and Applications,* p. 115, ©1993, Technomic Publishing Co., Inc., Lancaster, PA.)

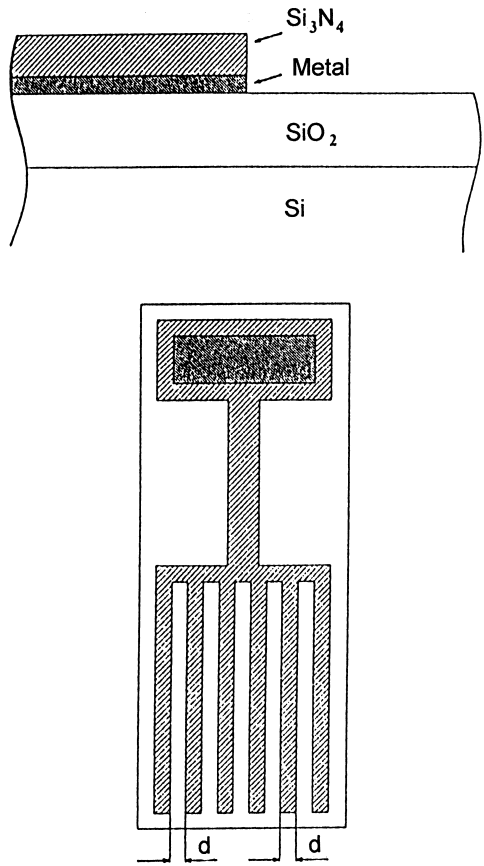

FIGURE 6.39. Cross section (a) and top view (b) of the microstep electrode produced on silicon substrate. (Reprinted with permission from M. Samuelsson, M. Armgarth and C. Nylander, "Microstep Electrodes: Band Ultramicroelectrodes Fabricated by Photolithography and Reactive Ion Etching," *Anal. Chem.,* Vol. 63, pp. 931–936, ©1993, American Chemical Society.)

RIE. The important feature of RIE patterns is that they have extremely sharp and vertical steps.

6.3.5 Miscellaneous Gas Sensor Applications

Gas-compound monitoring and analysis also has important biomedical applications, even in cases when the sensor elements are in the atmosphere without any contact with the human body.

Direct control of incubator *atmosphere* is generally performed by means of

atmospheric oxygen sensors rather than by blood oxygen sensors that serve monitoring purposes. Other life-supporting equipment often apply oxygen sensors for monitoring and/or controlling inspired O_2 concentration, FiO_2. Oxygen sensors in these applications are, for example, amperometric electrochemical sensors, the structure and operation of which is very similar to the Clark oxygen sensors with the exception that, instead of a semipermeable membrane, a small capillary or a porous film acts as the diffusion controlling object. Inorganic solid-state sensors employ heated zirconia ceramic-based dielectric films showing ionic conductivity at elevated temperatures (Asada and Yamamoto, 1990). Polymer electrolyte-based types can be operated even at room temperatures (Harsányi, 1995b; Yan and Lu, 1989). Another approach is to apply fuel cells that are practically O_2/H_2 batteries (Teledyne, 1994).

Exhalation gas compound analysis is another potential application field of gas sensors. A number of solid-state gas sensors have already been built into various alcohol tester appliances. Hydrogen testers applied in indigestion analysis may employ hydrogen sensors, such as Pd-gate MOSFETs or heated Pd-doped SnO_2 thin- or thick-film semiconductor resistors. Their operation is based on well-known hydrogen solubility and the related work function shift of Pd, that can modulate the conductivity of a MOSFET and of thin-film or porous thick-film semiconductor resistors. A more detailed discussion of these atmospheric gas sensors is beyond the scope of this book, and we refer to the literature (Mandelis and Christofides, 1993).

6.4 REFERENCES

Alcock, S. J. and Turner, A. P. F., "Continuous Analyte Monitoring to Aid Clinical Practice," *IEEE Engineering in Medicine and Biology,* June/July (1994), pp. 319–326.

Asada, A. and Yamamoto, H., "Limiting Current Type of Oxygen Sensor with High Performance," *Sensors and Actuators B,* Vol. 1 (1990), pp. 312–318.

Baumberger, I. P. And Goodfriend, R. B., "Determination of Arterial Oxygen Tension in Man by Equilibration Through Intact Skin," *Fed. Proc. Fed. Am. Socs. Exp. Biol.,* Vol. 10 (1951), pp. 10–11.

Bezegh, K., Bezegh, A., Black, P. G. and Janata, J., "Integrated Probe for Sweat Analysis," *J. of Clinical Laboratory Analysis,* Vol. 2 (1988), pp.16–18.

Bezegh, K., Bezegh, A., Janata, J., Oesch, V., Xu, A. and Simon, W., "Multisensing Ion-Selective Field-Effect Transistors Prepared by Ionophore Doping Technique," *Anal. Chem,* Vol. 59 (1987), pp. 2846–2848.

Boisde, G., Blanc, F. and Machuron-Mandard, X., "pH Measurements with Dyes Co-Immobilization on Optrodes: Principles and Associated Instrumentation," *Int. Journal of Optoel.,* Vol. 6, No. 5 (1991), pp. 407–423.

Buerk, D. G., *Biosensors, Theory and Applications,* Technomic Publishing Co., Inc., Lancaster, PA (1993).

Cha, C. S., Shao, M. J. and Liu, Ch.-Ch., "Problem Associated with the Miniaturization of a

Voltammetric Oxygen Sensor: Chemical Crosstalk among Electrodes," *Sensors and Actuators B,* Vol. 2 (1990), pp. 239–242.

Clark, L. C., "Monitoring and Control Blood and Tissue Oxygen," *Trans. Am. Soc. Artif. Intern. Organs,* Vol. 2 (1958), pp. 41–48.

Colvin, A. E. Jr., Phillips, T. E., Miragliotta, J. A., Givens, R. B. and Bargeron, C. B., "A Novel Solid-State Oxygen Sensor," *John Hopkins APL Technical Digest,* Vol. 17, No. 4 (1996), pp. 377–385.

Diamond, D., *Principles of Chemical and Biological Sensors,* John Wiley & Sons, New York (1998).

Fraser, D. M., *Biosensors in the Body: Continuous in vivo Monitoring,* John Wiley & Sons, New York (1997).

Göpel, W., Jones, T. A., Kleitz, M., Lundström, I. and Seiyama, T., *Sensors: A Comprehensive Survey, Vol. 2-3, Pt. H, Chemical and Biochemical Sensors,* John Wiley & Sons, New York (1991).

Gumbrecht, W., Schelter, W., Montag, B., Bos, J. A. H., Eijking, E. P. and Lachmann, B., "Monitoring of Blood pO_2 with a Thin-Film Amperometric Sensor," *Proc. of 1991 Int. Conf. on Solid State Sensors and Actuators (Transducers 91),* San Francisco, CA (1991), pp. 85–87.

Harsányi, G., "Electrochemical Processes Resulting in Migrated Short Failures in Microcircuits," *IEEE Transactions on Components, Packaging, and Manufacturing Technology—Part A,* Vol. 18, No. 3 (1995a), pp. 602–610.

Harsányi, G, *Polymer Films in Sensor Applications,* Technomic Publishing Co., Inc., Lancaster, PA (1995b).

Harsányi, G., Péteri, I. and Deák, I., "Low Cost Ceramic Sensors for Biomedical Use: A Revolution in Transcutaneous Blood Oxygen Monitoring?" *Sensors and Actuators B,* Vol. 18–19 (1994), pp.171–174.

Huch, A., Huch, R. and Lübbers, D. W., "Quantitative Continuous Measurement of Partial Pressure (PO_2 Measurement) on the Skin of Adults and Newborn Babies," *Pflügers Arch. Ges. Physiol.,* Vol. 337 (1972), pp. 185–198.

Jinghong, H., Dafu, C., Yating, L., Jine, C., Zheng, D., Hong, Z. and Chenglin, S., "A New Type of Transcutaneous pCO_2 Sensor," *Sensors and Actuators B,* Vol. 24–25 (1995), pp. 156–158.

Kästle, S., Noller, F., Falk, S., Bukta, A., Mayer E. and Miller, D., "A New Family of Sensors for Pulse Oximetry," *Hewlett-Packard Journal,* February (1997), pp. 39–53.

Keplinger, F., Glatz, R., Jachimowicz, A., Urban, G., Kohl, F., Olcaytug, F. and Prohaska, O. J., "Thin-Film Ion-Selective Sensors Based on Neutral Carrier Membranes," *Sensors and Actuators B,* Vol. 1 (1990), pp. 272–274.

Keplinger, F., Urban, G., Jobst, G., Kohl, F. and Jachimowicz, A., "Solid Contact Neutral Carrier pH-ISE with Conducting Polymers," *Eurosensors VII. Conf.,* Budapest, Hungary (abstracts) (1993) p. 24.

Leiner, M. J. P. and Hartmann, P., "Theory and Practice in Optical pH Sensing," *Sensors and Actuators B,* Vol. 11 (1993), pp. 281–289.

Mandelis, A. and Christofides C., *Solid State Gas Sensor Devices,* John Wiley & Sons, New York (1993).

Mendelson, Y., "Invasive and Noninvasive Blood Gas Monitoring," in *Bioinstrumentation and Biosensors* (ed. Wise, D. L.), Marcel Dekker, New York (1991), pp. 249–279.

Morita, K. and Shimizu, Y., "Microhole Array for Oxygen Electrode," *Anal. Chem,* Vol. 61 (1989) pp. 159–162.

Papkovsky, D. P., "Luminescent Porphyrins as Probes for Optical (Bio)sensors," *Sensors and Actuators B,* Vol. 11 (1993), pp. 293–300.

Parker, D., "Sensors for Monitoring Blood Gases in Intensive Care," *J. Phys. E: Sci. Instrum.,* Vol. 20, No. 9 (1987), pp. 1103–1112.

Peterson, J. I., Goldstein, S. R., Fitzgerald, R. V. and Buckhold, D. K., "Fiber Optic pH Probe for Physiological Use," *Anal. Chem.,* Vol. 52 (1980), pp. 864–869.

Rolfe, P., "Intra-Vascular Oxygen Sensors for Neonatal Monitoring," *IEEE Engineering in Medicine and Biology,* June/July (1994), pp. 336–346.

Samuelsson, M., Armgarth, M. and Nylander, C., "Microstep Electrodes: Band Ultramicroelectrodes Fabricated by Photolithography and Reactive Ion Etching," *Anal. Chem.,* Vol. 63 (1991), pp. 931–936.

Schelter, W., Gumbrecht, W., Montag, B., Sykora, V. and Erhardt, W., "Combination of Amperometric and Potentiometric Sensor Principles for On-Line Blood Monitoring," *Sensors and Actuators B,* Vol. 6 (1992), pp. 91–92.

Severinghaus, I. W. and Bradely, A. F., "Electrodes for Blood PO_2 and PCO_2 Determination," *J. Applied Physiol.,* Vol. 13 (1958), pp. 515–520.

Soller, B. R., "Design of Intravascular Fiber Optic Blood Gas Sensors," *IEEE Engineering in Medicine and Biology,* June/July (1994), pp. 327–335.

Spichiger-Keller, U. E., *Chemical Sensors and Biosensors for Medical and Biological Applications,* John Wiley & Sons, New York (1998).

Suzuki, H., Sugama, A. and Kokima, N., "Micromachined Clark Oxygen Electrode," *Sensors and Actuators B,* Vol. 10 (1993), pp. 91–98.

Takatani, S. and Ling, J., "Optical Oximetry Sensors for Whole Blood and Tissue," *IEEE Engineering in Medicine and Biology,* June/July (1994), pp. 347–357.

Teledyne Brown Engineering/Sensor Technologies, "Oxygen Monitors and Sensors for the Health Care Industry," Product Catalogue (1994).

Thybaud, L., Depeursinge, C., Rouiller, D., Mondin, G. and Grisel, A., "Use of ISFETs for 24h pH Monitoring in the Gastrooesophageal Tract," *Sensors and Actuators B,* Vol. 1 (1990), pp. 482–485.

Tsukada, K., Miyahara, Y., Shibata, Y. and Miyagi, H., "An Integrated Micro Multi-Ion Sensor Using Platinum-Gate Field-Effect Transistors," *Proc. Conf. Solid State Sensors and Actuators, Transducers '91,* San Francisco, CA (1991), pp. 218–221.

Tsukada, K., Miyahara, Y., Shibata, Y. and Miyagi, H., "An Integrated Chemical Sensor with Multiple Ion and Gas Sensors," *Sensors and Actuators B,* Vol. 2 (1990), pp. 291–295.

Varlan, A. R. and Sansen, W., "Micromachined Conductometric p(CO_2) Sensor," *Sensors and Actuators B,* Vol. 44 (1997), pp. 309–315.

Wolfbeis, O. S., "Biomedical Application of Fiber Optic Chemical Sensors," *Int. Journal of Optoel.,* Vol. 6, No. 5 (1991), pp. 425–441.

Wolfbeis, O. S., Fürlinger, E., Kroneis, H. and Marsoner, A., "A Study on Fluorescent Indicators for Measuring Near Neutral ('Physiological') pH Values," *Fresenius Z. Anal. Chem.,* Vol. 314 (1983), pp. 119–124.

Yan, H. Q. and Lu, J. T., "Solid Polymer Electrolyte-Based Electrochemical Oxygen Sensor," *Sensors and Actuators,* Vol. 19 (1989), pp. 33–40.

CHAPTER 7

Biosensors

Currently, biosensors are in the focus of research efforts in sensorics and analytical chemistry. Several hundreds of papers are published annually on this topic. New results are published almost weekly in leading journals. A journal (*Biosensors and Bioelectronics*) and a series of annual conferences were established that specifically addressed this topic.

The definition of biosensors was not uniform in the literature a few years ago, but it became general recently: *biosensor* is a sensor using a living component or a product of a living thing for measurement or indication. Thus, they are characterized by the nature of interaction that is the basis of the sensing effect, i.e., the very specific chemical reactions that are typical in biological systems.

The general structure of biosensors is schematically shown in Figure 7.1; they consist of two main parts, the *receptor* and the *transducer* (this does not mean that they are physically separated). The receptor interacts with the analyte selectively, while the transducer produces an electrical or optical signal as a result of the former interaction. This signal carries information about the concentration of the analyte.

Receptor parts contain the biologically active components that are capable for specific chemical reactions with the analyte. Nature has created an almost endless variety of biological compounds that may act as receptors. According to the type of receptor, biosensors can be distinguished into the following groups:

- *Enzymatic (or metabolism) biosensors* employ immobilized enzymes as receptors. Enzymes are catalysts, substances that enable biochemical processes to proceed. They are specific to their substrate which can be the analyte of interest. The enzymatic reaction makes it possible for a signal to be produced by the transducer.

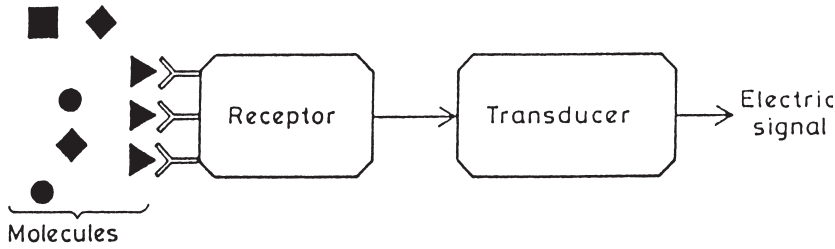

FIGURE 7.1. The general block diagram of biosensors. (Reproduced with permission from *Polymer Films in Sensor Applications* by G. Harsányi, ©1995, Technomic Publishing Co., Inc., Lancaster, PA, p. 382.)

- *Affinity biosensors* are based on specific chemical binding. In *immunosensors,* this means the antigen-antibody reaction. They employ the phenomenon that the immunosystem of living things produces specific antigens against foreign objects (bacteria, viruses, molecules, etc.) that are able to form stable complexes for biological recognition. In DNA sensors (also called DNA chips), the selective chemical binding is the hybridization of molecule clusters with DNA molecules to form a double structure.
- *Living biosensors* employ microorganisms or living tissues as receptors for selective sensing.

The first biosensors that dominated research in this field were enzymatic. Nowadays, this domination has been partly balanced by the other two types. The many enzymes present in living bodies and the phenomenon that the immune systems of living things may synthesize a great variety of antibodies specifically against a number of antigens, assure a practically endless variety of possible receptor molecules that are available in nature. Thus, the most important problems with biosensors are not the availability of the receptors, but are instead, their immobilization technique, their stability during operation, and the process of choosing appropriate transducer elements.

Biosensors employ the following *transducer types:*

- calorimetric
- electrochemical, including potentiometric, amperometric, and conductimetric electrochemical cells, as well as modified ISFETs
- fiber-optic transducers (almost all structures and sensing effects can be imagined)
- gravimetric resonator transducers

Different receptor types have different chemical behaviors that determine the approaches used in sensor applications:

- Enzymatic sensors are based on the catalytic chemical reaction of the enzyme and substrate. The reaction products, the charge exchange, or the heat generation may be the bases for the indirect transduction. The substrate material is continuously consumed by the enzymatic reaction during the operation of the sensor.
- Affinity sensors are based on the specific receptor-analyte chemical binding. This may be used for transduction in direct-operation sensors (for example, by measuring the resulted mass change, refractive index change, etc.). In indirect sensing, chemical labeling (by means of enzyme molecules, indicators, etc.) is applied for the analyte, as a usual practice in immunoassays, and the detection of these labels is the basis of transduction. Since immunoreactions are not always reversible, only a single immunoassay is possible with these sensors. The renewal of the receptor surface has to be performed periodically; thus, a continuous operation is not possible. In the case of labeled immunoassays, only *in vitro* applications can be realized practically.
- Living biosensors contain living cells and/or tissues, the supply of which must be continuously delivered, and their products should be removed. These products, or the reactions themselves, are used for transduction. By applying neurons that give a direct electrical output, not only the receptor, but also the transducer consist of living cells.

The origin of analytes is not always a living body. Accordingly, their application is not limited to the biomedical field. The most important application perspectives can be distinguished as follows (White and Turner, 1997):

- clinical bedside and personal medical monitoring instruments for measuring the concentration of biologically active, physiologically important compounds, such as glucose, urea, cholesterol levels in blood, etc.
- biotechnological and pharmaceutical industries for research and testing and analytical purposes
- food and beverage industries and gastronomy for the objective testing of row-material quality and product flavor
- environmental contaminant monitoring of air, water, and soil
- immunoreaction tests with immunosensors
- fast genetic analysis using DNA chips

It is obvious that medical applications of biosensors are not exclusive. Although this book concentrates on biomedical applications, the other fields cannot be neglected.

Biosensors have appeared not only in laboratory research but also in commercially available appliances as well. Practically all of these instruments were developed for the determination of glucose in blood. Only a very small por-

tion of the medical biosensor market is for the determination of other compounds, such as urea, lactate, cholesterol, etc. In spite of great research efforts, no breakthrough for their wide-range application has yet been reached—with the exceptions of glucose and DNA sensors (Turner, 1996; Weetall, 1999). Commercialization of most biosensor technologies has continued to lag behind research by several years. The most important problems to be solved can be summarized as follows:

- to choose appropriate receptors and transducers for various analytes
- to develop technologies for immobilizing the receptors on transducer surfaces
- to assure the appropriate stability of the receptors within a requested operation period (which may even be as short as one day or one hour)
- to prevent the receptors from poisoning during the operation
- to compensate interferences and disturbing effects
- to develop such fabrication, storage, preoperative treatment, calibration, and data-processing techniques that enable the wide-range mass application of low-cost, short-lifetime, disposable sensor families

7.1 ENZYMATIC BIOSENSORS

Biosensors that were developed first belong to the group of enzymatic sensors. A great number of different types have been developed since their appearance. The greatest efforts have been made in the field of glucose sensors, where devices with a possible operation period of several months could be fabricated. Meanwhile, a great development has been achieved in enzyme immobilization techniques. Without giving a detailed theoretical description of biocatalytic processes, the most important definitions and reaction models are summarized in the next section. In subsequent sections, the possible measuring methods, transducer types, enzyme immobilization techniques, and sensor types and properties are described.

7.1.1 Theoretical Bases

Enzymes are high-molecular-weight proteins synthesized inside living cells. They influence the reaction speed of chemical processes. With hormones and vitamins, they form the biocatalytic system of living things. The reagent, the chemical transition of which the enzyme catalyzes specifically, is called its substrate. Enzymatic analysis is a special branch of analytical chemistry, the goal of which is to detect enzymes or substrates by means of their specific reaction. Enzymatic sensors employ enzymes to measure the concentration of their substrate in the analyte of interest.

Enzymes can easily be decomposed by various environmental effects that can limit the lifetime of enzymatic sensors to a few days or hours. By using appropriate immobilization techniques on sensor surfaces, this behavior may be favorably modified.

The simplest scheme for describing a biochemical reaction catalyzed by a single enzyme E is the irreversible conversion of a substrate S to a product P:

$$\mathrm{E} + \mathrm{S} \xleftrightarrow{k_1,k_{-1}} \mathrm{ES} \xrightarrow{k_2} \mathrm{E} + \mathrm{P} \tag{7.1}$$

through the reversible formation of an intermediate enzyme-substrate complex ES. The reactions are characterized by the equilibrium constants shown in Equation (7.1). The kinetics of the reaction can be described by the Michaelis-Menten model. According to this model, the relationship between reaction rate (v) and substrate concentration (c_s) can be described by the following equation:

$$v = -\frac{dc_s}{dt} = \frac{dc_p}{dt} = \frac{v_{\max} c_s}{k_m + c_s} \tag{7.2}$$

where $v_{\max}$ is the maximal possible reaction rate ($v_{\max} = k_2 c_e$, c_e is the enzyme concentration), c_p is the concentration of the product, and k_m is the Michaelis-Menten constant that can be expressed with the equilibrium constants:

$$k_m = k_{-1} + k_2/k_1 \tag{7.3}$$

It can also be defined as the substrate concentration at which the reaction rate is reduced to half of the maximum rate. One International Unit (1 U) of the enzyme is defined as the amount that catalyzes 1 μM of the product per minute at a saturation substrate concentration ($c_s > 100\ k_m$), at a given temperature and pH, or at other relevant factors at a reference state.

Normalized reaction rates for the Michaelis-Menten model are shown in Figure 7.2 as a function of substrate concentration normalized to k_m (Buerk, 1993). At low substrate concentrations, the reaction is approximately first order (i.e., linearly dependent on concentration). At high concentrations, the rate becomes constant (saturation). The inset of the figure shows the double-reciprocal plot:

$$v_{max}/v = 1 + k_m/c_s \tag{7.4}$$

The situation is much more complicated if several substrates take part in the process, and several products are formed simultaneously.

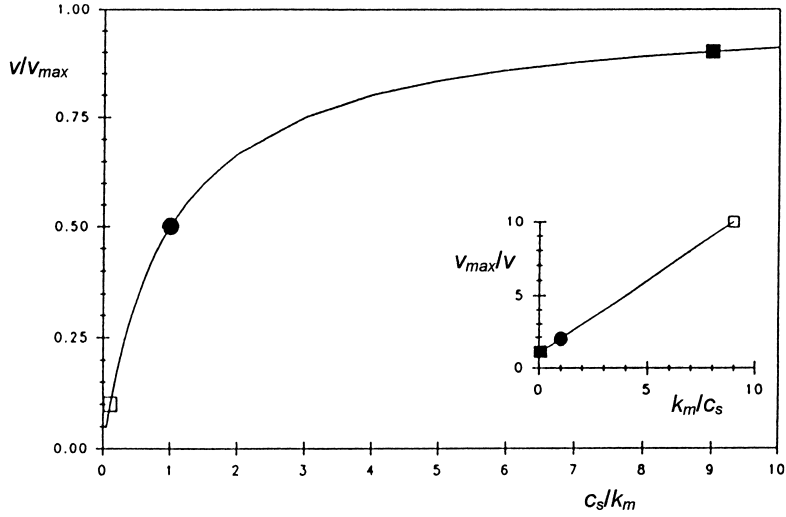

FIGURE 7.2. Concentration-dependent reaction rate of enzymatic reactions according to the Michaelis-Menten model. (Used with permission from *Biosensors, Theory and Applications* by D. G. Buerk, ©1993, Technomic Publishing Co., Inc., Lancaster, PA, p. 64.)

Two typical enzymatic reaction types characteristic of a number of biosensors will be demonstrated here as examples. Oxidase enzymes employ molecular oxygen as an electron acceptor in the reaction. The overall reaction scheme is as follows (Coulet et al., 1991):

$$S + O_2 + (H_2O) \xrightarrow{\text{oxidase}} P + H_2O_2 \tag{7.5}$$

Oxygen is a reagent (or cosubstrate) here. Similarly, water is also often consumed by the reaction. One of the reaction products is hydrogen peroxide, which plays an important role in biosensors since the majority of transducers are based on the indirect detection of this reaction product.

Another important example is the reaction catalyzed by hydrolase enzymes that are able to decompose the substrate with the addition of water, resulting in generally ionic products, the indirect sensing of which is also possible:

$$S + H_2O \xrightarrow{\text{hydrolase}} P_1^{+} + P_2^{-} \tag{7.6}$$

7.1.2 Time-Dependent and Stationary Measuring Methods

Enzymatic biosensors, like a number of chemical sensor types, operate by means of a membrane that incorporates the immobilized active receptors—the

enzymes in this case. Depending on the membrane-transducer cooperation mechanism, as well as the related transduction and measurement techniques, time-dependent and stationary operation modes can be distinguished as follows:

- *Time-dependent measurement technique:* As shown in Figure 7.2, the reaction rate is a monotonically increasing function of the substrate concentration, therefore, the former can be used for the determination of the latter (Buerk, 1993). The reaction rate can be determined by measuring the concentration of the product and forming its first derivative by time [see Equation (7.2)]. This type of measurement technique requires a small reaction chamber where the enzymatic reaction takes place uninfluenced by its environment (Bousse et al., 1990). The effect of the diffusion must be minimized, therefore, the enzyme should be immobilized directly onto the transducer surface as a thin film. Continuous monitoring cannot be realized, only the periodical sample taking and subsequent measuring process is applicable. The great advantage is the short response time within a single measurement cycle. This may even compensate the drawback of noncontinuous operation. Recent sensor types try to exploit the advantages of the time-dependent measurement technique (Watson et al., 1987).
- *Stationary technique:* This is a static measurement method of a stationary parameter. Calorimetric transducers measure, for example, a constant temperature difference between the sensing film and its environment due to the power dissipation of the enzymatic process. This temperature difference is a function of the reaction rate. Electrochemical and optical transducers measure the cosubstrate (reagent) or product concentrations in a stationary state. The transducer is separated from the analyte by a biocatalytic membrane that contains the enzyme in a homogenous distribution and acts as a diffusion membrane for each of the reagents, the substrate, and the reaction products. Inside the membrane, the concentration of the substrate (c_s), the reagent (or cosubstrate, c_r), and the product (c_p) are governed by diffusion mass transport mechanisms coupled with the enzymatic reaction acting as a reagent drain and a reaction-product source. By superposition of Fick's second law of diffusion and Michaelis-Menten kinetics, the following net equations describe the processes (Macholán, 1991):

$$\frac{\partial c_s}{\partial t} = D_s \frac{\partial^2 c_s}{\partial x^2} - \frac{v_{\max} c_s}{k_m + c_s} \tag{7.7a}$$

$$\frac{\partial c_p}{\partial t} = D_p \frac{\partial^2 c_p}{\partial x^2} + \frac{v_{\max} c_s}{k_m + c_s} \tag{7.7b}$$

$$\frac{\partial c_r}{\partial t} = D_r \frac{\partial^2 c_r}{\partial x^2} - \frac{v_{\max} c_s}{k_m + c_s} \tag{7.7c}$$

where the D_i coefficients are the diffusion constants, and x is the distance from each point of the membrane to the external surface. Supposing small c_s values relative to k_m, which allows the linear approximation, the above net differential equation also becomes linear. In a stationary state, derivatives by time are zero; thus, Equation (7.7a) becomes a simple linear differential equation of the second order. Supposing an external substrate concentration of c_{s0}, the solution of the equation is as follows:

$$c_s = c_{s0} \exp(-Ax), \text{ where } A^2 = v_{\max}/k_m D_s \tag{7.8}$$

Accordingly, the substrate concentration at the membrane surface facing the transducer (at $x = d$, where d is the thickness of the membrane) is a linear function of the external substrate concentration, c_{s0}. Functions for c_r and c_p are received by integrating Equations (7.7b) and (7.7c). Solutions without the Michaelis-Menten part represent the diffusion through the membrane without the enzyme, the differences above this solution are linear functions of c_{s0} because of the linearity of the differential equations. Consequently, it can be stated that at small external substrate concentrations in a stationary state, when comparing the behavior of enzymatic and nonenzymatic membranes, the cosubstrate and product concentration difference on the transducer side of the membrane is a linear function of the external substrate concentration. That represents the necessity of a dual-membrane transducer system that employs enzymatic and nonenzymatic membrane parts. The differential output is measured as a function of the substrate concentration. This is the basic model of the stationary measurement technique using biocatalytic membrane-based sensors. In special cases, when the external product concentration is zero (i.e., the product is formed exclusively by the reaction), the application of a single transducer is enough to obtain the measurement. We assumed in the former model that the substrate consumption of the transducer from the analyte is negligible. However, this is not always true with amperometric transducers. On the other hand, in the limiting current stationary operation mode, the amount of reagent or product is consumed by the amperometric cell, the limiting current of which is determined by the maximum material current, thus, providing the concentration gradient at the membrane transducer interface. Because of the linearity, it can be shown easily that the concentration gradient is also a linear function of the external substrate concentration. The greatest shortcoming of the sta-

tionary mode sensors is their slow response; equilibrium can often be reached in several minutes. Thus, the monitoring of fast-changing concentrations is impossible by means of this method.

- *Combined technique:* In this version, stationary mode sensors are used in nonequilibrium states by putting small amounts of analytes into a flow-through cell that contains the sensor element. Time-dependent transients of the parameters are measured and evaluated in a rather complicated way.

7.1.3 Transducer Types

In this section, the most important transducer types and their operation principles in enzymatic biosensors are surveyed, independent of the actual enzyme in question.

Amperometric electrochemical cells are widely used in biosensors, usually combined with oxidase enzymatic membranes following the typical reaction scheme of Equation (7.5).

Dual Clark-type oxygen cells were the first transducers applied successfully in enzymatic biosensors (Updike and Hicks, 1967). Their schematic structure is demonstrated in Figure 7.3 (Buerk, 1993). The cells have a common Ag/AgCl reference electrode and a common internal electrolyte. Over one cathode, the enzyme was immobilized into the membrane, while over the reference cathode, the enzyme was inactivated by local heating. The limiting current difference between the two cathodes is linearly proportional to the substrate concentration, independent from the external O_2 tension within a

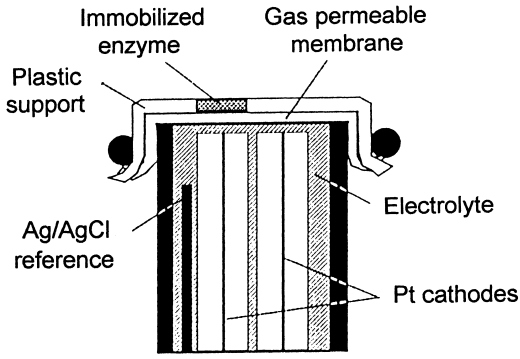

FIGURE 7.3. Schematic model of a dual-structure enzymatic biosensor using two Clark-type oxygen sensors. (Used with permission from *Biosensors, Theory and Applications* by D. G. Buerk, ©1993, Technomic Publishing Co., Inc., Lancaster, PA, p. 70.)

reasonable operating range. The greatest shortcoming of this type may occur with an inadequate O_2 tension when this becomes the rate-limiting factor and causes unreliable measurements.

The reaction product H_2O_2 can also be used for amperometric transduction. Using a Pt or Au electrode polarized at a positive potential of 0.6–0.7 V, hydrogen peroxide can be reduced electrochemically through the following reaction:

$$H_2O_2 \longrightarrow 2H^+ + O_2 + 2e^- \tag{7.9}$$

Since hydrogen peroxide is generally absent from the external environment of the sensor, there is no necessity for dual-differential measurements, which is a great advantage over the amperometric O_2 transducers. Practically the same structure can be used as in the Clark sensors with a single H_2O_2-permeable enzymatic membrane. The amperometric signal is directly proportional to the substrate concentration under steady state conditions. Since the electrochemical reaction is a fast process, the amount of hydrogen peroxide produced is consumed at the membrane-transducer interface. Thus, there is no need for a special H_2O_2 diffusion-limiting membrane. However, the reaction is still rate limited at low O_2 tension. In such cases, the initial rate of current change (dI/dt) can also be related to the substrate concentration, since it is proportional to the reaction rate (Buerk, 1993). Presently, due to the above mentioned advantages, *amperometric H_2O_2 cells are the most widely and successfully used transducers in enzymatic biosensor applications,* although enzyme stabilization and immobilization problems are the same as with any other types of transducers.

Biosensors based on *calorimetric transducers* are thought to be the first types that were successfully realized. The primary enzymatic reaction generally does not generate enough power for stable transducer operation. At (7.5)-type reactions, the heat dissipation can considerably increase by means of the secondary reaction of H_2O_2 in the presence of a catalase enzyme (Guilbeau, 1987):

$$2H_2O_2 \xrightarrow{\text{catalase}} 2H_2O + O_2 + 100\ \text{kJ} \tag{7.10}$$

Figure 7.4 shows schematically a possible realization (Yao, 1991). The bienzyme membrane is immobilized over one set of thin-film temperature-sensing thermoelectric junctions. The heat produced by the catalytic reaction increases their temperature relative to the reference junctions. This temperature difference, in the order of millidegrees, generates a potential difference, a thermoelectric electromotive force that is a function of the reaction rate, thus, also of the substrate concentration. The disadvantages of thermoelectric transducers are associated with the stability of the bienzyme system and oxygen

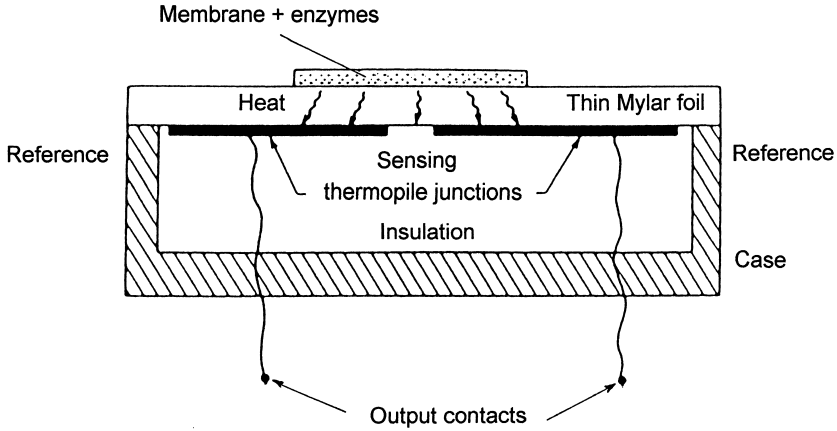

FIGURE 7.4. Schematic model of a thermopile-based calorimetric biosensor. (Reprinted after Yao, 1991, p. 236, courtesy of Marcel Dekker Inc., New York.)

limitation. Also, the measurement of very small temperature differences causes difficulties; thus, the application of this method is limited to *in vitro* analysis. Thermistor-based flow-through systems combined with pulse injection of the analyte and measurement of the temperature transients have also been developed for analytical purposes (Danielsson, 1991; Xie et al., 1995).

The application of *potentiometric (ion-selective) transducers* is limited primarily to the enzymatic reactions in which ionic compounds are produced by the reaction, as shown by Equation (7.6). It is especially favorable to employ ion-selective transducers that detect such ion types that are absent from the environment of the sensor, the enzymatic reaction produces them only. Examples include NH_4^+-sensitive electrodes and ISFETs, since this ion type is often produced by biocatalytic reactions (see urea sensors in Section 7.1.8). In spite of this, pH transducers have found the widest applications due to their simple structure, as well as their well-developed processing and measurement background, even though environmental pH fluctuations must be compensated (Van der Schoot et al., 1990). Figure 7.5 schematically shows a dual ENFET-REFET transducer consisting of an enzyme-modified FET and a reference pH-ISFET, called REFET, for compensating environmental pH and temperature variations (Buerk, 1993). The transistors are fabricated by SOS (silicon on sapphire) processing which assures special advantages for biosensors. Its advantages are the application of an insulating substrate and the absence of Si/SiO_2 interfaces that are present in conventional silicon-substrate-based FETs that might show instabilities and parasitic currents between the individual elements due to the irreversible penetration of ionic compounds. Of

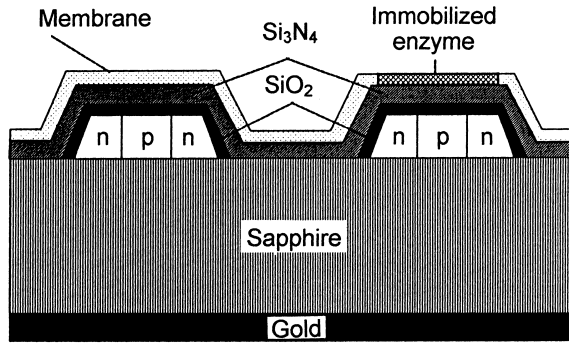

FIGURE 7.5. Schematic structure of a dual ENFET-REFET potentiometric biosensor based on SOS processing. (Used with permission from *Biosensors, Theory and Applications* by D. G. Buerk, ©1993, Technomic Publishing Co., Inc., Lancaster, PA, p. 70.)

course, conventional enzyme-modified ion-selective electrodes also have widespread application as potentiometric transducer-based biosensors.

CO_2 is often produced by enzymatic reactions, the tension of which can be measured potentiometrically, using the Stowe-Severinghaus technique (see Section 6.1.1).

Potentiometric measurements can also be performed for oxidase catalyzed enzymatic reactions [see Equation (7.5)], even though the primary products are nonionic compounds (Karyakin et al., 1996). In some cases, they may dissociate like weak acids or bases, and these secondary products can be followed potentiometrically (such as gluconic acid produced by the oxidation of glucose in glucose sensors, see Section 7.1.7). The measurement of small variations and the pH dependence of the enzymatic activity are the most important drawbacks to this technique, although some sensor types use this principle.

Another interesting approach is the potentiometric measurement of H_2O_2 production by means of a Pt electrode. The source of the potentiometric response is unclear. It may be involved with the oxidation or reduction of the Pt surface functional groups caused by hydrogen peroxide (Yao, 1991). Since the sensitivity depends on the Pt surface quality, the reproducibility of this type of transducer is rather poor. Recently, H_2O_2-sensitive MOS structures have been operated successfully with sputtered Pt/LaF_3 membrane (Katsube et al., 1991). In general, the passive nature of potentiometry, the large response time, and the possible drifting of the electrode potential preclude its usefulness for *in vivo* sensing.

Conductimetric electrochemical cells can be used for measuring conductivity changes caused by ionic products. In this case, polarization-free measurements must be performed without consuming ionic compounds from the

electrolyte. This can be realized by means of an AC excitation with moderate frequencies (typically with 10 mV amplitude at 1 kHz). The most favorable current range can be reached by applying an interdigital (see Figure 3.1) or double-meander electrode arrangement (Watson et al., 1987). The measurement method also enables transient analysis, without needing to wait for steady state. Thus, short response times may be reached with this technique.

Solid-state nonelectrochemical *gas sensors* can be applied as transducers in combination with those enzymatic processes in which gaseous compounds (mostly H_2 or NH_3) are produced by the reaction. Mainly, MOSFET devices with catalytic metal (Pt, Pd, or Ir) gates have been applied for such purposes, utilizing the absorption and ionization effect and the related work function shift of these metal films. More recently, Pt/*n*-GaAs Schottky barrier diodes (see Section 3.2) with discontinuous platinum thin film have been shown to be effective transducers for the detection of ammonia. In combination with a polyetherimide membrane in which the enzyme urease has been immobilized, it can be used as a urea sensor (Lechuga et al., 1992) (see also Section 7.1.8).

Optical transducers have wide application perspectives in all types of enzymatic biosensors. Until recent years, the biggest problem was the lack of an appropriate optical indicator for H_2O_2 that was a typical product of oxidase-enzyme-catalyzed reactions [see Equation (7.5)]. The indirect transduction methods and related transducer types can be distinguished as follows:

- Transduction with fluorescent O_2 optrodes (see Section 6.1.4) at (7.5)-type enzymatic reactions (Wolfbeis, 1991) is one method.
- Transduction with colorimetric (or fluorescent) pH optrodes (see Section 6.1.4) at (7.6)-type enzymatic reactions and at the (7.5)-type if acidic or basic products are produced (Wolfbeis, 1991; Yao, 1991; Buerk, 1993) is possible.
- NH_4^+-sensitive optrodes can be used based on the coimmobilization of specific ionophores and pH-indicators [see Equation (4.24)], if ammonium ions are present among the reaction products.
- Under basic conditions, the chemiluminescent detection of H_2O_2 in the presence of luminol, which reacts with hydrogen-peroxide with light emission, is possible; the practical application is limited by the low quantum yield of the reaction (Buerk, 1993).
- More recently, fluorescent detection of H_2O_2 has also been successfully performed with tris(bpy)Ru(II)Cl-hexahydrate dye.

In several cases, direct detection can be realized without the necessity of a secondary chemical or electrochemical reaction:

- If the enzyme is fluorescent and the substrate-enzyme intermediate has a different emission spectrum, the enzyme itself can be used as a fluores-

cent dye for measuring the ratio of free and complex forms, which is dependent on the substrate concentration in equilibrium.

- Biocatalytic processes often employ fluorescent co-factors or reagents that can be applied as dyes. For example, the hydrogen mediator NAD (nicotinamide-adenine-dinucleotide), excited at the 340 nm wavelength, emits at 460 nm, which is shifted at the hydrogenated NADH form [also see Equations (7.16) and (7.17)] (Schubert, 1993).
- There are biocatalytic reactions that show chemiluminescence and proceed with light emission [see Equation (4.30)]. In such processes, the emitted light intensity is characteristic for the reaction rate and, thus, the substrate concentration (also see Table 7.2) (Gautier et al., 1990).

The schematic structure of a simple enzymatic optrode is shown in Figure 7.6.

Chemomechanical transducers converting a chemical parameter into mechanical deformation represent a new development area. Mechanical changes can be subsequently converted into electrical or optical signals or used directly for actuator purposes. At first, the reversible swelling or shrinking of hydrophobic hydrogel polymers varying with pH was exploited (Buerk, 1993). A membrane can be prepared with a special material, the thickness changes of which can be followed either capacitively or optically [see Figures 3.1(c) and 3.10(e)]. The newly developed MICSPOMS (metal-island-coated swelling polymer over mirror system) device represents an optical approach (Schalkhammer et al., 1995). It is actually a special kind of optical reflection interference filter. It consists of a metal mirror covered by a thin film of optically transparent swelling polymer and a discontinuous metal-island film. The reflection interference from both metal films depends on the interlayer thickness, which varies with the swelling and, thus, the environmental pH. Since the metal-island film is highly permeable, the sensor layer is directly exposed to the analyte. Colorimetric transducers can be built in this way with a physical indicator; thus, the dissolution problem of chemical indicator dyes

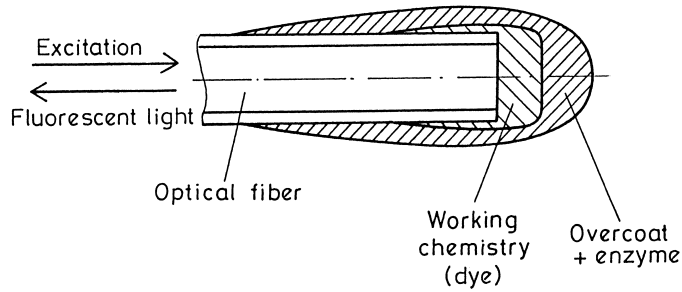

FIGURE 7.6. Schematic structure of a biocatalytic fluorescent optrode.

is eliminated. The devices can be operated within a wide pH range, allowing rather short response times. Enzymes can also be immobilized into the hydrogels, which represents great possibilities for biosensors. A special advantage is the possibility of direct application in chemically excited actuators.

7.1.4 Multienzyme Reactions, Reagents in Enzymatic Processes

In this section, those complex enzymatic reaction models and related reagent types that may have important roles in biosensor applications are surveyed.

Coupled multienzyme reactions can be competitive when several enzymes utilize the same substrate in parallel reaction pathways:

$$S \xrightarrow{\text{enzyme1}} P_1;\; S \xrightarrow{\text{enzyme2}} P_2 \tag{7.11}$$

In chain reactions, the second enzyme utilizes the product of the first one (Macholán, 1991):

$$S_1 \xrightarrow{\text{enzyme1}} P_1 = S_2 \xrightarrow{\text{enzyme2}} P_2 \tag{7.12}$$

Chain reactions may have great importance in those sensors, in which the first enzymatic reaction product cannot be detected by the available transducer types. The kinetics becomes more complicated in these cases. At competitive reactions:

$$\frac{v}{v_{\max}} = \sum_{i=1}^{n} f_i \frac{c_s}{c_s + k_{m,i}} \tag{7.13}$$

where the summation of the fractional components, f_i must be equal to one (Buerk, 1993). In some cases, several enzymes produce the same reaction product:

$$S_1 \xrightarrow{\text{enzyme1}} P,\; S_2 \xrightarrow{\text{enzyme2}} P \tag{7.14}$$

This can be the situation in multienzyme sensor arrays, in which the products must be separated for eliminating cross-sensitivities. In cooperative reactions, the second enzyme catalyzes the regeneration of the original substrate:

$$\begin{array}{c} S_1 \xrightarrow{\text{enzyme1}} P_1 = S_2 \xrightarrow{\text{enzyme2}} P_2 = S_1 \\ \uparrow \underline{\qquad\qquad\qquad\qquad\qquad\qquad} \hookleftarrow \end{array} \tag{7.15}$$

The two chain reactions create a closed loop, in which signal amplification can also be reached (Schubert et al., 1991). Cooperative reactions may have great importance in biosensor applications when the substrate concentration is too low, and its consumption by the first reaction cannot be neglected. In special cases, even cofactors can be regenerated by the second reaction when their concentration becomes rate limiting [i.e., O_2 at (7.5)-type reactions]. Oxidase/peroxidase and oxidase/dehydrogenase cooperative reactions are often utilized in biosensors.

As was already demonstrated, enzymatic reactions often need not only the substrate but also further reagents, so-called *cofactors* and *cosubstrates,* to proceed. Oxidase reactions generally (but not exclusively) need oxygen since the oxidation is the process that is catalyzed. NAD may also have an important role as a cosubstrate in reactions with hydrogen transfer. For example, a dehydrogenase reaction can proceed as follows:

$$S + NAD^+ \xrightarrow{\text{dehydrogenase}} P + NADH + H^+ \qquad (7.16)$$

where the reaction product NADH can be used as an indicator dye in fluorescent or chemiluminescent optical transducers, or it can be detected amperometrically by electrochemical dehydrogenation (Schuhmann et al., 1992). An opposite direction hydrogen transfer is catalyzed at hydroxylase reactions (SH represents the substrate) (Macholán, 1991):

$$SH + O_2 + NADH + H^+ \xrightarrow{\text{hydroxylase}} SOH + NAD^+ + H_2O \qquad (7.17)$$

NAD phosphate (NADP) is also often applied in similar catalytic processes.

Coenzymes are cooperating reagents in enzymatic reactions forming intermediate complexes with the substrate or the substrate-enzyme complex and acting as a carrier. In opposition to enzymes, they generally are small-molecular-weight compounds. According to the present comprehension, they are different from the cosubstrates, such as NAD, which was handled formerly as a coenzyme.

Mediators (electron mediators) have a special function in biosensors; their role is to replace the electron transfer performed by oxygen in (7.5)-type reactions, thus, preventing the process from the problem of having a low oxygen concentration. When applying amperometric transduction, oxygen has the following role in enzymatic and subsequent anodic reactions [see Equations (7.5) and (7.9)]:

in the membrane: $$S + O_2 \xrightarrow{\text{oxidase}} P + H_2O_2 \qquad (7.18a)$$

at the anode: $$H_2O_2 \longrightarrow 2H^+ + O_2 + 2e^- \qquad (7.18b)$$

In the overall reaction, oxygen is regenerated. Actually, it has only an electron transfer role that can be replaced by other materials, called mediators. Such a compound can be used as an electron mediator that can be transferred from its oxidized form (Me_{ox}) into its reduced form (Me_{red}) during the enzymatic reaction and can be recycled by the anodic oxidation:

in the membrane: $$S + Me_{ox} \xrightarrow{\text{oxidase}} P + Me_{red} \tag{7.19a}$$

at the anode: $$Me_{red} \longrightarrow nH^+ + Me_{ox} + ne^- \tag{7.19b}$$

A further advantage of applying mediators is that the amperometric measurement can be performed with lower polarographic polarization potentials than at H_2O_2, which reduces the possibility of interfering reactions.

A number of mediator types have been applied, mostly in glucose sensors. Classical examples are the ferrocene (Foulds and Lowe, 1988), ferrocyanide (Shul'ga et al., 1995), and quinone derivatives (Kajiya et al., 1991), and more recent examples include some organic salts, such as TTF-TCQN (tetrathiafulvalene-tetracyanoquinodimethane) (Hale et al., 1991), phenoxazines, phenothiazines, and tungsten and ruthenium complexes (Buerk, 1993). Their applications will be discussed in connection with glucose sensors (see Section 7.1.7).

The biggest problem of mediator application is that the competitive electron transfer for oxygen cannot totally be eliminated; moreover, the dissolution of the mediator may cause poisoning and false output signals. The immobilization of mediator molecules limits their transporting function. A good approach for solving this problem is to apply conducting polymer beds for immobilization (see Section 7.1.5).

Inhibitors have a great influence on enzymatic processes. They are substances that combine with the enzyme molecule to form an inactive complex, thus, reducing the rate of the enzyme-catalyzed reaction. Some of them inactivate the enzyme irreversibly, but others reversibly; that is, their effect can be abolished by removing the inhibitor, which enables a sensor-type operation for the inhibitor. The inhibition can be expressed in terms of percentage according to the following relation:

$$\text{Inhibition, } \% = 100 \times (X_0 - X_i)/X_0 \tag{7.20}$$

where X_i and X_0 are sensor responses with and without the presence of an inhibitor with the same substrate concentration. At a saturated substrate concentration, the sensor output is a function of the inhibitor concentration; thus, the biosensor can be used for measuring it. The application of biosensors for determining toxic compounds is becoming a dynamic trend in environmental

monitoring. Their application can be of great use mainly in organophosphorous pesticides (Yuan et al., 1991; Cagnini et al., 1995) and heavy-metal ion (Zhylyak et al., 1995) detection.

7.1.5 Enzyme Immobilization Techniques

One key issue of biosensor fabrication is the appropriate stable immobilization of enzyme molecules onto a transducer surface or into a functional membrane. A great number of techniques have been developed, but their wide variety and the appearance of even newer processes show that the optimal general solution has not yet been met.

Immobilization means the conversion of an enzyme from a water-soluble, mobile state into a water-insoluble state without affecting its catalytic activity. Coimmobilization of several enzymes or enzyme cosubstrate/mediator systems is often necessary. Since the immobilization method strongly influences how the enzyme molecules are exposed to environmental effects and how they react to them, it determines the stability and lifetime of the sensor. Basically, the following methods can be distinguished: encapsulation of a free soluble enzyme, physical adsorption and entrapment, direct cross-linking, covalent binding, and embedment of enzymatic molecules into conducting polymers.

An active layer of a *soluble enzyme* has been used at the initial stages of biosensor development (Macholán, 1991). This is the simplest method of physical immobilization and consists of capturing the enzyme on the surface of a transducer by means of a dialysis membrane. This ensures free diffusion of the substrate and reaction products, whereas the macromolecular enzyme remains a component of the sensing device. Soluble enzymes face a serious challenge when the sensor is exposed to various analytes, which results in unstable operation and a short lifetime. The dry-out, refreshing, and calibration problems are also causes of why this type has already become part of the historical background.

Enzymatic molecules can be immobilized physically by *adsorption* on membrane surfaces or by *entrapment* into the membrane. Most membrane materials will adsorb enzyme molecules directly on the surface, although the strength of attachment may not always be adequate causing reversible binding and dissolution of the enzyme. High-molecular-weight enzymes can be immobilized effectively by physical entrapment into a synthetic or natural gel matrix. The effectiveness of incorporation can be improved when cross-linking a polymer over an enzyme film adsorbed previously onto the transducer surface or polymerizing the membrane from a monomer solution containing the dissolved enzyme molecules. Since enzyme activity may be destroyed by the reagents during polymerization and/or cross-linking, the first sensor types developed this way had low sensitivity and high instability. A great variety of materials

and techniques have been tried out; a few promising examples are summarized as follows:

- entrapment into a ready-made membrane of cellulose acetate (Xie and Ren, 1989), silicone rubber (Guilbault et al., 1991), cellophane (Buerk, 1993), or some kind of gel, such as gelatin or agar gel (Macholán, 1991)
- adsorption of enzyme molecules onto the transducer surface and a subsequent membrane deposition on the structure using polyurethane (Koudelka et al., 1989) or polysuphone (the latter is a polymer electrolyte with a favorite small resistivity) (Kulys et al., 1991)
- polymerization of the membrane from a monomer precursor containing the dissolved enzyme molecules has led to the achievement of promising results with PAA (Macholán, 1991) and PVPy (Haemmerli et al., 1992). Recently, photolithographically patterned PHEMA hydrogel films were used for enzyme immobilization. Their advantage is the water and ion buffering capacity of the hydrogel, however, the enzyme dissolution had to be prevented by a second membrane system (Urban et al., 1994).
- deposition of a lipid-enzyme molecular multilayer structure onto transducer surfaces using the Langmuir-Blodgett method (see Figure 2.10 can be realized). Applying a subsequent photopolymerization of the lipid layer, the system can be immobilized (Zaitsev, 1995).

Chemical immobilization techniques have led to more successful solutions. One approach is the *cross-linking* of enzyme molecules with each other or other protein molecules forming continuous films. Bifunctional reagents form intermolecular connections during their reaction with enzymes, giving rise to an insoluble film in which a considerable part of the enzyme activity is retained and the enzyme molecules cannot easily be dissolved. Attachment must be carried out using the functional groups on the enzyme, which are not essential for its catalytic activity, such as amine, phenol, carboxyl, etc. Among the possible reagents, the method utilizing glutaraldehyde is very simple and useful. The scheme of this chemical reaction is shown in Figure 7.7 (Guilbault et al., 1991). Loss of enzymatic activity was found to be reduced when the enzyme was cross-linked with an inert protein rich in lisine, like albumin, etc. To improve the stability, the cross-linked film can be covered with further membranes. Such sensors can be operated for thousands of assays.

Another approach for immobilizing enzymes is *covalent binding* directly to the transducer surface that might need a series of complex chemical process cycles that are specific both to the enzyme and to the surface chemistry.

On graphite electrodes or on transducers with surfaces covered by some kind of organic film (such as collagen), the covalent binding is formed to the carbon atoms. One example is given in Figure 7.8(a) (Schuhmann et al., 1990). The electrochemical oxidation of graphite leads to the formation of carboxylic

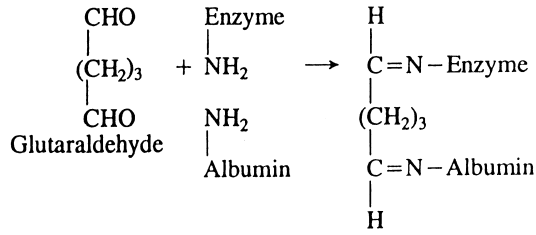

FIGURE 7.7. Reaction scheme of a typical enzyme cross-linking immobilization process. (Reprinted after Guilbault, 1991, p. 660, courtesy of Marcel Dekker Inc., New York.)

groups that can be activated by water-soluble carbodiimides, and the reaction with the *e*-amino groups of lysine residues of the enzyme (e.g., glucose oxidase) results in a covalent immobilization of the latter.

The situation is more complicated with SiO_2 or precious metal electrode (Pt) surfaces that are often used in electrochemical, microelectronical, and optical-fiber transducers (Lee et al., 1991). One example is given in Figure 7.8(b) (Mann-Buxbaum et al., 1990). The oxidized surface is first silylated resulting in a Si-O net, and the enzyme molecules are coupled through organosilane, and subsequent amine and quinone groups (using 3-aminopropyltriethoxysilane and *p*-tetrachloroquinone treatments in the example). The stability can be improved when applying a polymer membrane coating over the enzymatic film. The figure illustrates the technique on Pt surfaces, however, similar processes can be used for SiO_2. A recent promising method is to form a coupling through polysiloxane films with organic functional groups.

Another approach is that enzyme molecules are coupled onto an electroconducting polymer [e.g., polypyrrol, see Figure 7.8(c)] film which is previously deposited electrochemically on the electrode surfaces (Schuhmann et al., 1990). After having been nitrated, the nitro-derivative can be reduced electrochemically. Immobilization of the enzyme can be carried out with these surfaces by activating the carboxylic side-chains of the protein with carbodiimide.

The idea of applying conducting polymers has led to the most developed and rather successful technique of enzyme immobilization: *embedding enzyme molecules into a conducting polymer bed.* At first, PVPy films containing $Os(bpy)_2Cl$ complexes were used, in which the enzyme was immobilized during the synthesis of the layer (Buerk, 1993). Later, with the appearance of electrochemically deposited electroconducting polymers, their application for embedding functional receptors naturally arose. They offer a number of advantages that can be exploited mostly in electrochemical transducers:

- Electroconducting conjugated polymers (ECPs) can be deposited onto metallic transducer surfaces by a well-controlled electrochemical deposi-

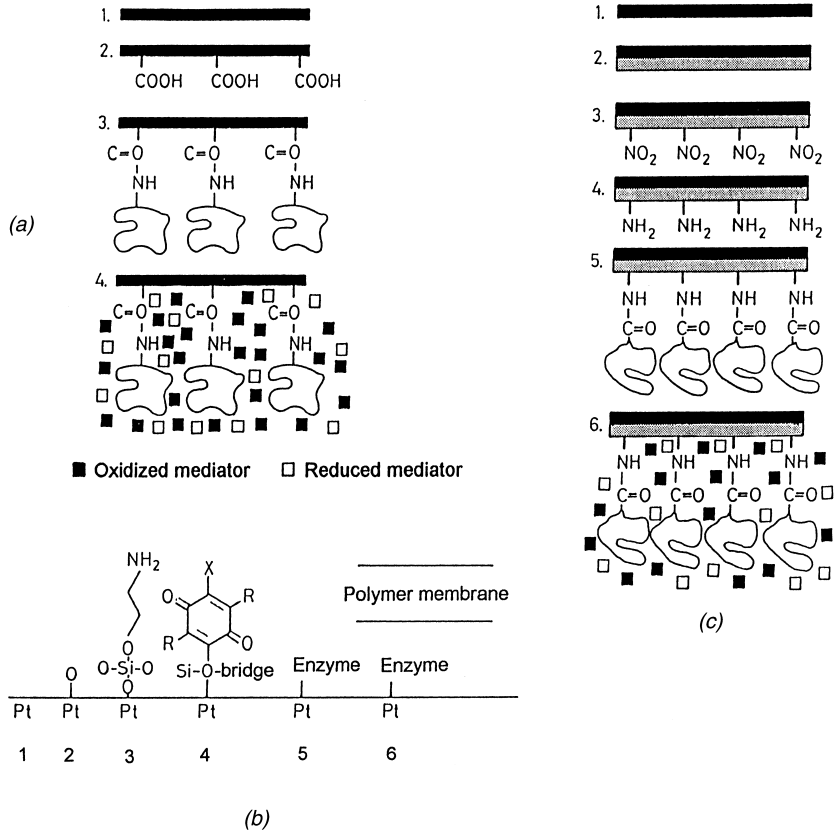

FIGURE 7.8. Covalent immobilization methods of enzymes to various surfaces: (a) graphite electrode (1—graphite electrode, 2—electrochemical oxidation, 3—activation of the carboxylic groups and immobilization of the enzyme molecules through their lysine residues, 4—adsorption of the appropriate mediator), (b) Pt-electrode (1—Pt electrode, 2—oxidation, 3—sylilation, 4—activation with quinone groups, 5—enzyme immobilization, 6—membrane covering), and (c) PPy (polypyrrole) surface (1—Pt-electrode, 2—electropolymerization of pyrrole, 3—nitration, 4—electrochemical reduction, 5—activation and enzyme immobilization through their carboxylic groups, 6—adsorption of the mediator). [Reprinted with permission from: (a) and (c) from W. Schuhmann, R. Lammert, B. Uhe and H. L. Schmidt, "Polypyrrole, a New Possibility for Covalent Binding of Oxidoreductases to Electrode Surfaces as a Base for Stable Biosensors," *Sensors and Actuators B,* 1, pp 537–541, ©1990; (b) from E. Mann-Buxbaum, F. Pittner, T. Schalkhammer, A. Jachimowicz, G. Jobst, F. Olcaytuy and G. Urban, "New Microminiaturized Glucose Sensors Using Covalent Immobilization Techniques," *Sensors and Actuators B,* 1, pp. 518–522, ©1990, Elsevier Science S.A., Lausanne, Switzerland.]

tion process, and the subsequent, coulombmetrically controllable doping-dedoping enables the incorporation of ionic dopants determining the conductivity of the film. This conductivity can be varied in wide ranges.
- Side chains of enzyme molecules can be polarized easily, which enables their coulombmetrically controllable incorporation into the polymer bed during the deposition.
- Multienzyme systems and enzyme-mediator combinations can be immobilized within the same deposition process.
- The polymer bed forms an electrical wiring for the enzyme molecules and the mediators. Thus, electrons can be conducted directly from the charge-exchange sites to the electrode surface (Bidan, 1995). Therefore, the physical electron carrying function of the mediator becomes unnecessary; its role may be limited to the chemical interaction. This enables a stronger immobilization of the mediator molecules, preventing them from dissolution.

Several electrochemically deposited polymer types, such as polypyrrol (PPy), poly(N-methylpyrrol) (PMePy), and polyanaline (PANi) were applied to immobilize various enzymes (e.g., glucose oxidase, cholesterol oxidase, and uricase) and mediators (Hämmerle et al., 1992; Bidan, 1995; Karyakin, 1996; Vidal et al., 1999; Dobay et al., 1996, 1999). The application of mediators is also reasonable because they prevent the formation of H_2O_2 which can be harmful for the conducting polymer layer. Mediatorless solutions have also been developed where the excess H_2O_2 is decomposed by a secondary catalytic process with enzymes like catalase or peroxidase (Urban et al., 1994), or when the active parts of the enzyme and the conducting polymer can communicate directly with each other (Koopal et al., 1994; Dobay et al., 1999).

Multilayer polymer/enzyme structures have also been fabricated by subsequent deposition processes in a number of combinations, but the best sensor parameters have been achieved with simultaneous deposition, when embedding the enzyme molecules into the polymer bed, although the real nature of the binding mechanism (physical embedding or covalent binding) has not been clarified for these cases (Hämmerle et al., 1992).

7.1.6 Operation Characteristics

The operation of enzymatic biosensors is influenced by a number of processing parameters and environmental conditions. The most important ones are listed below:

(1) Chemical circumstances:
   - the enzyme concentration and immobilization technique
   - the substrate concentration (it may influence not only the output signal which is expected, but also the response time)

- the pH of the analyte solution
- the concentration of interfering ions
- the concentration of cofactors (cosubstrates, coenzymes)
- the concentration of activators and inhibitors
- the presence of mediators

(2) Physical circumstances
- temperature
- thickness of the enzymatic film
- diffusion constant of the substrate and cofactors inside the enzymatic membrane
- thickness and permeability of the optional secondary membrane

The most important characteristic of the sensors is their sensitivity that has different dimensions with various types; thus, their comparison is not possible with this parameter. The measurable substrate concentration is typically in the range of 0.01–100 mM/l. According to the Michaelis-Menten model, this characteristic becomes nonlinearly saturated at high concentrations, independent from the actual sensor. Amperometric sensors that consume the reaction product of enzymatic processes are capable of extending the range of linearity, which is one of the reasons for their widespread application. With potentiometric transducers, the maximal sensitivity is determined by the Nernst equation: the ideal value is 59 mV/decade at room temperature. The logarithmic characteristic causes difficulties when measuring small substrate concentrations; it needs the application of an inverse-logarithmic amplifier.

The largest differences in sensor characteristics can be found in response time and lifetime values. Amperometric sensors generally have 10–100 s response times, the equilibrium-based potentiometric and fiber-optic types sometimes need several minutes. Kinetic types, using time-dependent measurement methods, have the shortest response times of 1–30 seconds. Lifetime of enzymatic sensors varies within the widest range; depending on the actual enzyme and its immobilization technique, it may range from a few hours to several months and from a few measurement assays to several thousand assays, respectively.

7.1.7 Glucose Sensors

One of the most important applications of enzymatic biosensors is the monitoring of blood glucose levels in diabetic patients by means of a glucose sensor. Normally, fasting blood glucose levels are in the range of 3.6–6.4 mM/l, and the peak response to an oral glucose tolerance test would not exceed 11 mM/l, falling below 7.8 mM/l two hours later. The diabetic patient will have a peak response exceeding 11 mM/l, and his/her blood glucose level will re-

main above this level after two hours. A person is diagnosed as being diabetic when his/her fasting blood glucose level is greater than or equal to 7.8 mM/l. The blood glucose level can reach 30 mM/l in extreme conditions. One of the major medical advances of this century has been the development of insulin to regulate glucose metabolism. The insulin dose for an individual must be adjusted to minimize hyperglycemia, while avoiding the serious conditions of hypoglycemia. This requires frequent and accurate testing to monitor the diabetic's blood glucose level.

It is now possible for diabetics to determine their blood glucose level at home using electronic home monitor appliances. Usually, the measurement should be taken four times daily, before each meal and before bedtime. A drop of blood is obtained by pricking the finger. The blood sample is placed on a reagent strip that is then analyzed by the instrument using reflectance photometry. This optical method is inherently nonlinear and requires somewhat more complicated signal analysis than other methods. Other disadvantages include the need for periodic recalibration, and the interferences of various blood compounds, such as erythrocytes and plasma proteins. In spite of these problems, the reagent strip method has been successfully implemented, and a number of instrument types have been commercially available for many years.

The goal of glucose biosensor research and development was to replace the reagent strip method with sensors and to enable the fabrication of portable instruments for *in vivo* or *ex vivo* blood glucose monitoring. Battery-operated portable appliances employed electrochemical cells equipped with an enzymatic membrane, first on O_2, and later on H_2O_2 transducer surfaces (Buerk, 1993). The instrument is simple to use, operated by only one button, with instructions shown on a liquid crystal display. The instrument prompts the user to supply either a calibration solution or a drop of blood in a small plastic well. The sample can be as small as 7 μl. The plastic well holds the sample over an electrochemical sensor that is covered with the enzyme-activated membrane. The biosensor is linear with glucose concentration in the range of 0 to 30 mM/l. Since the current required for the electrochemical biosensor is much less than that needed to operate LEDs that are used in reagent strip photometric instruments, the appliance can be battery operated. Simpler electronics are required, allowing the instrument to be miniaturized to the size of a handheld calculator. It detects when the sample has been applied and automatically times the analysis, which is completed in 30 seconds. After completing the measurement, the liquid crystal display prompts the user to wipe out the sample and place a drop of cleaning solution into the well. A tight plastic cover is then closed to prevent evaporation or spillage, keeping the membrane hydrated until the instrument is used again. Measurement tests have shown a good correlation with the results of conventional analytical methods. Furthermore, interferences of blood compounds are much less than with pho-

tometric instruments. The membrane has a lifetime of 500–1000 measurements or six weeks before degradation in performance. The sensitivity of the instrument can be restored simply by replacing the enzyme-activated membrane. The only limitation of the glucose biosensor was found with measurements taken when the blood pO_2 was low, as anticipated from the rate-limited reaction [see Equation (7.18)]. At the highest blood glucose levels, the instrument may underestimate the true level by approximately 10% when $pO_2 < 5$ kPa. When blood $pO_2 > 10$ kPa, there is practically no detectable error due to O_2 limitation. Nowadays, a number of pocket-portable instruments employ this measurement method.

Recent research and development is directed toward implantable systems that are able either for *in vivo* or *ex vivo* continuous monitoring of blood glucose. Ideally, a closed loop system for regulating the delivery of insulin could be developed, using an implantable biosensor and an insulin pump actuator. A more tightly regulated control of insulin during the early stage of the disease may spare the diabetic from more severe microcirculatory complications later in life. For widespread practical applications, a number of problems of glucose sensors have to be solved, such as:

- miniaturization of the sensor elements and their integration with other sensors and circuitry components
- improvement of biosensor lifetime and stability with sophisticated enzyme immobilization techniques
- toxicology and stability problems due to mediator dissolution
- biocompatible packaging and implantation methods
- problems of enzyme refreshment, system recalibration and sensor interchangeability

Glucose biosensors fabricated to date are almost entirely based on the catalytic effect of the glucose oxidase (GOD) enzyme. The active part of the macromolecule, the flavin-adenin-dinucleotide (FAD) radical is able to react with hydrogen to form $FADH_2$. The two forms of GOD are often marked, therefore, as "GO(FAD)" and "GO($FADH_2$)," respectively. The other part of the enzyme molecule is able to make the reaction specific to its substrate, the glucose molecule. In further description, the abbreviation "GOD" will be used for glucose oxidase with the exception of when the dehydrogenation nature of a chemical reaction should be emphasized.

Glucose is a six-carbon molecule with the empirical formula of $C_6H_{12}O_6$ and with the possible structures illustrated in Figure 7.9. Conventionally, the carbonyl group (C = O) of glucose is located on the C-1 position, while the OH groups and H atoms are bonded to the other five C atoms. Because there are two possible asymmetric arrangements of OH and H with respect to the C atoms in a glucose molecule, two stereoisomers exist, each the mirror im-

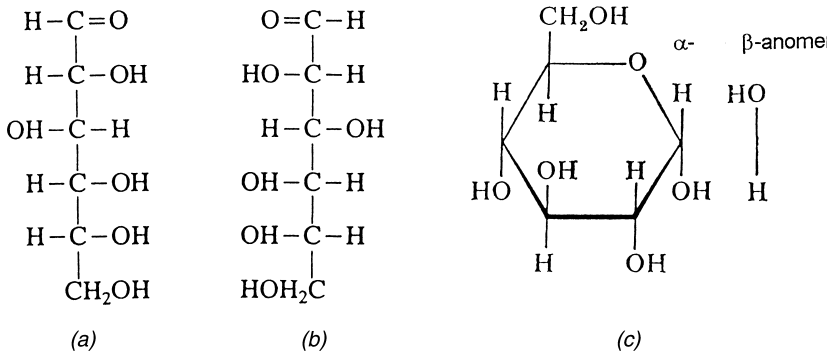

FIGURE 7.9. Structure of the glucose molecule: (a) D-glucose, (b) L-glucose, and (c) the two anomers of D-glucose. (Reprinted after Yao, 1991, p. 230, courtesy of Marcel Dekker Inc., New York.)

age of the other, as shown in Figures 7.9(a) and 7.9(b) (Yao, 1991). The two forms rotate the plane of polarized light in opposite directions: D-glucose to the right and L-glucose to the left. D-glucose is the form that is present in human body fluids. Its ability to rotate polarized light can be utilized for the optical determination of glucose. The C = O groups on C-1 and the OH group on C-5 of D-glucose can react to form hemiacetals with two anomeric structures as shown in Figure 7.9(c); they are called α- and β-anomers. The two anomers differ with respect to the optical rotation of plane-polarized light; this behavior is called mutarotation. In aqueous solution at 25°C, either form gives rise to an equilibrium mixture that contains about 37% of the α form and 63% of the β form. GOD only catalyzes the oxidation of β-D-glucose.

Depending on the pH of the solution, glucose will exist in either aldehyde or enol forms, shown in Figure 7.10 (Yao, 1991). The presence of a double bond and a negative charge in the enol anion makes glucose a relatively active reducing agent, that is, a reducing sugar. It is this property that is commonly used as the basis for the chemical analysis of glucose. For example, in high-pH solutions, glucose can cause the reduction processes of copper

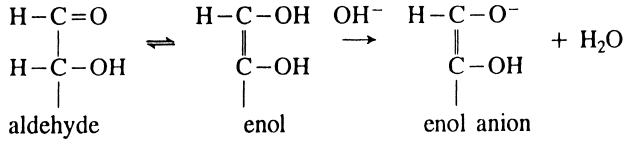

FIGURE 7.10. Aldehyde-enol reaction of the glucose molecule. (Reprinted after Yao, 1991, p. 231, courtesy of Marcel Dekker Inc., New York.)

$Cu^{2+} \rightarrow Cu$ and ferrocianide $Fe^{(III)}(CN)_6{}^{3-} \rightarrow Fe^{(II)}(CN)_6{}^{4-}$. The color changes in these reactions have been used in photometric analytical devices to indicate the presence and amount of glucose.

Glucose oxidase, reacting with glucose, dehydrogenates it in the first step, transforming the glucose into gluconolactone:

$$\text{glucose } (C_6H_{12}O_6) + \text{GO(FAD)} \longrightarrow \text{gluconolactone } (C_6H_{10}O_6) + \text{GO}(FADH_2), \quad (7.21a)$$

which reacts with water and forms gluconic acid that dissociates:

$$\text{gluconolactone } (C_6H_{10}O_6) + H_2O \longrightarrow \text{gluconic acid } (C_6H_{12}O_7) \Longleftrightarrow C_6H_{11}O_7{}^- + H^+ \quad (7.21b)$$

Potentiometric glucose biosensors are based on the pH shift resulting from the latter reaction. Meanwhile, glucose oxidase will return to its oxidized state in the presence of oxygen, resulting in H_2O_2 formation:

$$\text{GO}(FADH_2) + O_2 \longrightarrow \text{GO(FAD)} + H_2O_2 \quad (7.21c)$$

Hydrogen peroxide can be detected amperometrically [see Equations (7.9) and (7.10)]. In the presence of a mediator (see Section 7.1.4), this reaction is modified:

$$\text{GO}(FADH_2) + Me_{ox} \longrightarrow \text{GO(FAD)} + Me_{red} \quad (7.21d)$$

and will be followed by an anodic electrochemical oxidation described by Equation (7.19b). The multiple-cycle chain reactions of amperometric glucose detection with GOD are well illustrated in Figure 7.11 (Bidan, 1995).

Glucose biosensors apply mainly ferrocene, ferrocianide [$Fe(CN)_6$] and hydroquinone-sulphonate (HQS) mediators (Bidan, 1995).

First-generation glucose biosensors employed the dual Clark-type oxygen transducer structure (see Figure 7.3). Later, the application of amperometric H_2O_2 transduction became widespread. Nowadays, potentiometric ENFETs are the focus of interest due to their miniature size and their ability to be produced by silicon processing. It is simply impossible to demonstrate all realized types within the frame of this book, only a few examples and their typical behaviors will be described here.

As illustrated in Figure 7.12, upon increasing the substrate concentration, the response rate to glucose of an amperometric transducer increases and a faster response time is observed (Guilbault et al., 1991). Figure 7.13 compares the stability of various amperometric glucose sensors by illustrating the cur-

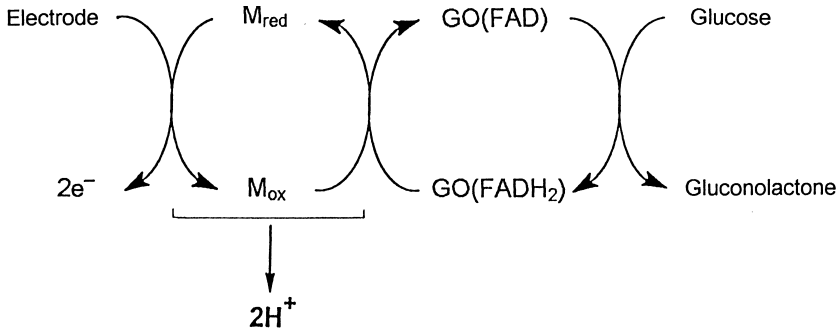

FIGURE 7.11. The multiple-cycle chemical-electrochemical reaction chain in the amperometric detection of glucose. (Reproduced with permission from *Polymer Films in Sensor Applications* by G. Harsányi, ©1995, Technomic Publishing Co., Inc., Lancaster, PA, p. 227.)

rent response via time when the sensor was kept in a constant-concentration glucose solution. The sensors were prepared using different enzyme immobilization techniques. The advantages in long-term behavior of chemical immobilization over physical methods are well demonstrated. Figure 7.14 shows the effect of a mediator. A similar characteristic can be achieved as without

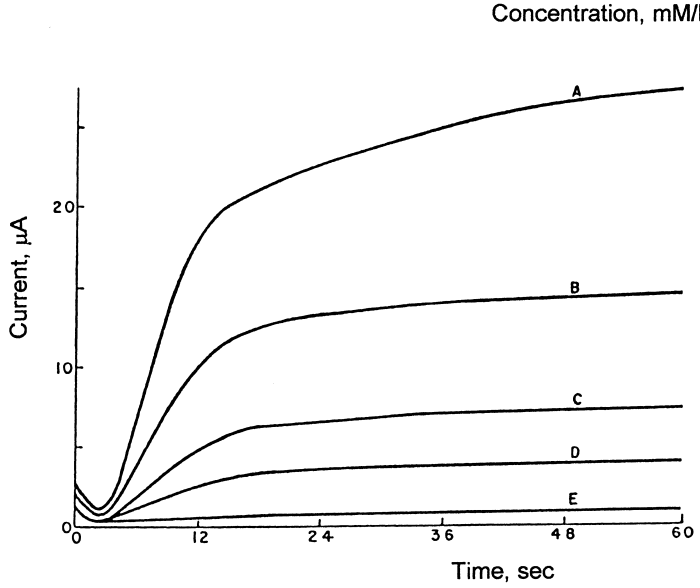

FIGURE 7.12. Family of current versus time curves for a typical amperometric glucose sensor polarized with 0.6 V in various glucose concentration solutions. (Reprinted after Guilbault, 1991, p. 669, courtesy of Marcel Dekker Inc., New York.)

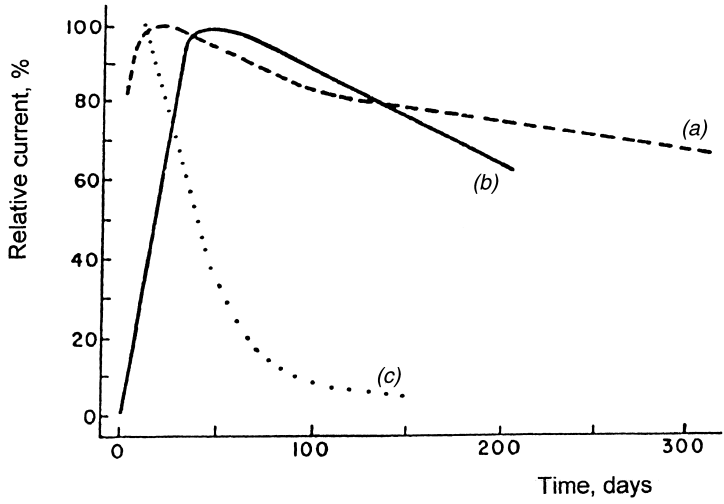

FIGURE 7.13. Long-term stability of glucose sensors prepared using various GOD immobilization techniques: (a) covalent immobilization, (b) cross-linking with polyacrylamide, and (c) physical immobilization. (Reprinted after Guilbault, 1991, p. 666, courtesy of Marcel Dekker Inc., New York.)

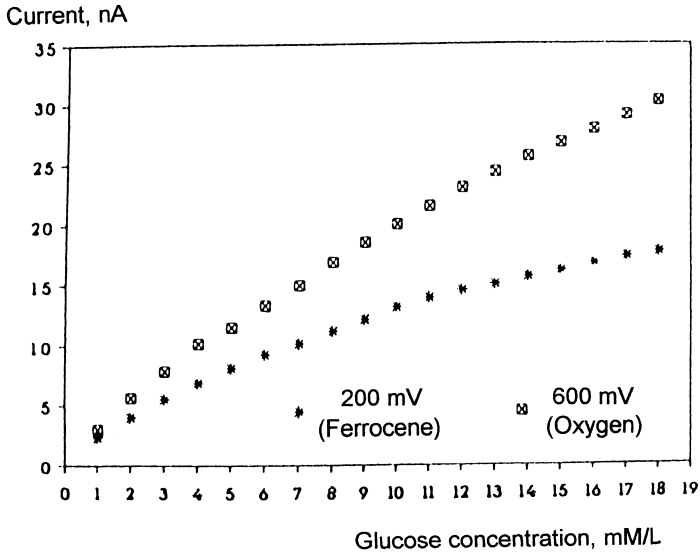

FIGURE 7.14. Characteristics of oxygen and ferrocene mediated Pt/PPy/GOD glucose electrodes. (Reprinted with permission from W. Schuhmann, R. Lammert, B. Uhe and H. L. Schmidt, "Polypyrrole, a New Possibility for Covalent Binding of Oxidoreductases to Electrode Surfaces as a Base for Stable Biosensors," *Sensors and Actuators B,* 1, pp. 537–541, ©1990, Elsevier Science S.A., Lausanne, Switzerland.)

mediators, but with a much smaller polarization of the electrochemical cell (Schuhmann et al., 1990).

Figure 7.15 shows the linear output voltage characteristic of a potentiometric glucose ENFET sensor (Katsube et al., 1990). The structure of the sensor is shown in Figure 7.16. The silicon MOSFET structure was deposited onto a sapphire substrate by CVD using the SOS (silicon on sapphire) processing method. The thermophilic glucokinase enzyme was immobilized in a polypyrrole film deposited electrochemically onto the pH sensitive IrO_x electrode that controls the gate voltage of the MOSFET (extended gate).

ENFETs have also been fabricated on silicon substrates containing the REFET and the integrated temperature compensating CMOS circuitry as well (Saito et al., 1991; Shul'ga et al., 1995).

In multiple-enzyme sensors, several sensor elements are used with various enzymatic membranes. They are able to simultaneously monitor several sub-

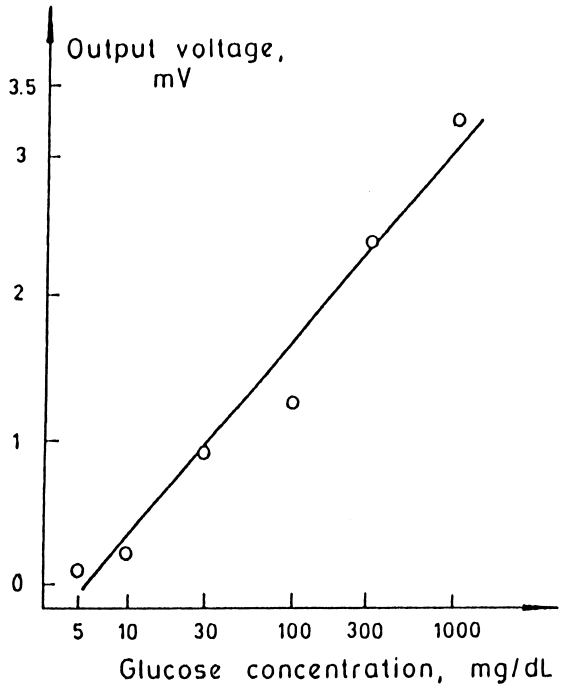

FIGURE 7.15. Characteristic of a potentiometric glucose ENFET. (Reprinted with permission from T. Katsube, M. Katoh, H. Maekawa, M. Hara, S. Yamaguchi, N. Uchida and T. Shimomura, "Stabilization of an FET Glucose Sensor with the Thermophilic Enzyme Glucokinase," *Sensors and Actuators B,* 1, pp. 504–507, ©1990, Elsevier Science S.A., Lausanne, Switzerland.)

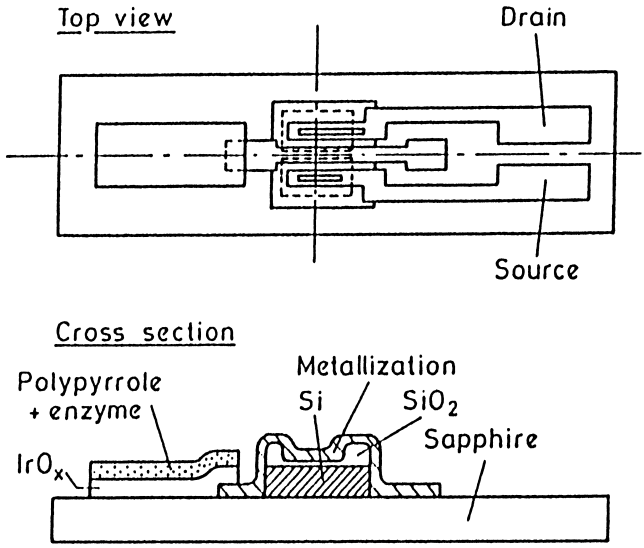

FIGURE 7.16. Structure of a glucose sensitive SOSENFET. (Reprinted with permission from T. Katsube, M. Katoh, H. Maekawa, M. Hara, S. Yamaguchi, N. Uchida and T. Shimomura, "Stabilization of an FET Glucose Sensor with the Thermophilic Enzyme Glucokinase," *Sensors and Actuators B,* 1, pp. 504–507, ©1990, Elsevier Science S.A., Lausanne, Switzerland.)

strates in the analyte. A cross talk between the individual sensor elements may result from the migration of H_2O_2 that can be suppressed with an additional membrane containing catalase enzyme reacting with H_2O_2 (Urban et al, 1994).

Glucose optrodes have also been developed with O_2, pH, and more recently with H_2O_2 transducers covered by GOD-activated membranes (Wolfbeis, 1991; Buerk, 1993). Their advantage over electronic transducers is that there is no need for mediators and electron-transferring media.

7.1.8 Urea Sensors

Just behind glucose sensors, urea sensors represent the second most developed area of biosensor research. Urea level of blood is an important indicator of kidney operation. Urea, uric acid, creatinine, and methylguanidine can accumulate in the bloodstreams of patients with renal disease, eventually reaching toxic levels if they are not removed. The detection of urea also has potential medical applications, particularly for portable hemodialysis systems for treating patients with renal disease either at home or in the hospital. A demand for combined multiple glucose-urea sensors has also emerged.

TABLE 7.1. Summary of Urea Sensors. (The Majority of Information Reproduced with Permission From Polymer Films in Sensor Applications *by G. Harsányi, ©1995, Technomic Publishing Co., Inc., Lancaster, PA, p. 384.)*

Transducer	Membrane	Urease Immobilization	Detection Range, M/l
NH_4^+-ISFET (Miyahara et al., 1991)	PVC + ionophore	cross-linking	10^{-6}–10^{-1}
pH-ISFET+REFET (Van der Schoot et al., 1990)	PAA	entrapment	10^{-3}
pH-electrode (Glab et al., 1993a)	aminated PVC	cross-linking	10^{-4}–10^{-1}
pH-electrode (Glab et al., 1993b)	carboxylated PVC + ionophore	cross-linking	10^{-4}–10^{-1}
Pt/*n*-GaAs Schottky-diode for NH_3 (Lechuga et al., 1992)	polyetherimide	adsorption	$4 \cdot 10^{-4}$
pH-optrode (Gauglitz and Reichert, 1992)	PAA + phenol red	entrapment	$4 \cdot 10^{-5}$–$25 \cdot 10^{-5}$
pH-optrode (Brennan et al., 1993)	polysiloxane + fluorescent dye	covalent	$4 \cdot 10^{-5}$
Conductimetric (Watson et al., 1987)	polyimid-azole	cross-linking	10^{-2}

Urea is catalyzed by urease enzyme according to the following reaction (Miyahara et al., 1991):

$$CO(NH_2)_2 + H_2O \xrightarrow{\text{urease}} 2NH_3 + CO_2, \tag{7.22a}$$

which may be followed by secondary reactions in aqueous solutions:

$$NH_3 + H_2O \longrightarrow NH_4^+ + OH^- \tag{7.22b}$$

$$CO_2 + H_2O \longrightarrow HCO_3^- + H^+ \tag{7.22c}$$

The reaction products enable a number of transduction methods for preparing urea biosensors. In conventional urea sensors, pH electrodes, ammonium-

ion-selective electrodes, ammonia gas sensors, or carbon dioxide sensors have been used to detect the variations indirectly. The principles were also adapted to the urea microsensors in which an ISFET, a microelectrode, or an optrode is used as the transducer. Even conductimetric types have been developed based on the global conductivity measurement of an electrolyte within a microreactor chamber. Table 7.1 summarizes a few recently developed urea sensors.

The response of urea sensors based on the measurement of pH changes caused by the enzymatic membrane depends on the buffer capacity and initial pH of the sample solution. Urea-ENFET and pH-REFET pairs have successfully been used to compensate the effect of initial external pH (Van der Schoot et al., 1990).

The maximum achieved sensitivity of the potentiometric sensors is 55 mV/decade, which is a good approximation of the Nernstian behavior (59 mV/decade at room temperature). Conductimetric sensors are operated with AC voltage in kinetic mode. They measure the current rate, not waiting for the equilibrium state (see Section 7.1.2). Optrodes operated with phenol red pH indicator dye have the disadvantage of a limited detection interval due to the narrow pH-sensitive range of the dye (see Section 6.1.4).

7.1.9 Other Enzymatic Sensor Types

Several review studies in early nineties tried to estimate the number of available enzymatic biosensor prototypes—it was over 100 already at that time (Coulet et al., 1991; Buerk, 1993). Thus, an entire overview is simply impossible to provide here, only the most important types are summarized in Table 7.2.

In clinical practice, those sensor types have great importance in that they might be used for continuous monitoring of one or several blood components that have importance in some kind of diagnosis. A few examples are listed as follows:

- creatinine and uric acid (as well as urea) in kidney diseases
- L-lactate (a by-product of insufficient muscle operation) in monitoring athletes, or heart disease
- cholesterol and free fatty acids in preventing arteriosclerosis and related diseases
- amino acids (arginine and tyrosine) in special diseases
- alcohol in treating alcoholism
- acetylcholine in indicating parasympathetic stimulation
- penicillin in pharmacology
- ATP in muscle operation, metabolism, and the operation of nerves

TABLE 7.2. Important Enzymatic Biosensor Types. (Sources: Coulet et al., 1991; Schubert et al., 1991; and Buerk, 1993—courtesy of Marcel Dekker Inc. and Technomic Publishing Co., Inc.)

Substrate	Enzyme(s)	Cofactor(s)	Transducer Type
Creatinine	Creatininase	—	NH_3, NH_4^+
Uric acid	Uricase	O_2	N_2O_2, CO_2
Xanthine	Xanthine oxidase	O_2	H_2O_2
L-Lactate	Lactate oxidase	O_2	H_2O_2
L-Lactate	Lactate dehydrogenase	NAD	pH, NADH (fluorescent or amperometric)
Galactose	Galactosidase	O_2	H_2O_2
L-arginine	Arginine deaminase	—	NH_3, NH_4^+
Tyrosine	Tyrosine decarboxylase	—	CO_2
L-amino acid	L-amino acid oxidase	O_2	NH_3, NH_4^+, H_2O_2
Cholesterol	Cholesterol oxidase	O_2	H_2O_2
Acetylcholine	Acetylcholine esterase	—	pH
Acetylcholine	Acetylcholine esterase	O_2	H_2O_2
Penicillin	Penicillinase	—	pH
Alcohol	Alcohol oxidase	O_2	H_2O_2
Alcohol	Alcohol dehydrogenase	NAD	pH, NADH (fluorescent or amperometric)
Glucose	Glucose dehydrogenase	NAD	pH, NADH (fluorescent or amperometric)
α-D-Glucose	Mutarotase + GOD	O_2	H_2O_2
Sucrose	Invertase, mutarotase, GOD	O_2	H_2O_2
Free fatty acids	Acyl-CoA synthetase, acyl-CoA oxidase	ATP, Mg^{++}, O_2	H_2O_2
ADP (adenosine-diphosphate)	Hexokinase, pyruvate kinase, glucose-6-phosphate dehydrogenase	phosphoenol-pyruvate, glucose, NAD	pH, NADH (fluorescent or amperometric)
ATP (adenosine-triphosphate)	Luciferase	luciferin, O_2, Mg^{++}	chemiluminescent

Several bi- and tri-enzymatic types are listed in the table. Their application is necessary if a single enzymatic reaction does not lead to any reaction product detectable by well-established transduction methods. An interesting example is the case of sucrose, when the first enzymatic reaction gives the product α-D-glucose. This cannot be detected by a glucose sensor operated with

GOD, first it must be transformed into β-D-glucose by the catalytic effect of enzyme mutarotase.

Another interesting example is the sensing of uric acid. Uricase catalyzes its oxidation in slightly alkaline solutions, producing allantoin, hydrogen peroxide, and carbon dioxide; the production of hydrogen peroxide can electrochemically be detected using amperometry (Shaolin, 1994). Since uric acid dissociates in aqueous solutions, it may interfere with the electrochemical processes. Therefore, a specially designed differential amperometric (bipotentiostatic) measurement has been developed using an enzymatic polypyrrole and a pure polypyrrole film deposited electrochemically on precious metal thick-film electrodes (Dobay et al., 1999).

Cholesterol sensors also have application prospects. Promising results were published when immobilizing cholesterol oxidase into polypyrrole films (Vidal et al., 1999).

Since the various sensor types apply a number of membrane types and immobilization techniques, listing their sensitivity parameters in the table makes no sense here.

7.1.10 Application Prospectives of Enzymatic Biosensors

The most important application fields of biosensors were mentioned in the first paragraphs of this chapter.

Biomedical areas include the following:

- continuous monitoring in clinical practice
- pharmacology, adjusting personal dosage and researching new medicines
- portable and home monitors for patient self-control
- implantable sensors for continuous monitoring in everyday life
- implantable sensor-actuator systems that may replace the hormonal regulating function of one of the endocrine glands

As was already mentioned in connection with glucose sensors, the first two fields are still dominated by conventional analytical methods. The practical application of sensors is spreading in portable and home monitors, and implantable monitoring sensors are in the first stage of practical application, while the long-term operating implantable regulating systems are in the research and development stage. It is important to mention here that miniature, electronically controllable medicine pumps have already been realized with silicon micromachining for continuous medicine delivery, however, there is a lack of long-term operating reliable biosensors. Thus, the realization of implantable regulating systems is hindered mainly by the instability and short lifetime of the biosensor elements.

Recently, an important research area is concentrating on body-sensor interface realization problems. Intravascular application of sensors, placing sen-

sor elements into the bloodstream, is not an appropriate approach for long-term monitoring. Taking blood samples for analysis does not enable a continuous operation of the system. *Subcutaneous implantation* seems to be the most promising approach nowadays, when the sample-taking dialysis cell or the sensor element itself is placed into the subcutaneous tissue, mainly in the abdominal fat of human bodies. The analyte is actually the tissue liquid and not the blood in this case.

Figure 7.17 shows three versions of the subcutaneous technique (Fischer and Freyse, 1993). Based on the principles of diffusion, microdialysis is a method for removing chemical substances from the extracellular fluid of the body without removing any liquid (Harsányi, 1995). The double-lumen microdialysis probe using hollow fibers (e.g., polysulphonic or cellulosic, generally with a molecular weight cut-off size of 15,000–20,000) functions as an artificial blood vessel. A physiological buffer solution is pumped at a constant flow-rate (1–100 μl/min) into the fiber placed subcutaneously and retrieves compounds of low molecular weight [see Figure 7.17(a)]. The dialysate of the tissue is subjected to investigation by analytical methods. If, for example, GOD is contained in the dialysate, the resulting pO_2 in it may be taken as a measure of glucose concentration using sensors for determining it (Mascini et al., 1992).

According to other approaches, the enzyme is immobilized onto the transducer surface, forming a real biosensor (Volpe et al., 1995; Steinkuhl et al., 1996). In both cases, however, the measurement is dependent on the flow-rate, pressure, active membrane surface, etc. In recent practical solutions, the probe is connected to a specially designed micromachined silicon/glass chip flow-through cell containing the integrated biosensor together with a system of capillaries and flow channels where the dialysate is pumped through (Steinkuhl et al., 1996). The electrodes of the electrochemical biosensor are located in two pyramid-like microcontainments etched through the silicon by anisotropic etching (see Appendix 5). The amperometric current may be measured with miniaturized amplifier electronics with LCD displays that has been developed to result in a handheld monitoring system with the overall size of a cigarette packet.

If an appropriately low pressure (vacuum) is applied to the subcutaneously inserted tubing of a sufficiently high molecular weight cut-off ultrafiltration membrane (Harsányi, 1995), the interstitial fluid may be sampled and analyzed directly [see Figure 7.17(b)].

According to the third version, the sensor element is directly implanted [see Figure 7.17(a)] (Pickup, 1993).

Until now, nearly all devices were laboratory-designed and -manufactured. In considering time constants, microdialysis probes may provide an excellent description of glucose kinetics in subcutaneous tissue over relatively short in-

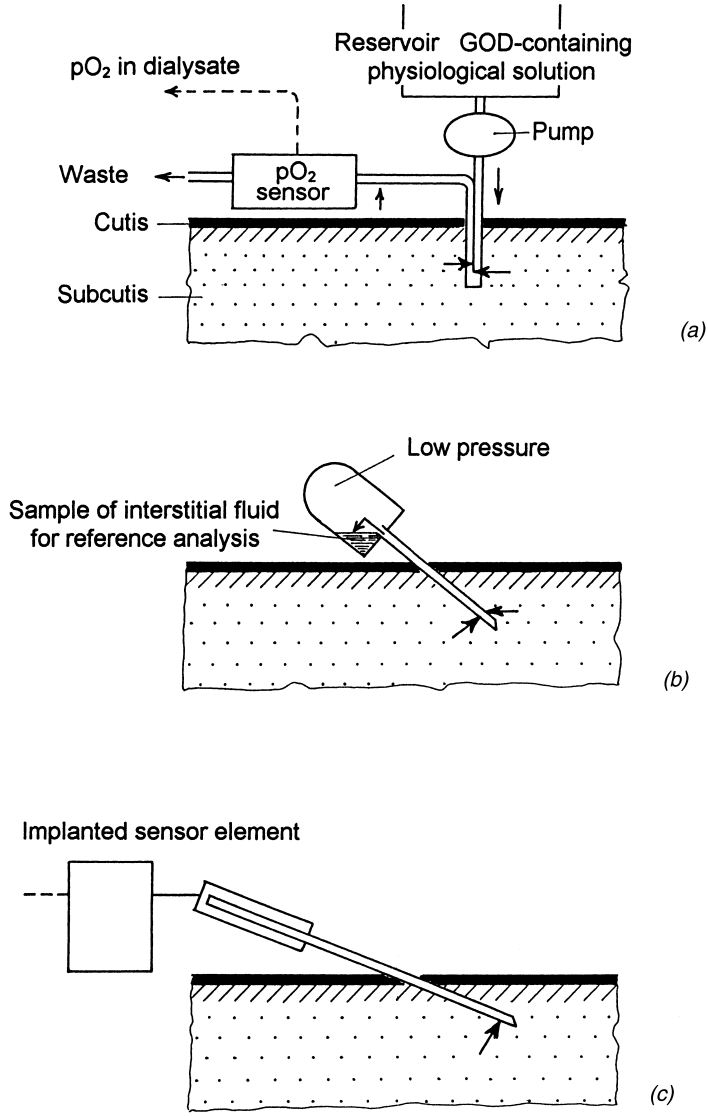

FIGURE 7.17. Various techniques of the subcutaneous implantation method: (a) microdialysis, (b) ultrafiltration, and (c) direct implantation (Fischer and Freyse, 1993).

tervals. But, any figure on the absolute glucose level can be obtained only retrospectively. In contrast, the ultrafiltration technique may reveal the real glucose concentration in the subcutaneous interstitial fluid, but at relatively large intervals. All sample-taking methods suffer from a slow alteration of real subcutaneous conditions. On the other hand, for the practical application of direct implantation of the sensor itself, a number of biocompatibility problems, such as fibrosis, blood clotting, and immunogenic effects, as well as the toxicity of the enzyme or mediator leakage (also see Chapter 8) have to be overcome.

A discussion about biosensors cannot be complete without mentioning their application possibilities in some fields other than biomedicine. In the *food processing industry,* it is anticipated that there will be increased commercial applications for biosensors for monitoring the quality of different production methods (Buerk, 1993). Fermentation processes are essential in a number of food production methods, and these processes might result in the production of glucose and a number of similar compounds (such as sucrose, fructose, lactose, maltose, etc.). The continuous monitoring of these compounds may have great importance for testing the reproducibility and for quality control of food processes. The short lifetime of enzymatic biosensors as a limiting factor can be overcome if the application is designed for only a few measurement cycles.

One frequently mentioned example is the fish freshness sensor developed recently in Japan (Watanabe and Tanaka, 1991). The ATP in the fish breaks down in a seven-step reaction to result in the formation of uric acid as tissue undergoes enzymatic autolysis and eventual spoilage. The depletion of high-energy phosphates (ATP, ADP, etc.) and accumulation of inosine and hypoxanthine alters the taste and quality of the meat. The chemical species for the last stages of the process were monitored by the sensor using four enzyme-modified O_2 electrodes, the signals of which were measured and digitized by a computer. The fish freshness factor was defined as the ratio of inosine and hypoxanthine concentration over the overall concentration of all seven components taking part in the breakdown process.

Enzymatic biosensors are beginning to have further applications for the *analysis of environmental contaminants* in air, water, and soil. Contaminants such as heavy-metal ions (Zhylyak et al., 1995), organophosphorous pesticides, and carbamates (Yuan et al., 1991; Cagnini et al., 1995) (that have widely been used for pest control in the agricultural industry for many years) can be detected by enzymatic biosensors based on their inhibition effect on enzymatic reactions [see Equation (7.20)]. For the operation, these sensor types need measurement media saturated with the substrate of the applied enzyme. Such enzyme types are useful for these sensor purposes that show reversible reaction with the inhibitor to be detected, or the enzyme can be refreshed easily for a subsequent measurement cycle. Figure 7.18 shows the typical charac-

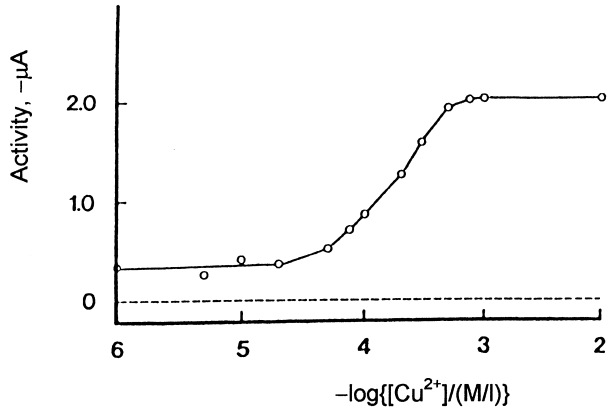

FIGURE 7.18. Typical characteristic of a Zn/Co/Cu ion sensor based on enzyme inhibition. (Reprinted with permission from I. Satoh and Y. Iijima, "Multi-Ion Biosensor with Use of a Hybrid-Enzyme Membrane," *Sensors and Actuators B,* 24–25, pp. 103–106, ©1995, Elsevier Science S.A., Lausanne, Switzerland.)

teristics of a Zn/Co/Cu ion sensor based on enzyme inhibition (Satoh and Iijima, 1995).

Some more details about the application problems of biosensors can be collected from several recent monographs (Freitag, 1996; Fraser, 1997; Cunningham, 1998; Diamond, 1998; Ramsay, 1998; Spichiger-Keller, 1998; Scheller and Schubert, 1999; Valarcel and de Castro, 1999).

7.2 AFFINITY BIOSENSORS

The basis of affinity sensors is the selective chemical binding between high-molecular weight biochemical substances. Practically, immunosensors based on antigen-antibody reactions were the first group and even nowadays are the major group in this field, although, DNA sensors have also gained an important role and commercial availability since 1997. In further discussion, the focus is on immunosensors, while the special features of DNA chips are described in a separate section (see Section 7.2.4).

There are many practical applications for immunosensors if they can be made to be reliable. They might be useful for quantifying how well the living (mainly human) immune system is functioning, and they could serve as valuable tools not only in clinical diagnostics but also in biochemical analytical methods. Although there has been a great deal of scientific research on immunosensors, which began in the early 1970s, commercial immunosensors are just beginning to emerge into the marketplace.

Since the chemical reactions in affinity sensors are often irreversible, the necessity of removing complexes and renewing transducer surfaces makes their operation somewhat different from that of the conventional sensors. Continuous monitoring is generally not realistic; thus, a quasi-continuous operation can be realized in flow-through cells, in which the transducer surface can be refreshed periodically by removing reaction-product complexes and by immobilizing new receptors onto them, subsequently. Immunosensors based on antigen-antibody reactions and DNA sensors based on the formation of double-spiral segments theoretically have very high selectivity because of the highly specific biochemical reactions that are the basis of operation. In practice, chemical binding and adsorption, or deposition of low-molecular-weight species can disturb the measurement, and thus, limit the theoretical selectivity. A number of problems similar to those of the enzymatic biosensors need to be solved before the practical realization and measurement method of affinity biosensors are implemented.

7.2.1 Operation Principles of Immunosensors

Immunology began its rapid development in the early 1950s by clarifying the nature of basic immune mechanisms and the types and structures of immune reagents, as well as the genetic correlation. Meanwhile, a number of laboratory techniques have been developed to perform qualitative and quantitative analysis of immune reagent materials.

The human immune system is extraordinarily complex, and antigen-antibody reactions are not fully understood at the present time. Antigens (AGs) are objects (molecules, viruses, bacteria) that are recognized by living systems, and an immune reaction is provoked by them. Antibodies (ABs) are Y-shaped glycoprotein molecules that are composed of equal numbers of heavy and light polypeptide amino-acid chains held together with disulfide bonds. These highly specialized immunoglobulin (Ig) proteins are produced by living cells against antigens and are able to recognize and bind only certain types of antigen molecules at receptor sites on the tip of each arm to form antigen-antibody complexes:

$$\mathrm{AB} + \mathrm{AG} = \mathrm{AB\text{-}AG} \tag{7.23}$$

Antibodies are divided into five classes (IgG, IgA, IgM, IgD, and IgE) according to their heavy chain structure. According to the number of receptor sites per antibody molecule, the following types are distinguished:

- monoclonal antibodies that have a single receptor site
- polyclonal antibodies that are able to bind several antigens

Immunoassays are processing sequences used in analytical chemistry for detecting objects by means of immune reactions. Antibodies are generally extracted from animal blood after immunization. Some types can be manufactured in relatively large quantities without great expense by exposing cultured cells or microbes to an antigen.

A useful method of the immunoassays is to immobilize receptor (antigen or antibody) molecules on a solid-state surface and follow the effect of AB-AG complex formation. This is also adapted for immunosensors, where the receptors are immobilized on the transducer surface, and the complex formation gives the transduction effect. Immunosensors can be developed by incorporating antigens or antibodies on the surface, although the latter design is used most often. Since the association and dissociation factors of antigen-antibody reactions correspond to relatively large response times (1–30 minutes!) in comparison with conventional chemical reactions, equilibrium can only be reached after a long time delay even when the complex formation is reversible. In irreversible processes, the transient behavior may have great importance in the evaluation. Independent from the reversibility, the quick refreshment of the transducer surface is often necessary, which means removing the complexes from the surface and immobilizing new receptors onto it. With irreversible immunoreactions, only a single immunoassay is possible without refreshing. Considerable research efforts have been directed toward the development of renewable receptor surfaces so that repetitive immunoassays can be made without loss of sensitivity (Buerk, 1993).

Immunosensor assays can be divided into two major categories: direct or nonlabeled types that rely on some change in physical properties in the transducer caused directly by the AB-AG formation, and indirect or labeled types that rely on the detection of chemical labels or markers bonded onto the analyte molecules. Figure 7.19 illustrates the characteristic chemical process sequences for various immunosensor operation modes. The direct operation is shown in Figure 7.19(a). At first, an interface layer (polysiloxane, protein molecules either cross-linked with glutaraldehide or embedded into a polymer film) appropriate for receptor immobilization is deposited onto the transducer surface, and the receptors are subsequently bound. During the operation, complex formation on the surface is followed by various methods.

The labeled operation differs from the former one in that the analyte molecules have specific chemical labels artificially coupled to them for detection. Figure 7.19(b) shows the competitive case, when the labeled antigens added to the measurand analyte in a well-known concentration are competing for the receptor sites with nonlabeled antigens, the concentration of which has to be determined. In equilibrium, the surface concentration ratio of labeled and nonlabeled antigens corresponds to their ratio inside the analyte. The transducer output is a function of the surface label concentration, from which the nonla-

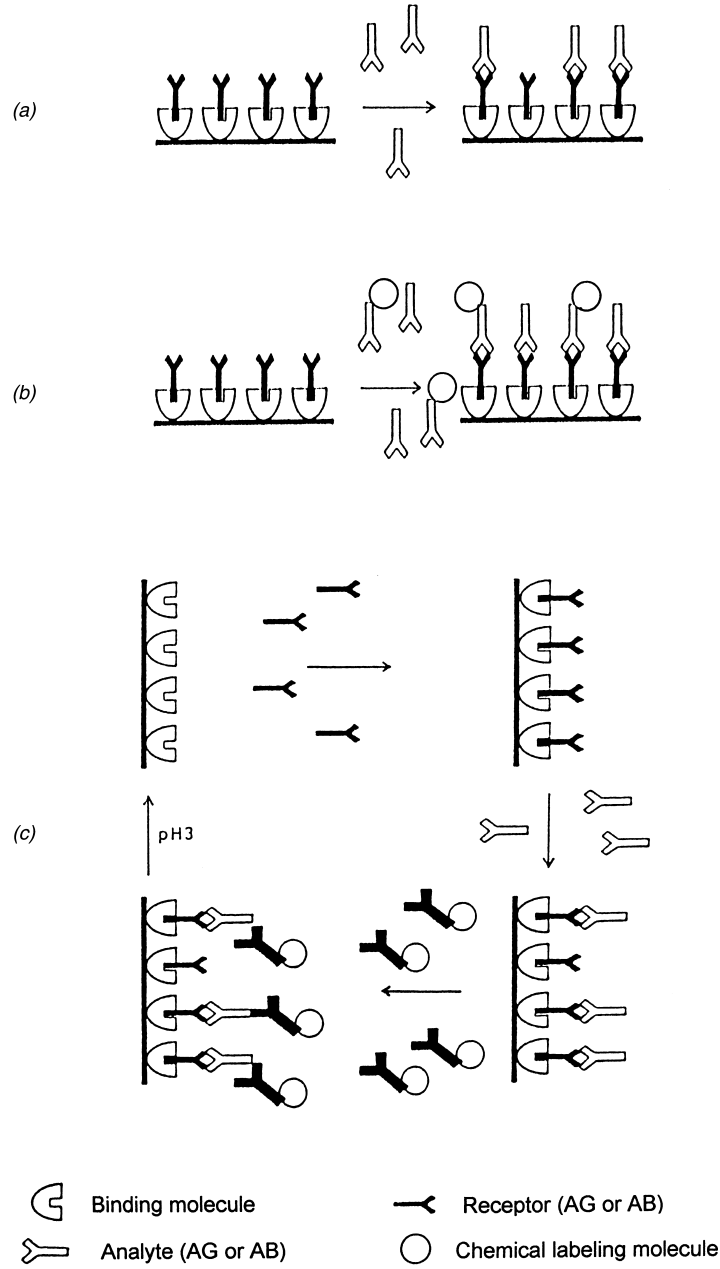

FIGURE 7.19. Complex formation mechanisms used in immunosensors: (a) direct, (b) indirect (labeled) competitive methods, and (c) the overall assay cycle of the indirect sandwich technique. [Reprinted with permission: (c) from C. Collapicchioni, A. Barbaro, F. Porcelli and I. Giannini, "Immunoenzymatic Assay Using CHEMFET Devices," *Sensors and Actuators B,* 4, pp. 245–250, ©1991, Elsevier Science S.A., Lausanne, Switzerland.]

beled antigen concentration originally present inside the analyte can easily be calculated. An important feature of this saturation method is that it can successfully be used even in irreversible complex formation processes. An important condition is that the chemical label must not alter the complex formation properties of labeled antigens.

Figure 7.19(c) illustrates a whole measurement cycle of the more complicated immunometric sandwich technique that can be used only for polyclonal analyte molecules. In the first step, the analyte molecules are bound to the receptors and then, in the second step of the process, labeled or nonlabeled receptor molecules are bound to them, forming a receptor/analyte/receptor molecular sandwich structure on the transducer surface. A new assay can be started when the complexes are removed by an acidic solution, and new receptors are immobilized. Both direct and indirect transduction methods can be used in combination with the sandwich technique. The figure illustrates the labeled indirect process.

Biomedical application of immunosensors include the detection of the following compounds:

- special medicines: digoxin, theophylline, antiepileptics, etc.
- hormones: LH (luteinizing hormone), FSH (follice-stimulating hormone), HCG (human chorionic gonadotrop hormone), TSH (thyrotrop stimulating hormone) prolactin, T_3 (triiodothyronine), T_4 (thyroxine), etc.
- steroids: testosterone, progesterone, estriol
- proteins: ferritin, HSA (human serum albumin)
- immunocompounds: immuno-globulins (IgG, IgE), HIV (human immunodeficiency virus) antibodies, etc.
- tumor markers
- metabolites

More details of potential applications are described in recent monographs about biosensors (Freitag, 1996; Fraser, 1997; Cunningham, 1998; Diamond, 1998; Ramsay, 1998; Spichiger-Keller, 1998; Scheller and Schubert, 1999; Valarcel and de Castro, 1999).

In the following sections, the indirect and direct operation mode transducers will be surveyed.

7.2.2 Indirect (Labeled) Immunosensors

The actual design of indirect transducer types is determined by the nature of chemical markers used for labeling antigens and antibodies. Labeling and related immunoassay methods of analytical chemistry are as follows:

- In RIA (radioimmunoassay), the labels are radioactive isotopes (for example, ^{125}J for T_3/T_4 analysis). The technique enables the application of

radiation detectors (see Section 4.11) as demonstrated in connection with the *in vitro* application of a tritium sensor APDs (see Section 5.5.4). Real immunosensors can be fabricated by combining radiation detectors with immobilized receptor films; their application, however, has not become a real part of practice due to the inconveniences of radioactive labeling.

- In EIA (enzyme immunoassay), otherwise called ELISA (enzyme-linked immunosorbent assay), enzyme molecules are used for labeling, and the transducer signal is provided by the enzyme-substrate reaction. This technique is very popular in recent immunosensor examples.
- In FIA (fluorescent immunoassay) and LIA (luminescent immunoassay), fluorescent or chemiluminescent dyes are applied for labeling in combination with optical transducers for signal generation.
- There are further methods that have found applications in immunosensors, such as labeling with ionic compounds combined with electrochemical transducers, signal amplification with liposomes, and labeling with magnetic dipoles.

Several widely used or recently developed examples of indirect immunosensors are given below.

A frequently used technique for fabricating immunosensors is the combination of *ELISA with electrochemical transducers.* Figure 7.20 shows the schematic structure of an immunosensitive electrode, where a membrane with immobilized antibodies is placed onto an amperometric probe (Macholán, 1991). The probe is then immersed in the buffered mixture of nonlabeled antigen to be assayed and a known amount of enzyme-labeled antigen; two competitive reactions take place on the electrode membrane during the bathing period. When adsorption equilibrium is reached, the probe is thoroughly washed to remove the nonspecifically adsorbed antigens, and then it is put into a solution containing the substrate for determining the initial rate of reaction catalyzed by the enzyme complexed on the electrode surface (in the figure, the case of catalase labeling and H_2O_2 substrate is illustrated). The amperometric detection of the reaction product O_2 is performed with a conventional Clark cell. The amperometric signal corresponds to the concentration of nonlabeled antigen within the sample solution.

GOD is also an often-used labeling enzyme. A glucose solution saturated for the enzyme must be applied during the evaluation, which can be performed amperometrically using the electrochemical decomposition of either O_2 or H_2O_2.

Figure 7.21 (Aberl et al., 1991, 1992) shows an interesting recent example developed by the Fraunhofer Institute: an ISFET pair and a connected flow-injection system for detecting HIV-antibodies. The sample is transported by the continuous carrier stream into the reaction cartridge where the HIV-anti-

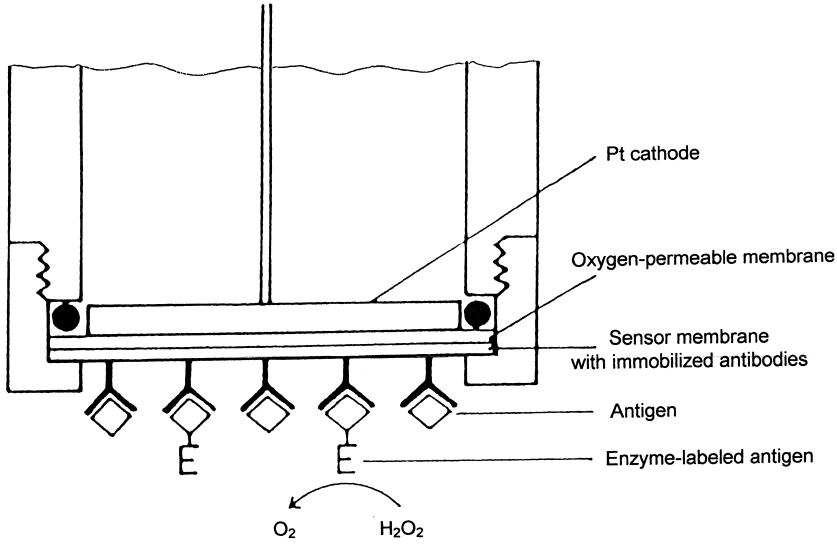

FIGURE 7.20. Schematic representation of an enzyme immunoelectrode based on membrane-bound antibodies, and its mode of operation. (Reprinted after Macholán, 1991, p. 353, courtesy of Marcel Dekker Inc., New York.)

bodies can react with p24 peptide antigens immobilized in a nitrocellulose membrane. For the recognition of immunoprecipitates, the sandwich ELISA procedure was applied using specific urease-labeled anti-antibodies. The enzyme urease yields a pH-shift in the presence of urea, which can be detected by means of an ISFET. The second ISFET acts as a REFET for compensating pH and temperature variations of the carrier solution. Figure 7.21(b) shows the calibration curve. Actually, the system applies a pH-sensing ISFET-REFET pair that can be used for a great number of measurement cycles. The immunoreaction takes place inside the reaction chamber, the membrane of which is disposable. The evaluation is made using a computer. This technique has a number of advantages over the conventional immunoassays used for HIV tests, such as its low cost and fast turnaround. It would be very useful for a prescreening process before making further laboratory tests for setting up a reliable diagnosis.

Real ImmunoFETs can be prepared by immobilizing receptor molecules onto the gate-membrane of the device. The sandwich-ELISA method was used, for example, for detecting human immunoglobulin-G (h-IgG) molecules with immobilizing anti-h-IgG antigen molecules as receptors onto the gate membrane of an ImmunoFET (Colapicchioni et al., 1991). According to the sandwich method, GOD-labeled antigen was used for recognizing immunocom-

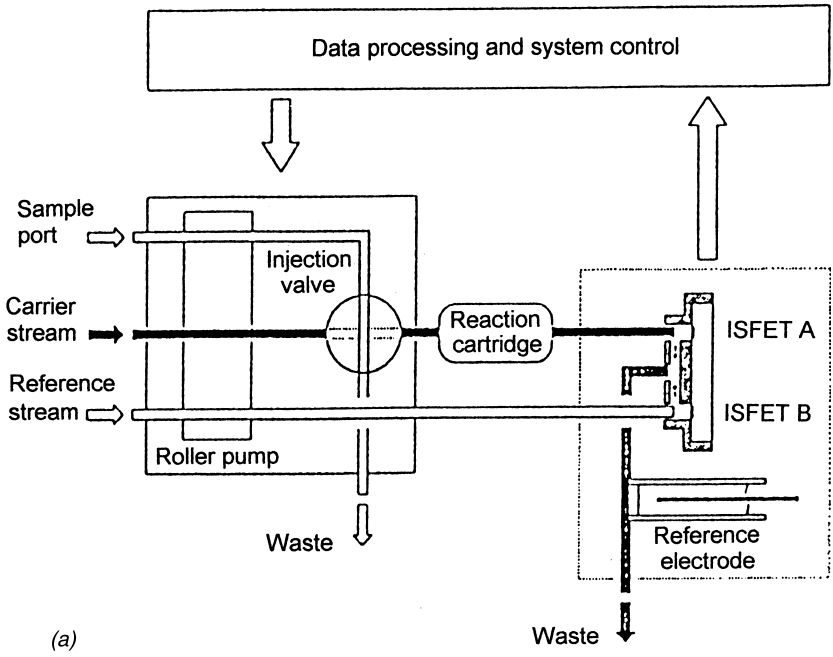

(a)

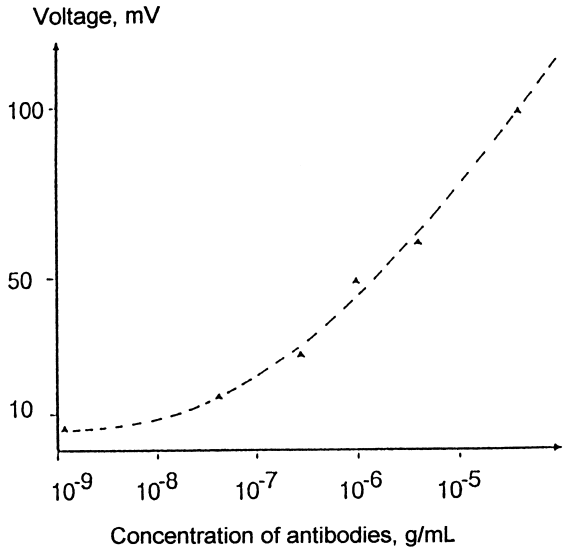

(b)

FIGURE 7.21. ISFET-ELISA flow injection system for immunosensing of HIV-antibodies: (a) block diagram and (b) calibration curve. [Reprinted with permission: (a) from F. Aberl, S. Modrow, H. Wolf, S. Koch and P. Woias, "An ISFET-Based FIA System for Immunosensing," *Sensors and Actuators B,* 6, pp. 186–191, ©1992, Elsevier Science S.A., Lausanne, Switzerland.]

plex formation and providing a pH shift in the presence of glucose [see Equation (7.21b)].

Another example for ImmunoFET operation is the ion-step method designed to measure immunoreactions via a change in charge density, which occurs in an antibody-loaded membrane deposited on an ISFET upon reaction with a charged antigen (Schasfoort et al., 1990, 1992). For detecting progesterone, anti-progesterone was immobilized into a polystyrene-agarose membrane deposited onto the gate of an ISFET. A competitive immunoassay was used by adding charged progesterone-lysozyme conjugate into the sample solution. A great advantage of this method over the ELISA is that it provides a direct potentiometric signal without a secondary enzymatic reaction.

In the case of ELISA, further well-known enzymatic effects (calorimetric effect, detection of substrate concentration, etc., see Section 7.1) can also be applied, however, they are not widespread. The greatest disadvantage is the necessary presence of enzyme substrates, sometimes also mediators, for the transduction effect. The enzymatic reaction is detected indirectly; thus, a double indirect transduction mechanism is applied. This might cause a number of erroneous readings.

Another approach for labeled immunosensors is the application of *optical transducers in combination with FIA and LIA processes.*

In the case of LIA, the chemiluminescent effect is used for detection (Kricka et al., 1984; Aizawa, 1994). Luminescent materials can be oxidized by active oxygen in basic media in the presence of a catalysator. This is followed by monochromatic light emission, the intensity of which is characteristic for the concentration of the luminescent material. In practice, luminogen molecules are used for labeling those catalyses (like the enzymes) and the light-emitting reaction between luminol and H_2O_2. When adding the basic hydrogen peroxide solution, the luminescent light emission starts immediately, reaches its maximum after a few seconds, and slowly decays exponentially. Light emission is followed by photodetection, the analysis is performed by evaluating the overall time-dependent intensity response curves. On these bases, immuno-optrodes can be fabricated by immobilizing receptors on the surface of optical-fiber tips. Excitation light is not necessary for the operation; thus, only a photodetector should be coupled to the other end of the fiber. The greatest disadvantage of this method is that the presence of luminol and hydrogen peroxide must be assured for the evaluation.

The FIA technique can also be utilized for preparing immuno-optrodes. Fluorescent dye molecules are used here for labeling that emits secondary light due to fluorescent quenching when excited by an external light source (see Section 4.16). Figure 7.22 shows the operation principles, the available structures, and a measuring setup for evanescent wave FIA immuno-optrodes (Anderson et al., 1994). The sensor structure is practically a cladding-based op-

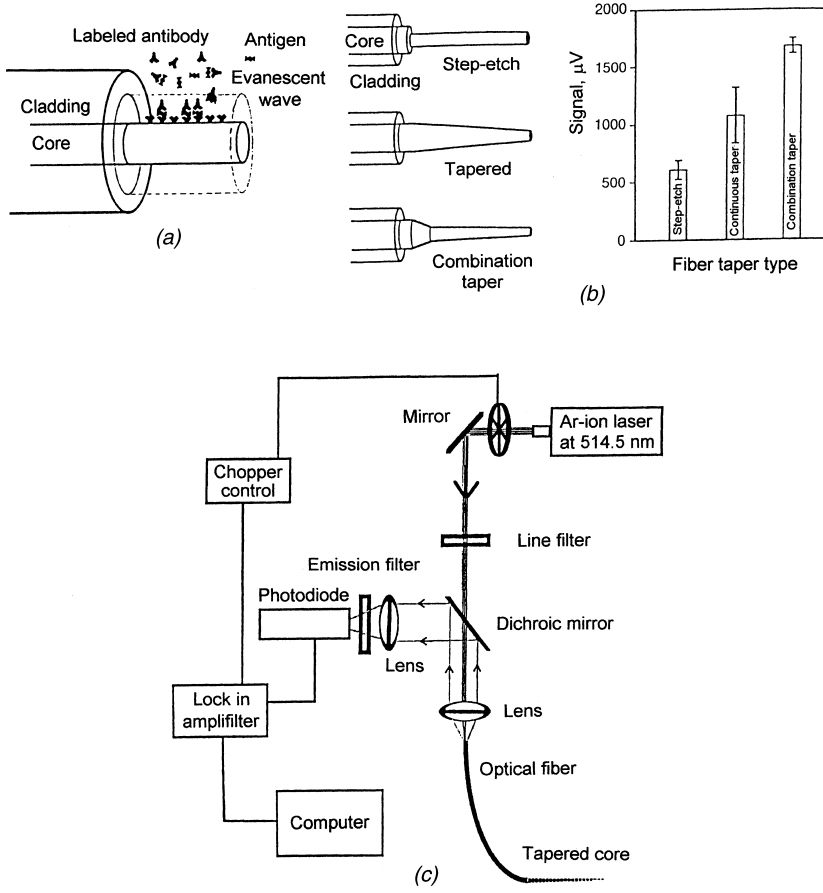

FIGURE 7.22. Evanescent-wave cladding immuno-optrode: (a) operation principle, (b) geometrical solutions and their coupling efficiencies, and (c) the measurement setup. (Reproduced with permission from G. P. Anderson, J. P. Golden, L. K. Cao, D. Wijesuriya, L.C. Shriver-Lake and F. S. Ligler, "Development of an Evanescent Wave Fiber Optic Biosensor," *IEEE Engineering in Medicine and Biology,* June/July, pp. 358–363, ©1994, IEEE.)

trode (see Section 3.6) where the original cladding of the fiber end was removed and a new cladding with fluorescent dye is formed by the immunocomplex precipitation [see Figure 7.22(a)]. The example in the figure shows a sandwich immunoassay. The receptor antibodies are immobilized onto the declad core of the optrode where the immunocomplexes are formed during the assay using labeled antibodies on the top of the sandwich. The evanescent wave effectively penetrates a distance less than one wavelength beyond the core into the surrounding medium, and this is what excites the fluorescent

molecules in the complex bound to the surface of the waveguide core. The penetration depth (d) of the evanescent wave, or the distance at which the magnitude of the electric field at the surface decays to its 1/e value, is defined as follows:

$$d = \frac{\lambda}{2\pi(n_c^2 \sin^2 \theta - n_{cl}^2)^{1/2}} \tag{7.24}$$

where λ is the wavelength, θ is the incident ray angle with the normal to the core/cladding interface, and n_c and n_{cl} are the refractive index values for core and cladding, respectively. The resulting fluorescent light couples into the declad core of the immersed optical fiber. The immersed probe acts as a waveguide with the aqueous buffer as a cladding. The coupling efficiency of the fluorescent light can be optimized with optrode geometry, as shown in Figure 7.22(b). The separation of the excited fluorescent light is possible by chopping the excitation and applying a dichroic mirror, as shown in Figure 7.22(c). The laser beam, after being modulated by the chopper, passes through the dichroic mirror and launches into the fiber via a biconvex-fused silica lens. The fluorescent light, which is generated at the declad probe regions, returns through the clad fiber and is collimated by the same lens that focused the laser light into the fiber. The fluorescent light is reflected by the dichroic mirror and focused by another lens through an emission filter onto a photodiode. The disadvantage of this technique is the complicated measurement setup. Its advantage is that there is no need for secondary chemical reactions and substrates as with the ELISA and LIA techniques.

An interesting solution of the indirect sensing operation is *signal amplification with liposomes* (Choquette et al., 1992) Liposomes are spherical-shaped artificial double-layer phospholipids that are able to close an aqueous solution inside the sphere. Liposomes can be bound to antigens with a number of labeling agents inside. The immunocomplex formation destroys the liposome bulb, therefore, the closed labels (enzyme or luminogen molecules) become free and can produce a multiplied signal. Since the labels are not bound to the immunocomplex, the application of this method in combination with transducers is limited mainly to kinetic techniques when transient signals are evaluated.

A very interesting approach is the *laser magnet immunoassay* developed by Japanese researchers for HIV tests. A suspension of AIDS virus was magnetically labeled using ultrafine magnetic dipole particles. The viruses can be concentrated at a local region by focusing an external magnetic field. This concentrated object is dissolved when the sample solution added contains HIV-antibodies. This effect can be followed using a laser to detect optical scattering changes in the sample (Buerk, 1993).

By applying magnetic transducers that follow the changes of magnetic permeability, *magneto-immunoassay* (MIA) can be performed. The feasibility of this method was demonstrated by the detection of the protein Concanavalin A (Kritz et al., 1998).

7.2.3 Direct (Nonlabeled) Immunosensors

Recently, great research efforts have been concentrated on developing direct immunosensors that can produce a signal directly from the antigen-antibody immunocomplex formation on its surface without applying labeling. The general disadvantage of this type of immunosensor is that the measurement can be disturbed by the adsorption of nonspecific particles, resulting in selectivity problems. The advantage over labeled types is, however, that there is no need for secondary chemical reagents and reactions for the transduction effect. At reversible immunoreactions, even *in vivo* monitoring can be realized. A number of transducer types have been used to fabricate direct immunosensors, but only a few groups of them seem to have sensitivity and other properties good enough for practical applications. These promising approaches and measurement techniques will be surveyed in this section, distinguished into the groups of potentiometric, amperometric, capacitive solid state, optical, and acoustic-wave transducers.

There are several types of direct *potentiometric* immunosensors. The principle of operation common to each type is that, due to the presence of several polarized sites in large organic molecules, a measurable change in electrical potential occurs when the combined surface charges are altered by the immunocomplex formation on the surface of the electrode. The following types have been fabricated (Buerk, 1993):

- *modified electrode:* the receptor molecules are immobilized directly on the electrode surface
- *modified membrane electrode:* the receptors are immobilized onto or into an ion-selective membrane deposited onto the surface of the electrode. The immunocomplex formation is followed by a transmembrane potential change due to the charge redistribution on both sides of the membrane.
- *impedance-type immunosensors:* these are based on the permittivity and/or conductivity changes of the film containing the immobilized receptor molecules when immunocomplex formation occurs
- *direct operation ImmunoFETs:* in these, the gate is controlled by the immunocomplex formation, as at the sensitive electrodes
- *immunocomplex formation* with catalytic antigens: this process may result in a pH shift around the transducer, which can be detected by pH-sensitive electrodes or ISFETs

Amperometric detection is also possible since the side chains of antigen molecules may be oxidized or reduced electrochemically, which enables their polarographic analysis. Since the reaction is more characteristic to the actual side chain than to the overall molecule, the technique is much less specific than the other ones. On the other hand, receptor immobilization and immunocomplex formation are not necessary for the transduction.

Enzymatic amperometric transducers with redox mediator blocking represent an interesting approach for immunosensors that are based on an indirect sensing mechanism, but they do not use labeling. An example for this type of operation is shown in Figure 7.23 (Umana et al., 1988). GOD with ferrocene redox mediator was immobilized in a polypyrrole film deposited onto a glassy carbon electrode that was then operated in a glucose solution saturated for the enzymatic system. The ferrocene redox mediator was conjugated with antigen as the receptor. The sensor's operation is based on the electron exchange blocking of the mediator due to the immunocomplex formation.

Capacitive solid state transducers are actually based on the phenomenon that the immunocomplex formation alters the permittivity of the surface layer. Receptor molecules can covalently be bound onto Si/SiO_2 surfaces after silylation (see Section 7.1.5). One electrode of the capacitor is the semiconductor silicon substrate, while the other is the sample solution itself that shows general ionic conductivity. Practically, the capacitance is measured by means of an AC voltage (Newman et al., 1986). *Conductimetric sensors* have also

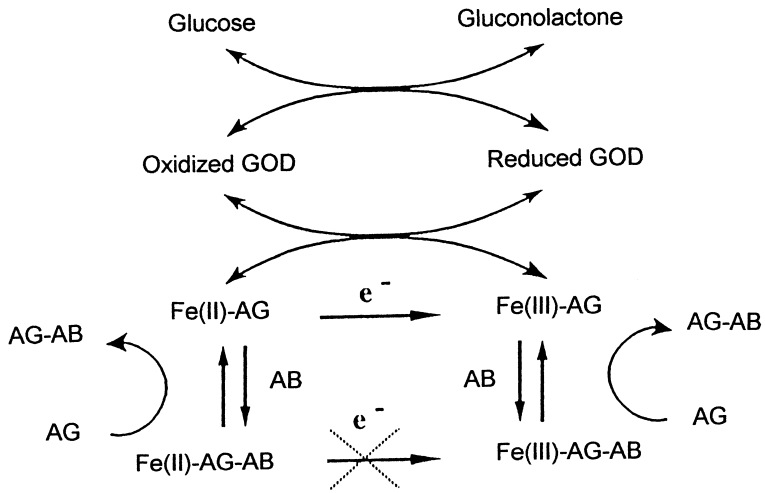

FIGURE 7.23. Reaction model of a glucose sensor operated as an immunosensor based on a redox mediator electron transfer blocking mechanism. (Reproduced with permission from Buerk, 1993, p. 168, after Umana et al., 1988.)

been realized with similar structures depositing an ultrathin (noncontinuous) Pt film onto the isolated silicon surface (Hardeman et al., 1995).

There are also several types of *direct optical immunosensor* designs (see Section 3.6).

Simple *reflection optrodes* can be realized with immobilizing receptors on the tip of an optical fiber. Their operation is based on reflectance variations due to immunocomplex formation (Sutherland et al., 1984).

Cladding optical immunosensors can be fabricated using either planar or fiber optical waveguides when immobilizing the receptors on declad waveguide surfaces. The immunocomplex formation causes refractive index variations in the surface film which results in transmission efficiency changes of the waveguide core. Since the complex refractive index is changing, it can also be followed by polarimetry (Kooyman et al., 1991) or by interferometry (e.g., by means of a Mach-Zehnder interferometer). The best detection limit can be reached with the latter types (Schipper et al., 1995).

A relatively new approach is the combination of planar grating couplers with optical waveguide lightmode spectroscopy (OWLS) (Ramsden, 1997). The basic principle of this method is that linearly polarized laser light is coupled by a diffraction grating into the waveguide layer, provided that the incoupling condition is fulfilled. The incoupling is a resonance phenomenon that occurs at a precise angle of incidence, which depends on the refractive indices of the analyte at the surface (Tiefenthaler, 1992). When immobilizing receptor molecules onto the grating surface, the formation of immunocomplexes causes a refractive index change of the film. In the waveguide layer, the light is guided by total internal reflection to the ends where it is detected by photodiodes. By varying the angle of incidence of the light, the mode spectrum can be obtained, from which the effective refractive indices are calculated for the electric and magnetic modes. Sensor chips are fabricated onto glass substrates by depositing the waveguide film using a sol-gel technology. OWLS sensors became commercially available during recent years (MicroVacuum, 1998).

Highly sensitive detection can be realized with the *surface plasmon resonance (SPR)* method (Liedberg et al., 1995). Since the conventional Kretschmann configuration [see Figure 3.10(f)] is rather complicated in biosensor applications, a new optrode transducer structure combined with the SPR spectroscopy (SPRS) measurement method has been developed recently, as shown in Figure 7.24 (Katerkamp et al., 1995). The cladding of a multimode fiber (with a diameter of 400 μm) was removed over a length of 5 mm at the end zone. The fiber core was then covered by a silver film and a chrome mirror was deposited onto the fiber tip. Surface plasmons are excited by polychromatic light, and the resonant excitation is detected as an intensity minimum in the measured output spectrum at a certain wavelength. The transducer is sensitive to changes of the refractive index and thickness of the layer that is deposited on it.

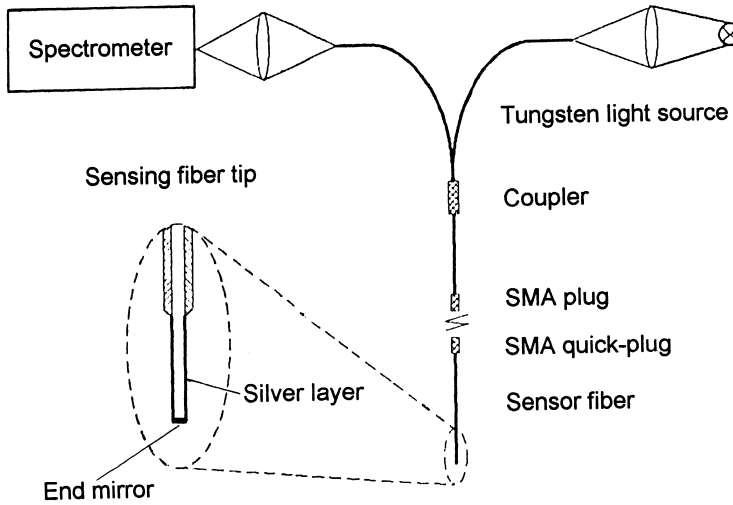

FIGURE 7.24. Application of surface plasmon resonance spectroscopy (SPRS) in optrode style immunosensors. (Reproduced with permission after Katerkamp et al., 1995, from the *Proceedings of SENSOR '95.*)

A similar construction became commercially available recently. In this "BIACOREprobe" device, the SPR phenomenon occurs in a gold film at the tip of a sensor probe. White light passed into the optical fiber of the probe is totally internally reflected at the surface interfaces. Biomolecular binding events cause changes in the refractive index close to the surface, and the wavelength of the reflected light intensity minimum shifts. By monitoring the output spectrum of the reflected light, the sensor is able to detect biomolecular binding occurring at the probe surface (http://www.biacore.com).

The SPRS optrode seemed to be the most promising candidate of direct optical immunosensor designs for highly sensitive practical applications for several years, however, recent advancements of conventional planar devices enabled the commercial availability of sensor arrays, called BIACORE chips (Jönsson et al., 1991; Alfthan, 1998). The sensor chip follows the Kretschmann configuration where the sample is injected into a flow-through cell. The signals (minimum intensity reflection angles) are generally followed kinetically (http://www.biacore.com).

Almost all types of *acoustic wave-based transducers* can be applied for immunosensor purposes. With the highly sensitive SPR and interferometric types, BAW and SSBW transducers (see Section 3.3) are the most sensitive. Table 7.3 summarizes the properties of the most promising direct immunosensor approaches.

Recently, some efforts have been concentrated on comparing optical and acoustic transducers. This comparison is realistic only if the same receptors

TABLE 7.3 Properties of Direct Immunosensor Types.

Transducer Type	Analyte	Detection Limit, μg/ml
Mach-Zehnder (Heideman et al., 1993)	HCG[1]	1
SPRS (Katerkamp et al., 1995)	FABP[2]	0.1
SPR (Löfås et al., 1991)	IgE[3]	0.1
SPR (Aldinger et al., 1998)	Staphylokinase IgA protease	50 nM/l —
SPR (O'Brien et al., 1999)	Anti-biotin	—
BAW (QMB) (Aberl et al., 1994)	HIV-antibodies	0.5
BAW (QMB) (Sakai et al., 1995)	HSA[4]	1
SSBW + PMMA (Gizeli et al., 1992)	anti-IgG	5–10
SH-APM (Andle et al., 1993)	IgG	0.02

[1]HCG = human chorionic gonadotropin (pregnancy) hormone
[2]FABP = fatty acid binding protein, characteristic in heart infarcts
[3]IgE = Immunoglobulin-E, characteristic of allergy
[4]HSA=human serum albumin, characteristic of diabetic nephrosis

are immobilized, and the immobilization technique is similar. This is true mostly for the SPR and BAW types, since quartz is a good medium both for acoustic and optical waveguide purposes, and the immobilization takes place on SiO_2 surfaces in both cases (Kösslinger et al., 1995). A considerable difference between the two sensor types has not been found when comparing the detection limits. The advantage of the SPR type is the small sensing area that is able to detect a very low number of immunocomplexes. BAW sensors have a much larger sensing area and, their signal-to-noise ratio is better by one order of magnitude.

A comparative study of spectral and angle-dependent SPR devices has been made (Aldinger et al., 1998). Generally, the angle-independent detection is less prone to interferences by vibrations.

7.2.4 DNA Sensors

DNA sensors, the most sophisticated transducers with molecular receptors, became available by combining the latest results of modern microbiology,

supramolecular organic chemistry, and sensorics. Actually, they form a special family of affinity sensors; their operation is based on specific chemical reactions similar to the immunosensors.

The use of nucleic acid recognition layers in biosensor design represents a new and exciting area in analytical chemistry. Such recognition layers add new and unique dimensions to the arsenal of modern biosensors. In particular, DNA hybridization biosensors offer considerable promise for obtaining sequence-specific information in a faster, simpler, and cheaper manner compared to traditional hybridization assays. Thanks to these advantages, great progress has been made in their research, and several types are commercially available (http://www.affymetrix.com, http://www.nanogen.com). Such devices possess great potential for numerous applications, ranging from decentralized clinical testing, to environmental monitoring, food safety, and forensic investigations.

In the first realized sensors, DNA spirals were immobilized onto transducer surfaces and the formation of the double-spiral DNA structure, as well as the binding process of protein or amino-acid molecules could be followed by signal variations. DNA molecules are specific to their counterparts and to proteins built-up of amino-acid sequences according to DNA "encoding." The basis for nucleic acid hybridization devices is the DNA base pairing, namely, the strong interaction between two complementary nucleic acid strands. Accordingly, such devices rely on the immobilization of a single-stranded (ss) DNA molecule ("the probe") for hybridizing with the complementary ("target") strand in a given sample (containing also noncomplementary nucleic acids) (Wang, 1998).

Various transduction modes, including optical, gravimetric, and electrochemical, have been used. Highly sensitive direct methods have been the first candidates in sensor designs. Sensors were realized using the dual-delay-line SH-APM transducer (see Section 3.3) with immobilizing DNA molecules of cytomegaloviruses onto its surface (Andle et al., 1995). The sensitivity was found to be -115 (± 5) ppb/ng (relative frequency shift per mass change). At these sensors, the sensitivity is strongly influenced by the thickness of the immobilization film. Good results have been achieved with diacetylene-acid films deposited by LB-technique. The immobilization of DNA molecules is possible, similar to the enzyme molecules, through carboxylic groups synthesized onto the surface of the transducer (Karymov et al., 1992). Embedding DNA or peptide molecules into electrochemically synthesized polypyrrole film deposited onto silicon chips was also successful (Livache et al., 1998).

Later, numerous direct transduction methods were applied, similar to the immunosensors, including potentiometric (Wang et al., 1996 and Wang et al., 1997), amperometric (Hashimoto et al., 1998), voltammetric (Oliveira Brett et al., 1998; Palecek et al., 1998), SPR, QMB (Caruso et al., 1997) and grat-

ing coupler evanescent wave (Bier et al., 1997) sensors. Indirect operation sensors generally apply fluorescent labeling (Vo-Dinh, 1998) and sometimes chemiluminesce (Aurora™).

Recently, a new approach has been applied for DNA-sequence analysis—the replacement of DNA recogniton molecules with peptide nucleic acid (PNA) molecules that contain the counterpart of the DNA segments. PNA, originally developed as a gene-targeting drug, has demonstrated remarkable hybridization properties toward complementary oligonucleotides. Biosensors, on replacement of the DNA recognition layer with a PNA layer, offer a greatly improved distinction between related sequences and several attractive advantages (Wang, 1998).

The commercially available DNA chips, called also genechips, are arrays of DNA sensor elements that have built up various oligonucleotide recognition layers. One successfully applied approach is the light-directed, spatially addressable, parallel chemical synthesis for building up oligonucleotide molecule layers in array arrangements (Fodor et al., 1991). The process, which is applied by Affimetrix in the production of GeneChips and is illustrated in Figure 7.25(a), consists of the following steps:

(1) A photo-protected glass substrate is selectively illuminated by light passing through a photolithographic mask. (The substrate S bears amino groups, or rather hydroxyl groups, nowadays, that are blocked with photolabile group X. Illumination of specific regions through the mask M_1 leads to photodeprotection.)
(2) Deprotected areas are activated by development. Amino groups in the exposed sector become accessible for chemical coupling.
(3) With nucleoside incubation, chemical coupling occurs at activated positions. The first chemical building block A (which can be adenine, cytosine, guanine, or tyrosine), also containing a photolabile protecting group X, is then attached.
(4) A new mask pattern M_2 is applied for the second illumination.
(5) The coupling step is repeated for the B-X group.
(6) This process is repeated until the desired set of probe sequences is produced.

Using a series of photolithographic masks to define chip exposure sites, followed by specific chemical synthesis steps, the process constructs high-density arrays of oligonucleotides, with each probe in a predefined position in the array. Multiple probe arrays are synthesized simultaneously on a large glass wafer. This parallel process enhances reproducibility and helps achieve economies of scale. For example, the complete set of polyonucleotides of length N (which represents a number of 4^N different array elements) can be

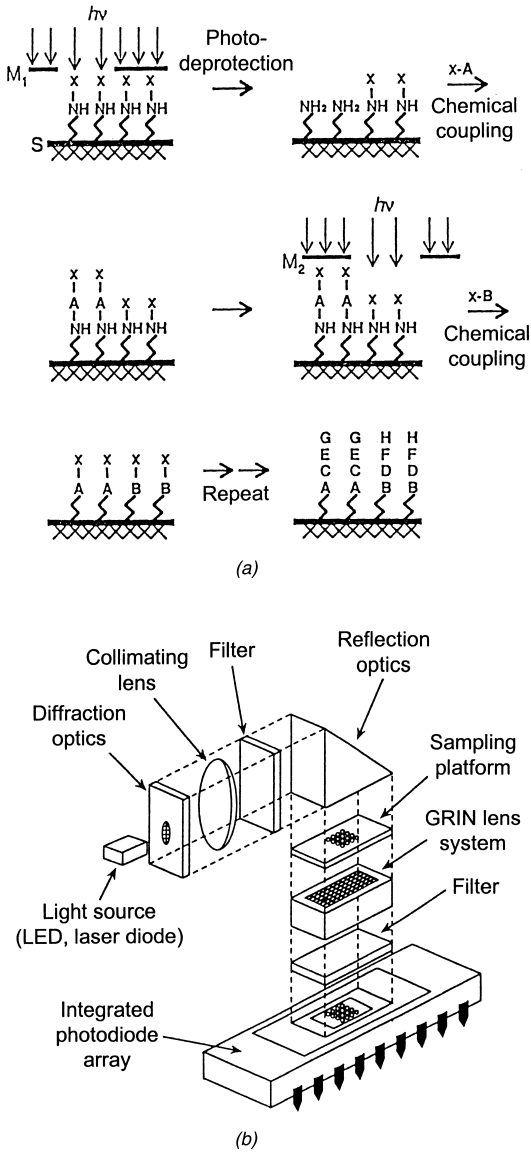

FIGURE 7.25. Typical processing and application of DNA biochips: (a) concept of light-directed spatially addressable parallel chemical synthesis of oligonucleotide probes on microchip surfaces and (b) fluorescent readout of the hybridization result from a DNA sensor array. [Reprinted with permission: (a) from S. P. A. Fodor, J. L. Read, M. C. Pirrung, L. Stryer, A. T. Lu and D. Solas, "Light-Directed, Spatially Addressable Parallel Chemical Synthesis," *Science,* Vol. 251 (15 February 1991), ©1991, American Association for the Advancement of Science; (b) from T. Vo-Dinh, "Development of a DNA Biochip: Principle and Applications," *Sensors and Actuators B,* Vol. 51, pp. 52–59, ©1998, Elsevier Science S.A., Lausanne, Switzerland.]

synthesized in only $4 \times N$ cycles. The amount of nucleic acid information encoded on the array is limited only by the physical size of the array and the available lithographic resolution. Current large-scale commercial manufacturing methods (developed mainly for the semiconductor industry) allow for approximately 300,000 polydesoxynucleotides to be synthesized on small 1.28 $\times$ 1.28 cm arrays—experimental versions now exceed one million probes per array (Lipshutz et al., 1999). After processing, the wafers are diced as in semiconductor processing, and individual probe arrays are packaged in injection-molded plastic cartridges, which protect them from the environment and serve as chambers for hybridization.

Once fabricated, the DNA chip probe arrays are ready for hybridization. The nucleic acid to be analyzed—the target—is isolated and labeled with a fluorescent reporter group. The labeled target is then incubated with the array using the fluidics station. After the hybridization reaction is complete, the array is inserted into the scanner, where patterns of hybridization are detected. Hybridization data are collected as light emitted from the fluorescent reporter groups is incorporated into the target, which is now bound to the probe array. Probes that perfectly match the target produce stronger signals than those that have mismatches. Since the sequence and position of each probe on the array are known, by complementarity, the identity of the target nucleic acid applied to the probe array can be determined. Figure 7.25(b) shows a parallel readout system that applys diffraction optics and a photodiode array under the DNA chip (Vo-Dinh, 1998). Signal processing is performed by a CMOS integrated circuitry. However, the laser scanning readout system combined with CCD seems to be more widely used currently.

Another approach applied by Nanogen (http://www.nanogen.com) is the electronic addressing and binding of DNA single-stranded fragments, called DNA captures, on microchip electrode surfaces, and the electronic concentration and hybridization of target DNA molecules.

Electronic addressing is the placement of charged molecules at specific test sites. Since DNA has a strong negative charge, it can be electronically moved to an area of positive charge (Heller, 1996). A test site or a row of test sites on the microchip is electronically activated with a positive charge. A solution of DNA captures is introduced onto the microchip. The negatively charged probes rapidly move to the positively charged sites, where they concentrate and are chemically bound to that site. The microchip is then washed and another solution of distinct DNA probes can be added. Site by site, row by row, an array of specifically bound DNA probes can be assembled or addressed on the microchip. Following electronic addressing, electrostatic forces are also applied to move and concentrate target molecules to one or more test sites on the microchip. The electronic concentration of sample DNA at each test site promotes rapid hybridization of sample DNA with complementary capture

probes. In contrast to the passive hybridization process, the electronic concentration process has the distinct advantage of significantly accelerating the rate of hybridization. To remove any unbound or nonspecifically bound DNA from each site, the polarity or charge of the site is reversed to negative, thereby forcing any unbound or nonspecifically bound DNA back into the solution away from the capture probes (electronic stringency control). In addition, since the test molecules are electronically concentrated over the test site, a lower concentration of target DNA molecules is required, thus reducing the time and labor otherwise required for pretest sample preparation. The electronic multiplexing feature allows the simultaneous analysis of multiple tests from a single sample. Electronic multiplexing is facilitated by the ability to independently control individual test sites (for addressing capture probes and obtaining the concentrations of test sample molecules), and this allows for the simultaneous use of biochemically unrelated molecules on the same microchip. Sites on a conventional DNA array cannot be individually controlled and, therefore, the same process steps must be performed on the entire array.

These DNA microchips utilize design technologies developed within the semiconductor industry and are manufactured using current microlithography and wafer processing techniques. These microchips are coated with a permeation layer onto which capture probes are attached, and the chip is then mounted into the disposable cartridge. Currently, microchip designs containing both 100 and 400 Pt electrodes arrays are under evaluation.

The permeation layer, which is critical to the proper functioning of the analytical system, is the interface between the surface of the microchip and the actual biological test environment. This general-use permeation layer isolates the biological materials from the harsh local electrochemical environment at the electrode surface and presents the chemistry necessary for physical attachment of the DNA capture probes. The chips are mounted using flip/chip implementation into a single-use cartridge. This single-use cartridge is constructed with the following components: a molded polycarbonate fluidics flow cell, a silicon microchip, a Ni/Au-plated polyimide flex interconnect circuit, 120 interconnect bumps, either Ag epoxy or various solder alloys, and an underfill that forms the flow cell seal. A fluorescent laser scanning readout system and a pattern recognition algorithm are used for the decoding (LeClair et al., 1998).

A recent review of the commercially available solutions is published by Bowtell (1999).

7.3 LIVING BIOSENSORS

A common special feature of living biosensors is that they employ living cells, tissues, or organisms as receptors in contrast to the other biosensor types

that contain only materials extracted from living things. Unique combinations of enzymes or highly sensitive physiological receptor mechanisms become available that are present in intact cells or tissues but may be impossible to duplicate using isolated enzymes in the biosensor. Another advantage should be that the materials can fulfill their biological functions within their natural biological media. In these circumstances, bioactive compounds may have the best activity and lifetime, and they can even be regenerated or resynthesized by the living organisms. Thus, a better stability of the sensors may be expected. If the living organisms perish, abrupt observable changes occur in the sensor's behavior, instead of a slow drift due to the receptor dissolution that is characteristic for other types. The common problems of living biosensors can be summarized as follows:

- The natural environmental conditions, in which the organisms can stay alive for a long period, must be maintained continuously, and this requires a severe control of physical and chemical parameters of the environment.
- The metabolism of the organisms must be maintained; they must be fed continuously.
- The living organisms must be immobilized around or on the surface of the transducer without limiting their biological functions. For appropriate solutions, the latest research results of supramolecular organic chemistry and cellular mimicry should be exploited in the future (Aizawa, 1994).
- The lifetime of the sensors is mainly determined by the lifetime of the organisms.

The particular advantages of using living biosensors are as follows:

- They are less sensitive to inhibition by solutes and are more tolerant of suboptimal pH and temperature values than enzyme electrodes (but exceeding a narrow range, the organisms can die).
- A longer lifetime can be expected than with the enzymatic sensors.
- They are much cheaper because an active enzyme does not need to be isolated.

Their disadvantages (beyond the general problems mentioned above) are as follows:

- Some types may have a longer response time than enzymatic sensors.
- They need more time to return to the baseline level after use.
- Cells contain many enzymes, and care must be taken to ensure selectivity.

Despite some successful research results with various biological elements described in the following sections, living biosensors have not been as widely

explored as other types of biosensors and may be perceived as having fewer commercial applications.

7.3.1 Microbial Biosensors

Microbial biosensors incorporate microorganisms (algae, bacteria, yeast, and fungi) as sensing elements that specifically recognize species of interest. The concentration of these species is related to the assimilation capacity of the microorganisms, measured as a change in respiration activity (metabolism). The transducers follow these changes, similar to the enzymatic sensors, by measuring oxygen consumption or reaction product formation. A number of different transducer types can be applied, as was shown in connection with enzymatic biosensors (see Section 7.1).

Figure 7.26 shows the two basic modes of operation for a microbial biosensor using an electrochemical transducer. The microbes are either cultured in an aerated broth in which the transducer is immersed, or they are immobilized within a membrane on the transducer surface (Buerk, 1993). The best approach for immobilizing microbes within a membrane was found so far to be physical entrapment in polymeric or gel materials, such as polyacrylamide,

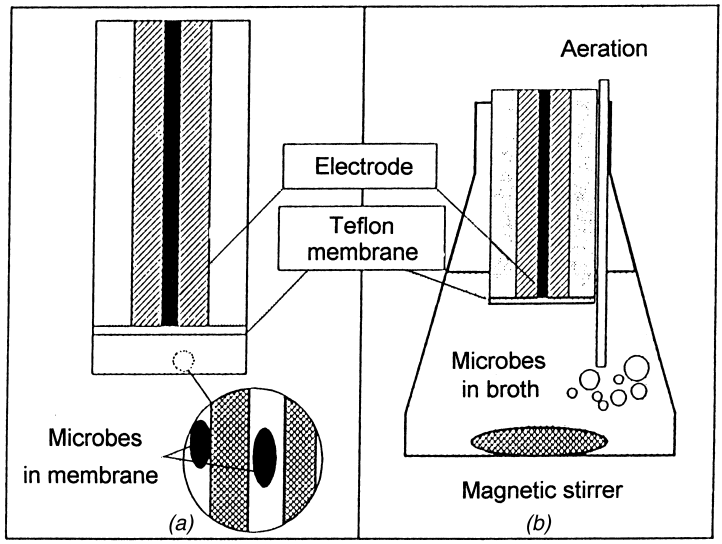

FIGURE 7.26. Basic modes of operation for a microbial biosensor using (a) immobilization within a membrane or (b) a cultured broth. (Used with permission from *Biosensors, Theory and Applications* by D. G. Buerk, ©1993, Technomic Publishing Co., Inc., Lancaster, PA, p. 180.)

poly(vinyl alcohol), collagen, agar gel, gelatin, etc. Apparently, there has not been much success using chemical methods to immobilize microbes by the covalent or other chemical binding techniques that are successful with enzymes, probably due to cell membrane damage and unacceptable losses in biological activity. However, physical methods were appropriate because whole organisms do not need to be incorporated as strongly as enzyme molecules that can be dissolved more easily. On the other hand, the membrane must be permeable not only for analyte and reaction product molecules, but also for all compounds that are necessary for maintaining the continuous metabolism of the living organisms.

Table 7.4 surveys a few interesting and often mentioned microbial sensor examples (Macholán, 1991; Karube and Nakanishi, 1994).

The table shows entirely the application of electrochemical (mostly amperometric and a few potentiometric) transducers. A further example is the photo microbial sensor based on the catalytic chemiluminescence in processes similar to those described by Equations (4.29) and (4.30). The luminescent

TABLE 7.4. Examples of Microbial Sensors. [Adapted with Permission from: Macholán (1991) and Karube and Nakanishi (1994).]

Analyte	Microbe	Transducer	Detection Range, mg/l	Lifetime, days
Glucose	*Saccharomices cerevisiae*	O_2	3–20	14
Acetic acid	*Trichosporon brassicae*	O_2	10–200	30
Ammonia	*Nitrosomonas, Nitrobacter*	O_2	3–45	20
Ethanol	*Trichosporon brassicae*	O_2	3–30	30
Nystatin	*Saccharomices cerevisiae*	O_2	1.2–800	—
Nicotin amide	*Escherichia coli*	NH_3	28–200 mM/l	—
Nicotinic acid	*Lactobacillus arabinosus*	pH	10^{-2}–5	30
L-glutamic acid	*Escherichia coli*	CO_2	8–800	20
Mutagenes	*Bacillus subtilis*	O_2	1–10	—
Ascorbic acid	*Enterobacter agglomerans*	O_2	4–700 μM/l	—
BOD[1]	*Trichosporon cutaneum*	O_2	3–60	30

[1]BOD = biological oxygen demand

light intensity emitted by photobacteria (luminobacteria) is dependent on their metabolic activity. Therefore, high-sensitivity microbial biosensors can be constructed by combining photobacteria with a photo detector (PEM or photodiode). Luminescence is strongly influenced by changes in external conditions. Therefore, the concentration of nutrients required by the microorganisms (e.g., glucose, amino acids) and inhibitors of their luminescence (e.g., toxicants, heavy metals) can be measured (Karube and Nakanishi, 1994).

7.3.2 Tissue-Based Sensors

This group of sensors employs intact tissue slices from living things as biocatalytic membranes combined mostly with electrochemical, but potentially also with other transducer types. With animal tissues, surprisingly good stability and lifetime have been achieved, but the results with plant tissues (the *botanical biosensors*) are also promising. Their great advantages over microbial sensors are that they have no immobilization problems, the decayed or inactivated tissue can easily be replaced, and there is no need for membrane preparation. One tissue slice can be used in combination with several transducer types for different purposes. The lifetime can be considerably extended by cooling and by adding preservatives to inhibit bacterial or yeast growth (Buerk, 1993). Table 7.5 summarizes a few examples (Macholán, 1991).

TABLE 7.5 Tissue-Based Biosensors. (Used with Permission from Macholán, 1991, p. 351, Courtesy of Marcel Dekker Inc., New York.

Analyte	Tissue	Transducer	Detection Range, mM/l	Lifetime
L-glutamine	Porcine kidney	NH_3	0.064–5.2	6 months (at 25°C)
L-glutamic acid	Yellow squash	CO_2	0.2–13	1 month (at 4°C)
L-ascorbic acid	Cucumber peel	O_2	0.004–1	5–6 days
Hydrogen peroxide	Bovine liver	O_2	from 0.01	1 day
L-tyrosine	Sugar beet	O_2	0.03–0.9	8 days
Guanine	Rabbit liver	NH_3	0.013–0.3	7 months (at 25°C)
Adenosine-monophosphate	Rabbit muscle	NH_3	0.05–10	7 months (at 25°C)
Dopamine	Banana pulp	O_2	0.2–1.2	2 weeks
Oxalate	Banana pulp	CO_2	0.1–2	10 days (at 4°C)

7.3.3 Microphysiometers

The microphysiometer is a sensor-based instrument designed to measure the metabolic rates of a small number of cultured living cells, actually measuring extracellular pH changes (acidification) induced by the cellular metabolism. The latter responds to a variety of external stimuli, such as the presence of toxic or irritating substances, chemotherapeutic agents, antiviral drugs, and various receptor ligands (Bousse et al., 1991).

Living cells constantly consume free energy for a variety of purposes, such as maintaining chemical concentration gradients, mechanical motion, and the synthesis of biological molecules. This energy is present in the form of ATP and must constantly be replenished. A variety of catabolic pathways exist in which nutrient compounds are broken down to provide energy in the form of ATP. The two major pathways are aerobic respiration, a complex breakdown of glucose, with CO_2 as the ultimate product, and glycolysis, which is the conversion of glucose to lactic acid without the presence of oxygen. Since part of the carbon dioxide is hydrated into carbonic acid, in both cases, the end result of an energy-yielding metabolic pathway is an acidic substance. The metabolism of living cells, therefore, tends to acidify the extracellular environment. If the volume of the acidic substance produced during the observation period is comparable with the volume of the overall closed compartment, a continuous pH shift can be measured according to the rate of metabolism. The smaller this volume, the larger the pH change that can be measured. The slope of the pH change via time is characteristic for the metabolic rate in a given volume. The metabolic rate depends on a number of environmental conditions, the influence of which can be detected. Since the effect is nonselective, multiple-channel monitoring is desired in which not only the effects of samples but also of reference solutions can be followed simultaneously. Thus, the various effects can be better screened, separated, or compensated.

The acidification of the exracellular fluid cannot be maintained unlimitedly without damaging the living organisms. Moreover, the feeding reagents are also consumed in a small closed system. Therefore, a material transport is needed to remove waste and deliver feeding material continuously. In the *stationary operation mode,* the cultured cells are placed into a flow-through chamber supplied with a continuous carrier flow while the pH difference between the inlet and outlet is monitored. When injecting reagents into the carrier stream, peaks on the curve can be observed. The great advantage of this method is the short response time, but since it consists of measuring a very small pH difference, it tends to be noisy and sensitive to flow-rate fluctuations. In the *kinetic method,* the flow is periodically stopped and the rate of pH change inside the chamber is measured with a single sensor. The time resolution of this method is less, but the rate of pH change can accurately be measured by us-

ing enough data points, moreover, it is independent of the absolute calibration of the pH sensor.

The rate of pH change is determined not only by the metabolic rate (R) producing dn H^+ ions during a period of dt ($R = dn/dt$), but also by the chamber volume (V) and its pH buffering capacity (β_v) defined by the following expression:

$$dn/d\text{pH} = \beta_v V \tag{7.25a}$$

In applying small chambers, the surface area (A) and its buffering capacity (β_a) must be considered:

$$dn/d\text{pH} = \beta_v V + \beta_a A \tag{7.25b}$$

from which the rate of pH change inside the microvolume reaction chamber is:

$$d\text{pH}/dt = R/(\beta_v V + \beta_a A) \tag{7.26}$$

Based on the preceding description, the requirements that the sensors must fulfill can be listed as follows:

- In order to create a microvolume, small geometrical sizes are required; the goal is to have linear sizes in the range of 10 μm.
- A multichannel structure is desired.
- High-resolution and low-noise measurement techniques are needed; the total pH change is in the order of 0.1, thus, a millipH resolution is necessary. Noises and interferences must not exceed this level.
- Rapid measurement should be available; the rate of pH change should be determined within a few seconds, otherwise, the time resolution will be inappropriate.
- Low drift is a typical rate of extracellular acidification in a small realizable volume, about 10–100 millipH/min. Thus, the drift must be lower than 1 millipH/min. Supposing a Nernstian electrode response (59 mV/pH), this allows a maximum drift level of 1 μV/s for the electrode.
- The sensor must survive at 37°C in physiological saline for a reasonable length of time.

The sensor that was chosen to meet these requirements is a type of silicon field-effect device called a light-addressable potentiometric sensor (LAPS). The schematic diagram of the sensor is shown in Figure 7.27(a) (Bousse and Parce, 1994). It consists of an electrolyte/insulation/silicon capacitor that is illuminated from the back by an AC-modulated light source at a wavelength

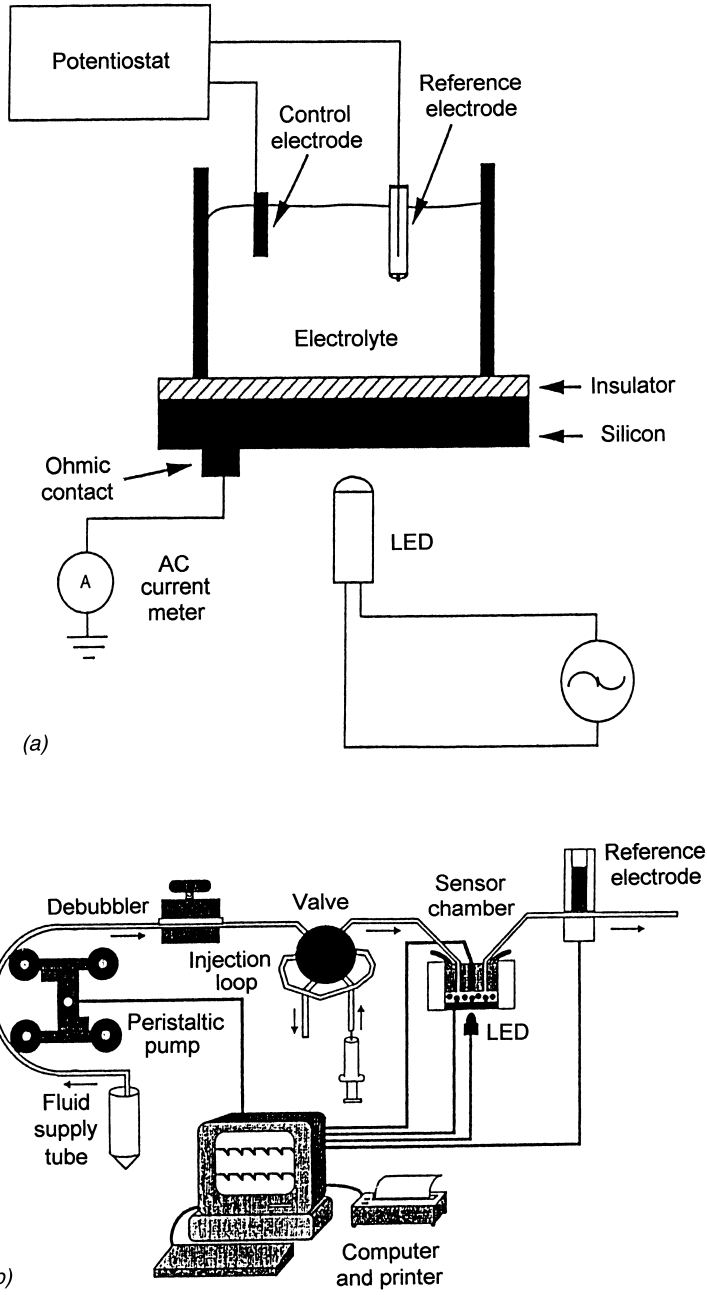

FIGURE 7.27. Schematic structure (a) and measurement setup (b) for a light addressable potentiometric sensor (LAPS) microphysiometer device. (Reproduced with permission from L. Bousse and W. Parce, "Applying Silicon Micromachining to Cellular Metabolism," *IEEE Engineering in Medicine and Biology,* June/July, pp. 396–401, ©1994, IEEE.)

short enough to generate carriers in silicon (usually 940 nm). The isolating film is Si_3N_4, that acts as a pH-sensitive membrane modulating the surface potential and, therefore, the conductivity in the silicon similarly to the channels MOSFETs. The generated AC photocurrent is dependent on the surface potential; thus, the pH value of the electrolyte can be measured by means of this effect. Compared to other field-effect silicon sensors, the LAPS has no front-side leads or wires to isolate and encapsulate. The light addressing enables the multiplexed readout of parallel channels, even when they are on the same substrate.

The measurement system [shown in Figure 7.27(b)] needs several components in the fluid path, including a pump to drive fluid flow (with periodic interruptions), a valve to switch a new solution to the cells with the sample injected, and a debubbler to remove air bubbles and reduce the dissolved gas (usually air) to inhibit bubble formation when the solution is heated up from room temperature to 37°C, since bubbles inside the chamber could destroy the measurement. "Debubbling" is achieved by using heat or vacuum to drive the dissolved gas through a gas permeable membrane.

An example of the sensor output during metabolic rate detection is shown in Figure 7.28, together with the rate data that follow from it. As illustrated, an important capability of a microphysiometer is the ability for real-time detection of receptor/ligand interactions. The response to the sample ligand is quite rapid; the maximum response is achieved within 25 seconds. The detection of cellular metabolism gives direct evidence of the activation of a receptor. This is valuable for drug screening in pharmacology, as well as for various applications in cell biology, toxicology, and environment measurements. It contains more information than binding measurements, which only tell that a compound binds to a cell.

A great advantage of the LAPS device structure is that multichannel systems can be fabricated by silicon micromachining. Figure 7.29 shows a three-dimensional view and a schematic cross section of an eight-channel flow-through chip, with a glass coverslip, LEDs, and fluid connections (Bousse and Parce, 1994). Flow channels are formed by etching channels into the surface of a silicon chip and placing a cell-coated glass coverslip over them so that a seal around the channels is formed. The access to these channels must be through the chip itself, from the back, and is available through holes made by anisotropic etching from both sides of the silicon. The active pH-sensitive area of the silicon is covered with a thin Si_3N_4 film, and the other parts are isolated from the solution with a thick SiO_2 layer. The photocurrent measurement pads are deposited on the backside of the silicon. The counterelectrode may be deposited onto the glass as a thin film or may have contact with the solution outside of the device. The volume of the sensing location inside the microchamber is in the range of 0.1 μl. Recently, a new method has also been

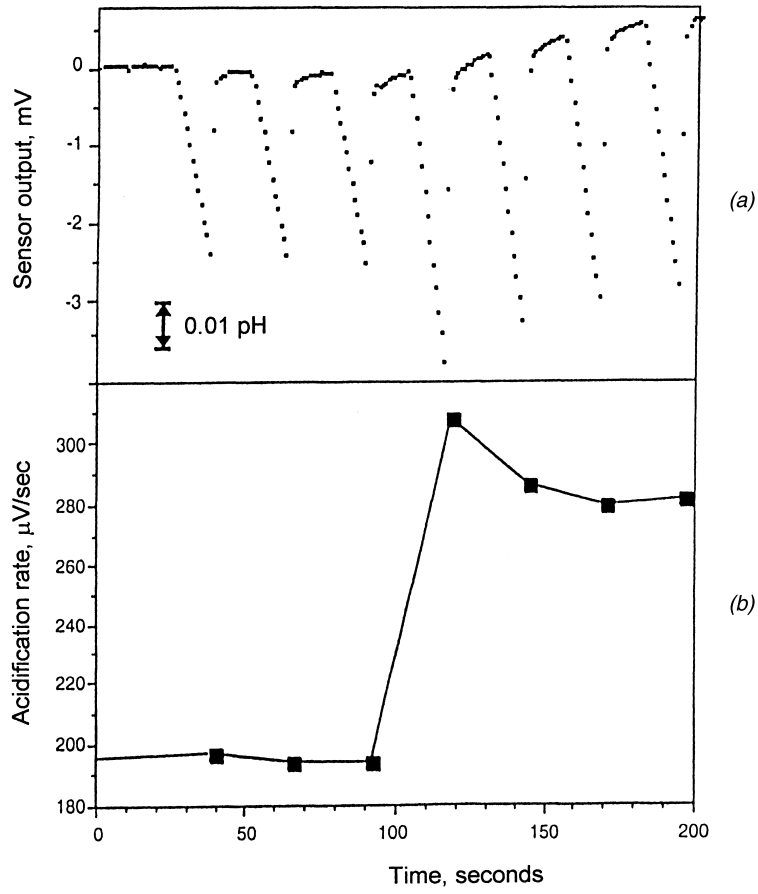

FIGURE 7.28. Typical output signal of a LAPS device (a) and plot of the slopes of the pH change/time data during the flow-off periods, obtained by least squares fitting (b). The increase in metabolic rate caused by the addition of the receptor stimulating ligand can be seen well. (Reproduced with permission from L. Bousse and W. Parce, "Applying Silicon Micromachining to Cellular Metabolism," *IEEE Engineering in Medicine and Biology,* June/July, pp. 396–401, ©1994, IEEE.)

developed to culture different adherent cell types at thirty-two locations of the chip by fabricating four active areas in each channel, thereby increasing the information throughput by a factor of four (Bousse, 1996).

Another approach for monitoring cellular viability, position, adhesion, and response to external stimuli is *impedance imaging,* in which the impedance characteristics of individual cell/electrode systems are used for characterization (Borkholder et al., 1996). A planar microelectrode system consisting of

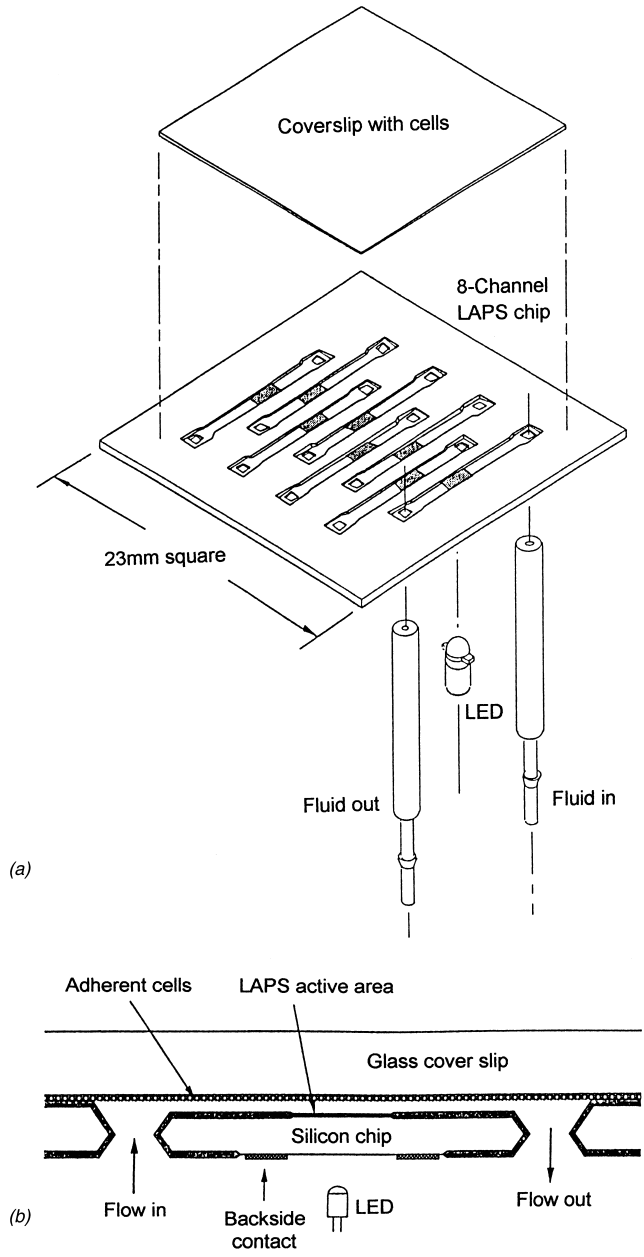

FIGURE 7.29. Realization of a LAPS device by means of silicon micromachining: (a) the structure of a multiple channel device and (b) schematic cross section of an individual cell. (Reproduced with permission from L. Bousse and W. Parce, "Applying Silicon Micromachining to Cellular Metabolism," *IEEE Engineering in Medicine and Biology,* June/July, pp. 396–401, ©1994, IEEE.)

thirty-six platinized iridium electrodes (10 μm diameter) deposited onto an oxidized silicon surface was used as a substrate for the culture of cells. Electrode impedance is monitored across the array as different environmental factors are changed. Maps of electrode impedance have been shown to correlate directly to cell positioning over an electrode and general cellular viability.

7.3.4 Neuronal Biosensors

Receptor neurons are actually living transducers of animals and human bodies. When stimulating the receptors, action potential impulses are generated that propagate along the axon. The frequency of action potential impulses is a function of the stimulation intensity. If a neuron is removed from the body and the action potential is measured by a simple microelectrode, a biosensor is created in which not only the receptor, but also the transducer, originates from a living thing.

The first neuronal biosensors were prepared with antennae of various crabs and animals (Buch and Rechnitz, 1989). These contain specialized chemosensory cells that allow the animal to locate food. The antennae was dissected free, and a sensory nerve was exposed. The nerve was implanted with a glass microelectrode filled with physiological salt solution for standard neurological recording of nerve activity spikes in response to chemosensory simulation. The effect of various biomolecules was monitored by an oscilloscope. According to the concentration of stimuli, such as amino acids, hormones, or toxins, the neuronal biosensor gives a varying frequency output, and the response is very quick and sensitive. Figure 7.30 shows the structure and operation of such sensors. They are sensitive for several compounds and insensitive for a number of other ones, depending on the type of antennae (Buerk, 1993). The frequency characteristic is nonlinear with a basic frequency of 30–80, and a maximum around 150 spikes/second. Depending on the analyte, the sensors could be used in the concentration ranges of 10^{-10}–10^{-4} M/l with nonlinear, saturation characteristics, and also limited linear regions. The lifetime of the neuronal living biosensor was only 8 to 10 hours.

7.4 DIRECT METHODS FOR MONITORING BIOACTIVE COMPOUNDS

The detection of large-molecular-weight bioactive compounds is possible not only with biosensors, but also with conventional chemical sensors as well. The great advantage of these methods for biomedical applications is that they do not employ compounds of living things, which are the most critical lifetime limiting factors. Their common disadvantage is the poor selectivity.

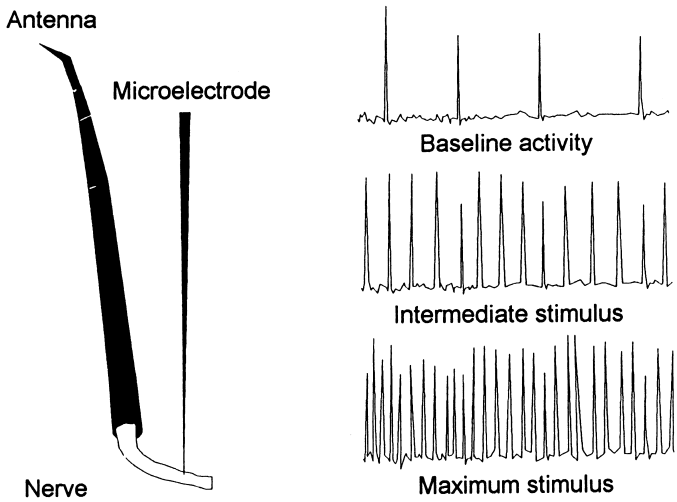

FIGURE 7.30. Example of a biological element with chemosensory transduction—the antennae of an animal. Neural action potential frequency increases with the concentration of analyte. (Used with permission from *Biosensors, Theory and Applications* by D. G. Buerk, ©1993, Technomic Publishing Co., Inc., Lancaster, PA, p. 190.)

Since the detection of those analytes that are the substrates of biosensors are discussed, they are placed into this chapter, however, the devices and methods belong in Chapter 6 which deals with chemical sensors. The greatest efforts have been made for detecting glucose, therefore, the examples are given for this analyte in the following sections.

7.4.1 Direct Electrochemical Sensing of Glucose

The use of direct electrochemical reactions for glucose sensing, without the presence of an enzyme catalyst, began more than twenty years ago. The first approaches almost entirely employed the concept of glucose oxidation. The prospectives that glucose is an aldehyde and can be oxidized to an acid and reduced to an alcohol, and that this reduction and the redox couple could be utilized for a more selective sensing process, were exploited only much later. Amperometric, and later, voltammetric, methods have been used in the direct, three-electrode electrochemical technique. Most sensors employ platinized platinum for working and counterelectrodes, sometimes carbon for the latter one. The reference is usually Ag/AgCl electrode. The physiologic buffer solution provides sufficient chloride ions for the stability of the reference. In *amperometry,* the oxidation current of glucose was measured at a constant potential. The greatest disadvantage of this method was nonselectivity and a grad-

ual loss in catalytic activity of the working electrode. Special techniques of *cyclic voltammetry* can assure better selectivity (Yao, 1991):

- The overall voltammogram contains several peaks that are characteristic for glucose. When evaluating them together, some interference may be screened out.
- With the use of suitable potential waveform, the interference of amino acids on glucose signals can be suppressed.
- By applying a technique of *differential pulse voltammetry,* interferences by low-molecular-weight substances, such as urea, can be reduced in the linear response range of the glucose signal.
- The *compensated net charge* method involves the mathematical integration of the current of a cyclic voltammogram over one complete cycle. Several interferences can significantly be diminished in this way.
- *Low-potential cyclic voltammetry,* an alternative approach for the enhancement of the selectivity and sensitivity of the working electrode, is to operate the voltammetry within a narrow potential range where the glucose signals are most pronounced and where the electrode is less susceptible to interferences. Figure 7.31 shows the complete cyclic voltammogram system of glucose in the range from -1.00 to $+1.00$ V, and Figure 7.32 shows the reaction mechanisms responsible for the different peaks. Two distinct and well-defined redox current peaks can be seen in the low negative range: a reduction peak at -0.80 V in the cathodic scan and an oxidation peak at -0.72 V in the anodic scan. The peaks represent a reversible redox couple in which the adsorbed hydrogen species generated by the interaction of Pt surface with glucose molecules have the determining role according to the mechanism shown in Figure 7.32(a). The reduction peak at -0.65 V is generated by the irreversible reduction of glucose to sorbitol through the mechanism shown in Figure 7.32(b). In the actual glucose sensing, the potential range of the cycle is confined to a narrow region, from -0.9 to -0.4 V, which is rather free from interferences, since amino acids, carbohydrates, urea, etc., are all oxidizable in the high and positive potential range (versus Ag/AgCl). The response time, that is, the time of cycle, can be reduced to less than 1 min. This would be a suitable response time for monitoring the glucose level of blood. The inflection points of the voltammograms can be used for calibration of the sensor *in vivo.* The sensing method needs further improvements before it can be studied *in vivo.* These include the use of a differential pulse technique to enhance selectivity, to rejuvenate the activity of the electrode, and to develop a glucose permeable membrane to cover the electrode, preventing the passage of macromolecules that can poison the electrode.

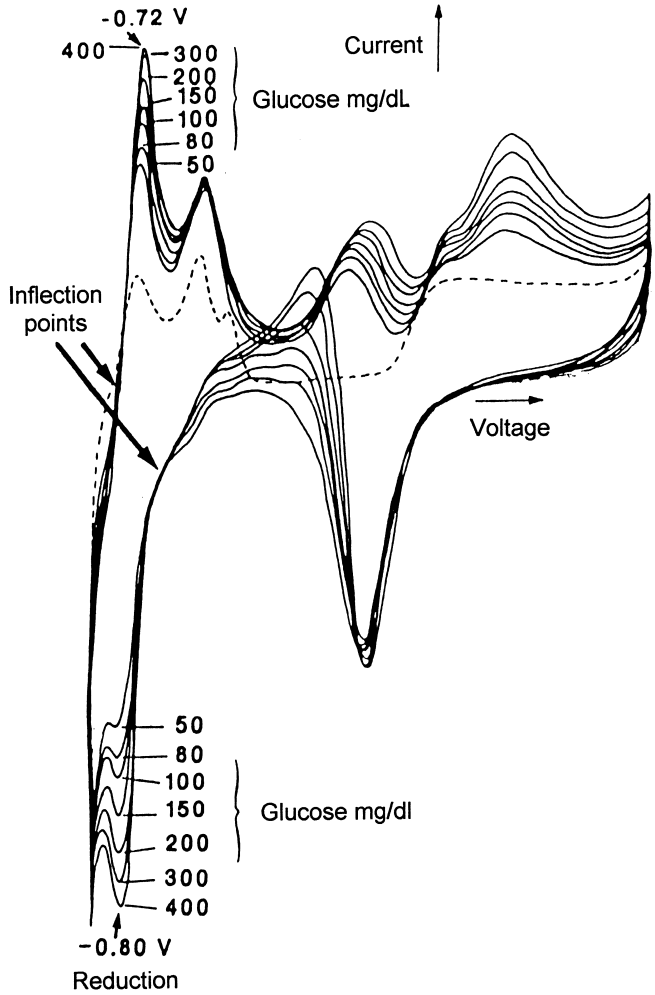

FIGURE 7.31. Cyclic voltammograms of glucose. (Reprinted after Yao, 1991, p. 238, courtesy of Marcel Dekker Inc., New York.)

7.4.2 Direct Optical Approaches

The measurement of glucose *optical rotation activity* on a plan-polarized light has been used for the determination of D-glucose concentrations in physiologic fluids: supposing a constant optical path length, the rotation angle is a function of the concentration.

Miniature optical integrated systems have been fabricated for such *in vivo*

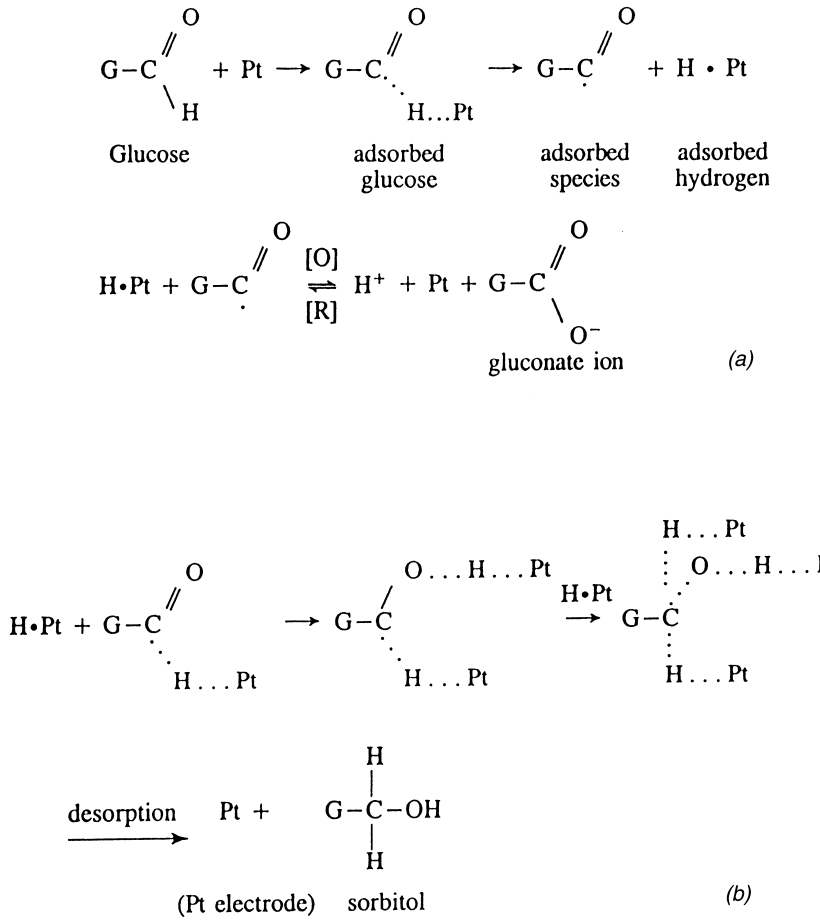

FIGURE 7.32. Mechanisms responsible for voltammetric peaks of glucose: (a) a reversible redox process couple at −0.8 V and −0.72 V, respectively and (b) an irreversible reduction of glucose at −0.65 V. (Reprinted after Yao, 1991, p. 239–240, courtesy of Marcel Dekker Inc., New York.)

polarimetry measurements. A (780 nm wavelength) laser diode/photodiode pair was mounted facing each other across a short (ca. 10mm long) V-groove created by anisotropic etching into a silicon substrate. The V-groove, isolated with Si_3N_4 and covered with a semipermeable membrane, serves as a reservoir for the glucose solution. Both diodes were covered with polarizator films oriented perpendicularly to each other. The output signal is the current of the photodiode, which is equal to the dark current if the reservoir does not contain glucose, and its intensity is a function of the glucose concentration. Amino

acids and other blood or tissue fluid compounds having optical rotation effects may cause interferences, and thus, the efficiency of the permselective membrane has a significant effect on the operation (Burk et al., 1987).

The detection of some biomolecules (glucose and urea) was also investigated by an optical sensor based on *laser-excited SPR* (see Section 3.6). The operation is based on SPR angle shifts caused by the refractive index variation external to the metal surface (Namira et al., 1995). Its practical application is not realistic at present, because of the selectivity problems.

7.4.3 Infrared Spectroscopy

Infrared spectroscopy is a technique of organic analytical chemistry that employs infrared absorption spectra of analytes for qualitative, quantitative, and structural analysis based on the phenomenon that various molecular groups and bond types give specific peak configurations in the spectra.

A unique property of infrared multiple *attenuated total reflectance (ATR) spectroscopy* is that these spectra from an analyte are independent of the sample thickness. The basis of operation is that the reflectance spectrum of a large-refractive-index optical waveguide/sample analyte interface may be characteristic for the sample composition. The measurement could easily be realized *in vitro,* and, by means of an optrode structure, also *in vivo,* invasively.

At first, the resonance peak at 9.676 μm characteristic for the C=O bond of glucose molecules was used for measuring glucose concentration applying a tunable CO_2 laser light source. *In vitro* study of glucose in whole blood gave a resolution of 1.6 mM/l. Since the interference of all blood-constituting molecules having C=O stretching vibration is the major problem, a multiple wavelength approach is necessary (Mendelson et al., 1990).

A system for *in vitro* spectral analysis of human blood serum was realized recently, based on ATR fiber-optic evanescent wave spectroscopy using a Fourier transform infrared spectrometer. The blood serum samples were introduced into a special cell designed for the analysis, with an IR transmitting silver halide fiber as the sensing element. The fiber was in direct contact with the sample. The transmission spectra were analyzed by models of neural networks, which is an effective tool for multicomponent analysis with undefined nonlinear cross-sensitivities. The concentrations of protein and cholesterol in uric acid in human blood serum were obtained with good correlation with ordinary analytical methods. The method can be used for in situ real-time blood analysis (Gotshal et al., 1997).

The great prospective of multiple infrared ATR spectroscopy is the possibility of *noninvasive* blood glucose determination through the skin using the skin's "transmission window" that exists in the near infrared region from 0.7 to 2.5 μm wavelength.

Molecular transitions that occur within the NIR spectrum are associated primarily with overtones and combinations of fundamental CH, NH, and OH vibrational transitions (Arnold, 1996a, 1996b). The fundamental transitions are much stronger and appear in the midinfrared region. Unfortunately, water strongly absorbs midinfrared radiation, which limits the depth of penetration into the human body to only a few hundred micrometers, which makes it impossible to perform noninvasive blood analysis. The fact that CH, NH, and OH stretches can be observed also in the NIR spectrum, where the absorption of water is much less, enables the potential noninvasive application of NIR spectroscopy. Absorbance features directly associated with the glucose molecule are present in the long-wavelength portion of the NIR spectrum. These features represent overtone and combination bands associated with CH vibrations within the glucose molecule, and make this region preferred in terms of potential measurement selectivity and sensitivity. Since other organic molecules also show CH vibrations, their interference cannot be eliminated. The only solution could be the multivariate calibration analysis using principal component regression with partial least squares method or neural network analysis. The description of these techniques is out of scope of this chapter, but more about this topic can be found in the literature (Small and Arnold, 1998; Burmeister et al., 1998; Hazen et al., 1998a; Arnold et al, 1998). Great research efforts have been done recently to realise such multicomponent analysis systems for measuring glucose, cholesterol, urea, triglycerides, and lactate *in vitro* (Hazen et al., 1998b). It must be stressed, however, that no one has ever successfully demonstrated an ability to measure *in vivo* glucose levels in a noninvasive manner (Arnold, 1996). On the other hand, the tremendous potential of this approach will continue to drive advancements in both spectroscopic and computer-based data analysis technologies.

In the near infrared (NIR) spectroscopy, photoacoustic interactions (excited by pulsed laser beam) cause absorption peaks in the spectrum that are more characteristic to the molecular weight and shape than the peaks characteristic for C-H bond resonance effects. Using a laser photoacoustic NIR spectroscopy at the wavelength of 1.7 μm, a relative absorption change of 20% was measurable within the concentration range from 0 to 50 mM/l. However, it is envisaged that any device will use multiple wavelengths for the analysis (Christison, 1993). Recently, the evaluation method was combined with a skin electrical impedance measurement to detect hypoglycemia (Pruna, 1995). NIR spectroscopy has also gained attention as a possible noninvasive method for monitoring blood oxygen (Liem et al., 1992).

7.5 REFERENCES

Aberl, F., Modrow, S., Wolf, H., Koch, S. and Woias, P., "An ISFET-Based FIA System for Immunosensing," *Sensors and Actuators B,* Vol. 6 (1992), pp. 186–191.

Aberl, F., Wolf, H., Kösslinger, C., Drost, S., Woias, P. and Koch, S., "HIV Serology Using Piezoelectric Immunosensors," *Sensors and Actuators B,* Vol. 18–19 (1994), pp. 271–275.

Aberl, F., Wolf, H., Woias, P., Koch, S., Kösslinger, C. and Drost, S., "Development and Evaluation of Biosensors for HIV-Serology," from *Proc. Biosensoren: Grundlagen, Technologien, Anwendungen* (1991), Mai, Bogensee, pp. 1–5.

Aizawa, M., "Molecular Interfacing for Protein Molecular Devices and Neurodevices," *IEEE Engineering in Medicine and Biology,* February/March (1994), pp. 94–102.

Aldinger, U., Pfeifer, P., Schwotzer, G. and Steirücke, P., "A Comparative Study of Spectral and Angle-Dependent SPR Devices in Biological Applications," *Sensors and Actuators B,* Vol. 51 (1998), pp. 298–304.

Alfthan, K., "Surface Plasmon Resonance Biosensors as a Tool in Antibody Engineering," *Biosensors & Bioelectronics,* Vol. 13 (1998), pp. 653–663.

Anderson, G. P., Golden, J. P., Cao, L. K., Wijesuriya, D., Shriver-Lake, L. C. and Ligler, F. S., "Development of an Evanescent Wave Fiber Optic Biosensor," *IEEE Engineering in Medicine and Biology,* June/July (1994), pp. 358–363.

Andle, J. C., Weaver, J. T., McAllister, W. D., Josse, F. and Vetelino, J. F., "Improved Acoustic-Plate-Mode Biosensor," *Sensors and Actuators B,* Vol. 13–14 (1993), pp. 437–442.

Andle, J. C., Weaver, J., Vetelino, J. F. and McAllister, W. D., "Selective Acoustic Plate Mode Sensor," *Sensors and Actuators B,* Vol. 24–25 (1995), pp. 129–133.

Arnold, M. A., "New Developments and Clinical Impact of Noninvasive Monitoring," *Handbook of Clinical Automation, Robotics, and Optimization* (eds. Kost, G. J. and Welsh, J.), John Wiley & Sons, New York (1996a), pp. 631–647.

Arnold, M. A., "Noninvasive Glucose Monitoring," *Current Opinion in Biotechnology,* Vol. 7 (1996b), pp. 46–49.

Arnold, M. A, Burmeister, J. J. and Small, G. W., "Phantom Glucose Calibration Models from Simulated Noninvasive Human Near-Infrared Spectra," *Analytical Chemistry,* Vol. 70, No. 9 (1998), pp. 1773–1781.

Bidan, G., "Sensing Effects in Electroconducting Conjugated Polymers," in Harsányi, G, *Polymer Films in Sensor Applications,* Technomic Publishing Co., Inc., Lancaster, PA (1995), pp. 206–236.

Bier, F. F., Kleinjung, F. and Scheller, F. W., "Real-Time Measurement of Nucleic-Acid Hybridization Using Evanescent-Wave Sensors: Steps Towards the Genosensor," *Sensors and Actuators B,* Vol. 38–39 (1997), pp. 78–82.

Borkholder, D. A., Maluf, N. I. and Kovacs, G. T. A., "Impedance Imaging for Hybrid Biosensor Applications," *Proceedings of the Solid-State Sensor and Actuator Workshop,* Hilton Head, SC (1996), pp. 156–160.

Bousse, L., "Whole Cell Biosensors," *Sensors and Actuators B,* Vol. 34 (1996), pp. 270–275.

Bousse, L., Kirk, G. and Sigal, G., "Biosensors for Detection of Enzymes Immobilized in Microvolume Reaction Chambers," *Sensors and Actuators B,* Vol. 1 (1990), pp. 555–560.

Bousse, L. J., Miller, D. L., Owicki, J. C. and Parce, J. W., "Rapid Determination of Cellular Metabolic Rates with a Silicon Microphysiometer," *Proc. of 1991 Int. Conf. on Solid State Sensors and Actuators (Transducers '91),* San Francisco, CA (1991), pp. 74–77.

Bousse, L. and Parce, W., "Applying Silicon Micromachining to Cellular Metabolism," *IEEE Engineering in Medicine and Biology,* June/July (1994), pp. 396–401.

Bowtell, D. D. L., "Options Available—From Start to Finish—For Obtaining Expression Data by Microarray," *Nature Genetics Supplement,* Vol. 21 (1999), pp. 25–32.

Brennan, J. D., Brown, R. S., Della Manna, A., Kallury, K. M. R., Krull, U. J. and Piunno, P. A., "Covalent Immobilization of Amphiphilic Monolayers Containing Urease onto Optical Fibers for Fluorimetric Detection of Urea," *Sensors and Actuators B,* Vol. 11 (1993), pp. 109–120.

Buch, R. M. and Rechnitz, G. A., "Neuronal Biosensors," *Anal. Chem.,* Vol. 61 (1989), pp. 533A–542A.

Buerk, D. G., *Biosensors, Theory and Applications,* Technomic Publishing Co., Inc., Lancaster, PA (1993).

Burk, E. D., Arrieta, I. C. and Batich, D. C., "The Feasibility of an Implantable Optoelectronic Glucose Sensor," *Proc. 9th Annual Conference of the IEEE Engineering in Medicine and Biology Society* (1987), p. 788.

Burmeister, J. J., Arnold, M. A. and Small, G. W., "Spectroscopic Considerations for Noninvasive Blood Glucose Measurements with Near Infrared Spectroscopy," *Leos Newsletter,* April (1998), pp. 6–9.

Cagnini, A., Palchetti, I., Lionti, I., Mascini, M. and Turner, A. P. F., "Disposable Ruthenized Screen-Printed Biosensors for Pesticides Monitoring," *Sensors and Actuators B,* Vol. 24–25 (1995), pp. 85–89.

Caruso, F., Rodda, E., Frulong, D. N. and Haring, V., "DNA Binding and Hybridization on Gold and Derivatized Surfaces," *Sensors and Actuators B,* Vol. 41 (1997), pp. 189–197.

Choquette, S. J., Locascio-Brown, L. and Durst, R. A., "Planar Waveguide Immunosensor with Fluorescent Liposome Amplification," *Anal. Chem.,* Vol. 64 (1992), pp. 55–60.

Christison, G. B., "Summary of Near Infrared Glucose Sensing Research Towards a Noninvasive Measurement Technique," *Chemical Sensors for In Vivo Monitoring* (a newsletter published by a European Union Concerted Action), No.11, March (1993), pp. 8–10.

Collapicchioni, C., Barbaro, A., Porcelli, F. and Giannini, I., "Immunoenzymatic Assay Using CHEMFET Devices," *Sensors and Actuators B,* Vol. 4 (1991), pp. 245–250.

Coulet, P. R., Bardeletti, G. and Séchaud, F., "Amperometric Enzyme Membrane Electrodes," in *Bioinstrumentation and Biosensors* (ed. Wise, D. L.), Marcel Dekker Inc., New York (1991), pp. 753–793.

Cunningham, A. J., *Introduction in Bioanalytical Sensors,* John Wiley & Sons, New York (1998).

Danielsson, B. "Enzyme Thermistor Devices," in *Biosensor Principles and Applications* (eds. Blum, L. J. and Coulet, P. R.), Marcel Dekker Inc., New York (1991), pp. 83–106.

Diamond, D., *Principles of Chemical and Biological Sensors,* John Wiley & Sons, New York (1998).

Dobay, R., Harsányi, G. and Visy, Cs., "Detection of Uric Acid with a New Type of Conducting Polymer-Based Enzymatic Sensor by Bipotentiostatic Technique," *Analytica Chimica Acta,* Vol. 385 (1999), pp. 187–194.

Dobay, R., Harsányi, G. and Visy, Cs., "Enzymatic Microbiosensors Using Conducting Polymer Films and Thick Film Technology," *Proceedings of Eurosensors X.,* Leuven, Belgium, Vol. 3 (1996), pp. 945–948.

Fischer, U. and Freyse, E. J., "Glucose Analyses in Subcutaneous Tissue: References to the Electrochemical Approach," *Chemical Sensors for In Vivo Monitoring* (a newsletter published by a European Union Concerted Action), No.11, March (1993), pp. 11–15.

Fodor, S. P. A., Read, J. L., Pirrung, M. C., Stryer, L., Lu, A. T. and Solas, D., "Light-Directed, Spatially Addressable Parallel Chemical Synthesis," *Science,* Vol. 251 (15 February 1991), pp. 767–772.

Foulds, N. C. and Lowe, C. R., "Immobilization of Glucose Oxidase in Ferrocene-Modified Pyrrole Polymers," *Anal. Chem.,* Vol. 60 (1988), pp. 2473–4278.

Fraser, D. M., *Biosensors in the Body: Continuous in vivo Monitoring,* John Wiley & Sons, New York (1997).

Freitag, R., *Biosensors in Analytical Biotechnology,* Academic Press, San Diego (1996).

Gauglitz, G. and Reichert, M., "Spectral Investigation and Optimization of pH and Urea Sensors," *Sensors and Actuators B,* Vol. 6 (1992), pp. 83–86.

Gautier, S. M., Blum, L. J. and Coulet, P. R., "Alternate Determination of ATP and NADH with a Single Bioluminescence-Based Fiber-Optic Sensor," *Sensors and Actuators B,* Vol. 1 (1990), pp. 580–584.

Gizeli, E., Goddard, N. J., Lowe. C. R. and Stevenson, A. C., "A Love Plate Biosensor Utilising a Polymer Layer," *Sensors and Actuators B,* Vol. 6 (1992), pp. 131–137.

Glab, S., Holona, I., Koncki, R. and Hulanicki, A., "Animated PVC as Material for the Construction of pH-Based Urea Sensors," *Eurosensors VII* (abstracts), Budapest (1993a), p. 44.

Glab, S., Koncki, R., Holona, I. and Kopczewska, E., "pH-Membrane Electrodes with Chemically Immobilized Urease," *Eurosensors VII* (abstracts), Budapest (1993b), p. 45.

Göpel, W., Jones, T. A., Kleitz, M., Lundström, I. and Seiyama, T., *Sensors: A Comprehensive Survey, Vol. 2-3, Chemical and Biochemical Sensors,* John Wiley & Sons, New York (1991).

Gotshal, Y., Simhi, R., Ben-Ami Sela and Katzir, A., "Blood Diagnostics Using Fiber-Optic Evanescent Wave Spectroscopy and Neural Networks Analysis," *Sensors and Actuators B,* Vol. 42 (1997), pp. 157–161.

Guilbault, G. G., Suleiman, A. A., Fatibello-Filho, O. and Nabirahni, M. A., "Immobilized Bioelectrochemical Sensors," in *Bioinstrumentation and Biosensors* (ed. Wise, D. L.), Marcel Dekker Inc., New York (1991), pp. 659–692.

Guilbeau, E. J., Towe, B. C. and Muehlbauer, M. J., "A Potentially Implantable Thermoelectric Sensor for Measurement of Glucose," *Trans. Am. Soc. Artif. Intern. Organs,* Vol. 33 (1987), p. 329.

Haemmerli, S., Schaeffler, A., Manz, A. and Widmer, H. M., "An Improved Micro Enzyme Sensor for Bioprocess Monitoring by Flow Injection Analysis," *Sensors and Actuators B,* Vol. 7 (1992), pp. 404–407.

Hale, D. P., Boguslavsky, L. I., Inagaki, T., Karan, H. I., Lee, H. S. and Skotheim, T. A., "Amperometric Glucose Biosensors Based on Redox Polymer-Mediated Electron Transfer," *Anal. Chem.,* Vol. 63 (1991), pp. 677–682.

Hämmerle, M., Schuhmann, W. and Schmidt H. L., "Amperometric Polypyrrole Enzyme Electrodes: Effect of Permeability and Enzyme Location," *Sensors and Actuators B,* Vol. 6 (1992), pp. 106–112.

Hardeman, S., Nelson., T., Beirne, D., DeSilva, M., Hesketh, P. J., Maclay, G. J. and Gendel, S. M., "Sensitivity of Novel Ultrathin Platinum Film Immunosensors to Buffer Ionic Strength," *Sensors and Actuators B,* Vol. 24–25 (1995), pp. 98–102.

Harsányi, G., Polymer Films in Sensor Applications, Technomic Publishing Co., Inc., Lancaster, PA (1995).

Hashimoto, K., Ito, K. and Ishimori, Y., "Microfabricated Disposable DNA Sensor for Detection of Hepatitis B Virus DNA," *Sensors and Actuators B,* Vol. 46 (1998), pp. 220–225.

Hazen, K. H., Arnold, M. A. and Small, G. W., "Measurement of Glucose and Other Analytes in Undiluted Human Serum with Near-Infrared Transmission Spectroscopy," *Analytica Chimica Acta,* Vol. 371 (1998a), pp. 255–267.

Hazen, K. H., Arnold, M. A. and Small, G. W., "Measurement of Glucose in Water with First-Overtone Near-Infrared Spectra," *Applied Spectroscopy,* Vol. 52, No. 12 (1998b), pp. 1597–1605.

Heideman, R. G., Kooyman, R. P. H., and Greve, J., "Performance of a Highly Sensitive Optical Waveguide Mach-Zehnder Interferometer Immunosensor," *Sensors and Actuators B,* Vol. 10 (1993), pp. 209–217.

Heller, M. J., "An Active Microelectronics Device for Multiplex DNA Analysis," *IEEE Engineering in Medicine and Biology,* March/April (1996), pp. 100–104.

Jönsson, U., Fagerstam, L., Ivarsson, B., Johnsson, B., Karlsson, R., Lundh, K., Löfås, S., Persson, B., Roos, H., Rönnberg, I., Sjölander, S., Ståhlberg, R., Urbanicsky, C., Östlin, H. and Malmqvist, M., "Real-Time Biospecific Interaction Analysis Using Surface Plasmon Resonance and a Sensor Chip Technology," *BioTechniques,* Vol. 11 (1991), pp. 620–627.

Kajiya, Y., Sugai, H., Iwakura, C. and Yoneyama, H., "Glucose Sensitivity of Polypyrole Films Containing Immobilized Glucose Oxidase and Hydroquinonesulfonate Ions," *Anal. Chem.,* Vol. 63 (1991), pp. 49–54.

Karube, I. and Nakanishi, K., "Microbial Biosensors for Process and Environmental Control," *IEEE Engineering in Medicine and Biology,* June/July (1994), pp. 364–374.

Karyakin, A. A., Bobrova, O. A., Lukachova, L. V. and Karyakina, E. E., "Potentiometric Biosensors Based on Polyaniline Semiconductor Films," *Sensors and Actuators B,* Vol. 33 (1996), pp. 34–38.

Karymov, M. A., Kruchinin, A. A., Tarantov, Y. A., Balova, I. A., Remisova, L. A., Sukhodolov, N. G., Yanklovich, A. I. and Yorkin, A. M., "Langmuir-Blodgett Film Based Membrane for DNA-Probe Biosensor" *Sensors and Actuators B,* Vol. 6 (1992), pp. 208–210.

Katerkamp, A., Bolsmann, P., Kunz, U., Niggermann, M., Pellmann, M. and Cammann, K., "The Fiber Optical Surface Plasmon Resonance Sensor, a Promising Transducer for Chemical and Biochemical Sensors," *Proceedings of Sensor 95,* Nürnberg, Germany (1995), pp. 349–354.

Katsube, T., Katoh, M., Maekawa, H., Hara, M., Yamaguchi, S., Uchida, N. and Shimomura, T., "Stabilization of an FET Glucose Sensor with the Thermophilic Enzyme Glucokinase," *Sensors and Actuators B,* Vol. 1 (1990), pp. 504–507.

Katsube, T., Shimizu, M., Hara, M., Matayoshi, N., Miura, N. and Yamazone, N. "New Semiconductor Glucose Sensor Using Sputtered LaF_3 Film," *Proc. of 1991 Int. Conf. on Solid State Sensors and Actuators (Transducers '91),* San Francisco, CA (1991), pp. 78–81.

Koopal, C. G. J., Bos, A. A. C. M. and Nolte, R. J. M., "Third-Generation Glucose Biosensor Incorporated in a Polymer Conducting Printing Ink," *Sensors and Actuators B,* Vol. 18–19 (1994), pp. 166–170.

Kooyman, R. P. H., Heideman, R. G., Koster, R. and Greve, J., "Optical Fiber Immunosensor Based on Polarimetry," *Proc. of 1991 Int. Conf. on Solid State Sensors and Actuators (Transducers '91),* San Francisco, CA (1991), pp. 376–377.

Kösslinger, C., Uttenthaler, E., Drost, S., Aberl, F., Wolf, H., Brink, G., Stanglmaier, A. and Sackmann, E., "Comparison of the QCM and the SPR Method for Surface Studies and Immunological Applications," *Sensors and Actuators B,* Vol. 24–25 (1995), pp. 107–112.

Koudelka, M., Gernet, S. and de Rooij, N. F., "Planar Amperometric Enzyme-Based Glucose Microelectrode," *Sensors and Actuators B,* Vol. 18 (1989), pp. 157–165.

Kricka, L. J., Stanley, P. E., Thorpe, G. H. G. and Whitehead, T. P. (ed.), *Analytical Applications of Bioluminescence and Chemiluminescence,* Academic Press, San Diego (1984).

Kritz, D., Gehrke, J. and Johnson, K., "Magneto Immuno Assays," *Proc. of the 5th World Congress on Biosensors,* Berlin, Germany (1998), p. 70.

Kulys, J., Bilitewski, U. and Schmid, R. D., "Robust Graphite-Based Bienzyme Sensors," *Sensors and Actuators B,* Vol. 3 (1991), pp. 227–234.

Lechuga, L. M., Calle, A., Golmayo, D., Briones, F., De Abajo, J. and De La Campa, J. G., "Ammonia Sensitivity of Pt/GaAs Schottky Barrier Diodes. Improvement of the Sensor with an Organic Layer," *Sensors and Actuators B,* Vol. 8 (1992), pp. 249–252.

LeClair, T., Harper, A., Graham, S. and Ackley, D., "Film Chip Interconnection of DNA Chip Devices," *Proceedings of IMAPS '98,* San Diego (1998), pp. 758–762.

Lee, J. S., Nakahama, S. and Hirao, A., "A New Glucose Sensor Using Microporous Enzyme Membrane," *Sensors and Actuators B,* Vol. 3 (1991), pp. 215–219.

Liedberg, B., Nylander, C. and Lundström, I., "Biosensing with Surface Plasmon Resonance—How It Started," *Biosensors and Bioelectronics,* Vol. 10, No. 8 (1995), pp. i–ix.

Liem, K. D., Hopman, J. C. W. and Oeseburg, B., "Method for the Fixation of Optrodes in Near Infrared Spectrophotometry," *Med. Biol. Eng. Comput.,* Vol. 30 (1992), pp. 120–121.

Lipshutz, R. J., Fodor, S. P. A., Gingeras, T. R. and Lockhart, D. J., "High Density Synthetic Oligonucleotide Arrays," *Nature Genetics Supplement,* Vol. 21 (1999), pp. 20–24.

Livache, T., Bazin, H., Caillat, P. and Roget, A., "Electroconducting Polymers for the Construction of DNA or Peptide Arrays on Silicon Chips," *Biosensors & Bioelectronics,* Vol. 13 (1998), pp. 629–634.

Löfås, S., Malmqvist, M., Rönnberg, I., Stenberg, E., Liedberg, B. and Lundström, I., "Bioanalysis with Surface Plasmon Resonance," *Sensors and Actuators B,* Vol. 5 (1991), pp. 79–84.

Macholán, L., "Biocatalytic Membrane Electrodes," in *Bioinstrumentation and Biosensors* (ed. Wise, D. L.), Marcel Dekker Inc., New York (1991), pp. 329–377.

Mann-Buxbaum, E., Pittner, F., Schalkhammer T., Jachimowicz, A., Jobst, G., Olcaytung, F. and Urban, G. "New Microminiaturized Glucose Sensors Using Covalent Immobilization Techniques," *Sensors and Actuators B,* Vol. 1 (1990), pp. 518–522.

Mascini, M., Moscone, D. and Bernardi, L., "In vivo Continuous Monitoring of Glucose by Microdialysis and a Glucose Biosensor," *Sensors and Actuators B,* Vol. 6 (1992), pp. 143–145.

Mendelson, Y., Clermont, A. C., Peura, R. A. and Lin, B.-C., "Blood Glucose Measurement by Multiple Attenuated Total Reflection and Infrared Absorption Spectroscopy," *IEEE Transaction on Biomedical Engineering,* Vol. 37 (1990), pp. 458–465.

MicroVacuum Ltd., "Optical Waveguide Lightmode Spectroscopy," (1998) http://www.microvacuum.com.

Miyahara, Y., Tsukada, K. and Miyagi, H., "Urea Sensor Based on an Ammonium-Ion-Sensitive Field-Effect Transistor," *Sensors and Actuators B,* Vol. 3 (1991), pp. 287–293.

Namira, E., Hayashida, T. and Arakawa, T., "Surface Plasmon Resonance Study for the Detection of Some Biomolecules," *Sensors and Actuators B,* Vol. 24–25 (1995), pp. 142–144.

Newman, A. L., Hunter, K. W. and Stanbro, W. D., "The Capacitive Affinity Sensor: A New Biosensor," *Proc. 2nd Int. Meet. Chemical Sensors,* Bordeaux, France (1986), pp. 596–598.

O'Brien II, M. J., Brueck, S. R. J., Perez-Luna, V. H., Tender, L. M. and Lopez, G. P., "SPR Biosensors: Simultaneously Removing Thermal and Bulk-Composition Effects," *Biosensors and Bioelectronics,* Vol. 14 (1999), pp. 145–154.

Oliveira Brett, A., Macedo, T. R. A., Faimundo, D., Marques, H. M. and Serrano, S. H. P., "Voltammetric Behaviour of Mitoxantrone at a DNA-Biosensor," *Biosensors and Bioelectronics,* Vol. 13 (1998), pp. 861–867.

Palecek, E., Fojta, M., Tomschik, M. and Wang, J., "Electrochemical Biosensors for DNA Hybridization and DNA Damage," *Biosensors and Bioelectronics,* Vol. 13 (1998), pp. 621–628.

Pickup, J. C., "Developing Glucose Sensors for *in vivo* Use," *Trends in Biotechnology,* Vol. 11 (1993), pp. 285–291.

Pruna, S., "Development of Noninvasive Method for in vivo Sensing of Glycaemia," *Chemical Sensors for In Vivo Monitoring* (a newsletter published by a European Union Concerted Action), No. 19, December (1995), pp. 30–33.

Ramsay, G., *Commercial Biosensors: Applications to Clinical, Bioprocess, and Environmental Samples,* John Wiley & Sons, New York (1998).

Ramsden, J. J., "Optical Biosensors," *Journal of Molecular Recognition,* Vol. 10 (1997), pp. 109–120.

Saito, A., Miyamoto, Sh., Kimura, J. and Kuriyama, T., "ISFET Glucose Sensor for Undiluted Serum Sample Measurement," *Sensors and Actuators B,* Vol. 5 (1991), pp. 237–239.

Sakai, G., Saiki, T., Uda, T., Miura, N. and Yamazone, N., "Selective and Repeatable Detection of Human Serum Albumin by Using Piezoelectric Immunosensor," *Sensors and Actuators B,* Vol. 24–25 (1995), pp. 134–137.

Satoh, I. and Iijima, Y., "Multi-Ion Biosensor with Use of a Hybrid-Enzyme Membrane," *Sensors and Actuators B,* Vol. 24–25 (1995), pp. 103–106.

Schalkhammer, Th., Lobmaier, Ch., Pittner, F., Leitner, A., Brunner, H. and Aussenegg, F. R., "The Use of Metal-Island-Coated pH-Sensitive Swelling Polymers for Biosensor Applications," *Sensors and Actuators B,* Vol. 24–25 (1995), pp. 166–172.

Schasfoort, R. B. M. and Eijsma, B., "The Ion-Step Method Applied to Disposable Membranes for the Development of Ion-Responding Immunosensors," *Sensors and Actuators B,* 6 (1992), pp 308–311.

Schasfoort, R. B. M., Keldermans, C. E. J. M., Kooyman, R. P. H., Bergveld, P.,and Greve, J., "Competitive Immunological Detection of Progesterone by Means of the Ion-Step Induced Response of an ImmunoFET," *Sensors and Actuators B,* Vol. 1 (1990), pp. 368–372.

Scheller, F. and Schubert, F., *Biosensors,* Elsevier Science, Amsterdam (1999).

Schipper, E. F., Kooyman, R. P. H., Heideman, R. G. and Greve, J., "Feasibility of Optical Waveguide Immunosensors for Pesticide Detection: Physical Aspects," *Sensors and Actuators B,* Vol. 24–25 (1995), pp. 90–93.

Schubert, F., "A Fiber-Optic Enzyme Sensor for the Determination of Adenosine Diphosphate Using Internal Analyte Recycling," *Sensors and Actuators B,* Vol. 11 (1993), pp. 531–535.

Schubert, F., Wollenberger, U., Scheller, F. W. and Müller, H. G., "Artificially Coupled Reactions with Immobilized Enzymes: Biological Analogs and Technical Consequences," in *Bioinstrumentation and Biosensors* (ed. Wise, D. L.), Marcel Dekker Inc., New York (1991), pp. 19–37.

Schuhmann, W., Lammert, R., Uhe, B. and Schmidt H. L., "Polypyrrole, a New Possibility for Covalent Binding of Oxidoreductases to Electrode Surfaces as a Base for Stable Biosensors," *Sensors and Actuators B,* Vol. 1 (1990), pp. 537–541.

Schuhmann, W., Lehn, Ch. and Schmidt H. L., "Comparison of Native and Chemically Stabilized Enzymes in Amperometric Enzyme Electrodes," *Sensors and Actuators B,* Vol. 7 (1992), pp. 393–398.

Shaolin, M., "The Kinetics of the Activated Uricase Immobilized on a Polypyrrole Film," *Electrochim. Acta,* Vol. 39 (1994), p. 9.

Shul'ga, A. A., Koudelka-Hep, M., de Rooij, N. F. and Netchiporouk, L. I., "Glucose-Sensitive ENFET Using Potassium Ferricyanide as an Oxidizing Substrate: The Effect of an Additional Lysozyme Membrane," *Sensors and Actuators B,* Vol. 24–25 (1995), pp. 117–120.

Simon, W., "Urea Sensor Based on an Ammonium-Ion-Sensitive Field-Effect Transistor," *Sensors and Actuators B,* Vol. 3 (1991), pp. 287–293.

Small, G. W. and Arnold, M. A., "Data Handling Issues for Near-Infrared Glucose Measurements," *Leos Newsletter,* April (1998), pp. 16–17.

Spichiger-Keller, U. E., *Chemical Sensors and Biosensors for Medical and Biological Applications,* John Wiley & Sons, New York (1998).

Steinkuhl, R., Sundermeier, C., Hinkers, H., Dumschat, C., Cammann, K. and Knoll, M., "Microdialysis System for Continuous Glucose Monitoring," *Sensors and Actuators B,* Vol. 33 (1996), pp. 19–24.

Sutherland, R. M., Dahne, C., Place, J. F. and Ringrose, A. S., "Optical Detection of Antibody-Antigen Reactions at a Glass-Liquid Interface," *Clin. Chem.,* Vol. 30 (1984), pp. 1533–1538.

Tiefenthaler, K., "Integrated Optical Couplers as Chemical Waveguide Sensors," in *Advances in Biosensors,* Vol. 2., JAI, Greenwich, CT (1992), pp. 261–289.

Turner, A. P. F., "Biosensors: Past, Present and Future," (1996) http://www.cranfield.ac.uk/biotech/chinap.htm.

Umana, M., Waller, J., Wani, M., Whisnant, C. and Cook, E., "Enzyme-Enhanced Electrochemical Immunoassay for Phenytoin," *J. Natl. Inst. Stand. Technol.,* Vol. 93 (1988), pp. 659–661.

Updike, S. J. and Hicks, G. P., "The Enzyme Electrode, A Miniature Chemical Transducer Using Immobilized Enzyme Activity," *Nature (Lond.),* Vol. 214 (1967), pp. 986–988.

Urban, G., Jobst, G., Aschauer, E., Tilado, G., Svasek, P., Varahram, M., Ritter, Ch. and Riegebauer, J., "Performance of Integrated Glucose and Lactate Thin-Film Microbiosensors for Clinical Analysers," *Sensors and Actuators B,* Vol. 18–19 (1994), pp. 592–596.

Valarcel, M. and de Castro, L., *Flow-Through (Bio)Chemical Sensors,* Elsevier Science, Amsterdam (1999).

Van der Schoot, B. H., Voorthuyzen, H. and Bergveld, P., "The pH-static Enzyme Sensor: Design of the pH Control System," *Sensors and Actuators B,* Vol. 1 (1990), pp. 546–549.

Vidal, J. C., García, E. and Castillo, J. R., "In situ Preparation of a Cholesterol Biosensor: Entrapment of Cholesterol Oxidase in an Overoxidized Polypyrrole Film Electrodeposited in a Flow System, Determination of Total Cholesterol in Serum," *Analytica Chimica Acta,* Vol. 385 (1999), pp. 213–222.

Vo-Dinh, T., "Development of a DNA Biochip: Principle and Applications," *Sensors and Actuators B,* Vol. 51 (1998), pp. 52–59.

Volpe, G., Moscone, D., Compagnone, D. and Palleschi, G., "In vivo Continuous Monitoring of L-Lactate Coupling Subcutaneous Microdialysis and an Electrochemical Biocell," *Sensors and Actuators B,* Vol. 24–25 (1995), pp. 138–141.

Wang, J., "DNA Biosensors Based on Peptide Nucleic Acid (PNA) Recognition Layers. A Review," *Biosensors and Bioelectronics,* Vol. 13 (1998), pp. 757–762.

Wang, J., Rivas, G., Luo, D., Cai, X., Valera, F. S. and Dontha, N., "DNA-Modified Electrode for the Detection of Aromatic Amines," *Analytical Chemistry,* Vol. 68, No. 24 (1996), pp. 4365–4369.

Wang, J., Rivas, G., Ozsoz, M., Grant, D. H., Cai, X. and Parrado, C., "Microfabricated Electrochemical Sensor for the Detection of Radiation-Induced DNA Damage," *Analytical Chemistry,* Vol. 69, No. 7 (1997), pp. 1457–1460.

Watanabe, E. and Tanaka, M., "Determination of Fish Freshness with a Biosensor System," in *Bioinstrumentation and Biosensors* (ed. Wise, D. L.), Marcel Dekker Inc., New York (1991), pp. 39–73.

Watson, L. D., Maynard, P., Cullen, D. C., Sethi, R. S., Brettle, J. and Lowe, C. R., "A Microelectronic Conductimetric Biosensor," *Biosensors,* Vol. 3 (1987/88), pp. 101–115.

Weetall, H. H., "Chemical Sensors and Biosensors, Update, What, Where, When and How," *Biosensors and Bioelectronics,* Vol. 14 (1999), pp. 237–242.

White, S. F. and Turner, A. P. F., *Encyclopedia of Bioprocess Technology: Fermentation, Biocatalysis and Bioseparation* (eds. Flickinger, M. C. and Drew, S. W.) John Wiley & Sons, New York (1997).

Wolfbeis, O. S., "Biomedical Applications of Fiber Optic Chemical Sensors," *International Journal of Optoelectronics,* Vol. 6, No. 5 (1991), pp. 424–441.

Xie, B. and Ren, Sh., "A Versatile Thermal Biosensor," *Sensors and Actuators B,* Vol. 19 (1989), pp. 53–59.

Xie, B., Mecklenburg, M., Danielsson, B., Öhman, O., Norlin, P. and Winquist, F., "Development of an Integrated Thermal Biosensor for the Simultaneous Determination of Multiple Analytes," *Analyst,* Vol. 120 (1995), pp. 155–160.

Yao, S. J., "Chemistry and Potential Methods for in vivo Glucose Sensing," in *Bioinstrumentation and Biosensors* (ed. Wise, D. L.), Marcel Dekker, New York (1991), pp. 229–247.

Yuan, Z. Y., Hong, M., Wlodarski, W. B. and Ji, X. S., "A Novel Organophosphorous Pesticides Sensitive EN-FET," *Proc. of 1991 Int. Conf. on Solid State Sensors and Actuators (Transducers '91),* San Francisco, CA (1991), pp. 703–705.

Zaitsev, S. Y., "Polymeric Langmuir Films with Glucose Oxidase as Prototype Biosensors," *Sensors and Actuators B,* Vol. 24–25 (1995), pp. 177–179.

Zhylyak, G. A., Dzyadevich, S. V., Korpan, Y. I., Soldatkin, A. P. and El'skaya, A. V., "Application of Urease Conductometric Biosensor for Heavy-Metal Ion Determination," *Sensors and Actuators B,* Vol. 24–25 (1995), pp. 145–148.

CHAPTER 8

Biocompatibility of Sensors

A serious problem with all devices used in contact with tissue is that of *biocompatibility,* especially *hemocompatibility* when they are used in contact with blood. Since biocompatibility is a special issue of biomedicine, the present description is restricted only to some special problems of sensor applications.

The implanted device and blood need to coexist, in such that the device will function in the way intended and blood and tissues will not be adversely affected by the presence of the device. Insertion of catheters and catheter-tip sensors may stimulate a number of processes, which could lead to the failure of the sensor or blockage of the catheter due to the formation of fibrous deposits and blood clotting. Moreover, the presence of the device may cause a hazard to the patient due to the possible release of toxic products into the blood or body fluid and due to the increased possibility of thrombosis caused by the production of charges or current leakage exterior of the sensor.

Blood-clotting time is the most obvious indication of the biological incompatibility of materials that are in contact with blood. Blood-clotting time data in terms of percentage are presented in Table 8.1 for twelve different materials that are widely used in biomedical sensor technology (Poghossian, 1995). Blood coagulation time of PTFE, which is considered to be one of the most inert and biocompatible medical polymers having data from 11 to 13 min, was taken as 100%. Unfortunately, inorganic silicon-based and glassy surfaces show very short blood-clotting time below ten minutes. This is much less than the lifetime even of the most unstable sensor types. Thus, the length of the possible monitoring period using invasive sensors is mostly limited by incompatibility problems and not by the sensor's lifetime, even when this allows only a few hours of operation. This is why sensor and catheter surface design by fabrication procedures and by surface modification has become a key issue of invasive sensor research and development.

TABLE 8.1. The Average Time for the Beginning of Blood Coagulation on Various Materials (100% Represents 12 Minutes) (Reprinted with Permission from A. S. Poghossian, "Using the Site-Binding Model for an Explanation of the Blood Compatibility of Some Materials Used in Biomedical Sensors, Sensors and Actuators B, *24–25," pp. 159–161, ©1995, Elsevier Science S.A., Lausanne, Switzerland.)*

Material Type	Blood Clotting Time, %
PTFE	100
Si_3N_4	70–72
Ta_2O_5	70–72
Al_2O_3	70–72
Al	66
PVC	58–62
Akrylate glue	58–62
Photoresist	58–62
Epoxy	58–62
SiO_2	52
Si (n wafer)	44
Pyrex glass	38

A simplified form of the cascade of the most important reactions following contact between blood and the catheter sensor is generally described as follows (Rolfe, 1994):

- protein adsorption
- platelet adhesion
- platelet aggregation
- fibrin formation
- thrombus formation

There are several approaches to decrease blood coagulation possibilities on sensor surfaces that are described as follows.

Protein adsorption control. The deposition and attachment of the first layer of macromolecules is of critical importance. Proteins are bound to the surface, for example, by an electrostatic bond between charged groups on the surface and opposite charges on the protein. It is supposed that the negative surface charge appears as a result of electrochemical phenomena at the foreign body—blood interface prevents the adsorption of negatively charged proteins of the blood plasma that stimulate thrombus formation (Poghossian, 1995). Surface texture and chemistry are also important influencing factors. Generally, smooth surfaces will allow a lower rate of protein adsorption than rough surfaces, and plasma proteins have a greater affinity for hydrophobic material surfaces than for hydrophilic ones (Mannhalter, 1993). The adsorption is extremely low on

hydrogels that are very useful on sensor surfaces for a number of other reasons as well (see Figure 6.6).

Thrombus formation control. Protease inhibitors (e.g., antithrombin III) can inactivate the coagulation enzymes, particularly thrombin, the inactivation of which means that fibrin is not formed from fibrinogen, and so the clot is not formed. Heparin is a sulphated polysaccharide, providing an anticoagulant effect by accelerating the inactivation of proteases that work within the coagulation cascade. Heparin can be infused with saline directly into the patient, resulting in a more general anticoagulation, which is often not desired. Heparin immobilization, especially by its covalent bonding onto polymeric surfaces seems to be an appropriate solution for sensor applications (Vulic et al., 1993).

Despite significant improvements in the understanding of the critical processes of blood clotting, only limited success has been achieved in modifying these processes in order to improve sensor performance. The best approach seems to be, therefore, the application of the new results of cellular engineering.

Cellular mimicry. Vascular endothelial cells, which line the blood vessels, interact very favorably with blood and ensure freedom from thrombus formation. The cell membrane is structured as a phospholipid bilayer, with the external surface having an appropriate charge distribution to provide an ideal interface with plasma proteins and blood cells. Phospholipid bilayers can be produced using the Langmuir-Blodgett technique, and for improving their mechanical stability, they might be polymerized on sensor surfaces (Rolfe, 1994). Another new promising approach is endothelial cell adhesion to polymer surfaces to obtain biocompatible devices.

Platelet adhesion/activation blocking by NO release. The variety of biological functions of nitric oxide (NO) caused the wide interest in chemistry of this radical molecule during the last ten years. This completely new method is based on fabricating implantable sensors with outer polymeric films that slowly release low levels of nitric oxide locally, at the implant site. Such in situ release of NO should prevent platelet adhesion/activation on the surface of the sensors and, concomitantly, could provide sustained release of NO. The feasibility of this method was demonstrated with novel NO donor compounds (e.g., diazeniumdiolates) that were built into polymeric films on electrochemical blood-gas sensors. Results from *in vitro* and *in vivo* platelet adhesion studies indicate that the polymers that release NO exhibit greatly enhanced biocompatibility compared to corresponding blank polymer films formulated without the NO release chemistry (Meyerhoff et al., 1998).

Invasion of the body with implantable devices also demands the use of tested *sterilization* protocol. According to International standards, the term "sterile" means free from viable microorganisms. From a product point of view, it should mean that there is no risk of infection when the patient uses this prod-

uct. Several pharmacopoeia demand a sterility assurance level (SAL) of 10^{-6}, i.e., among 1 million objects sterilized, only one object is allowed to be nonsterile. Various strategies are currently employed and researched in biomedical sensorics to achieve sensor sterility since bacterial contamination of devices may reduce the local biocompatibility and cause reaction against the implant.

The most effective conventional methods of sterilization comprise either moist or dry heat that are unsuitable for enzymatic biosensors (Rigby, 1994). Sterilization by means of gas (ethylene hydroxide) and chemical exposure (thiomersal) have associated problems with enzyme degradation, problems of absorption and retention when used with polymeric materials (acting as carcinogens), and may often result in toxic effects to the local environment. Exposure to a controlled dose of gamma radiation (2.5 MRad) from a ^{60}Co source affords the safest, most reliable reduction in bacterial challenge and confers minimal effects even on enzymatic sensors (Koudelka-Hep et al., 1993).

Three combinations for glucose sensor sterilization are recommended (Woedke et al., 1998):

- action of low concentrated hydrogen peroxide parallel to low-dose gamma irradiation
- universal homogenous ultraviolet (UHUV) irradiation followed by low-dose gamma irradiation
- UHUV irradiation followed by the action of inclusion compounds of tensides with hydrogen peroxide in urea

Recent anxieties from HIV infections caused by clinical devices have changed the general opinion about recycling and sterilization of blood-contact medical tools. It seems that the application of disposable low-cost devices is much more desirable in this field than the use of very special sterilization methods causing high costs and possible hazards both for devices and patients.

A recent trend is that sensors for invasive applications should belong in the nearest future to the category of low-cost, disposable elements that are designed for a stable operation within a single monitoring period, ranging from a few minutes to a maximum of one day.

8.1 REFERENCES

Koudelka-Hep, M., Strike, D. J. and de Rooij, N. F., "Miniature Electrochemical Glucose Biosensors," *Anal. Chim. Acta,* Vol. 281 (1993), p. 461.

Mannhalter, Ch., "Biocompatibility of Artificial Surfaces such as Cellulose and Related Materials," *Sensors and Actuators B,* Vol. 11 (1993), pp. 273–279.

Meyerhoff, M. E., Mowery, K. A., Schoenfisch, M. H., Baliga, N., Saavedra, J. E. and Keefer,

L. K., "Improving the Biocompatibility of Intravascular Chemical Sensors via In-Situ Nitric Oxide Release," *Int. Symp. on Electrochemical and Biosensors,* Mátrafüred, Hungary (1998), p. PL-12.

Poghossian, A. S., "Using the Site-Binding Model for an Explanation of the Blood Compatibility of Some Materials Used in Biomedical Sensors," *Sensors and Actuators B,* Vol. 24–25 (1995), pp. 159–161.

Rigby, G., "Diffusion Limiting Membranes and Sterilisation Methods for Glucose Sensors," *Chemical Sensors for In Vivo Monitoring* (a newsletter published by a European Union Concerted Action), No. 17, Dec. (1994), pp. 20–22.

Rolfe, P., "Intra-Vascular Oxygen Sensors for Neonatal Monitoring," *IEEE Engineering in Medicine and Biology,* June/July (1994), pp. 336–346.

Vulic, I., Okano, T. T., van der Gaag, F. J., Kim, S. W. and Feijen, J., "Heparin-Containing Block Copolymers, Part II, in vitro and ex vivo Blood Compatibility," *Journal of Materials Science: Materials in Medicine,* Vol. 4 (1993), pp. 448–459.

Woedtke, von Th., Jülich, W.-D. and Abel, P. U., "Gentle Sterilization of Enzyme Glucose Sensors," *Proc. of the 5th World Congress on Biosensors,* Berlin, Germany (1998), p. 39.

CHAPTER 9

Summary and Future Trends

Detection techniques, sensing effects, sensor structures, and their present status is summarized in Tables 9.1, 9.2, and 9.3 (without the demand of covering all available types) of this chapter according to the various biomedical application fields distinguished into the following groups:

- medical imaging appliances
- appliances for personal and clinical use
- sensors mainly for clinical and laboratory applications

The wide variety of biomedical sensor applications is obvious from the tables. Because of this wide variety, any statement about present status and potential development must be carefully adjusted according to the sensor type and its application technique. Although, therefore, it is rather difficult to draw general conclusions, some trends could be highlighted that are typical for particular sensor groups. From this aspect, physical sensors should be distinguished from chemical and biosensors.

The rather well-described transduction effects of *physical sensors,* as well as the rapid and continuous development resulting in integrated smart sensors and sensor arrays with increasingly better performances (such as signal-to-noise ratio, long-term stability, reliability, etc.) and lower costs results in the fact that potential application fields are gradually invaded by them. Their application is concentrated mainly on the following areas:

- *medical imaging appliances:* The application of sensors enabled not only the practical realization and several generations of new appliances (such as ultrasound-echo, CT, MEG, etc.), but also the introduction of computer-aided image processing into conventional imaging areas (like radiology). Great progress can be predicted for the latter areas in the near future.

TABLE 9.1. Detection Techniques, Sensing Effects, Sensor Structures, and Their Present Status in Various Biomedical Applications: Medical Imaging Appliances.

Biomedical Application Field	Measurand	Sensor/Measurement Type	Basis of the Sensing Effect	Sensor Structure	Present Status
Body surface temperature image	temperature mapping	pyroelectric vidicon	pyroelectric	capacitor	CA*
		parabolic antenna	EM waves	microwave antenna	CA
		IR camera	photo- or pyroelectric	SSD, POSFET	CA, R&D*
Ultrasound imaging	ultrasound impulse time of flight	transmitter/receiver arrays	piezoelectric	capacitor array	CA
				POSFET array	R&D
Digital teleradiology	X-ray image	Charpak-detector	ionization	vacuum tube array	R&D, CA
		scintillation detector array	fluorescence + electron-hole generation	phosphor-CCD array or mosaic	CA
X-ray computer tomography (CT)	X-ray intensity profile(s)	scintillation or semi-conductor detector array	fluorescence + photoelectric effect	BGO/LSO/CWO + PEM/PIN/APD	CA
			photoelectric effect	Si-SSD, HPGe	R&D
Angiography	γ-intensity map	scintillation Anger camera	fluorescence + photoelectric effect	NaI + PSPEM	CA
Single photon emission CT (SPECT)	γ-intensity distribution	scintillation γ-camera array	fluorescence + photoelectric effect	div. collimator + NaI + PSPEM	CA
			photoelectric effect	Ge, CZT array	R&D
Positron emission tomography	γ-intensity distribution	scintillation γ-detector block rings	fluorescence + photoelectric effect	segmented BGO + PSPEM/PIN/APD	CA
Nuclear magnetic resonance imaging	magnetic pulses	special arrangement of coil inductors	EM induction	cooled Cu or HTS (planar) coils	CA
Biomagnetism	magnetic pulses	SQUID	superconductor quantum interference	1 or 2 Josephson junctions	CA
Ophthalmoscopy	light parameters	SLO, SLT, SLP, OCT	optical	photodiode, APD	CA
Blood vessel lumen	flow mapping	Doppler sonography	piezoelectric	capacitor array	CA
		NMRI	EM induction	EM coils	CA
		MBI	Hall effect	Hall sensor	R&D

*CA = Commercially Available; R&D = Research and Development

TABLE 9.2. Appliances for Personal and Clinical Use.

Biomedical Application Field	Measurand	Sensor/Measurement Type	Basis of the Sensing Effect	Sensor Structure	Present Status
Body core temp.	temperature	body thermometer	thermoresistive	thermistor	CA
		ear thermometer	thermoelectric, pyroelectric	metal junction capacitor	CA CA
Blood pressure	pressure	Korotkoff oscillometric	piezoelectric piezoresistive	capacitor Si resistor bridge	CA
Heart rate, apnea Breathing wave Fetal heart rate	pressure pulses	fingertip sensor, phonocardigraph, flexible belt	piezoelectric	capacitor	CA
Glucose in blood and tissues	glucose concentration	GOD-based biosensors	catalytic reaction and transduction with the products	electrochemical cells, optrodes, and calorimetric types	some types CA, others in R&D
		low-potential cyclic voltammetry	acidic behavior of glucose	electrochemical cell	R&D, some types CA
		optical polarimetry	optical rotation	interferometer	
		SPR	plasmon resonance	optrode	R&D
		near IR spectroscopy	attenuated total reflection	optosensors	R&D, CA
Hearing aid	acoustic pressure	microphones	electret-based	capacitor, Si-micromachined	CA
Artificial retina	optical image	planar array on VLSI signal conditioner	photoelectric	photodiode array	R&D
Artificial limbs	tactile image	tactile sensor array	piezoresistive	resistor array	R&D, some types CA
			optical	phototr. array	
			capacitive	capacitor array	
			magnetoresistive	permalloy array	
			piezoelectric	capacitor array	
			ultrasonic	transmitter array	

TABLE 9.3. Sensors Mainly for Clinical and Laboratory Applications.

Biomedical Application Field	Measurand	Sensor/Measurement Type	Basis of the Sensing Effect	Sensor Structure	Present Status
Hemodynamic blood pressure	pressure	invasive catheter tip	piezoresistive	Si resistor bridge	CA
			piezoresistive	Si resistor bridge	
			optical reflectance	optrode	R&D
Blood temp.	temperature	catheter tip	thermoelectric, thermoresistive	Si-diode, thermo-couple, thermistor	CA
			phosphorescency	optrode	R&D
Blood flow	flow rate, velocity	SBF sensor	calorimetric	thermopiles	R&D
		hot-film anemometer	calorimetric	thermistor	CA
		Doppler sonography	piezoelectric	twin-capacitor	CA
		electrodynamic	Lorentz-force effect	magnet + contacts	CA
Joint angle	angular displacement	monitor gloves, etc.	piezoresistive	strain gauge	CA
Internal ocular pressure (IOP)	pressure	tonometer	piezoresistive	Si resistor bridge	R&D
Respiratory flow	air flow rate	Fleish sensor	Venturi + piezoresistive	Si resistor bridge	CA
		turbine	Hall effect	Hall sensor	CA
		vortex shedding	piezoelectric	capacitor	R&D
		catheter tip	freflectance	optical fiber	R&D
		nose clip	calorimetric	Si or film thermistor bridge	CA
in vitro nuclear diagnostics	β-intensity distribution	β-detector array	photoelectric effect	Si-APD array	R&D, CA
Electronic dosimeter	X- or γ-dosis	semiconductor detector + CMOS counter	photoelectric effect	Si-SSD	CA
Bioelectric signals	electric impulses	pickup electrodes	no transduction effect	electrode array	CA, R&D

TABLE 9.3. (continued).

Biomedical Application Field	Measurand	Sensor/Measurement Type	Basis of the Sensing Effect	Sensor Structure	Present Status
Blood dissolved O_2	pO_2	Clark electrochemical cell	permeation through membranes	amperometric cell	CA
		transcutaneous Clark cell	permeation through skin and membranes	heat-controlled amperometric cell	CA
		optical-fiber technique	fluorescence	optrode	CA
Blood dissolved CO_2	pCO_2	Stow-Severinghaus cell	permeation through membranes	poteniometric cell, pH-ISFET	CA
		transcutaneous Stow-Severinghaus cell	permeation through membranes	heat-controlled potenciometric cell	CA
		optical-fiber technique	colorimetric effect	optrode	CA, R&D
Blood acidity	pH	electrochemical	H^+-ion-complexation in membranes	potentiometric cell, pH-ISFET	CA CA
		optical fiber	colorimetric effect fluorescence	optrode optrode	R&D
Blood oxygen saturation	SO_2	invasive oximetry	absorbance/reflectance	pure-fiber optrode	CA
		ear oximetry	spectrum variations of hemoglobin	photodiodes	CA
		pulse oximetry		photodiodes	CA
Cerebral oxygenation	Cytochrome oximetry	tissue oximetry	reflectance variations of cytochrome oxidase	photodiodes	R&D
Ionic compounds in blood	Na^+, K^+, Ca^{2+}, Mg^{2+}, Cl^-, NH_4^+ concentrations	electrochemical	ion complexation in membranes	poteniometric cells, ISFETs	CA, R&D
Gastric acidity	pH	electrochemical	ion complexation in membranes	poteniometric cells, ISFETs	CA, R&D
		optical fiber	colorimetric	optrode	R&D
Sweat analysis	Na^+/Cl^- concentration	electrochemical	ion complexation in membranes	Na^+/Cl^- ISFETs	R&D

TABLE 9.3. (continued).

Biomedical Application Field	Measurand	Sensor/Measurement Type	Basis of the Sensing Effect	Sensor Structure	Present Status
Tissue acidity and oxygenation	pH/pO_2 mapping	scanning electrochemical microscopy	electrochemical	microelectrodes and their arrays	R&D
Metabolites and other substrates in blood	urea, uric acid, lactate, cholesterol, ATP, etc.	enzymatic biosensors living biosensors	catalytic reaction and transduction with the products	electrochemical cells, optrodes, and calorimetric types	mainly R&D
Immunoreaction reading	antigens/antibodies	immunosensors	chemical affinity and recognition + indirect/direct sensing	electrochemical, gravimetric SPR, SPRS	mainly R&D CA
Macromolecules in blood and tissues	DNA or DNA segment recognition	DNA sensors DNA or genetic chips	chemical recognition + direct sensing or with labeling	BAW, SPR fluorescent readout	R&D CA
Pharmacological effects on bacteria	*d*pH/*dt*	microphysiometer	pH-shift due to bacterial metabolism	LAPS	R&D

- *small personal and portable electronic diagnostic devices* (such as blood pressure meters, thermometers, etc.): Their widespread, low-cost commercial availability is based mainly on the application of sensors. Electronic data storage and processing enabled the clinical or ambulatory monitoring of the measured parameters.
- *invasive measurements:* The miniaturization of sensors enabled the direct continuous intravascular monitoring of parameters such as blood pressure, temperature, and flow rate, which has given new practical tools for clinical diagnostics. Although commercial products are available, their practical potentials have not yet been fully exploited.

The situation is much more contradictory in connection with *chemical and biosensors.* Chemical and biosensor technologies can play an important role in the documentation and improvement of public health by finding application in areas where rapid detection, high sensitivity, and specificity are important. Clinicians or patients also need a way to monitor the concentration of several key metabolites of the human body in many diseases. Great efforts have been made recently to extend the conventional clinical *in vitro* chemical analysis with the possibilities of chemical and biosensors. Although several hundreds of papers are published about research results, there are only a few well-defined areas where they really have found commercial applications:

- *blood oxygen monitoring:* Both intravascular and transcutaneous sensors have already been commercialized, but their application is rather limited. The easy and reliable operation of noninvasive oximeters, relying practically on physical sensors, keeps physicians from using the former two techniques that are somewhat harmful and more risky.
- *continuous* in vivo *monitoring of key metabolites:* The sensors can operate inside the body for a given period and give information on an analyte concentration; this approach can be used to establish real-time feedback control and treatment. The most important breakthrough has been made with glucose in applying the sensors in microdialysis systems.
- *portable screening appliances for personal use or for fast screening tests performed by physicians:* This area is also currently dominated by glucose test meters, however, the application of sensors has not exclusively replaced conventional photometry in such appliances. The main reason of this is that the possibilities of integrated multisensor-based systems for multianalyte testing have not yet been exploited. Commercially available medical enzymatic biosensor production is fully (98%) dominated by glucose sensors (http://www.cranfield.ac.uk/biotech/biomark.htm). The rest of the portion is for lactate, urea, and creatinine.
- *affinity sensors:* The greatest breakthrough of recent years is that two *affinity sensors* have gained commercial success: SPR immunosensors for

pharmaceutical research and DNA chips for genetic diagnostics and research (http://www.biacore.com, http://www.affimetrix.com, http://www.nanogen.com). Since they are applied for *in vitro* testing, the patient contact problems do not limit their rapid spread.

In spite of these commercial successes, however, even today, commercialization of sensors for the chemical, bioprocessing, and clinical diagnostic industries is rather limited in comparison with the great number of research results. Commercialization of most chemical sensor and biosensor technologies has continued to lag behind research by several years (Weetall, 1999). The reasons are complex. The large number of research articles related to the well-elaborated glucose sensor topic indicates that a number of problems still exist. There have always been cost considerations, and this includes the poor integration of many biosensor and chemical sensors into easy-to-use systems. An ever-existing problem of biosensors is the poor stability for long-term operation, which may be overcome with disposable sensors. A clear requirement for the successful commercialization of these devices is an applications need, either established or successfully predicted. In addition, the technology must offer advantages over existing technologies. There are still major barriers to the citizen-oriented application of sensors for the clinical diagnostic industries. Many of these barriers are not technical and include technology transfer, funding in early stages of development, and establishment of effective interdisciplinary partnerships. The other part of the barriers is technical and includes such specific concerns as follows:

- proper placement of the chemical or biocomponent on microfabricated devices
- reproducible placement of nanoliter quantities of biocomponents
- stabilization and storage of biosensors and biosensor components under an assortment of conditions
- improvement of electron transfer and mediation in electrochemical sensing devices to eliminate effects of contaminants
- methods of producing inexpensive, reliable, and sensitive biosensors in large quantities
- internal calibration and reference
- *in vivo* biosensors that are biocompatible and can remain in the body for weeks or months
- market diversity
- lack of company integration for production of chemical sensor or biosensor systems

The stability of biosensors remains a prime issue in the manufacture and deployment of these devices into many application areas in the real world. If stability remains a secondary issue in academic publications, in commercial

terms, it is of paramount importance. Stability can be subdivided into two main areas: shelf-stability, which is a measure of the storage capacity of the manufactured device, and operational stability, which is a measure of the longevity of the device in use. In many cases, operational stability is the described parameter in the literature, whereas in commercial applications, it is shelf stability that is more important. Indeed, in many cases, there is no need for operational stability as the commercial devices are disposable.

The most important technical and innovative concerns for finding a citizen-oriented road map for biosensor application can be summarized as follows:

- to find a specific application area where the possibilities of biosensors indisputably exceed those of the presently available technologies
- to establish an appropriate interdisciplinary cooperation between research centers and industry for production of biosensor systems
- to design inexpensive, single use, reliable, sensitive, and specific devices that exceed the possibilities and can perform these tasks at a low cost to the user

The indications are that sensor technology could follow the same trends as microelectronics (Turner, 1996). As chemical analysis becomes simpler and more widely available, one can expect to see a proliferation of uses in conjunction with microprocessors and telecommunications equipment. Equipment capable of acquiring data as well as processing it could find wide application in monitoring personal health. In order to facilitate this analytical revolution, biosensor technologists must resolve the remaining problems hindering the exploitation of biological molecules and their analogues in conjunction with microelectronics.

A more detailed description about the history and potentials of biosensors is given in the references.

9.1 REFERENCES

Turner, A. P. F., "Biosensors: Past, Present and Future," (1996) http://www.cranfield.ac.uk/biotech/chinap.htm.

Weetall, H. H., "Chemical Sensors and Biosensors, Update, What, Where, When and How," *Biosensors and Bioelectronics,* Vol. 14 (1999), pp. 237–242.

Sensor for Hemodynamic Pressure Monitoring in Invasive Applications

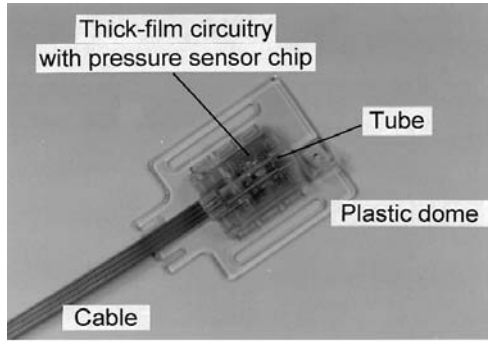

Top view

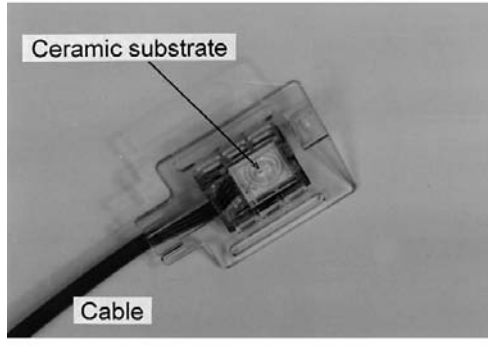

Bottom view

By courtesy of HIPOT, Slovenia (thanks to Mr. Darko Belavic).

Pressure Sensor Chips for Invasive Applications Fabricated by Silicon Surface Micromachining

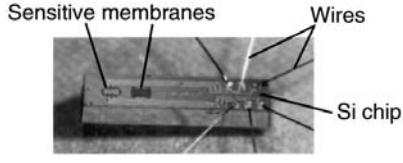

Piezoresistive pressure sensor chip
(2.3 x 0.5 x 0.5 mm)

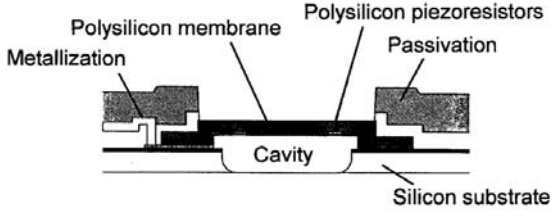

Schematic cross section of the sensor

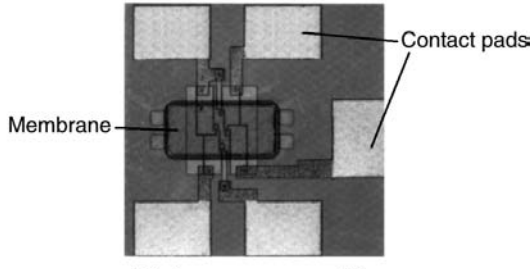

Minimum-area sensor chip
(0.5 x 0.5 mm)

By courtesy of Fraunhofer-Institut für Siliziumtechnologie, Germany (thanks to Dr. Berndt Wagner).

Transcutaneous Blood Oxygen Sensor

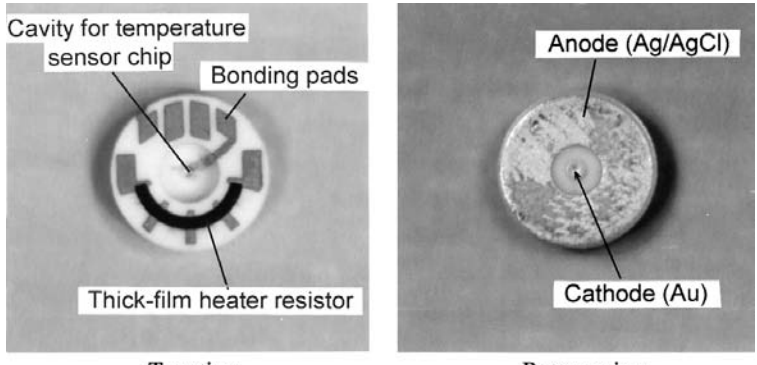

Top view Bottom view

Ceramic sensor body

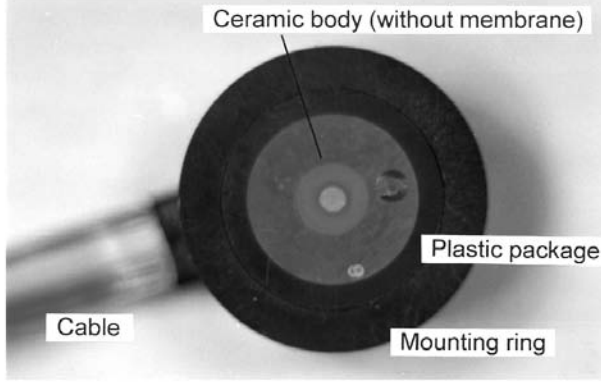

Sensor with its package

By courtesy of MELCOM Co., Hungary (thanks to Mr. Imre Göblös).

Integrated NaCl Probe for Sweat Analysis

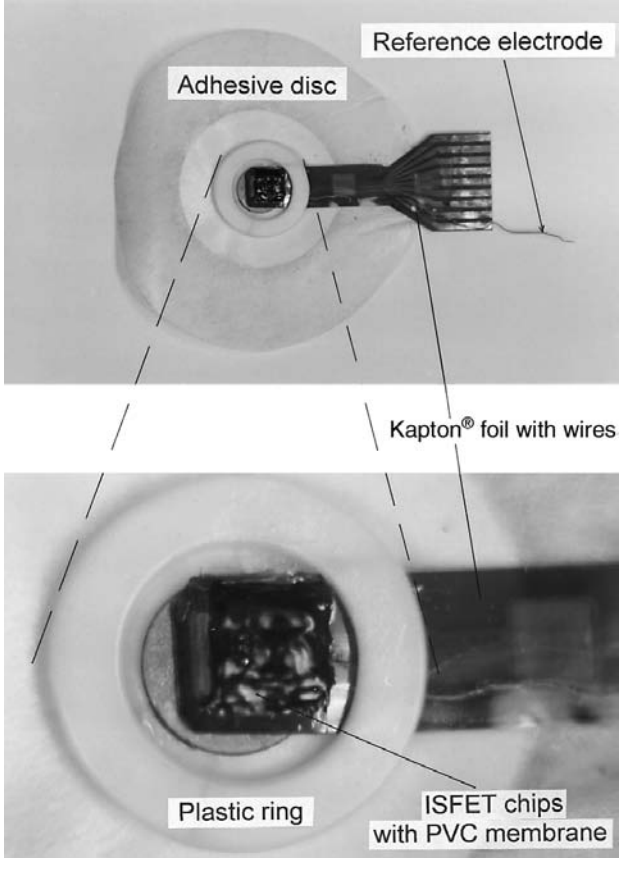

By courtesy of Dr. Klára Bezegh and Dr. András Bezegh.)

Flow-Through Cell for Biosensors in Microdialysis Systems

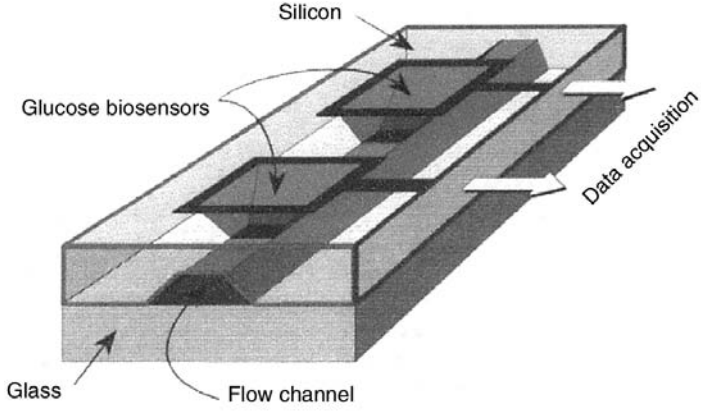

Schematic structure

Reproduced with permission from R. Steinkuhl, C. Sundermeier, H. Hinkers, C. Dumschat, K. Cammann and M. Knoll, "Microdialysis System for Continuous Glucose Monitoring," *Sensors and Actuators B,* pp. 19–24, ©1996, Elsevier Science S.A., Lausanne, Switzerland.

APPENDIX 6

Cost and Reliability Oriented Material Design Aspects of Electrochemical Cell Biomedical Sensors*

Electrochemical cells have an essential role in chemical sensors and biosensors. Although a number of other approaches have appeared, electrochemical cells represent the classical solution for a number of analytical problems. The application of precious metal electrodes is the main limit of their cost effectiveness. Three main solutions may be followed to achieve cost reduction:

- replacing high-cost materials with lower-cost precious metals, e.g., applying silver instead of gold and platinum (carbon has shown instabilities and reliability problems)
- decreasing the amount of precious metal materials by applying electrodes made by thick- or thin-film processing
- enabling refreshment methods for the electrolyte and the (semipermeable or enzymatic) membrane, thus, the electrode system can be used for a number of measurement cycles, but its long-term reliability must be guaranteed in this case

When turning to lower-cost solutions, reliability deterioration may generally occur; thus, a careful material design must be performed. This discussion concentrates on the reliability of the electrode system itself and does not deal with electrolyte and membrane-related problems that are emphasized in the book.

The reliability of the electrode system is strongly dependent on the possible corrosion/migration processes that can occur with the applied materials at the particular conditions of use. These important conditions are the composition of the electrolyte and the applied cell polarization. Since these may vary strongly according to the application, a general description cannot be given here. We try to summarize the available processes causing electrode deterioration the availability of which must be investigated at the given application field individually.

Electrode processes causing reliability problems may be distinguished as follows:

*A special contribution by the Author.

(1) *Anode consumption.* This is especially dangerous when applying thin films. It occurs in anodic processes that result in the dissolution of the metallic electrode. In the case of silver, for example (Krumbein, 1994):

$$Ag \rightarrow Ag^{+} + e^{-} \tag{A1}$$

This may lead not only to electrode consumption, but also result in the presence of silver ions inside the electrolyte. In many cases, the electrolyte contains KCl, which will prevent the formation of free silver ions by the electrochemical process characteristic for the Ag/AgCl reference electrodes:

$$Ag + Cl^{-} \Longleftrightarrow AgCl + e^{-} \tag{A2}$$

If traces of H_2O_2 are present [e.g., in enzymatic reactions and also in oxygen sensors due to their intermediate formation according to Equation (6.3), characteristic for gold cathodes], their anodic reaction shifts the electrode potential significantly to the positive direction, and the silver is continuously converted into AgCl, resulting again in electrode consumption, thus limiting the lifetime (Cha et al., 1990). Using Pt-Ag and Pd-Ag conductors, the platinum or palladium, respectively, reduces the dissolution of silver, but this cannot totally be eliminated. However, at special ternary Pd-Pt-Ag compositions, the dissolution can be prevented (Harsányi, 1995). These alloys can only be used, however, for counterelectrode materials in three-electrode cells, but not for reference purposes. In oxygen sensors, the H_2O_2 production was typically found at gold conductors. The process could be eliminated by applying platinum.

Dissolution may also occur even from Au, Pt, and Pd anodes in the presence of Cl^{-} ions by the formation of water soluble complexes, such as (Grunthaner et al., 1975):

$$Au + 4\ Cl^{-} \rightarrow AuCl_4^{-} + 3\ e^{-} \tag{A3}$$

The tetrachloro-gold complex-ion formation is typical at a standard potential of 1.0 V, which is fortunately out of the polarization ranges applied in most sensor cells. But, the deterioration may be started even during hazardous transients or special calibration cycles that are not kept within the narrow polarization range. The situation is worse with Pd, which shows similar behavior at a much lower standard potential level of 0.62 V (Sbar, 1976).

(2) *Cathodic deposits.* If metal ions are present in the electrolyte due to the anodic dissolution and/or complex formation and subsequent processes, they can be deposited on the cathode surface at relatively low polarization levels (Krumbein, 1994):

$$Me^{n+} \rightarrow Me + ne^{-} \tag{A4}$$

This effect not only causes interferences in the sensor signal, but also may lead to the formation of dendrite-like deposits that can grow through the isolation gap to-

ward the anode resulting in a catastrophic short circuit failure. High ionic salt concentration inside the electrolyte can prevent this process by two ways: one is the precipitate formation with the possible cations, like in Equation (A2), and the other is that rather than a continuous film deposition, dendritic growth is typical on the cathode surface in high conductivity electrolytes. The sensor operation will be, however, disturbed in this situation as well.

Although the reduction of oxygen is considerable for many metals in neutral solutions [as shown in Equation (6.3)], hydrogen evaluation as a result of the reduction of hydrogen ions (Shan et al., 1992) might also occur:

$$2\,H^+ + 2\,e^- \rightarrow H_2 \tag{A5}$$

This process cannot be totally disclosed, especially at polarization levels close to 1V in electrolytes showing some acidity. The hydrogen evaluation can cause the reduction of isolating oxide compounds that are applied as binder materials in thick-film conductor and insulator materials (such as CuO and Bi_2O_3) (Harsányi 1992, 1993):

$$Me_2O_n + 2nH^+ \rightarrow 2Me^{n+} + nH_2O \tag{A6}$$

This process may again lead to metal ion formation that can form deposits and dendrites on the cathode surface. Moreover, the decomposition of the binder oxides may cause the delamination of the films.

The most important failure mechanisms leading to electrode deterioration in electrochemical cell sensors have been summarized above. All electrochemical processes on the electrode surfaces are strongly dependent on the electrolyte composition, polarization voltage, and cell current density. Since the exact conditions of the various processes have not yet been determined, a careful design and test process has to be performed when selecting materials, fabrication processes, and geometrical sizes for properly adjusting them to the operating conditions.

A.1 REFERENCES

Cha, C. S., Shao, M. J. and Liu, Ch. -Ch., "Problem Associated with the Miniaturization of a Voltammetric Oxygen Sensor: Chemical Crosstalk among Electrodes," *Sensors and Actuators B,* Vol. 2 (1990), pp. 239–242.

Grunthaner, F. G., Griswold, T. W. and Clendening, P. J. "Migratory Gold Resistive Shorts: Chemical Aspects of Failure Mechanism," in *Proc. Int. Symp. Reliab. Physics* (1975), pp. 99–106.

Harsányi, G., "Electrochemical Processes Resulting in Migrated Short Failures in Microcircuits," *IEEE Transactions on Components, Packaging, and Manufacturing Technology—Part A,* Vol. 18, No. 3 (1995), pp. 602–610.

Harsányi, G., "Dendritic Growth from Dielectric Constituents: a Newly Discovered Failure Mechanism in Thick Film ICs?" *Int. J. Microcircuits & Electronic Packaging,* Vol. 16, No. 3 (1993), pp. 207–216.

Harsányi, G., "New Type Short Circuits at Fritless Thick Film Conductors—Formed From Reduced Oxides," in *Proc. Intern. Symp. on Microelectronics, ISHM* (1992), pp. 140–143.

Krumbein, S. J., "Metallic Electromigration Phenomena," in *Electromigration and Electronic Device Degradation* (ed. A. Christou), John Wiley & Sons, New York (1994), pp. 139–166.

Sbar, N. L., "Bias Humidity Performance of Encapsulated and Unencapsulated Ti-Pd-Au Thin-Film Conductors in an Environment Contaminated with Cl_2," *IEEE Trans. Parts, Hybrids, Packaging,* Vol. 12 (1976), pp. 176–181.

Shan, X., Pecht, M. and A. Christou, "Corrosion Modeling in Microelectronic Devices," *Int. J. Microcircuits & Electronic Packaging,* Vol. 15, No. 1 (1992), pp. 1–10.

GLOSSARY

ABPM	Ambulatory Blood Pressure Monitoring
AC	Alternating Current
A/D	Analog to Digital
ADP	Adenosine-5′-diphosphate
AFM	Atomic Force Microscopy
APD	Avalanche Photodiode
APM	Acoustic Plate Mode
ATP	Adenosine-5′-triphosphate
ATR	Attenuated Total Reflection
BAW	Bulk Acoustic Wave
BGO	$Bi_4Ge_3O_{12}$
BOD	Biological Oxygen Demand
bpy	2,2′-Bipyridine
CBI	Compton-Backscatter Imaging
CCD	Charge Coupling Device
CHEMFET	Chemically sensitive FET
CMOS	Complemented MOS
CT	Computer Tomography
CTA	Constant Temperature Anemometry
CVD	Chemical Vapor Deposition
CW	Continuous Wave
CWO	$CdWO_4$
CZT	CdZnTe
DC	Direct Current
DNA	Desoxyribonucleinic Acid
ECG	Electrocardiography
EEG	Electroencephalography

EIA	Enzyme Immunoassay
EKG	Electrocardiography
ELISA	Enzyme-Linked Immunosorbent Assay
EM	Electromagnetic
ENFET	Enzymatic FET
FAD	Flavin Adenin Dinucleotide
$FADH_2$	Reduced form FAD
FET	Field Effect Transistor
FIA	Fluorescent Immunoassay
FiO_2	Inspired O_2 concentration
FHR	Fetal Heart Rate
Ge(Li)	Lithium-ion-drifted germanium
GF	Gauge Factor
GOD	Glucose Oxidase
Hb	Hemoglobin
HCG	Human Chorionic Gonadotropin Hormone
HIV	Human Immunodeficiency Virus
HPGe	High-Purity Germanium
HPTS	Hydroxy-pyrene-trisulphonate
HSA	Human Serum Albumin
HTS	High-Temperature Superconductor
IDT	Interdigital Transducer
IgE	Immunoglobulin-E
IgG	Immunoglobulin-G
ImmunoFET	Immunosensitive FET
IOP	Internal Ocular Pressure
IR	Infrared
ISE	Ion-Selective Electrode
i-Si	Intrinsic Silicon
ISFET	Ion-Selective FET
LAPS	Light-Addressable Potentiometric Sensor
LB	Langmuir-Blodgett
LCD	Liquid Crystal Display
LED	Light-Emitting Diode
LIA	Luminescent Immunoassay
LPE	Liquid Phase Epitaxy
LSO	Luthetium-ortosilicate
MBE	Molecular Beam Epitaxy
MBI	Magnetic Backprojection Imaging
MCG	Magnetocardiography
MEG	Magnetoencephalography
MEMFET	Membrane Modified FET

MICSPOMS	Metal-Island-Coated Swelling Polymer Over Mirror System
MIS	Metal-Insulator-Semiconductor
MLC	Multilayer Ceramic
MOSFET	Metal Oxide Semiconductor FET
MRI	Magnetic Resonance Imaging
MRMI	Magnetic Resonance Microimaging
MUX	Multiplexer
NAD	Nicotinamide-Adenine-Dinucleotide
NADH	Reduced form NAD
NADP	NAD Phosphate
NIR	Near Infrared
NMOS	N-channel MOS
NMR	Nuclear Magnetic Resonance
OCT	Optical Coherent Tomography
OSAS	Obstructive Sleep Apnea Syndrome
OWLS	Optical Waveguide Lightmode Spectroscopy
PAA	Polyacrylamide
PAA	Polyacrylamide
PANi	Polyaniline
pCO_2	Partial pressure of carbon dioxide
PEI	Polyetherimide
PEM	Photoelectron Multiplier
PET	Positron Emission Tomography
PEV	Pyroelectric Vidicon
PFEP	Poly(fluoroethylene propylene)
PHEMA	Poly(hydroxyethyl methacrylate)
PID	Proportional Integral Derivative
PIN	P-intrinsic-n structure diode
PMePy	Poly(N-methylpyrrol)
PMMA	Poly(methyl methacrylate)
PMOS	P-channel MOS
pO_2	Partial pressure of oxygen
POSFET	Piezopolymer Oxide Semiconductor FET
PPy	Polypyrrole
PSPEM	Position-Sensitive PEM
PTF	Polymer Thick Film
PTFE	Polytetrafluoroethylene
PVA	Poly(vinyl alcohol)
PVC	Poly(vinyl chloride)
PVDF	Poly(vinylidene fluoride)
PVI	Poly(*N*-vinylimide-azole)

PVPy	Poly(vinyl pyridine)
PW	Pulsed Wave
PWD	Printed Wiring Board
PZT	Lead-Zirconate-Titanate
QMB	Quartz Microbalance
ROM	Read-Only Memory
REFET	Reference FET
RF	Radio Frequency
RIA	Radio Immunoassay
RIE	Reactive Ion Etching
RTD	Resistance Temperature Detector
$Sa\mathrm{O}_2$	Arterial blood oxygen saturation
SAW	Surface Acoustic Wave
SBF	Skin Blood Flow
SH-APM	Share Horizontal APM
Si(Li)	Lithium-ion-drifted silicon
SLO	Scanning Laser Ophthalmoscopy
SLP	Scanning Laser Polarometry
SLT	Scanning Laser Tomography
$S\mathrm{O}_2$	Blood oxygen saturation
SOS	Silicon On Sapphire
SPECT	Single-Photon Emission Tomography
$Sp\mathrm{O}_2$	Pulse oximetry blood oxygen saturation
SPR	Surface Plasmon Resonance
SPRS	SPR spectroscopy
SQUID	Superconductor Quantum Interference Device
SSBW	Surface Skimming Bulk Wave
SSC	Silver/Silver-Chloride (electrode)
SSD	Solid State Detector
$Sv\mathrm{O}_2$	Venous (or mixed) blood oxygen saturation
TBCCO	$\mathrm{Tl_2Ba_2CaCu_2O_8}$
TCGF	Temperature Coefficient of the GF
TCQN	Tetracyanoquinodimethane
TCR	Temperature Coefficient of Resistance
TGS	Triglycine Sulphate
UFCT	Ultrafast CT
UV	Ultraviolet
VLSI	Very Large-Scale Integration
VPE	Vapor Phase Epitaxy
YBCO	$\mathrm{YBa_2Cu_3O_7}$

ABOUT THE AUTHOR

Gábor Harsányi, Ph.D., is presently Associate Professor and Head of the Sensors Laboratory at the Department of Electronics Technology, Technical University of Budapest. He graduated in electrical engineering in 1981 and received his Ph.D. in microelectronics technology. He spent several years in industry conducting research projects on chemical microsensors. His current research activity focuses on sensors in biomedical applications, polymers in sensorics, fiber optic sensors, and reliability physics of high-density electronic interconnection systems. He spent half a year at fellowship at the Florida International University in 1996.

Dr. Harsányi has an international reputation in the field of microelectronics and sensorics. And, he is very active professionally in international conferences and societies: he was President of the Hungarian Chapter of IMAPS (International Microelectronics and Packaging Society) in 1993/94; he received a Best Paper of Session Award at the International Symposium on Microelectronics (Orlando, FL, 1991); he is a member of the Technical Program Committee of European Microelectronics Conferences, and became a Fellow of IMAPS in 1998. He has been involved in various international projects, including PHARE-ACCORD, NATO-ARW, COBASE (a NSF program), INCO-COPERNICUS (a European Union funded program), and others. His scientific research, publication, and related coordinating and traveling activity is also supported by several Hungarian national institutions, such as the National Committee for Technological Development (OMFB), the National Scientific Research Fund (OTKA), the Ministry for Culture and Education (MKM), and the Foundation for Hungarian Higher Education and Research (AMFK). He has authored more than 100 research publications and technical papers in international journals and conference proceedings books, coedited several books,

and authored one monograph *Polymer Films in Sensor Applications* published by Technomic Publishing Co., Inc. in 1995. In various sensor application topics, he has also conducted several high level international professional seminars and courses sponsored by IMAPS, Europractice, and Technomic Publishing Co., Inc.

INDEX